EPSTEIN-BARR VIRUS IN THE PATHOGENESIS OF POST-TRANSPLANT LYMPHOPROLIFERATIVE DISEASE

By

DAVID MERITON BURNS

A thesis submitted to the University of Birmingham

for the degree of DOCTOR OF PHILOSOPHY

School of Cancer Sciences

College of Medical and Dental Sciences

University of Birmingham

December 2014

Abstract

Post-transplant lymphoproliferative disease (PTLD) is a life threatening complication of transplantation, often associated with the B-lymphotrophic Epstein-Barr virus (EBV). In order to further our understanding of the relationship between EBV infection and PTLD, a series of clinical and laboratory studies were undertaken. A multicentre United Kingdom study defined current outcomes and prognostic factors for patients with PTLD arising after solid organ transplant. A study to define incidence and risk factors for EBV reactivation and PTLD amongst patients undergoing allogeneic haematopoietic stem cell transplant (allo-HSCT) revealed greatly reduced risk amongst patients with Non-Hodgkin lymphoma previously treated with Rituximab. Complementary laboratory studies to explore the pathophysiology of EBV reactivation after allo-HSCT demonstrated that the virus maintains selectivity for, and can drive the expansion of, circulating $CD27^+$ memory B-cells; these are normally scarce for many months after transplant. Investigations were also performed to examine the role of cell survival, DNA damage signalling and mutations as possible drivers of clonal selection in EBV-infected B-cell cultures, as an *in vitro* model for PTLD. Finally, work was undertaken to characterise EBV-epitope specific T-cell responses expanding in patients successfully treated with donor lymphocyte infusion for Rituximab-refractory PTLD arising after allo-HSCT.

Acknowledgments

I wish to thank my supervisors Dr Andrew Bell and Prof Martin Rowe, and also Prof Alan Rickinson, for their guidance and support throughout the course of these studies. Particular thanks also go to Dr Heather Long as supervisor for the work on EBV-specific T-cells, and Dr Claire Shannon-Lowe and Dr Rose Tierney for additional supervision in the laboratory. I also wish to extend gratitude to Dr Sridhar Chaganti, Dr Ram Malladi and Prof Charles Craddock for their guidance with the clinical aspects of these studies. I also wish to thank Dr Sandeep Nagra, Janice Ward, Jane Nunnick, Dr Jo Croudace, Dr Charlotte Inman and Prof Paul Moss for their advice and assistance with accessing patient samples and clinical data from University Hospital Birmingham. Gratitude also goes to Pauline Cauldwell, Dr Shabeeha Rana and Dr Christopher Fox for provision of samples and clinical data from Nottingham University Hospital. I also wish to acknowledge clinical haematology trainees Dr Katherine Clesham, Dr Joanna Haughton, Dr Michelle Lannon and Dr Hayder Hussein, and their supervising consultants Dr Kate Cwynarski, Dr Roderick Johnson and Dr Anne Lennard, for provision of clinical data for the study on PTLD arising after solid organ transplant. Thanks also go to the statisticians Andrew Howman and Dr Jennifer Marsh for supervision of statistical analyses. My gratitude also goes to Dr Eszter Nagy, Gordon Ryan, Debbie Croom-Carter, Alison Leese and Roger Bird for their assistance. I also wish to thank Dr Jane Bryon and others from the West Midlands Genetics laboratory for their help with molecular studies. Finally I wish to thank the Wellcome Trust for their sponsorship.

Table of Contents

List of Figures

Page

List of Tables

Page

Abbreviations

AID	Activation-induced cytidine deaminase
Allo-HSCT	Allogeneic haematopoietic stem cell transplant
AML	Acute myeloid leukaemia
ATG	Anti-thymocyte globulin
BCR	B-cell receptor
BEAM	Carmustine / etoposide / cytarabine / melphalan
β2M	Beta-2-microglobulin
BL	Burkitt lymphoma
Bp	Base pairs
Bu	Busulphan
BZKO	BZLF1 knockout
CD	Cluster of differentiation
CD40L	CD40 ligand
cDNA	Complementary deoxyribonucleic acid
CDR	Complementarity determining region
CFSE	Carboxyfluorescein succinimidyl ester
CLL	Chronic lymphocytic leukaemia
CR	Complete response or complete remission
CSM	Class Switched Memory
CSR	Class-switch recombination
Cy	Cyclophosphamide
Cy TBI C	Cyclophosphamide / total body irradiation / Campath
DLBCL	Diffuse large B-cell lymphoma
DLI	Donor lymphocyte infusion
DNA	Deoxyribonucleic acid
EA	Early antigen
EBER	EBV encoded RNA
EBNA	EBV nuclear antigen
EBNA-LP	EBNA leader protein
EBV	Epstein-Barr virus

Elispot	Enzyme-linked immunosorbent assay
FACS	Fluorescence activated cell sorter (sorting)
FITC	Fluorescein isothiocyanate
FLAMSA	Fludarabine / cytarabine / amsacrine / ATG
Flu	Fludarabine
FMC	Fludarabine / melphalan / Campath
FSC	Forward scatter
FSC-H	Forward scatter - height
GAPDH	Glyceraldehyde-3-phosphate dehydrogenase
GC	Germinal centre
GvHD	Graft-versus-host disease
H2AX	Histone H2A family, member X
HIV	Human immunodeficiency virus
HL	Hodgkin lymphoma
HLA	Human leukocyte antigen
HRS	Hodgkin and Reed-Sternberg
HSCT	Haematopoietic stem cell transplant
IFN	Interferon
Ig	Immunoglobulin
IgH	Immunoglobulin heavy chain
IgVH	Variable region of immunoglobulin heavy chain
IL4	Interleukin 4
IM	Infectious mononucleosis
IMGT	ImMunoGeneTics (database)
IPTG	Isopropyl-β-D-thiogalactoside
KSHV	Kaposi sarcoma-associated herpesvirus
LCL	Lymphoblastoid cell line
LMP	Latent membrane protein
LPL	Lymphocytoplasmacytic lymphoma
MDS	Myelodysplasia
Mel	Melphalan
MF	Myelofibrosis

MFI	Median fluorescence intensity
$MgCl_2$	Magnesium chloride
MHC	Major histocompatibility complex
MOI	Multiplicity of infection
mRNA	Messenger RNA
MUD	Matched unrelated donor
NK-cell	Natural killer-cell
NK/T-cell	Natural killer T-cell
NHL	Non-Hodgkin lymphoma
NR	No response
NPC	Nasopharyngeal carcinoma
NSM	Non-switched memory
NT	Not tested
OriP	Origin of plasmid replication
PB	Plasmablast
PBMC	Peripheral blood mononuclear cells
PBS	Phosphate buffered saline
PBSC	Peripheral blood stem cells
PCR	Polymerase chain reaction
PET	Positron emission tomography
PR	Partial response or remission
PTLD	Post-transplant lymphoproliferative disease
qPCR	Quantitative PCR
RAG	Recombination-activating gene
RIC	Reduced intensity conditioning
RNA	Ribonucleic acid
rpm	Rotations per minute
RPMI	Roswell Park Memorial Institute
RT	Reverse transcription
RT-PCR	Reverse transcription polymerase chain reaction
SHM	Somatic hypermutation
SOT	Solid organ transplant

SSC	Side scatter
TBI	Total body irradiation
TCD	T-cell depletion
TCR	T-cell receptor
T-PLL	T-cell prolymphocytic leukaemia
Trans	Transitional cell
UV	Ultraviolet
VCA	Viral capsid antigen
VDJ	Variable-diversity-joining
X-Gal	5-bromo-4-chloro-3-indoyl-β-D-galactoside
XLA	X-linked agammaglobulinaemia
XLP	X-linked lymphoproliferative disease

1. Introduction

1.1 Beginnings

February 2014 marked the 50th anniversary of the discovery of the first human tumour virus, Epstein-Barr virus (EBV). This milestone in biomedical research has its origins in a chance meeting between Dennis Burkitt, an Irish surgeon working in Uganda, and Anthony Epstein, a pathologist in training at the Middlesex Hospital Medical School, United Kingdom[1]. It was during an evening seminar delivered by Burkitt at the Middlesex Hospital that Epstein first learnt of Burkitt's work describing a novel form of tumour affecting East African children, characterised by a curious localisation to the jaw and aggressive clinical course – Burkitt lymphoma (BL). Detailed epidemiological observation had shown that this lymphoma was restricted to geographical areas with high temperatures and rainfall, and in light of this Burkitt and his colleagues postulated that a virus might be responsible. Working at the time on Rous sarcoma virus, an agent which causes tumours in chickens, Epstein was enthused by this idea and promptly set about trying to identify a virus in specimens of BL transported from Africa. Working with his research assistant, Yvonne Barr, 3 years without success followed until late one evening in February 1964 when Epstein finally observed virus particles inside cultured BL cells using electron microscopy[2]. Subsequent work confirmed the presence of Epstein-Barr Virus, as it came to be known, in almost all cases of African (endemic) BL. It was also found in a proportion of non-African (sporadic) BL, as well as in cases arising in individuals with Acquired Immunodeficiency Syndrome (AIDS) due to Human Immunodeficiency virus (HIV) infection.

In the years that followed this seminal discovery, EBV was linked to numerous other disease

entities (Table 1). Thus, in 1968 EBV was shown to be the agent responsible for infectious mononucleosis (IM), a usually self-limiting lymphoproliferative disease characterised by fever, pharyngitis, lymphadenopathy and marked fatigue[3]. It was also causally implicated in diseases originating from epithelial cells, in particular nasopharyngeal carcinoma (NPC), a major cause of mortality in southern China, in which EBV is always found[4]. Furthermore, it was found to be associated with other forms of B-lymphocyte (B-cell) malignancy, including cases of classical Hodgkin lymphoma (HL)[5], as well as diseases arising from T-cells[6,7] or Natural Killer (NK)-cells[8].

Remarkably, EBV was also discovered to be the cause of lymphomas in organ transplant recipients. Thus, human organ transplantation had been pioneered in the early 1960s, facilitated by the introduction of the immunosuppressive drugs Azathioprine and then Cyclosporin. However, transplant physicians had soon noticed a worrying increase in the incidence of cancer in their patients. These were frequently lymphomas, which developed within 1 - 2 years of transplant and which were usually fatal. Although an infective cause was suspected, the agent responsible remained elusive until the landmark discovery, reported in June 1980, that EBV had been found in a lymphoma from a patient with a renal transplant[9]. Subsequently, EBV would be confirmed as an aetiological agent in many cases of what came to be known as post-transplant lymphoproliferative disease (PTLD). To this day, PTLD remains a significant cause of morbidity and mortality amongst transplant recipients, and an important paradigm in research.

Diseases
Infectious mononucleosis
X-linked lymphoproliferative disease
Haemophagocytic lymphohistiocytosis
Chronic active EBV
Hairy oral leukoplakia
Multiple sclerosis
B-cell lymphomas
Post-transplant lymphoproliferative disease
Burkitt lymphoma
Classical Hodgkin lymphoma
Diffuse large B-cell lymphoma
Acquired immunodeficiency syndrome lymphomas
Primary effusion lymphoma
T- and NK-cell lymphomas
Haemophagocytic lymphohistiocytosis T-cell lymphoma
Nasal NK/T-cell lymphoma
Epithelial cell malignancies
Nasopharyngeal carcinoma
Gastric carcinoma
Other malignancies
Leiomyosarcoma

Table 1. EBV-Associated Pathologies

Since its discovery EBV has been associated with a wide range of non-malignant and malignant disease entities[10].

1.2 B-Cell Biology

Humeral Immune Responses

EBV is primarily a B-lymphotrophic virus, and thus an appreciation of B-cell biology is crucial for understanding EBV and its associated pathologies. As mediators of the humeral arm of the adaptive immune system, the principal role of B-cells is to generate immunoglobulins (Ig), also known as antibodies[11]. These glycoproteins, secreted by plasma cells, bind target antigens to mediate numerous immune effects including elimination of bacterial pathogens via complement-activation, triggering of macrophage-mediated phagocytosis and recruitment of other immune cells. Antibodies are comprised of 2 identical immunoglobulin heavy (IgH) chains and 2 identical Ig light (IgL) chains, covalently linked to each other by disulphide bonds. Located at the amino terminus of each chain is a variable domain (VH for the heavy chain; VL for the light chain) containing 3 areas of highly variable amino acid sequence, known as complementarity-determining regions (CDR). When brought together in the overall structure of the antibody molecule, the CDRs collectively form an antigen binding site, which facilitate binding to specific target antigens. Meanwhile, the remainder of the Ig chains comprise 1-3 conserved constant (C) domains, the configuration of which determines which of 5 functionally distinct antibody classes the molecule belongs to: IgM, IgD, IgG, IgA or IgE. Mature B-cells express surface Ig complexed with the molecules CD79a and CD79b, constituting the B-cell receptor (BCR)[12].

Early B-Cell Development

The earliest events in B-cell development occur in the bone marrow (Figure 1). It is here that B-cell precursors develop from haematopoietic stem cells, and where Ig genes undergo ‘VDJ recombination,’ a process that contributes significantly to the generation of antibody

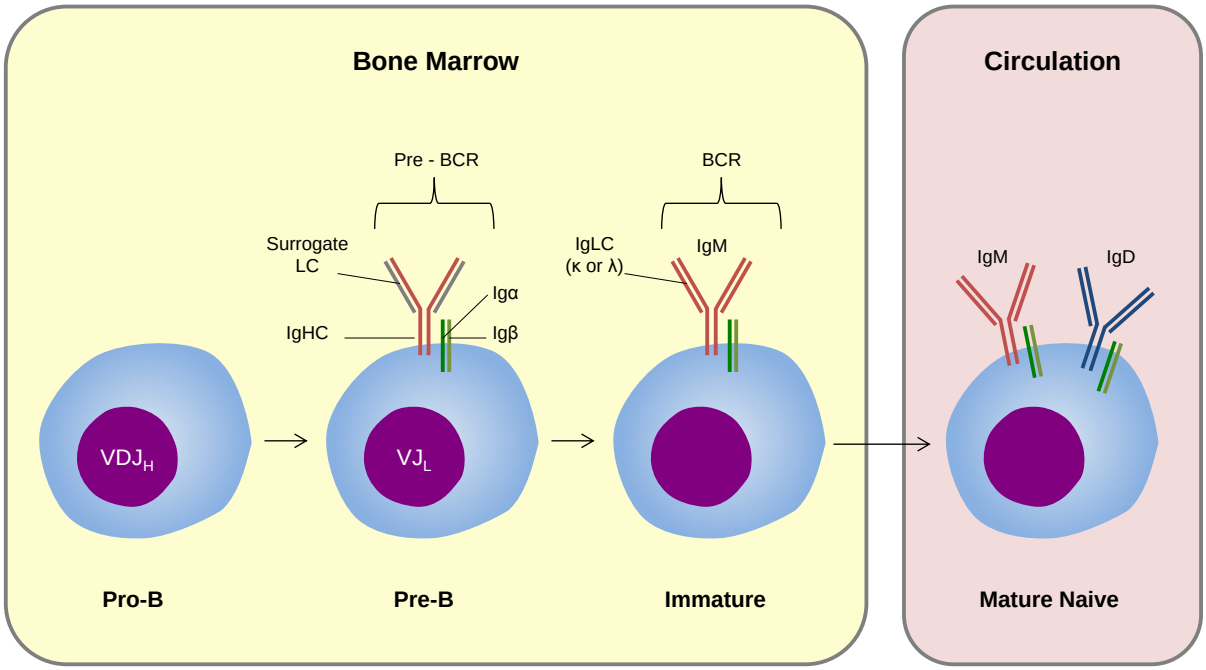

Figure 1 Early B-Cell Development

During B-cell development RAG-mediated VDJ recombination results in rearrangement of germ-line Ig sequences in a process that contributes hugely to Ig diversity by randomly bringing together sequences that generate the variable domains of IgH and IgL chains. The IgH chain undergoes rearrangement of VDJ segments at the pro-B-cell stage. The rearranged chain is expressed at the cell surface in combination with a surrogate light chain and CD79α (Igα) and CD79β (Igβ) molecules, a complex that comprises the pre-BCR. At the pre-B-cell stage, the IgL chain undergoes rearrangement of VJ segments, and this replaces the surrogate light chain generating the final BCR. Mature naive B-cells simultaneously expressing surface Ig with IgM and IgD constant regions, as a consequence of alternative splicing, are released into the circulation. Multiple regulatory mechanisms ensure that only B-cells successfully expressing Ig with a single specificity, and which lack self-reactivity, are generated. Figure adapted from Fried & Bonilla[13].

diversity[14]. In humans, the Ig genes are located on separate chromosomes: chromosome 14 (IgH locus), chromosome 2 (κ IgL locus) and chromosome 22 (λ IgL locus). In the germline, each IgH locus contains multiple variable (V), diversity (D), and joining (J) segments, and each IgL locus contains multiple V and J segments. As B-cells progress through the early stages of their development, they randomly recombine these gene segments to form a single 'rearranged' sequence that codes for each Ig V domain. Recombination events occur in sequence and define distinct stages of B-cell development. Thus the IgH gene first undergoes recombination during the 'pro-B-cell' stage, when single D and J segments recombine, after which a V segment recombines with the DJ segment. Subsequently, the rearranged VDJ sequence is expressed with a constant domain at the 'large pre-B-cell' stage. Later, rearrangement of the IgL segments occurs at the 'small pre-B-cell' stage, resulting in expression of a functional κ or λ IgL molecule. These VDJ recombination events are mediated by the recombination activating gene (RAG) recombinase complex, encoded by RAG1 and RAG2. This cleaves DNA at specific recombination signal sequences (RSS) flanking each V, D and J gene segment, after which DNA repair enzymes, including those of the non-homologous end joining (NHEJ) repair pathway, repair the DNA breaks[15]. Importantly, the VDJ recombination process is regulated by multiple mechanisms in order to ensure that B-cells express a single functioning BCR[16,17]. Thus, as each cell contains 2 copies of the Ig loci, a mechanism known as 'allelic exclusion' ensures that productive rearrangement of 1 copy prevents further rearrangement and expression of the other. Furthermore, if both Ig rearrangements are non-productive, resulting in the inability to express a functional Ig chain, then further differentiation of the cell is prevented. Moreover, in order to prevent the generation of autoreactive B-cell responses, cells bearing BCRs which recognise self-antigens are eliminated via the induction of apoptosis or anergy.

Naive B-cells

Consequent upon these early B-cell differentiation events, antigen-inexperienced naive B-cells are released from the marrow into the circulation, where they typically constitute around 70% of the total B-cell pool[18]. These cells are identifiable by simultaneous expression of surface IgM and IgD (and absence of the surface marker CD27, as described later), resulting from alternative splicing of IgH mRNA transcript, such that the recombined VDJ region can be associated with C regions of either Ig class[14]. Notably, the earliest emigrants from the bone marrow are known as transitional B-cells, which typically make up less than 5% of B-cells in healthy individuals[19-22]. Characteristically these cells express high levels of CD24, CD38 and CD10, which are gradually down-regulated as they differentiate into mature naive B-cells. A high proportion of transitional B-cells are thought to exhibit self-reactivity, and these are deleted such that only around 50% successfully develop into mature B-cells[22]. The latter circulate through the blood and secondary lymphoid tissues until they either encounter cognate antigen or otherwise apoptose.

B-Cell Activation

Antigen encounter by B-cells, typically in the follicular areas of secondary lymphoid tissues, initiates B-cell activation and differentiation[12,23,24]. Antigen binding triggers the aggregation of BCR complexes, resulting in activation of the Src family kinases LYN, BLK and FYN, as well as SYK and BTK tyrosine kinases. During this process, targets in the CD79a and CD79b subunits of the BCR are phosphorylated and a large ‘signalosome’ complex assembles, composed of the BCR, kinases and other important adaptor molecules including CD19, CD21 and BLNK. This triggers a signalling cascade resulting in pleiotropic downstream effects including modulation of gene expression, changes to cell metabolism, cytoskeletal

reorganisation and cell-cycle entry. However, effective B-cell activation also requires additional co-stimulatory signals, without which antigen-stimulated B-cells would either apoptose or become anergic[23]. T-cell independent antigens, such as the lipopolysaccharide (LPS) component of Gram-negative bacterial membranes and unmethylated CpG DNA of bacteria or viruses, provide intrinsic co-stimulatory signals in the form of 'pathogen-associated molecular patterns' (PAMPs) which are recognised by Toll-like receptors[25,26]. However, most other antigens are T-cell dependent and require additional signalling provided by $CD4^+$ (helper) T-cells[23]. Thus, within 6 hours of BCR engagement, B-cells exhibit cell-cycle entry and begin to proliferate[27], after which they up-regulate the chemokine receptor molecule CCR7 which triggers B-cell migration to the border between follicular and T-cell areas of secondary lymphoid tissues[28]. It is here that B-cells present antigen to $CD4^+$ T-cells. Thus, antigen-bound BCR complexes are internalised by B-cells, after which antigen is processed to generate peptides that are presented at the cell surface by MHC-class II molecules. T-cell receptor (TCR)-binding to the MHC-peptide complex triggers activation of the $CD4^+$ T-cells, which thereafter provide co-stimulatory signals via cell-cell contact and cytokine secretion.

The most important of the co-stimulatory signals provided by $CD4^+$ T-cells is the binding of CD40 ligand (CD40L, also known as CD154), which is upregulated on activated T-cells, to CD40 on B-cells[29]. Other important signals include binding of CD28, also upregulated on activated T-cells, to CD86 on activated B-cells[30], and secretion of the cytokine IL4. These interactions trigger a multitude of signalling events, operating via NFkB and other signalling pathways, which supporting B-cell survival, proliferation and further differentiation. Notably, the ability of CD40L to act as a potent stimulator of B-cells is evident from its use to generate

B-cell lymphoblasts *in vitro*. Thus, in one approach, resting B-cells cultured on a layer of mouse fibroblasts stably transfected with the coding region for human CD40L, in the presence of the cytokine IL4, rapidly differentiate into activated lymphoblasts[31,32]. These maintain proliferation for several weeks with repeated stimulation.

Within 1 to 2 days of initial antigen encounter, B-cells begin to proliferate[23]. Thereafter, stimulated B-cells undergo 1 of 3 principal fates[33]. As such, some cells differentiate into extra-follicular plasma cells, which produce low-affinity IgM antibodies. Other cells re-enter the circulation as early memory B-cells. Meanwhile, some B-cells establish areas of marked proliferation within lymphoid follicles known as 'germinal centres' (GC)[34-36] (Figure 2). In these GC structures, B-cells exhibit massive clonal expansion and undergo further diversification of their Ig genes in order to generate plasma cells that produce high-affinity antibody, as well as memory B-cells. Importantly, differentiation into plasma cells versus GC B-cells is influenced by key transcriptional regulators. Thus, plasma cell differentiation is dependent upon up-regulation of Blimp1 and MUM1 (IRF4), whilst GC differentiation depends on expression of the transcriptional repressor BCL6, an important marker of GC B-cells[37-40].

Germinal Centre Reactions

During GC formation, activated B-cells first differentiate into rapidly proliferating centroblasts that express BCL6[34,35]. Characteristically these cells also upregulate activation-induced cytosine deaminase (AID), an enzyme that plays a central role in 2 essential processes in GC B-cell maturation: somatic hypermutation (SHM) and class switch

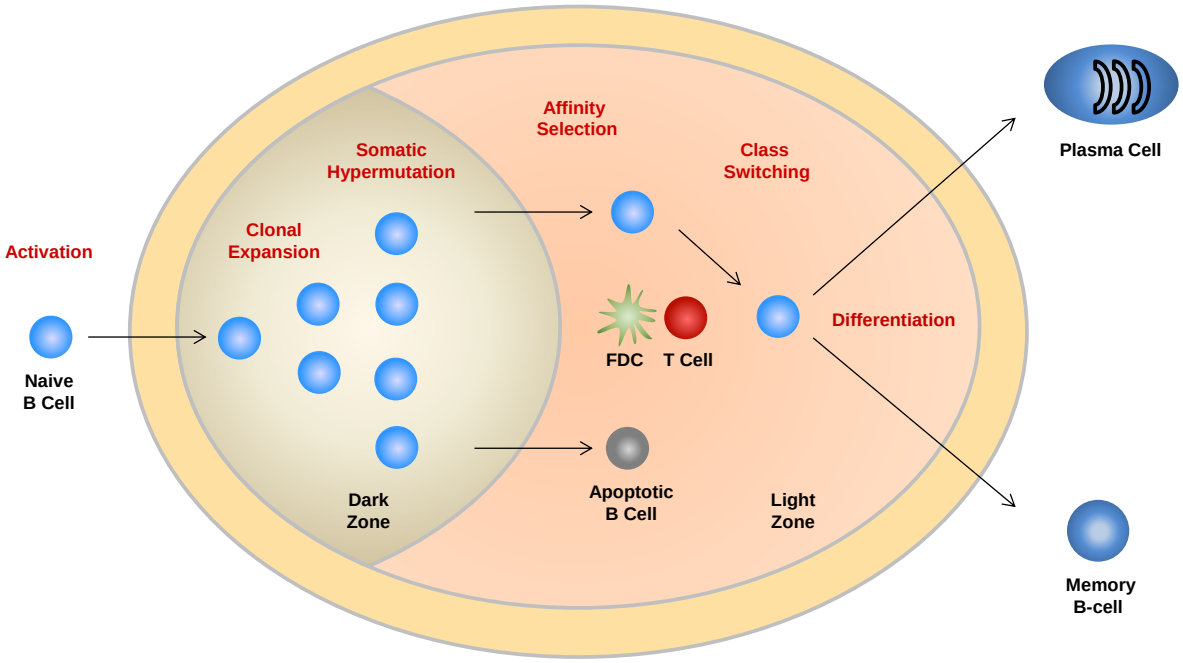

Figure 2. Germinal Centres

Events occurring during germinal centre (GC) transit. Following antigen-encounter, naive B-cells become activated and seed a GC. The cells first differentiate into centroblasts and exhibit massive clonal expansion in the dark zone of the GC. Here they undergo somatic hypermutation (SHM), mediated by the enzyme AID which is upregulated in GC cells. SHM introduces mutations into the variable region of the Ig sequence which may alter the affinity of antigen-binding. During affinity selection, B-cells that have acquired mutations which improve antigen-binding receive signals promoting cell survival and proliferation, whereas other cells either apoptose or become anergic. Selected cells then transit to the light zone of the GC where they differentiate into centrocytes and undergo Ig class-switch recombination (CSR). During CSR, the IgH variable region recombines with an alternative constant region, belonging to either the IgG, IgA or IgE antibody classes, in an AID-dependent mechanism. These GC processes are regulated by follicular dendritic-cells (FDCs) and CD4+ T-cells which engage in cell-cell contacts and secrete cytokines. Amongst the key signalling events is interaction of CD40L expressed on activated $CD4^+$ T-cells with CD40 on B-cells. Plasma cells with the capacity to produce high affinity Ig of alternative classes subsequently exit the GC. Memory B-cells also leave the GC and these can rapidly respond to future antigen-encounter. Figure adapted from Kuppers[41].

recombination (CSR)[42-45]. SHM facilitates the generation of high-affinity antibodies by introducing additional mutations into Ig genes[46]. Thus AID targets cytidine nucleotide residues localised in the V regions of Ig loci resulting in their deamination, after which error prone repair mechanisms mediated by enzymes including Pol η and θ can result in the introduction of random mutations. This can result in amino acid changes in IgH and IgL variable domains which alter the binding affinity of the BCR for its antigen. Subsequently, as centroblasts differentiate into centrocytes they are subjected to selection by follicular dendritic cells (FDCs), in a process known as affinity maturation[47]. B-cells which have acquired SHM mutations that confer improved affinity for target antigens are selected in preference to cells that bind antigen less avidly.

CSR is the mechanism through which B-cells, which initially express IgD and IgM antibody, alter their expression to alternative Ig classes[15,46]. This is beneficial because each of the Ig classes possess unique functional characteristics, determining properties such as antibody tissue distribution, the capacity to interact with other immune cells and the ability to polymerise. At the molecular level CSR is mediated by an AID-dependent mechanism that recombines the rearranged VDJ Ig region with an alternative CH region corresponding to the different Ig classes. In particular AID introduces double-stranded breaks in switch (S) regions, which consist of tandem repeats of short G-rich sequences (20-80 bp), located downstream of each CH region. Intervening DNA sections are removed, after which the DNA ends are reunited by end joining recombination. Notably, this process is regulated by $CD4^+$ T-cells and FDCs via cell-cell contacts and the secretion of cytokines including IL4, IL10, IL13, IL21 and TGFβ, which influence the frequency of specific switching events[48].

Importantly, AID is also responsible for the generation of mutations in non-Ig genes in B-cells. These mutations characteristically occur in the 5' non-translated promoter regions of affected genes, and resemble the SHM events in Ig genes. Thus, GC B-cells were first shown to possess mutations within the BCL6 gene[49]. Thereafter numerous other genes have been shown to be targeted, including known oncogenes and tumour suppressors[50,51]. Importantly, such mutations have also been found in several forms of lymphoma[52-57], implicating AID in tumourigenesis. Furthermore, AID has been linked to the generation of chromosomal translocations[58-60]. Notably, AID-induced mutations are only thought to affect actively transcribed genes because the open chromatin configuration associated with gene transcription is necessary for AID to access DNA.

Memory B-Cells

Memory B-cells are antigen-experienced cells that persist for many years after a primary immune response[18,23]. On secondary antigen encounter they respond by rapidly differentiating into plasma cells that produce high-affinity antibodies. In keeping with this, they can be distinguished from antigen-inexperienced naive B-cells because they are larger in size, possess mutated Ig genes and secrete high quantities of antibody following *in vitro* stimulation. Notably, expression of the TNF-receptor superfamily molecule CD27 has also been recognised as a reliable marker of B-cell memory in recent years. Thus, stimulation of B-cells bearing surface CD27 results in up to 100-fold more antibody secretion compared to that of $CD27^-$ cells[61,62]. Furthermore, $CD27^+$ B-cells cells possess somatically mutated Ig V region genes, whilst those lacking CD27 are non-mutated[63,64]. Moreover, immunised individuals carry antigen-specific B-cells exclusively within the $CD27^+$ B-cell subset[65]. An important caveat, however, is the consistent finding of a small population (around 1%) of

circulating B-cells which lack CD27 surface expression but which are larger than naive B-cells, possess mutated V regions and have undergone class-switching, and which are thus known as $CD27^-$ memory B-cells[66-69].

In light of the above, 2 principal circulating memory B-cell subsets can be identified using the surface markers CD27, IgM and IgD[18,63] (Figure 3). Thus, whereas antigen-inexperienced naive B-cells are reliably identified as $CD27^-IgM^+IgD^+$ cells, $CD27^+$ memory B-cells, comprising around 30% of all B-cells, can be further separated into 2 generally equal fractions. Thus, class-switched memory (CSM) B-cells are $CD27^+IgM^-IgD^-$ antigen-experienced cells which have transited through a GC reaction, where they have acquired Ig gene mutations and undergone switching to IgG, IgA or IgE classes. Meanwhile, a second subset of so-called 'non-switched memory' (NSM) B-cells possess mutated Ig genes and exhibit surface $CD27^+$ but they have *not* undergone class switching and thus retain surface IgM and IgD. Notably, a further memory B-cell subset are the so-called 'IgM only' memory B-cells. These exhibit a $CD27^+IgD^-IgM^+$ phenotype, carry mutated Ig genes, and constitute around 1% of circulating B-cells.

Interestingly, there has been considerable debate as to the origins of the NSM B-cell subset[18]. In particular, one hypothesis to explain why these cells possess mutated Igs but are not class-switched suggests that they derive from T-cell dependent pathways in the context of an abortive GC reaction, such that SHM occurs but CSR does not[63]. This view is supported by data showing that $CD27^+IgM^+$ B-cells exhibit 'off-target' mutations in BCL6, taken as evidence of GC transit, and moreover that they appear to be clonally related to CSM B-cells[70]. However, this has been disputed by subsequent data which failed to show any clonal

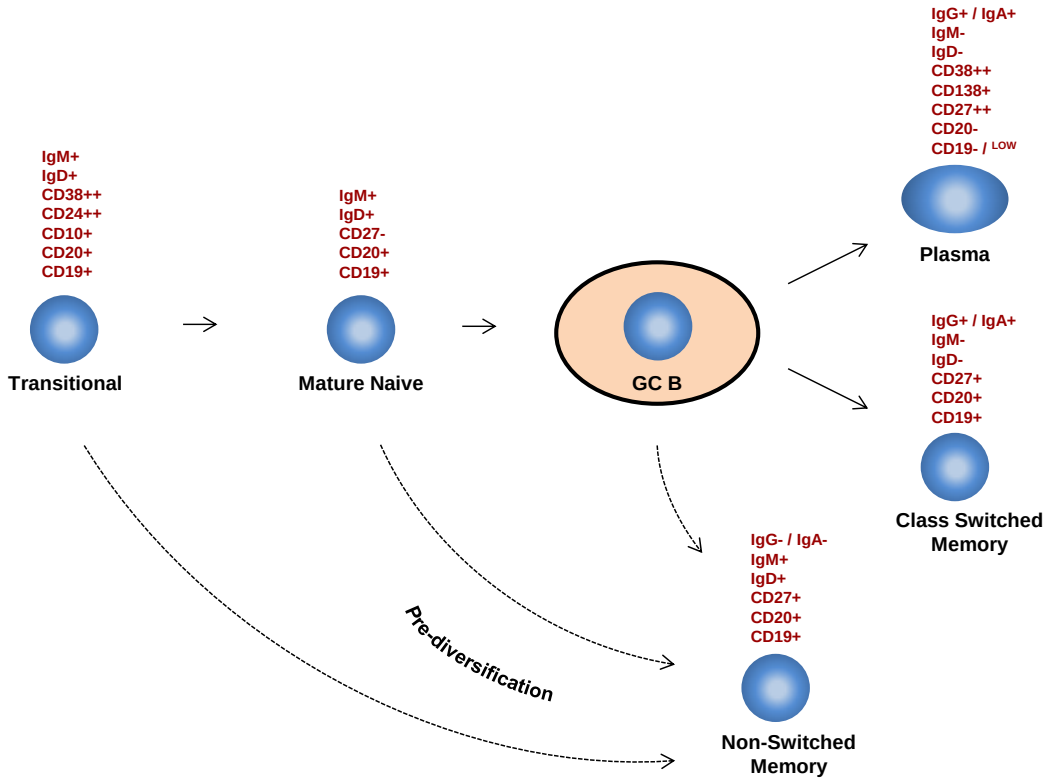

Figure 3. B-Cell Surface Markers

B-cells at different developmental stages can be identified by characteristic surface markers. The earliest B-cell emigrants from the bone marrow are transitional B-cells, which bear surface IgD and IgM, and also express high levels of CD38 and CD24, and also CD10. These markers are down-regulated as these cells differentiate into mature naive B-cells. Following antigen encounter, naive B-cells ultimately differentiate into antibody-secreting plasma cells which are $CD38^{++}$, $CD20^{-}$ and $CD138^{+}$. Memory B-cells (and plasma cells) can be distinguished from naive B-cells because they upregulate the TNF-receptor superfamily molecule CD27. CSM B-cells result from T-cell dependent antigen stimulation and GC transit, and undergo SHM and Ig class switching from IgM /IgD to either IgG, IgA or IgE. A small proportion of memory B-cells lack surface CD27 but have still undergone class switching and are known as 'CD27-negative' memory B-cells. A minority of $CD27^{+}$ B-cells also retain IgM but lose IgD; these 'IgM-only' memory B-cells are also considered to be GC-derived. NSM B-cells express CD27 and undergo SHM but retain surface IgM and IgD; their origin remains controversial (dotted lines); they may arise from T-cell independent antigen-stimulated pathways located in the spleen or via early exit from the GC.

relationships to CSM subsets[71]. Meanwhile a second hypothesis proposes that they may arise through a T-cell independent mechanism that occurs outside of GC[72,73]. This has been supported by evidence that $CD27^+IgM^+$ B-cells are retained in individuals with genetic conditions that abrogate GC development. Thus hyper-IgM syndrome is an inherited condition in which mutations in the genes for CD40 or CD40L interfere with normal B- and T-cell co-operation during immune responses[74,75]. As a consequence, GC do not form in these individuals, their B-cells fail to undergo class switching and they exhibit an excess of IgM antibody. Nevertheless, they retain somatically mutated circulating $CD27^+IgM^+$ B-cells[72,73,76]. Similarly, NSM B-cells are also found in patients with X-linked lymphoproliferative disease (XLP), in whom loss of a functional SAP protein prevents $CD4^+$ T-cell help for the production of antibody responses[68,77,78], and those with common variable immunodeficiency (CVID) resulting from mutations in ICOS[79]; both groups also fail to develop GC. Such evidence has formed the basis for proposing that the $CD27^+IgM^+$ B-cells may in fact be circulating splenic marginal zone cells, which arise following T-cell independent antigenic stimulation and which undergo SHM outside of GC. Supporting this is the finding that $CD27^+IgM^+$ B-cells are markedly reduced in asplenic individuals[80], and that they may be clonally related to splenic B-cells[73]. In addition, it has been proposed that these $CD27^+IgM^+$ B-cells may acquire Ig mutations prior to antigen exposure, through so called 'pre-diversification,' in the spleen[73,81]. Evidence in favour of this is the observation that infants less than 2 years old, in whom T-cell independent responses are thought to be absent, possess mutated $CD27^+IgM^+$ cells which retain a polyclonal repertoire, consistent with a lack of antigen driven stimulation[73,81]. However, a major criticism of this view is the failure to detect AID in splenic B-cells[82].

1.3 Epstein-Barr Virus

Taxonomy and Structure

EBV is a member of the herpesvirus family of double-stranded DNA viruses[10]. This family, characterised by the potential to establish chronic infections, contains over 100 members, several of which are known to infect humans. Notable examples of the latter include Herpes Simplex Virus (HSV), which causes oral and genital infections, Varicella Zoster Virus (VZV), the cause of Chicken Pox and Shingles, and Cytomegalovirus (CMV) which causes multi-system disease, particularly in the immunocompromised. EBV belongs to the gammaherpesvirus subfamily, along with Kaposi Sarcoma Herpes Virus (KSHV). As a member of the lymphocryptovirus (LCV) genus, EBV is closely related to other LCVs that cause B-cell transforming infections in non-human primate species including Old World monkeys such as the rhesus macaque, and New World monkeys including the marmoset[83-86].

EBV consists of a linear double-stranded DNA genome packaged inside a protein capsid, surrounded by tegument proteins and a glycoprotein-containing lipid envelope[87]. The genome is approximately 172 Kb in length, making it very large compared to most other viruses, and has the potential to code for approximately 80 proteins (Figure 4). The prototypic B95.8 strain of EBV, isolated from a patient with IM, was the first herpesvirus to be fully cloned and sequenced in 1984 (Accession no. V01555)[88]. Notably, this strain contains a deletion of approximately 11.8kb which has subsequently been repaired by insertion of corresponding sequence isolated from the Raji-BL strain[89], generating a hybrid reference sequence (Accession no. NC_007605). In addition, several other complete virus sequences, mainly derived from EBV-positive tumours, have recently been published[90-96]. The EBV genome is flanked by a number of terminal repeats (TR) which mediate genome circularisation. The

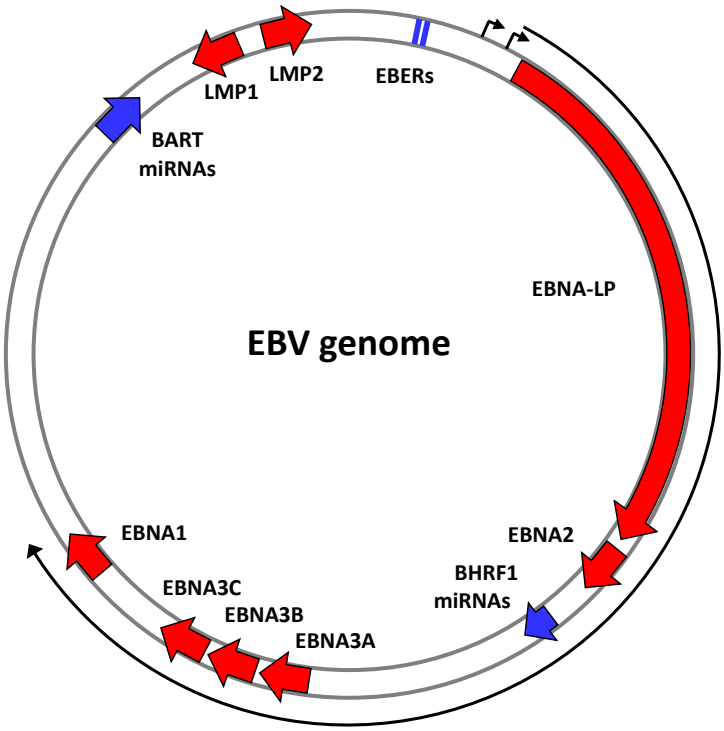

Figure 4. The EBV Genome

EBV possesses a double-stranded DNA genome that is approximately 172 Kb in length. When packaged inside its virion the genome is linear. Flanking terminal repeats mediate circularisation to the episomal form found in latent infection. The genome has potential to code for approximately 80 proteins in total. Of these, only a limited number are expressed during latent infection. Latent proteins (red arrows) comprise the 6 EBV nuclear antigens (EBNA1, EBNA2, EBNA3A, EBNA3B, EBNA3C and EBNA-leader protein (LP)), 3 latent membrane proteins (LMP1, LMP2A and LMP2B) and BHRF1. A series of non-coding RNAs are also expressed (blue arrows) including the 2 EBV-encoded RNAs (EBERs), and a complex of highly spliced polyadenylated transcripts known as the BamHI A rightward transcripts (BARTs) from which multiple micro RNAs (miRNAs) are derived. A second cluster of miRNAs originate from the BHRF1 region. Figure courtesy of Dr A. Bell, University of Birmingham.

sequence also contains several internal repeat regions, and separate latent and lytic origins of replication. By convention, the EBV genome sequence has been annotated with reference to fragments generated by BamHI restriction endonuclease digestion (labelled BamHI A-Z, a-e). EBV isolates are generally classified into 2 major subtypes, principally based on polymorphisms within the EBV nuclear antigens EBNA2, EBNA3A, EBNA3B and EBNA3C[97]. Type I viruses appear to predominate within most human populations[10], and show an enhanced ability to transform B-cells in comparison to Type II viruses, largely due to differences in the EBNA2 gene[98,99]. In addition, minor polymorphisms in several other regions including EBNA1[100], LMP1[101] and BHRF1[102,103] have been used to define intra-typic strains. Interestingly, studies have used these EBV genome polymorphisms to propose that immunocompromised[104] and immunocompetent individuals[105] may carry multiple EBV strains.

Latent Infection

EBV is principally trophic for B-cells, in which it establishes chronic latent infection[10,87]. However it can also infect epithelial cells in healthy carriers, and T-cells, NK-cells and smooth muscle cells in the context of disease. Much of our knowledge of EBV latency has been obtained through in vitro experimentation, making use of the virus's ability to transform B-cells into lymphoblastoid cells lines (LCLs)[87]. In these, the virus genome is carried in each cell as multiple extracellular double-stranded DNA episomes, and viral gene expression is a restricted to a small number of products, which exert pleiotropic effects on the cellular phenotype leading to transformation (Figure 4). Protein products comprise 6 EBNAs, (EBNA1, EBNA2, EBNA3A, EBNA3B, EBNA3C and EBNA-leader protein (LP)), 3 latent membrane proteins (LMP1, LMP2A and LMP2B) as well as the viral BCL2 homologue

BHRF1. In addition, EBV also expresses a series of non-coding RNAs including 2 non-polyadenylated, EBV-encoded RNAs (EBERs) and a complex of highly spliced polyadenylated transcripts of uncertain coding potential known as the BamHI A rightward transcripts (BARTs) which are precursors of more than 40 micro RNAs (miRNAs). Together this combination of gene expression is known as the 'Latency III' pattern, and in addition to being observed in LCLs it is found in infected B-cells from patients with IM and most PTLD tumours[106]. In Latency III, all of the EBNA proteins are expressed from individual mRNA species that are differentially spliced from a long primary transcript originating from either of 2 alternative upstream viral promoters, Cp or Wp, located in the BamHI C or W regions[107-110] (Figure 5). Activation of both promoters is dependent on the B-cell specific host transcription factor PAX-5 (also known as BSAP)[111,112]. Notably, switching from Wp to Cp occurs early after B-cell infection due to the trans-activating effects of both EBNA1 and EBNA2 on Cp. Meanwhile, LMP1 and LMP2A/B are expressed from separate promoters located in the BamHI N region, where their expression is dependent upon transactivation by EBNA2[113-115].

Alternative Forms of Latency

In addition to Latency III, EBV exhibits other patterns of gene expression. These were first described in the context of EBV-related tumours but may also be important for EBV persistence in the normally infected host. Thus, in many examples of BL, a 'Latency I' pattern is observed, characterised by expression of just EBNA1, the EBERs and the BARTs. In this, EBNA1 expression is driven from a primary transcript expressed from the Qp promoter located in the BamHI Q region[116,117]. However, in some forms of BL an alternative 'Wp Latency' is observed, in which transcription from the Wp promoter leads to expression of all EBNAs except EBNA2, in addition to BHRF1[118-121]. This pattern, present in 15% or more of

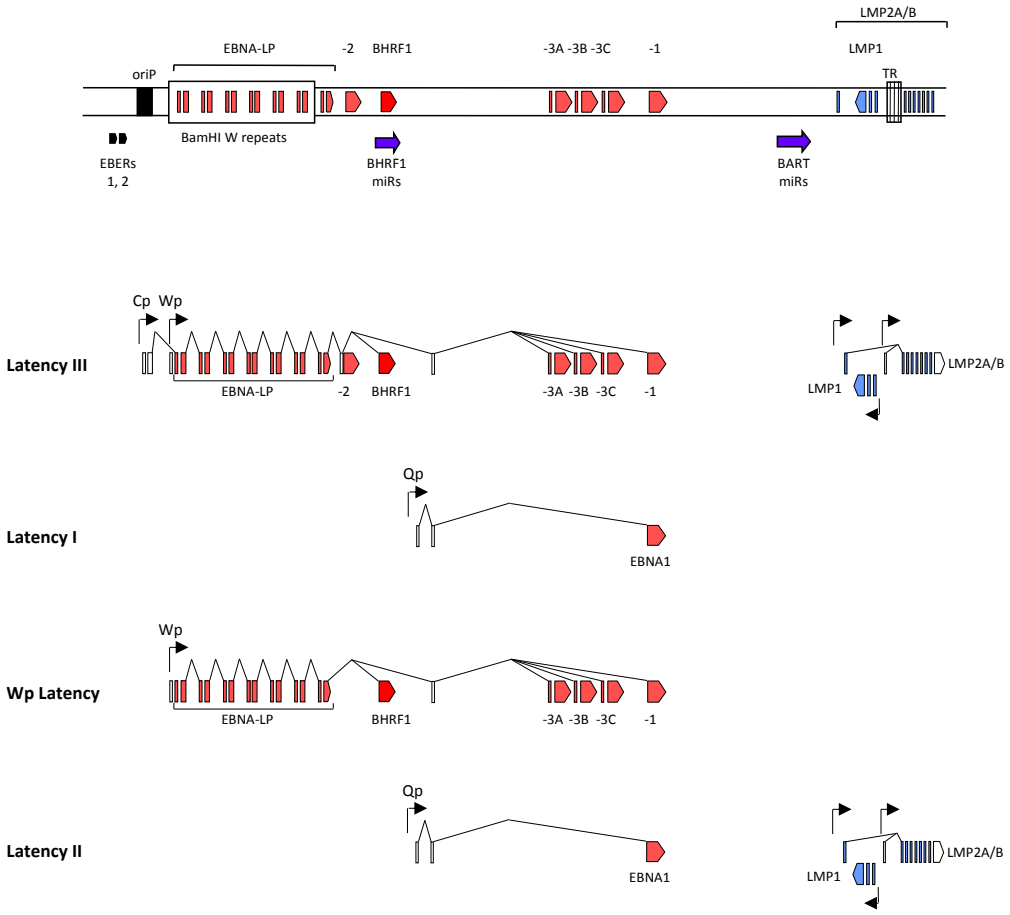

Figure 5. Patterns of EBV Latent Gene Expression

Transcripts expressed in different forms of EBV latency are shown below a schematic illustration of the linear EBV genome. In the Latency III pattern of expression, seen in LCLs and in most PTLDs, all EBNA proteins and BHRF1 are expressed from the BamHI W and C promoters (Wp and Cp), and the 3 LMP proteins are expressed from promoters in the BamHI N region. By contrast, in the Latency I pattern found in most endemic BLs, expression is limited to a single nuclear antigen, EBNA1, from a promoter in BamHI Q (Qp). Wp Latency is an alternative pattern of expression, found in around 15% of endemic BL tumours, in which transcription from the Wp promoter results in expression of all EBNAs, except EBNA2, and BHRF1. In the Latency II pattern, found in NPC and EBV-positive HL, expression of EBNA1 from the Qp promoter is accompanied by that of the LMPs. The non-coding EBER and BART RNAs, from which the BART miRNAs are derived, are found in all forms of Latency. The BHRF1 miRNAs are thought to be generated from Wp/Cp-initiated transcripts and are predominantly found in Latency III infection. Figure adapted from Rowe et al.[122]

endemic BL tumours, occurs when an EBV strain exhibits a deletion including the EBNA2 region, although it is currently unclear why activation of the Wp promoter is favoured over the Qp promoter. Interestingly, Latency I BL cell lines may also alter their pattern of gene expression when passaged *in vitro*, resulting in Latency III expression[123,124].

The Latency II pattern of virus gene expression was first identified in NPC biopsies[125-127] and was subsequently identified in gastric carcinoma[128,129], HL[130,131], and T-cell and NK-cell lymphomas[132], amongst others. In this, EBNA1 expressed from the Qp promoter is found along with the EBERs and BARTs as in Latency I, but these are also accompanied by expression of LMP1, LMP2A and LMP2B regulated by an EBNA2-independent mechanism.

Notably, the factors that determine why different cell types, and different malignancies, exhibit alternative expression patterns remains imperfectly understood. However, it is clear the B-cells can support all forms of latency, whereas non-B-cells exhibit more restricted expression patterns. This may be explained, at least in part, by the fact that non-B-cells lack the transcription factor PAX-5, which is required for activation of the Cp and Wp promoters essential for Latency III expression[111,112].

Latent Gene Products

The function of individual EBV latent gene products has been elucidated largely through experimentation using recombinant forms of EBV, in which viral genes have been manipulated. This work has shown that disrupted expression of any one of EBNA1, EBNA2 EBNA3A, EBNA3C or LMP1 results in either complete or significant abrogation of B-cell transformation[87].

EBNA1

EBNA1 is a DNA binding protein which is essential for maintenance and replication of the viral episome, acting by binding to and recruiting other factors to the viral latent origin of replication, OriP[133,134]. For this reason it is the only EBV protein found in all EBV-infected cells. In addition, the protein acts as a transactivator of viral gene expression, enhancing transcription from both the Cp promoter[135,136] and of LMP1[137]. It also negatively regulates its own transcription from the alternative EBNA1 promoter Qp[138,139]. Notably, the EBNA1 protein contains a glycine–glycine–alanine (gly–gly–ala) repeat sequence, which prevents its proteasomal degradation and also interferes with MHC class I-restricted presentation, resulting in evasion of EBNA1-specific $CD8^+$ T-cell responses[140,141].

EBNA2 and EBNA-LP

EBNA2 is an essential effector of viral transformation, as demonstrated by the inability of the P3HR1 strain, which carries a deletion of EBNA2, to transform B-cells[99,142]. Acting as a master transcription factor that, along with EBNA-LP, is expressed shortly after infection, EBNA2 activates target cellular genes which drive the host cell into cell-cycle, as well as triggering expression of the other EBNA proteins from the EBNA2-dependent Cp promoter[143], along with LMP1 and LMP2A[114]. The activity of EBNA2 is mediated, at least in part, by interaction with the DNA binding protein J-recombination-binding protein (RBP-J), which targets it to promoters containing the RBP-Jκ sequence[144,145]. Among the cellular targets which are upregulated by EBNA2 is the proto-oncogene c-myc[146]. EBNA-LP is encoded by the leading part of the EBV primary latent transcript. Its coding region includes an area of BamHI W repeats and therefore multiple isoforms of differing size can arise from a single infected cell[147]. The number of BamHI repeats varies between isolates[148,149]. Whilst it is

not essential, EBNA-LP increases the efficiency of B-cell transformation[150,151]. Furthermore, the presence of fewer than 5 BamHI W repeats impairs transformation[149]. In particular, EBNA-LP is thought to interact with EBNA2 to regulate transcriptional targets including LMP1[151-153].

EBNA3 Family

The EBNA3A, -3B and -3C proteins are related nuclear proteins which act as transcriptional regulators of multiple viral and cellular genes. EBNA3A and -3C are essential for transformation. They function as repressors of proteins associated with apoptosis, such as BIM (BCL2L11)[154], as well as senescence, including p16INK4A[155,156] and p14ARF (CDKN2A)[156]. They also appear to have important roles in the disruption of cell cycle checkpoints, including the G2 to M transition[157]. EBNA3C has also been reported to modulate DNA-damage signalling associated with proliferation-induced oncogenic stress[158]. In contrast, EBNA3B is dispensable for effective transformation, although its conservation in various LCV viruses implies an important role *in vivo*[159]. Recently, it has been reported to function as a tumour suppressor in mice infected with EBV carrying EBNA3B deletions[160].

LMP1

LMP1 is the major transforming oncogene of EBV[161]. It is essential for B-cell transformation *in vitro*[162,163], and for the tumourigenesis of EBV-infected B-cells in mouse models[164]. LMP1 functions as a viral oncogene, as demonstrated by its ability to induce oncogenic transformation in rodent fibroblast cell lines[165-167]. The structure of LMP1 consists of an amino-terminal cytoplasmic tail which tethers it to the plasma membrane, a transmembrane domain made up of 6 loops, and a long carboxy-terminal cytoplasmic tail which contains

signalling domains which activate multiple cell signalling pathways. Amongst these are C-terminal activation regions 1 and 2 (CTAR1 and CTAR2) which trigger signalling events through the $NF\kappa_B$ pathway by interacting with TRAF and TRADD adaptor proteins[168-174]. Other signalling pathways through which LMP1 operates include the MAP kinase[175,176], JAK/STAT[177] and phosphatidylinositol 3-kinase (PI3-K) pathways[178]. LMP1 functions as a constitutively active receptor of the tumour necrosis factor receptor superfamily[179,180]. In doing so, it acts as a functional mimic of the CD40 signalling pathway. Thus, CD40 can substitute for LMP1 in mediating proliferation and survival in LCLs *in vitro*[163,181]. Furthermore, it can at least partially substitute for CD40 *in vivo*[182]. The signalling events that originate from LMP1 exert pleiotropic effects on the host cell, to establish the transformed phenotype. Thus, LMP1 causes up-regulation of anti-apoptotic proteins such as BCL2[183,184], drives cells into cycle[163], and triggers the stimulation of multiple cytokines including IL6, IL8 and IL10[185,186], amongst many other effects.

LMP2

The LMP2 gene encodes 2 different protein isoforms, LMP2A and LMP2B, neither of which are essential for B-cell transformation[187]. Nevertheless, LMP2A has been shown to influence multiple signalling pathways, and in particular is thought to mimic signal transduction events normally triggered via the BCR. Thus, work using LCLs and mouse models has shown that the LMP2A terminal cytoplasmic domain constitutively phosphorylates downstream targets of the BCR including LYN, SYK, BLNK, BTK, RAS, PI3K, NFκB and MAP kinases[188]. Notably, expression of LMP2A can also act to block signalling that would normally result from BCR cross-linking[189,190], preventing lytic cycle entry in LCLs[191]; this may be an important role for LMP2A during chronic infection *in vivo*. Furthermore, LMP2A can support

the survival and proliferation of B-cells lacking surface Ig in mouse models[192-194], and this may explain some of its contribution to malignancy. Meanwhile, LMP2B is thought to play a role in antagonising the activity of LMP2A[195,196].

BHRF1

BHRF1 is a homologue of the anti-apoptotic cellular protein BCL2, and is dispensable for B-cell transformation[197]. Although originally thought to be expressed exclusively in virus lytic cycle, it is now known to be persistently expressed in Latency III LCLs, in which it is may confer resistance to apoptotic signals[121]. Notably, in Wp-restricted BL, BHRF1 is expressed as a consequence of deletions which remove the EBNA2 gene and bring the BHRF1 gene into close proximity to the highly active Wp promoter. Expression of BHRF1 in Latency I BL cell lines, which normally lack BHRF1, has been shown to enhance cell survival in the face of apoptotic triggers[121].

Non-Coding RNA Transcripts

EBV also produces a series of apparently non-coding RNA species during latent infection. These include the EBER1 and EBER2 transcripts, which are ubiquitously and abundantly expressed in all EBV-infected cells[198,199], such that their detection by *in situ* hybridisation forms the basis of a widely adopted method for establishing EBV infection[200]. EBERs are dispensable for B-cell transformation *in vitro*[201]. Although their function remains largely obscure, they have been implicated in various roles which may be relevant to EBV pathogenesis[202]. These include conferring resistance to apoptosis triggered by innate IFN-mediated immune responses[203-205], as well as enhancing proliferation of EBV-infected cells[206-208] and the induction of tumourigenesis[208-210].

The BARTs are a group of highly differentially spliced RNAs that are also ubiquitously expressed. These contain a series of open reading frames, the protein-coding potential of which remains controversial[211]. However, they also code for 1 of 2 clusters of micro-RNAs produced by the EBV genome; the other is located adjacent to the BHRF1 open reading frame. Although the function of these viral micro-RNAs is currently poorly characterised, they may play important roles in the negative regulation of gene expression [212,213]. Indeed, targets of the EBV micro-RNAs include viral LMP1, LMP2A and DNA polymerase, as well as cellular genes PUMA and CXCL11[213].

Lytic Cycle

Like other herpesviruses, EBV periodically exhibits lytic cycle activity, in order to generate new virus particles necessary for transmission of the virus between individuals[10]. Notably, around 5% of cells within an LCL exhibit spontaneous lytic cycle entry at any one time. Lytic cycle is orchestrated by a large number of EBV genes, which are expressed in a sequential cascade[87]. The principal switch from latency to lytic cycle entry is mediated by activation of the immediate-early (IE) lytic genes BZLF1[214-219] and BRLF1[216,220], which encode the proteins ZEBRA (also known as EB1 or Zta) and Rta respectively. These transactivate a number of downstream early (E) lytic genes, many of which encode enzymes and other proteins necessary for viral DNA replication. Notably, replication of the viral DNA is initiated from a distinct origin of replication from that used for latent genome maintenance, ori-lyt[221]. Subsequent amplification of the EBV genome is followed by expression of the late (L) lytic cycle genes, most of which encode structural proteins necessary for the manufacture of the capsids into which the viral genomes are subsequently packaged. These include the gene BLLF1 which encodes the envelope glycoproteins gp350 and gp220[222,223], and BALF4 which

encodes the glycoprotein gp110[224]. Once assembled, viral capsids bud through the nuclear membrane before fusing with the plasma membrane, after which they are released by exocytosis, in such a way that the host cell is eventually lysed.

1.4 *In Vitro* B-Cell Transformation by EBV

Key Events

In vitro B-cell transformation is initiated when resting B-cells are incubated with preparations of EBV, resulting in infection via interaction of the viral envelope glycoproteins gp350 and gp42 with their respective host cell targets, complement receptor CR2 (CD21)[225] and the HLA class II molecules[226,227]. Notably, quantitative studies have demonstrated that delivery of just a single EBV genome to the host cell nucleus is required to initiate viral transcription[228]. Within 2 days of infection, almost all EBV Latency III proteins are detectable and induction of cellular DNA synthesis is accompanied by acquisition of blastoid morphology and up-regulation of numerous surface markers associated with B-cell activation, including CD23, CD30, CD39, CD70, as well as the cell adhesion molecules leukocyte function associated molecule-1 (LFA-1; CD11a/18), LFA-3 (CD58) and intercellular adhesion molecule-1 (ICAM-1; CD54)[87,229-233]. Within 5 days of initial infection, microscopic colonies of proliferating lymphoblasts are apparent and the LCL is considered to be fully transformed within a few weeks.

Selective Outgrowth of LCLs

Several aspects pertaining to B-cell transformation remain imperfectly understood. In particular, recent interest has focused on the possibility that selective outgrowth of EBV-infected B-cells occurs during transformation. Thus, it is increasingly apparent that only a

proportion (1 – 10% in some estimations) of infected B-cells ever grow out to contribute to an established LCL[234,235]. Furthermore, additional selective processes may operate in the weeks following infection, and several groups (including our own) have demonstrated oligoclonal and thereafter monoclonal outgrowth of LCLs over a period of 3 to 4 months[236-239]. Intriguingly, this does not appear to occur in mitogen-stimulated B-cell blasts, which remain polyclonal when cultured for a similar period[236].

Interestingly, Nikitin et al. have recently proposed a model in which interactions between EBV proteins and DNA damage response (DDR) signalling pathways are considered important in determining selective outgrowth within the first few days of B-cell infection[158]. As such, several pathways exist for sensing, and responding to, DNA damage caused by exogenous and endogenous genotoxic insults, in order to maintain genomic integrity. Thus, the DDR kinase ATM, and its downstream target Chk2, are activated in response to the appearance of aberrant double-stranded DNA breaks, the presence of which is signalled by phosphorylation of histone H2AX at the site of these breaks[240]. Similarly the DDR kinase ATR, and its target Chk1, are activated in response to single-stranded DNA breaks[241]. These kinases relay signals to other factors, with extensive cross-talk, leading to imposition of cell cycle arrest, senescence or apoptosis, mediated by the master tumour suppressor protein p53, as well as inducing DNA repair machinery. Importantly, rapid or uncontrolled replication, including that driven by oncogenes such as c-myc, may result in oncogenic replication stress which also activates these pathways[242,243]. In view of this, Nikitin et al. have proposed that a period of very rapid proliferation (hyperproliferation) in the first few days after EBV-infection, thought to be a consequence of unhindered EBNA2-induced oncogene activity, causes replication stress resulting in activation of the ATM/Chk2 pathway and impaired LCL

outgrowth[158]. In this model, EBNA3C is subsequently thought to play an important role by acting as a transcriptional repressor that subsequently opposes EBNA2 activity, thus attenuating DDR activation and facilitating the outgrowth of LCLs with stable rates of proliferation.

Meanwhile, the factors determining clonal outgrowth in more established LCLs are largely obscure, and it remains to be seen whether machinery such as DDR signalling pathways are important for this phenomenon. However, it is notable from experiments in which LCLs have been generated from naive B-cells (carrying unmutated Ig VH regions), that many of the clones which come to dominate these cultures exhibit mutated Ig HV regions[236]. Importantly, these mutations are consistent with AID-induced SHM events, and furthermore they appear to be acquired during *in vitro* culture; interestingly, whilst LCLs do not undergo spontaneous Ig class-switching, this can be still be triggered by treatment with CD40L, IL4 and IL21, stimuli known to induce class switching in uninfected naive B-cells[236]. In keeping with these findings, AID, which is not expressed in resting B-cells, is upregulated in LCLs[236,244-246]. Such observations are interesting because, as discussed later, they inform debates about the role GC play in EBV colonisation *in vivo*. However, they also raise the possibility that AID-induced mutations might be an important influence on clonal selection. Regarding this, it is notable that Epeldegui et al. have reported that LCLs accumulate 'off-target' AID-induced mutations in the genes BCL6 and p53 in the first few months after infection[244]. It is possible that AID-induced mutations such as these, as well as mutations generated by other mechanisms, might confer proliferative or survival advantages that influence clonal LCL outgrowth.

EBV as Mutagen

Relevant to the above discussion is a wider discourse as to how EBV might interact with DDR signalling pathways, and whether it can directly induce genetic changes in host cells. As such, a growing body of evidence shows that other oncogenic viruses can both trigger and manipulate DDR pathways, resulting in genomic instability[247,248]. For example, the DNA tumour viruses Simian Virus 40 (SV40), Adenovirus, and Human Papilloma Virus (HPV), all inactivate the p53 tumour suppressor; with SV40 large T antigen[249,250], Adenoviral EIB p55[251] and HPV E6[249,252] proteins respectively. As a consequence of unhindered cell cycle progression, infected cells exhibit considerable genetic instability.

In the case of EBV, much of the evidence that it interacts with DDR pathways relates to its lytic cycle activity. Thus, although linear viral genomes produced by lytic cycle replication can trigger ATM, BZLF1 mediates repression of p53 checkpoint signalling in order to stall cells in S phase, to facilitate further viral replication[253]. Additionally, BZLF1 has been shown to effect the rapid destruction of p53 by promoting its ubiquitinylation and proteasomal degradation[254]. Meanwhile, in human epithelial cells, the lytic cycle protein BGLF5 has been implicated in the generation of genomic instability by directly damaging DNA and inhibiting expression of DNA repair proteins[255].

Regarding latent gene expression, early studies of latently infected B-cells showed that LCLs retain functional p53 activity and respond appropriately to DNA damaging insults by undergoing p53-mediated apoptosis[256,257]. This led to the conclusion that, unlike other DNA tumour viruses, latent EBV infection is primarily non-mutagenic[257]. Nevertheless, more recent evidence has increasingly implicated EBV latent gene expression in causing genetic

aberrations. Thus, EBV latent proteins have been shown to cause genomic instability when expressed in an EBV-negative BL background[258]; EBNA1 reportedly induces reactive oxygen species leading to double-stranded DNA breaks, LMP1 transcriptionally downregulates ATM, and EBNA3C causes mitotic spindle checkpoint disruption[259,260]. Furthermore, Lacoste et al. showed that LCLs, but not mitogen-stimulated B-cell blasts, frequently exhibit cytogenetic abnormalities including deletions, insertions and translocations in the first few weeks after infection[237]; although it is notable that the chromosomal defects were almost entirely non-clonal, suggesting that they occurred as isolated events that were not propagated. Interestingly, many of the cytogenetic abnormalities associated with EBV result from telomeric defects[237,258]. Consistent with this, EBV has been implicated in causing telomeric dysfunction by displacing the telomere capping protein TRF2, by a mechanism that may involve EBNA1[237,258,261,262]. Ultimately, although such studies are intriguing it nevertheless remains challenging to reconcile them with an apparent evolutionary strategy to maintain long term asymptomatic persistent infection. The full extent to which EBV infection directly contributes to genomic instability remains to be fully characterised.

1.5 *In Vivo* Colonisation by EBV

Primary Infection

Orally transmitted in saliva, EBV initially colonises cells within the oropharynx[10] (Figure 6). EBV is commonly acquired asymptomatically from parents or siblings during infancy. This is the principal mode of transmission in the developing world, where almost all individuals acquire the virus in the first decade of life, most by the age of 3 years[263,264]. In contrast, around 50% of those in the developed world remain EBV-negative by the end of the first decade of life, probably as a consequence of alternative hygiene practices[265]. A proportion of

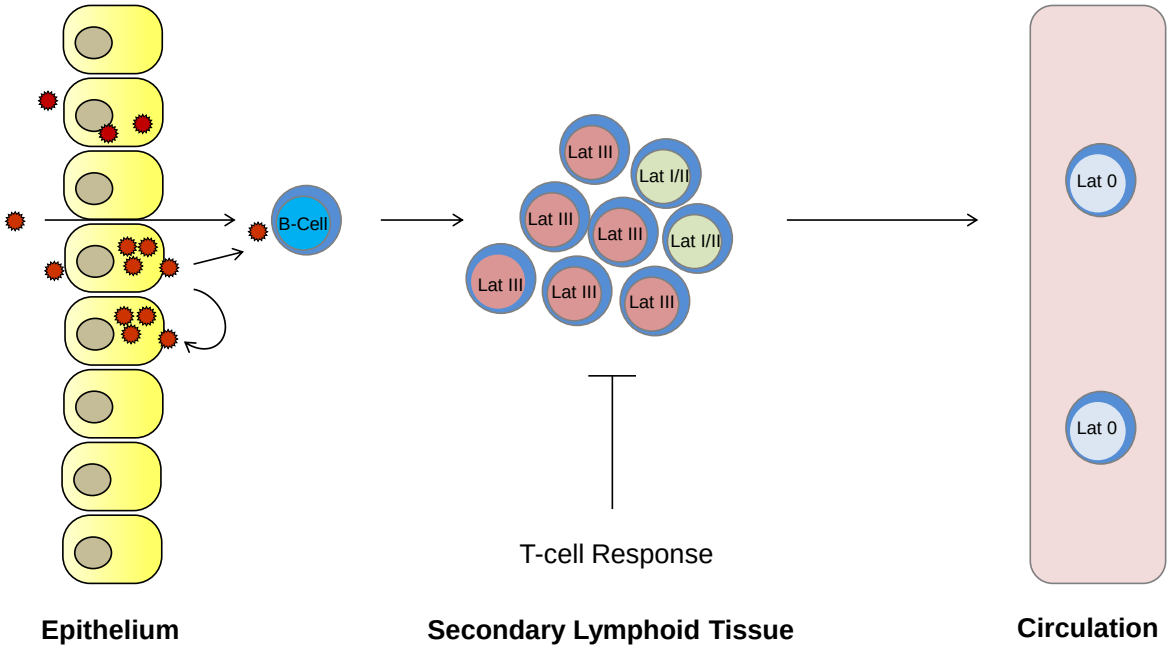

Figure 6. Primary EBV Infection

Primary EBV infection usually occurs asymptomatically during infancy but it may cause IM if delayed until after adolescence. Orally transmitted, EBV initially establishes infection in the oropharynx. Although some uncertainty remains regarding the earliest events, the virus probably first targets submucosal B-cells, with secondary infection of oropharyngeal epithelial cells in which productive lytic cycle occurs. Alternatively, EBV may target epithelial cells directly. Thereafter, latently infected B-cells, at least some of which express the Latency III growth transforming pattern of viral gene expression, accumulate in the oropharynx and circulation. An immune response, primarily involving $CD8^+$ and $CD4^+$ T-cells directed against lytic and latent EBV antigens, subsequently controls the acute infection. EBV avoids elimination by establishing low level chronic latency within circulating resting memory B-cells, in which viral gene expression is highly restricted. Figure adapted from Young and Rickinson[266].

those who become infected after adolescence develop IM. Thus, cohort studies have reported that 25 - 77% of university students who acquire EBV develop IM, and that the predominant mode of transmission in this group is kissing[267,268]. Interestingly, around 5% of individuals in the developed world never acquire EBV[10].

In IM, an incubation period of between 30 and 50 days follows initial virus expose[269]. By the time symptoms develop, high titres of infectious virus are detectable in oral secretions as a result of lytic replication within the oropharynx[270]. Simultaneously, latently infected B-cells accumulate in the blood and tonsils, some of which are transformed lymphoblasts positive for EBNA2 and LMP1, consistent with a Latency III pattern of viral gene expression[271-273]. This is accompanied by lymphocytosis, principally involving expansion of activated $CD8^+$ T-cells[274,275]. The latter is thought to cause much of the symptomology of IM, and therefore $CD8^+$ T-cell frequency, rather than circulating EBV DNA, has been correlated with the appearance of symptoms[276]. Notably, high levels of EBV are detectable in oral secretions for weeks after resolution of symptoms and the clearance of elevated circulating EBV DNA[277].

Site of Initial Infection

The earliest events in primary EBV infection remain relatively obscure, largely because the symptoms of IM do not present until several weeks after initial virus exposure. Given this, one unresolved issue regards the target cell of initial EBV infection. Thus, following early work in which EBV DNA and lytic viral transcripts were detected in epithelial cells in cytological preparations of IM tonsils, it was proposed that oropharyngeal epithelium is the site of initial infection[278]. However, more weight is now given to the alternative view that B-cells infiltrating the oropharyngeal mucosa are the initial target. Supporting this, IM tonsil

histology has failed to show EBV-infected epithelium, although small numbers of lytically infected B-cells have been detected[271,273]. Furthermore, individuals with the inherited immunodeficiency X-linked agammaglobulinaemia (XLA), in whom mutation of Bruton's tyrosine kinase (BTK) causes deficiency of all mature B-cells[279], show no evidence of EBV infection in blood or throat washings; moreover, they lack detectable EBV-specific T-cell responses, which even transient infection of tonsillar epithelium could be expected to generate[280].

In vitro experiments exploring EBV infection of epithelial cells have also informed this discussion. Thus, in comparison to B-cells, which are readily infected by EBV, epithelial cell infection is normally highly inefficient. This is consistent with a lack of CD21, the principal receptor for EBV, from epithelial cells. However, it is notable that rates of epithelial cell infection can be significantly increased by using strains of EBV in which gp350, the viral ligand for CD21, has been inhibited with an antibody[281] or has been knocked out[282], suggesting that gp350 may actually inhibit EBV binding to epithelial cells. Furthermore, the efficiency of epithelial cell infection can be dramatically enhanced if virus is first loaded onto B-cells[282,283]. Thus EBV virions appear to bind to the surface of B-cells in large numbers without being internalised, after which they can efficiently transfer to CD21-negative epithelial cells. This process may be facilitated by the unmasking of additional ligands after gp350 binding to CD21 on B-cells.[282] Such evidence supports the view that B-cells are the initial target of primary infection, after which secondary spread to epithelial tissues may occur.

Primary Immune Response

Antibody responses to EBV infection have principally been studied in the context of IM[10]. Of these, the earliest detectable is an IgM antibody response to viral capsid antigen (VCA), comprising several late lytic cycle viral proteins, which is diagnostic of primary infection. This is subsequently followed by an IgG response to VCA, accompanied by responses to a range of other lytic and latent proteins, all of which remain detectable (generally at lower levels) during the chronic carrier state. These include neutralising IgG responses to membrane antigen (MA), which predominantly comprises the gp350 envelope glycoprotein. Notably, anti-gp350 antibodies have been trialled clinically in an attempt to prevent primary EBV infection[284]. However, the overall contribution of humeral responses in controlling EBV remains unclear. Interestingly, IM is also associated with a polyclonal increase in non-EBV-specific antibodies of all classes, which include heterophile antibodies that can agglutinate sheep and horse erythrocytes. This forms the basis of the widely employed Paul-Bunell-Davidsohn test (Monospot test) for IM[285,286].

Cell-mediated immunity conferred by cytotoxic $CD8^+$ T-cells, plays a crucial role in the control of both primary and chronic EBV infection[10,287]. Interestingly, the marked $CD8^+$ T-cell lymphocytosis observed during IM was initially not thought to be EBV-specific, but rather a product of 'bystander-'[288] or 'superantigen-'[289] driven expansion. However, oligoclonal T-cell receptor usage in IM was consistent with antigen-driven expansion[290], and the subsequent application of immunological techniques, including IFN-γ Elispot assays and MHC tetramer staining, revealed that the majority of T-cells are indeed EBV-specific[291-299]. Notably, $CD8^+$ T-cell responses during acute IM are usually dominated by those against IE and early lytic antigens[292,293,295,296]. Thus, 25-50% of $CD8^+$ T-cells in HLA-B8 positive

individuals with IM are regularly specific for the RAK epitope of BZLF1[293], whilst up to 25% of $CD8^+$ T-cells in HLA-A2.01 positive individuals are specific to either the YVL epitope of the IE protein BRLF1 or the GLC epitope of the early protein BMLF1[296]. Meanwhile, $CD8^+$ T-cell responses to latent antigens typically occur later in IM, and are of lesser magnitude[295,296]. These are usually dominated by responses against the immunodominant EBNA3 family proteins, although in certain MHC I backgrounds responses against other antigens may predominate[291]. Notably, most of the T-cells which expand during acute IM bear activation markers such as CD38 and HLA-DR and are positive for the proliferation marker Ki-67[293,295]. During convalescence, most of these undergo apoptosis, probably due to loss of antigenic drive as EBV latent gene expression assumes a more restricted pattern (see below). Thus, $CD8^+$ T-cells isolated from individuals with IM readily apoptose *in vitro* if not rescued by antigenic or cytokine stimulation[300,301]. Although $CD4^+$ T-cell responses have not been characterised to the same extent as those of $CD8^+$ T-cells, recent work has been facilitated by the identification of $CD4^+$ EBV epitopes. This reveals that $CD4^+$ T-cells also undergo marked expansion during IM, albeit at lower levels than $CD8^+$ T-cells[302].

The role of NK-cells in controlling EBV infection is less established than that of T-cells. However, NK-cells also undergo expansion during acute IM[268,303]. Furthermore, they can impair B-cell transformation if added to cultures within the first few days of infection, acting at least in part through secretion of IFN-γ[304]. Recent studies have also shown that depletion of NK-cells from mice containing reconstituted human haematopoiesis results in increased symptoms and tumour formation following EBV infection, largely through failure to control viral lytic activity[305]. A specific NK-cell subset enriched in the tonsils of chronic EBV carriers, which is less mature than most circulating NK-cells and which secretes high amounts

of IFN-γ, appear to control *in vitro* EBV transformation most effectively[306,307].

Chronic Infection

Following primary infection, EBV assumes the chronic carrier state[10]. In this, EBV virions are continuously, or periodically, shed into the saliva as a consequence of productive lytic cycle within the oropharynx[277,308]. The cellular origin of viral shedding during chronic infection is debated; although EBV does replicate within oral epithelium in disease states such as oral hairy leukoplakia[309,310], the current evidence favours lytic infection of submucosal B-cells as the principal source of virus in healthy individuals[311,312]. Meanwhile, EBV establishes chronic latent infection of the B-cell system, which constitutes its principal reservoir. Thus, an estimated 1 - 50 per 10^6 circulating B-cells are thought to carry viral genomes in healthy immunocompetent adults[313,314]. Strikingly, these are found almost exclusively within the memory B-cell subset, as demonstrated by landmark studies in which B-cell subsets were isolated using magnetic beads or flow cytometric sorting and then tested using PCR assays specific for the EBV genome[315-317]. Subsequently, EBV-infected B-cells were shown to possess somatically mutated Ig genes, confirming their memory B-cell status[318]. Interestingly, the infected memory B-cells appear to be in a resting state, as demonstrated by cell-cycle analysis and staining for Ki-67[314,315]. Moreover, EBV gene expression is thought to be limited to a highly restricted pattern in these cells. Thus, the only reliably detected EBV transcripts found in circulating B-cells from healthy carriers are those for EBERs, BARTs and LMP2A[315,319,320]; although EBNA1 transcripts have also been detected by some[315,320]. However, it has been suggested that the bulk of circulating B-cells may, in fact, only express the EBERs and BARTs, an expression pattern dubbed 'Latency 0'[266,321]. By restricting its gene expression in this way, EBV is able to escape EBV-specific T-cell responses directed

again latent antigens and establish chronic infection.

During the chronic carrier state, surveillance by EBV-specific immune responses maintains strict control of viral infection. This is predominantly mediated by EBV-specific $CD8^+$ memory T-cells, with reactivity to lytic and latent antigens. These constitute a relatively high proportion of the total $CD8^+$ T-cell population in healthy carriers. Thus, it has been estimated that up to 2% of all $CD8^+$ T-cells may be specific for EBV lytic epitopes[322-324], and up to 1% for latent epitopes[324]. Unlike the T-cells observed in acute IM, those found in chronic infection exhibit a predominantly $CD38^-$, $HLA\text{-}DR^-$ and $Ki\text{-}67^-$ resting phenotype[293] but these are presumably able to respond rapidly to any reappearance of growth-transformed lymphoblasts. Notably, $CD4^+$ T-cell responses are also detected during chronic infection, and although they are present at around 10-fold lower frequency than those of corresponding $CD8^+$ T-cells[302], they recognise a broader distribution of latent and lytic antigens[325-327]. They predominantly exhibit a TH1 phenotype and generate IFN-γ, although they also exhibit direct cytotoxic function[326-328].

Alternative Models for EBV Persistence

The mechanism by which EBV achieves selective colonisation of the memory B-cell compartment has been much debated (Figure 7). One model, proposed by Thorley-Lawson and colleagues[329], originates from studies which examined tonsillar B-cells isolated from healthy EBV carriers, in which the only infected B-cells found to exhibit an EBV Latency III expression pattern possessed a naive phenotype[321,330]. Based on this finding, it was proposed that EBV gains entry to memory B-cells via a GC-dependent mechanism. Thus, it is argued, virions originating from the oropharynx (or acquired exogenously) target naive tonsillar B-

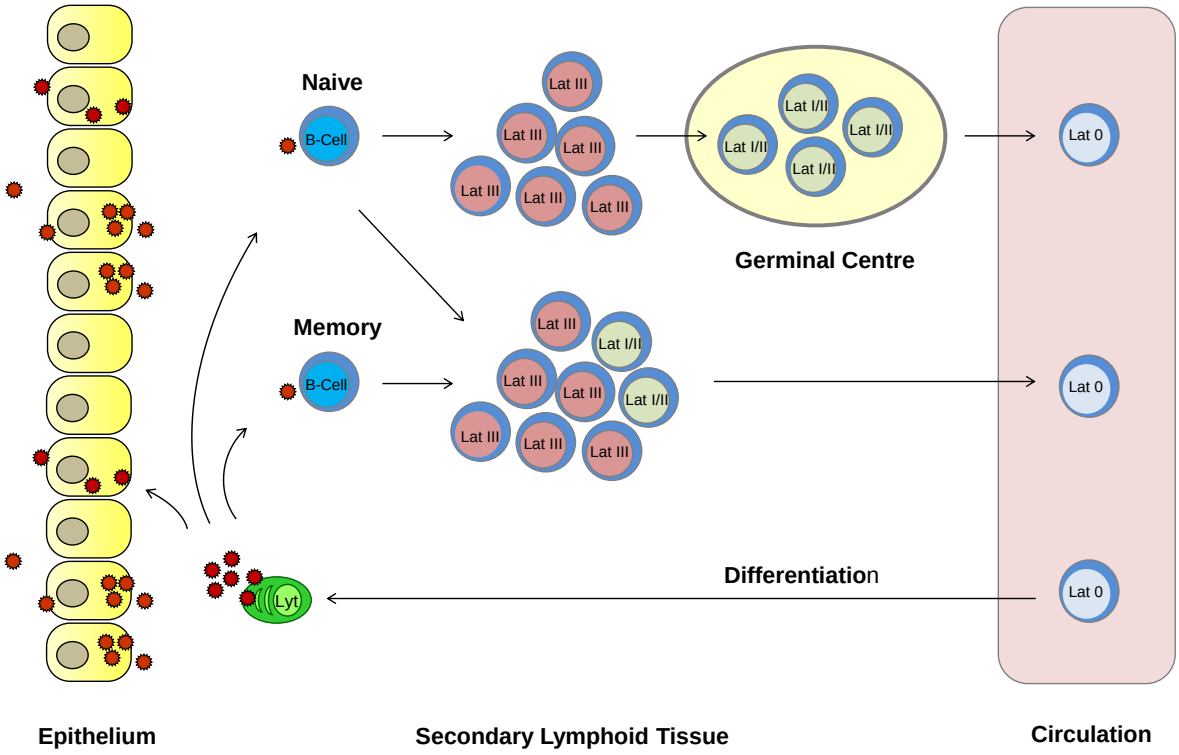

Figure 7. Alternative Models of EBV Persistence

The mechanism by which EBV establishes chronic latency in the resting memory B-cell compartment remains controversial. In the prevailing GC-dependent model[329] it is proposed that EBV initially infects naive B-cells resulting in a Latency III growth transforming infection. This may drive the infected cells to enter a GC reaction, during which the naive B-cells acquire a memory B-cell phenotype, undergoing SHM and CSR. Latent viral gene expression may be progressively down-regulated to Latency II and Latency I patterns, before resting memory B-cells bearing EBV expressing a highly restricted pattern of gene expression exit the GC into the circulation. Alternatively, EBV may enter B-cell memory by a GC-independent route. Thus it may infect pre-existing memory B-cells directly41, or it may infect both naive and memory B-cells with equal efficacy (as it does in vitro) but with preferential survival or proliferation of the latter[331]. It has also been proposed that circulating EBV-infected B-cells may undergo plasma cell differentiation and exit into the secondary lymphoid tissues, accompanied by a switch to virus lytic cycle. This may result in the generation of new EBV virions that can then infect other B-cells (or epithelial cells), establishing a cycle that maintains the latent EBV reservoir. Figure adapted from Young and Rickinson[266].

cells, establishing a Latency III transforming infection. The latter is believed to mimic normal B-cell antigenic stimulation, driving the EBV-infected B-cells to initiate a GC reaction[332]. Thereafter, as the B-cells transit through the GC, undergoing further expansion, they down-regulate viral gene expression to the more restricted Latency II and Latency I patterns. Ultimately, the GC B-cells differentiate into memory B-cells, which exit into the circulation as long-lived cells in a resting state. In these, EBV is transcriptionally silent, thus evading T-cell responses directed against EBV latent antigens. Based on other evidence that terminal differentiation of B-cells into plasma cells is associated with initiation of EBV lytic cycle [271,273,333-335], it is also proposed that infected memory B-cells may subsequently differentiate into plasma cells, triggering production of new virions. The latter may infect new naive B-cells, thus maintaining the EBV memory B-cell reservoir.

Although widely referenced, the GC-dependent model is not favoured by all, and alternative GC-independent models have been suggested (Figure 7). Thus it has been argued that EBV may preferentially infect pre-existing memory B-cells[41,272], or that both naive and memory B-cells may be infected but with preferential survival or proliferation of the latter[331]. Such proposals have cited several criticisms of the GC-dependent model. Thus, it is notable that EBV can infect naive and memory B-cells with equal efficacy *in vitro*[336], and it is therefore unclear why the virus would not directly colonise memory B-cells *in vivo.* Moreover, several histological studies have failed to demonstrate EBV within GC. Thus, analysis of tonsil sections from patients with IM has shown that EBV typically localises to extra-follicular areas, rather than GC[271-273]. Furthermore, analysis of Ig gene sequences from these specimens showed these to be dominated by clones with an absence of ongoing Ig hypermutation, refuting GC localisation; even rare $EBER^+$ cells within the GCs had memory genotypes

distinct from the adjacent GC reaction[272]. These findings have subsequently been supported by work on tonsillar B-cell suspensions from chronic carriers and patients with IM, showing that EBV is concentrated in cells with an extra-follicular, rather than GC, phenotype[331]. However, the virus *has* been reported within (occasional) GC cells in tonsillar tissues from healthy chronic carriers in other studies[337].

Strong support for GC-independent models also comes from evidence of EBV persistence within the NSM B-cell subset. This was first observed in individuals with XLP which, as described above, results in a lack of GC formation and inability to generate CSM B-cells, although NSM subsets are retained. Patients with XLP often develop a life-threatening EBV-driven lymphoproliferative disease following primary EBV infection, survivors of which become chronic EBV carriers. Given that NSM B-cells may arise independently of GC, as discussed previously, the finding that EBV genomes are concentrated within the NSM subset of such individuals has been interpreted as evidence against the GC-dependent model of EBV entry in memory[338]. Subsequently, EBV has also been detected in NSM B-cells from healthy carriers, as well as in individuals with IM, albeit at lower levels than those found in CSM B-cells[331]. Notably, the recent demonstration that LCLs established from naive B-cells may accumulate Ig mutations adds additional weight to the view that GC transit is not required[236]. Collectively, such studies provide compelling evidence that EBV is not exclusively dependent on a GC route into B-cell memory.

1.6 PTLD

Solid Organ Transplantation

Solid organ transplantation provides definitive treatment for end-stage organ failure.

Allografts can be harvested from cadaveric or living donors, and with the exception of renal allografts, donor and recipient HLA-antigens are not usually matched. Transplant recipients are managed indefinitely with immunosuppressive agents to prevent alloreactive immune responses, which would otherwise result in organ rejection[339]. Commonly used agents are cyclosporin and tacrolimus, both of which inhibit calcineurin, a serine-threonine phosphatase which mediates IL2 secretion and T-cell activation. Others agents target purine synthesis in lymphocytes, including the purine analogue azathioprine, and mycofenolate mofetil which inhibits inosine monophosphate dehydrogenase which is required for synthesis of guanosine. Glucocorticoids are also commonly used as adjunctive therapy, particular to treat episodes of organ rejection. The prolonged state of immunosuppression caused by these agents exposes patients to a range of opportunistic infections[340] and malignant complications[341], amongst which are uncontrolled herpesvirus infections and PTLD.

Allogeneic Haematopoietic Stem Cell Transplantation

Allo-HSCT is used to treat malignant haematological conditions including leukaemia, myelodysplasia, lymphoma and myeloproliferative disorders, as well non-malignant conditions such as bone marrow failure syndromes, haemoglobinopathies and congenital immunodeficiency[342]. The process of allo-HSCT involves delivery of preparative conditioning followed by infusion of donor-derived haematopoietic stem cells contained in a stem cell graft (Figure 8). The latter is usually collected from the peripheral blood of donors following treatment with granulocyte-colony-stimulating factor (GCSF), which mobilises stem cells into the peripheral circulation; compared to bone marrow, peripheral blood stem cell (PBSC) grafts produce more rapid immune recovery[343,344]. Donors are typically HLA-matched siblings or unrelated individuals, although umbilical cord blood grafts or

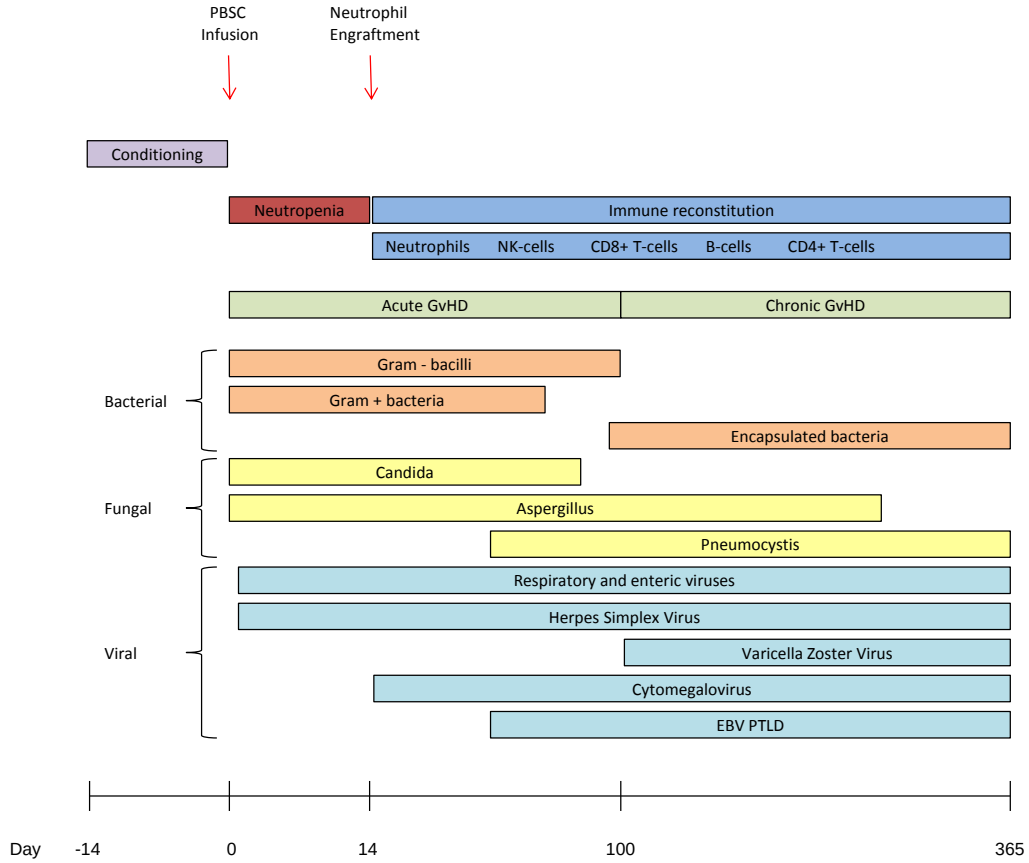

Figure 8. Overview of Allogeneic Haematopoietic Stem Cell Transplantation

During the course of allo-HSCT patients receive preparative conditioning comprising cytotoxic chemotherapy+/- radiotherapy, after which donor haematopoietic stem cells, usually in the form of a GCSF-mobilised PBSC graft, are infused on 'Day 0'. Immune reconstitution takes many months. Following a period of neutropenia, donor stem cell 'engraftment' occurs once the neutrophil count is >1.0 x10^9/L. Lymphocyte reconstitution occurs in a characteristic order, with NK-cells recovering first, followed by $CD8^+$ T-cells, then B-cells (which are almost entirely $CD27^-$ naive B-cells) and $CD4^+$ T-cells. Patients are exposed to numerous complications during allo-HSCT. Thus, GvHD is a potentially life threatening alloreactive immune response, largely originating from mature donor T-cells transferred in the stem cell graft. Acute GvHD usually occurs within the first 100 days after transplant and characteristically involves the skin, liver and gut. Chronic GvHD occurs later and may involve multiple organ systems, including the skin and joints. Infective complications are caused by bacterial, fungal and viral pathogens; the latter frequently include herpesviruses. Figure adapted from Mackall et al.[336].

haploidentical donors may also be used where a donor is not available.

It was originally believed that all anti-tumour effects resulting from allo-HSCT were due to the cytotoxic action of the preparative conditioning, and that the stem cell graft was just a means of providing haematopoietic system rescue. Thus, in conventional allo-HSCT myeloablative doses of cytotoxic chemotherapy, often accompanied by radiation, are used. However, studies conducted over the last 4 decades have led to the recognition of important graft-versus-leukaemic (GvL) immune effects mediated by donor-derived T-cells, and NK-cells[345,346]. Consequently, non-myeloablative (also known as reduced intensity conditioning or RIC) transplants, which use less toxic forms of preparative conditioning and instead rely on GvL effects, have been adopted. These are better tolerated by older and less fit patients and have thus become the predominant form of allo-HSCT. Although these can be complicated by states of mixed host and donor chimerism, this is managed with additional donor lymphocyte infusions (DLI)[347]. Patients undergoing allo-HSCT are also at risk of graft-versus-host-disease (GvHD), a potentially fatal alloreactive immune response in which donor T-cells react to antigens in recipient tissues[348]. Consequently, patients are treated with additional immunosuppressive agents to prevent (or treat) GvHD. Therefore they usually receive cyclosporin for the first few months after transplant. Furthermore, graft T-cell depletion (TCD) results in significantly reduced incidence of GvHD. This is commonly performed using either anti-thymocyte globulin (ATG)[349,350], which specifically targets T-cells, or Campath (Alemtuzumab)[351,352], a cytolytic monoclonal antibody specific to CD52 expressed on most lymphocytes.

Immune Reconstitution after Allo-HSCT

It takes many months for the transplanted haematopoietic system to reconstitute following allo-HSCT, and during this time patients are at high risk from infectious complications[353] (Figure 8). Individual cell types reconstitute in a predictable order after allo-HSCT[342,354]. Thus, following a short period of absolute pancytopenia, neutrophils (and other granulocytes), monocytes and NK-cells are the first cell types to recover to normal levels. These are followed by erythrocytes and platelets, before the eventual recovery of T- and B-cells. Notably, lymphocyte reconstitution is a prolonged process which occurs by 2 alternative pathways. In the first, new antigen-inexperienced cells differentiate from lymphocyte progenitors arising from recently engrafted donor haematopoietic stem cells[355]. In the second, reconstitution occurs through peripheral expansion of mature cells which have been carried across in the graft[356]. NK-cells, the first lymphocyte subset to recover, reconstitute almost exclusively through the first of these pathways. Normal NK-cell frequency is usually reached by 1 - 2 months following transplant, after which their numbers often become supra-normal. In contrast, T-cell recovery predominantly occurs through thymus-independent expansion of mature T-cells carried across in the graft. This 'homeostatic expansion' is driven by normal T-cell regulatory pathways, involving cytokines such as IL7 and IL15 which respond to T-cell lymphopenia[280,357], and is also stimulated by the presence of antigens present at the time of transplant[358]. Notably, the potential for T-cells to reconstitute from lymphoid progenitors is often severely limited by thymic incompetence, resulting from the effects of ageing, therapy and GvHD, which impairs the thymus-dependent maturation of naive T-cells[359,360]. The reconstitution of $CD4^+$ T-cells often lags behind that of $CD8^+$ T-cells, and this is reflected in reversal of the normal CD4/CD8 ratio which persists for many months after transplant[361]. This may be due to a relative insensitivity of $CD4^+$ T-cells to the homeostatic mechanisms which

drive the peripheral expansion of $CD8^+$ T-cells[361].

B-cell reconstitution is characterised by undetectable or low levels of circulating B-cells for around the first 2 months following allo-HSCT, after which there is a gradual increase in B-cell frequency, often culminating in supra-normal levels by 1-2 years after transplant[342,354,362]. B-cell recovery derives almost entirely from the differentiation of donor B-cell progenitors, as opposed to peripheral expansion of mature B-cells carried across in the graft. Thus, the circulating B-cell pool is dominated by $CD27^-IgD^+$ antigen-inexperienced naive B-cells for many months after transplant, with a concurrent paucity of $CD27^+$ memory B-cells which lasts for at least 12 months[363-365]. Furthermore, these naive B-cells exhibit a transitional cell phenotype, reflecting their recent emergence from the bone marrow, which gradually resolves over time[21,366,367]. However, some recipient B-cells may also persist after transplant, more commonly after reduced intensity conditioning[368]. Notably, levels of serum Ig remain normal for some time, due to the persistence of long–lived recipient-derived plasma cells, which appear to be relatively resistant to chemotherapy[369]. However, these levels subsequently drop, and recipients invariably become seronegative to antigens against which they (or their donor) were previously immunised[370,371], and therefore re-vaccination is required. Consistent with this, allo-HSCT recipients are particularly vulnerable to infections by encapsulated bacteria such as *Haemophilus influenza* and *Streptococcus pneumonia,* against which neutralizing antibodies normally provide a first line of defence[372-374]. They also exhibit poor responses to immunisation after transplant, such that vaccination is generally not recommended until 6 months afterwards[375]. The deficiency of humeral immunity that follows allo-HSCT is likely to reflect an impairment of T-cell dependent B-cell responses and GC development, consequent upon delays in $CD4^+$ T-cells reconstitution, as well as impaired recovery of other

important cells contributing to the secondary lymphoid tissue microenvironment, including follicular dendritic cells[376,377]. B-cell maturation is also highly susceptible to damage by the toxic effects of GvHD and its treatment, and patients who experience even a limited episode of GvHD show significantly impaired B-cell reconstitution and GC development[377-379].

Deranged Host-Virus Balance after Transplant

A measureable decrease in EBV-specific immunity accompanies the state of general immunocompromise that follows transplantation. Thus, EBV-specific T-cell responses are reduced in solid organ transplant patients taking even relatively low levels of immunosuppressive therapy[380,381]. Meanwhile, EBV-specific T-cells are absent or significantly reduced for at least 6 months after allo-HSCT[382,383]. As a consequence, transplant patients often exhibit impaired control of EBV, consistent with the view that cell-mediated immunity is crucial for exerting long-term control over EBV infection. Thus solid allograft recipients shed increased levels of EBV into the throat[381]. Furthermore, otherwise asymptomatic transplant recipients may develop increased levels of circulating EBV DNA (otherwise known as 'EBV DNAemia,' or 'EBV reactivation') as measured by PCR[384]. Notably, patients with established PTLD exhibit significantly elevated levels of EBV DNA, and therefore quantitative EBV-specific PCR (EBV qPCR) testing is now widely used as a clinical tool to aid diagnosis, to assess response to therapy, and to identify those with impending PTLD, as discussed in more detail later.

Regarding the basis of the increased EBV loads observed in transplant patients, it is apparent that EBV DNA can be detected in both cellular and plasma fractions of blood. However, although EBV can always be found in the cellular compartment it is only consistently found

in plasma when circulating EBV loads are very high or when PTLD is present[384]. EBV DNA in plasma is thought to comprise either fragments of free viral DNA released from EBV-infected cells that have been destroyed, or possibly viral DNA packaged into virions[385]. Meanwhile, cell-associated viral genomes principally result from an expansion of latently infected B-cells. Importantly, Babcock et al. demonstrated that solid organ allograft recipients with EBV DNAemia carry EBV genomes almost exclusively within the IgD^- memory B-cell compartment[386], and this was later confirmed by others[387]. Notably, it was originally assumed that the increased circulating EBV DNA found in transplant patients would originate from an expansion of B-cell lymphoblasts exhibiting a Latency III pattern of virus gene expression, as found in PTLD tumours. However, Babcock et al. reported that the IgD^- memory B-cells in which EBV is found are in a resting state, as determined by cell-cycle analysis[386]. Furthermore, EBV gene expression, as detected by RT-PCR, revealed an absence of EBNA2 in these cells[386]. Therefore, it was concluded that EBV DNAemia in transplant patients results from an accumulation of latently infected memory B-cells, existing in a resting state with highly restricted EBV gene expression. As such, these cells are identical to the latently infected B-cells that comprise the main EBV reservoir in healthy immunocompetent individuals[315-317].

Presentation and Epidemiology

The clinical presentation of PTLD may be highly variable but it commonly involves lymphadenopathy, often accompanied by systemic features including fever, sweats and weight loss[388]. Patients with EBV-associated disease may also develop a sore throat, similar to that observed in acute IM. PTLD may also present with manifestations including encephalitis, hepatitis or a fulminant sepsis-like picture that rapidly leads to multi-organ

failure, particularly in the allo-HSCT setting. A high incidence of extranodal disease is observed, with involvement of the gastrointestinal tract occurring most frequently. Disease affecting the transplanted organ is also relatively common. On occasions, PTLD is also diagnosed at post-mortem, highlighting the need for improved vigilance and early recognition of the condition. PTLD can occur at any time after solid allograft but it is most common during the first year[389]. Notably, disease occurring more than 1 year after transplant is less likely to be associated with EBV[390,391]. Meanwhile, most cases of PTLD arising after allo-HSCT occur within the first 6 months, peaking in incidence at around 2-3 months[392].

The reported incidence of PTLD varies from <1% up to 10% in most studies, although rates are highly variable with regard to transplant and host-related risk factors. Amongst risk factors for PTLD arising after solid allograft, the intensity of iatrogenic immunosuppression, and in particular the degree of T-cell suppression, is a fundamental determinant of PTLD risk. In particular, the cumulative level of immunosuppression is likely to be more important than the individual immunosuppressive agents used, because studies seeking to compare drugs have generated conflicting data[393]. However, agents that are specifically T-cell depleting, such as the anti-CD3 monoclonal antibody OKT-3 and ATG have been associated with a particularly high incidence of disease[389,394-398]. Patients undergoing cardiothoracic or intestinal transplants are at greater risk than those receiving liver or renal transplants, consistent with the requirement for more intensive immunosuppression with the former[389,395,399-401]. Interestingly, the incidence of lymphoma in renal transplant patients who lose their graft and subsequently cease immunosuppression reverts to pre-transplantation levels[402].

Importantly, negative EBV serological status at the time of transplant is also a major risk

factor for PTLD, and incidence is increased further when solid allografts are derived from an EBV seropositive donor[395,402-405]. For example, Ho et al. reported a 20-fold higher incidence in PTLD amongst EBV seronegative solid organ transplant recipients[405]. This reflects the consequence of undergoing primary EBV infection in the context of immunocompromise. Furthermore, it explains the elevated risk of PTLD, and shorter intervals from transplant to disease onset, observed amongst paediatric solid allograft recipients[389,406].

Specific to the allo-HSCT setting, several risk factors for PTLD (or EBV DNAemia), all of which are principally related to the degree of graft T-cell suppression, have been identified[392,407-420]. Thus, T-cell depletion using ATG or Campath is associated with significantly increased incidence of PTLD; T-cell replete transplants rarely develop PTLD. Interestingly, Campath is thought to be associated with lower risk than ATG because it also eliminates B-cells from the donor graft[392,407]. Other recognised risk factors are unrelated and/or HLA-antigen-mismatched donors, the occurrence of acute or chronic GvHD, increasing age at transplant and re-transplantation[392].

Pathological Subtypes

PTLD includes a heterogeneous spectrum of pathological subtypes that are categorised according to the World Health Organisation (WHO) classification system for PTLD[388,421] (Table 2). These include early benign proliferations, polymorphic disease and malignant monomorphic PTLD. It has been assumed that monomorphic lymphoma may arise from the early and polymorphic types, although this process remains poorly characterised[422]. The frequency of each type varies between transplant and patient groups, but the commonest forms are polymorphic PTLD and the diffuse large B-cell lymphoma (DLBCL) subtype of

Histological Type	Approximate Frequency
Early PTLD	5%
Plasmacytic hyperplasia	
IM-like PTLD	
Polymorphic PTLD	15-20%
Monomorphic B-cell PTLD	>70%
Diffuse large B-cell lymphoma	
Burkitt lymphoma	
Plasmacytoma-like lymphoma	
Plasmablastic lymphoma	
Other	
Monomorphic T-cell PTLD	<5%
Peripheral T cell lymphoma	
Other	
Classical Hodgkin lymphoma PTLD	<5%

Table 2. WHO Classification of PTLD

PTLD is a heterogeneous disease, with multiple pathological types. The most common forms are DLBCL-PTLD (which comprise >90% of monomorphic B-cell PTLD lesions) and polymorphic PTLD. Table adapted from the WHO Classification of Tumours of Haematopoietic and Lymphoid Tissues 2008[421].

monomorphic B-cell PTLD.

Early PTLD includes plasmacytic hyperplasia (PH) and IM-like PTLD subtypes. These are benign B-cell proliferations that are almost always EBV-associated, as determined by EBER *in-situ* hybridisation. They develop within the first year after transplant and usually occur in the context of primary EBV infection[423,424]. In PH, lymphoid tissues retain their architecture and contain sheets of plasma cells with scattered large $EBER^+$ B-cell immunoblasts, whereas IM-like PTLD lesions resemble true IM, showing at least partial preservation of lymphoid architecture and paracortical infiltrates containing plasma cells and large numbers of $EBER^+$ B-cell immunoblasts and reactive T-cells. Molecular analysis reveals polyclonal (or oligoclonal) IgH rearrangements in both subtypes[425].

Polymorphic PTLD lesions are typically EBV-associated and, as their name suggests, contain a diverse range of lymphoid cells, including small and intermediate-sized lymphocytes, immunoblasts and plasma cells that characteristically efface the underlying tissue architecture[426,427]. Malignant features, including nuclear atypia, necrosis and a high mitotic rate, may also be present. The lesions contain a mixture of $EBER^+$ B-cells, usually showing IgL restriction, and reactive T-cells. Molecular analysis typically reveals monoclonal IgH gene rearrangements[425].

The monomorphic B-cell PTLD category includes the DLBCL subtype, which makes up over 90% of cases, as well as rarer BL and plasma cell subtypes[428]. The DLBCL subtype exhibits histology typical of DLBCL occurring in immunocompetent individuals. Notably, there is variable positivity for EBV, ranging from 50 – 70% in many studies. In most cases these

lesions exhibit monoclonal IgH rearrangements. Of the other monomorphic B-cell PTLD lesions, the BL subtype resembles sporadic BL, and most cases are EBV-associated. Typical BL morphology is observed including the classical 'starry sky' appearance, and the tumour cells are positive for CD20, CD10 and BCL6, and negative for BCL2. Immunohistochemistry for Ki-67 reveals a proliferation fraction close to 100% and molecular studies show clonal IgH rearrangements and MYC translocation. Meanwhile, plasma cell myeloma and plasmacytoma-like lesions are rare subtypes composed of mature plasma cells[429,430]. In keeping with this they are usually negative for CD20 and PAX5 but positive for CD138. They show variable positivity for EBERs and exhibit IgL restriction and monoclonal IgH rearrangements. Notably, they may secrete monoclonal Ig into the serum or urine.

The monomorphic T/NK-cell PTLDs make up only a minority of PTLD lesions. This category encompasses the full spectrum of lesions recognised in immunocompetent individuals, the commonest subtype being peripheral T-cell lymphoma not otherwise specified[421]. Most of the T-cell lesions are negative for EBV[431], whilst the majority of NK-cell PTLD tumours show positivity for EBERs[432]. The T-cell lesions show clonality of TCR genes and NK-cell tumours exhibit clonal EBV episomal DNA.

Occasional PTLD cases are also of classical HL type[433,434]. Unlike in the non-transplant setting, almost 100% of post-transplant cases are positive for EBV. Histology demonstrates findings typical of classical HL, with HRS cells and a background composed of small lymphocytes, histiocytes and eosinophils. The RS cells exhibit a characteristic phenotype, being positive for CD30, CD15 and EBV, with weak or heterogeneous positivity for CD20.

EBV Gene Expression

In EBV-associated B-cell PTLD, Latency III viral gene expression is typically detected by immunohistochemical or molecular methods[435]. This supports the notion that EBV is a key aetiological agent in PTLD, actively driving cell proliferation. Consistent with this, PTLD-like tumours expressing the Latency III pattern have been documented in animal models including cottontop tamarins injected with EBV[436], or SCID mice inoculated with PBMCs from EBV seropositive individuals[437]. Meanwhile, rarer types of EBV-associated PTLD, including BL, plasma cell, and HL types exhibit more restricted forms of viral latency, as occur in equivalent tumour types in immunocompetent individuals. However, some B-cell PTLD lesions also exhibit more restricted forms of latency, and there is often heterogeneity of latency type within individual PTLD lesions[438-440]. Thus, although cells expressing EBNA2 and LMP1 are found in most tumours, the proportion of these is often highly variable[439,441-443]. Furthermore, the number of cells positive for EBV is often greater than the number of cells positive for EBNA2 and LMP1, suggesting that some of the cells may express Latency I, and some cells express LMP1 in the absence of EBNA2, indicating Latency II expression[439]. Consistent with these findings, Latency I Qp transcripts have been detected in some PTLD tumours, in addition to Latency III Cp and Wp transcripts[439].

EBV lytic cycle gene expression has also been documented within many B-cell PTLD tumours[439,442-444]. Interestingly, in some cases there has been failure to show full progression through to late lytic cycle gene expression[439,443], suggesting the occurrence of abortive lytic cycle activity. As lytic cycle expression is often limited to only a small number of cells in PTLD tumours its relevance to tumour pathogenesis has remained uncertain. Indeed, it is notable that drugs such as aciclovir, which impair EBV lytic cycle activity *in vitro*, have

failed to prevent or effectively treat PTLD. Nevertheless, recent findings have increasingly suggested that lytic cycle expression, whether or not it results in productive virus, might be important for tumourigenesis[445-448]. Thus, lytic cycle defective LCLs fail to develop PTLD-like tumours in SCID mice models[445]. This effect may be mediated, at least in part, by up-regulation of paracrine factors such as IL6 mediated by IE lytic gene expression[445,446].

Some cases of PTLD are negative for EBV, and the aetiology of these remains poorly characterised[449,450]. However, it is apparent that EBV-negative tumours often show an increased number of cellular mutations, as discussed below. It has been proposed that they may represent previously EBV-positive tumours that have lost the EBV genome, perhaps due to the acquisition of mutations that render the proliferative effects of EBV redundant. In support of this, some BL cell lines may lose their EBV genomes in culture[451,452]. It has also been suggested that they arise as a consequence of alternative infectious agents such as KSHV[453-455], although this has been disputed[456].

Histogenesis

Studies seeking to establish the histogenesis of B-cell PTLD tumours have shown that the majority of lesions arise from GC-experienced cells[457-461] (Figure 9). As such, mutational analysis of IgH V regions has shown that most PTLD tumours possess mutated Ig genes, consistent with GC transit. Furthermore, evidence of ongoing SHM in these lesions strongly indicates their GC origin; interestingly, in some biopsies $CD4^+$ T-cells and FDCs have been found to be absent, suggesting that SHM might have occurred in the absence of normal GC physiology[458]. Additional immunohistochemical analysis, using markers including BCL6, MUM1 (IRF4) and CD138, have also confirmed that most PTLD tumours arise from either

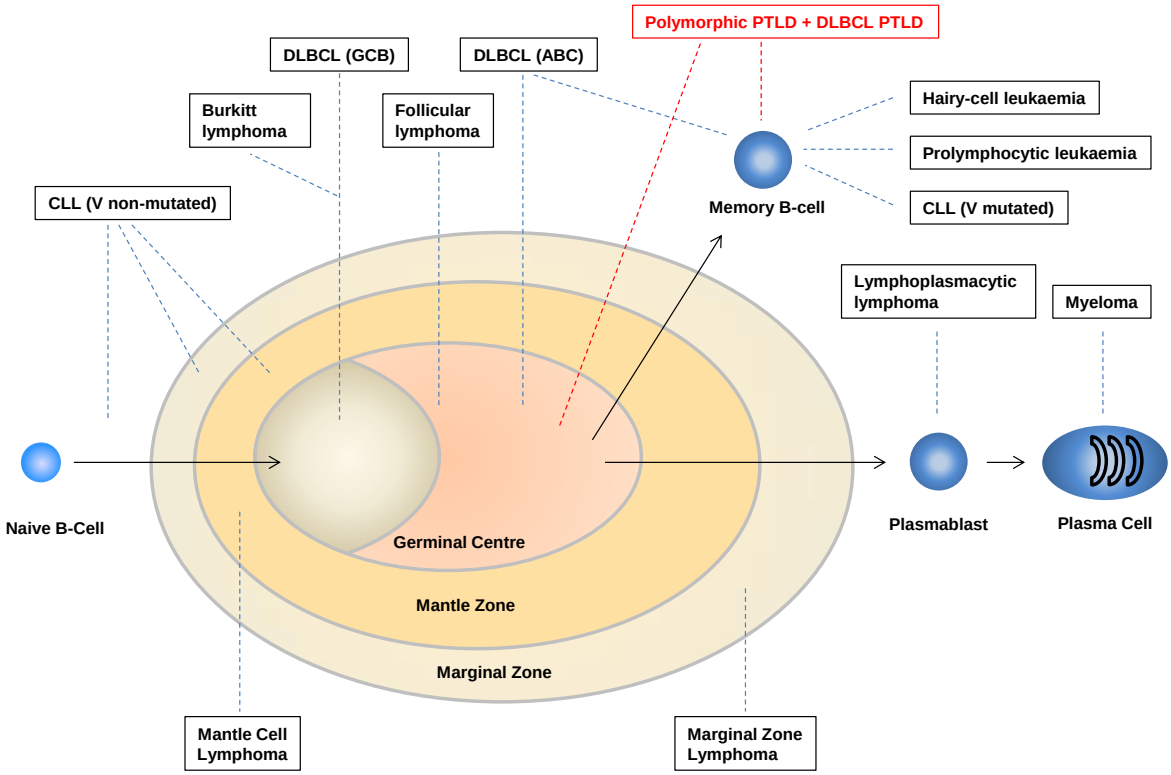

Figure 9. Histogenesis of PTLD Lesions

Immunophenotypic and molecular markers can be used to identify the stage of normal B-cell development from which B-cells malignancies are likely to originate. Positivity for BCL6 identifies cells of GC origin, MUM1 those of late (centrocyte) and post-GC origin, and CD138 those of plasmablastic and plasma cell origin. Analysis of SHM mutations identifies pre-GC cells as those lacking SHM, post-GC cells as those with intraclonally uniform SHM, and centroblast GC cells as those with intraclonally diverse SHM. Notably, DLBCL arising in immunocompetent individuals can be separated into 2 principal categories: germinal centre B-cell (GCB) DLBCL are $BCL6^{+}$/MUM1-/CD138- and carry a better prognosis than activated B-cell (ABC) DLBCL which derive from late or post-GC cells which are $BCL6^{+}$/$MUM1^{+}$/CD138-. Malignancies from plasmablastic or plasma cells stages are BCL6-/$MUM1^{+}$/$CD138^{+}$. Applying this scheme to B-cell PTLD, it can be seen that the majority of DLBCL-type PTLD and polymorphic PTLD lesions are of late or post GC B-origin, although a small proportion of DLBCL-PTLD lesions are of GCB type. Figure adapted from Kuppers[462].

GC or post-GC B-cells[461,463]. Notably, recent studies have used high throughput genomic techniques to categorise DLBCL in immunocompetent individuals into clinically important subtypes, such that GC B-cell (GCB) or activated B-cell (ABC) lesions are now recognised [464], with 5 year survival rates of 75% for GCB types, compared to 30% for ABC DLBCL[465]. According to this scheme, the majority of PTLD lesions of DLBCL (and polymorphic) type fall into the ABC category.

Interestingly, some of the studies mentioned above have also shown that PTLD lesions may arise from cells which exhibit inactivating mutations in previously productive Ig genes[458-460]. Thus, they contain IgH genes in which stop codons, deletions or other changes prevent expression of a functional IgH chain. This is remarkable because such 'crippling' mutations would normally be incompatible with survival of these B-cells during GC transit due to affinity selection. Notably, inactivating mutations such as these had already been identified in HL at the time they were found in PTLD[466,467]. In light of these findings it is hypothesised that EBV may confer essential survival and proliferative signals sufficient for the rescue of GC B-cells that would otherwise be destined for elimination. Furthermore, a selective advantage may be gained by cells which have lost the BCR through inactivating mutations, as they are no longer subject to regulatory mechanisms which operate through BCR signalling pathways.

The host versus donor origin of B-cells found in PTLD has also been investigated, revealing differences between transplant settings. Thus, PTLD arising after solid organ transplant is usually of recipient origin, although cases of donor-derived PTLD are also found; these are more common after liver or lung allografts, and frequently involve the donor organ[468-471]. In contrast, almost all cases of PTLD arising after allo-HSCT are of donor origin, although

recipient-derived tumours have been reported[415,472,473]. These patterns reflect important differences in the biology of these transplant settings, such that host B-cells are usually ablated by allo-HSCT transplant conditioning. Furthermore, relatively few donor B-cells are transferred to the recipient during the course of solid organ transplantation.

Genetic Aberrations

Efforts to characterise genetic abnormalities associated with PTLD have thus far failed to demonstrate any consistent changes. However, monomorphic lesions, those arising later after transplant and EBV-negative cases appear to exhibit greater frequency of genetic aberrations. Thus, conventional cytogenetics has revealed more abnormalities in monomorphic compared to polymorphic PTLD lesions[474-476]. Indeed, Djokic et al. found cytogenetic abnormalities in 72% of monoclonal B-cell PTLD tumours, in comparison to 15% of polymorphic PTLD lesions, with none found in early PTLD. The most frequent clonal abnormalities in the monomorphic PTLDs were trisomies of chromosomes 9 and 11, followed by rearrangements of 8q24 (containing c-Myc), 3q27 (BCL6) and 14q32 (IgH and Tcl1). Lesions with trisomy of chromosomes 9 or 11 were associated with EBV-positive DLBCL occurring early after transplant and showed improved survival, whereas rearrangements containing c-Myc were correlated with poor outcome[475]. Meanwhile, studies using comparative genomic hybridisation (CGH) have identified chromosomal imbalances already known to occur in non-transplant NHL, as well as some alterations unique to PTLD[325,328]. Thus, Poirel et al. reported chromosomal imbalances in 52% of PTLD lesions, and these were associated with worse clinical outcome[476]. These included gains of 8q24 (c-Myc), 3q27 (BCL6) and 18q21 (BCL2), and loss of 17p13 (p53). Notably, EBV-negative tumour status was associated with a greater number of chromosomal alterations.

Regarding specific mutations, early studies to identify changes in known oncogene and tumour suppressor genes revealed mutations of c-Myc, N-Ras and p53 in monoclonal PTLDs[391,425,477,478]. Furthermore, 5' non-coding region mutations of BCL6 have been detected in most monomorphic PTLD tumours, and around half of polymorphic PTLD lesions, and these have been associated with aggressive clinical outcome[479]. More recently, single nucleotide polymorphism (SNP) arrays have been used to analyse PTLD tumours. In one study, deletions targeting loci at the known fragile sites FRA1B, FRA2E and FRA3B were found to be more common in DLBCL arising in post-transplant versus immunocompetent individuals [480]. Meanwhile, an Affymetrix array identified prognostic markers amongst 36 cases of post-transplant DLBCL, showing gains of 1q or 18q that were significantly associated with poor overall survival[481]. Notably, a small number of studies have also performed gene expression profiling on PTLD tumours, and these have shown distinct profiles when comparing PTLD lesions to immunocompetent NHL, or EBV-positive versus EBV-negative lesions[482-484].

Interestingly, attempts have also been made to identify genotypes that might predispose to the development of PTLD. In particular, several studies have focussed on polymorphisms within cytokine genes[485-491]. For example, a genotype known to cause low production of IFN-γ has been associated with increased risk of EBV reactivation after allo-HSCT, as well as greater incidence of PTLD arising in patients with renal and liver allografts[485-487]. Similarly polymorphisms within the genes TNFα, TGFβ1, IL1, IL10, IL12 and CC chemokine ligand 2 (CCL2) have all been associated with the development of PTLD[489-491]. Meanwhile, a small number of studies have sought to identify associations between HLA types and PTLD[492-494]. In one study, HLA-A26 was shown to confer a 3-fold increase in the risk of PTLD after solid

allograft if present in either the recipient or the donor[494]. However, it is apparent that neither this, nor any of the other HLA-associations identified thus far, has been reproduced between studies. Overall, such insights, like those from the other studies discussed in this section, need to be evaluated in larger prospective studies.

1.7 Management of PTLD

Differences between PTLD arising after solid organ transplant and allo-HSCT mean that they require differing management strategies, and this is reflected in the following discussion. However, common to both transplant settings is a paucity of high quality data to guide clinical decision-making. Indeed, management practices have thus far been based almost entirely on expert opinion, retrospective analyses and a small number of prospective phase 2 studies, rather than on randomised controlled phase 3 trials.

Prophylaxis

Aside from the use of adoptive cellular approaches, as discussed below, there are currently no accepted strategies to prevent PTLD. However, pre-transplant screening of recipient and donor EBV serostatus allows the identification of high risk seronegative recipients. This provides the opportunity to avoid, where possible, T-cell depleting agents in these patients. Furthermore, it conceivably allows selection of a donor who is not EBV seropositive. Although some have advocated the prophylactic treatment of EBV seronegative patients with antiviral agents such as (val-) ganciclovir, or intravenous Ig, there is currently no robust data to support this practice[388,495,496].

Pre-emptive Management

As patients with (EBV-associated) PTLD develop high levels of circulating EBV DNA, EBV qPCR monitoring has been evaluated as means to identify patients with impending PTLD. This allows the institution of 'pre-emptive' management, comprising reduction of immunosuppression (RI) to facilitate endogenous EBV-specific T-cell responses, and/or the administration of Rituximab, a humanised anti-CD20 monoclonal antibody which effectively depletes B-cells and can prevent or treat PTLD[497].

In the solid organ transplant setting, evidence to support EBV qPCR monitoring and pre-emptive management is limited. It is apparent that many otherwise asymptomatic patients develop transiently raised EBV loads, and some exhibit chronically elevated levels, with no clear relationship to the development of PTLD[384,470,567-569]. Consequently, current guidelines do not support the routine use of EBV qPCR monitoring, except in EBV seronegative recipients of an organ from a seropositive donor, or in recipients of a cardiothoracic or intestinal transplant who have a particularly high risk of developing PTLD[388,495]. If these patients exhibit high EBV loads, it is advised that they receive thorough clinico-radiological assessment for evidence of PTLD, and should be considered for pre-emptive RI. However, the routine use of pre-emptive Rituximab therapy is not currently supported for solid organ allograft recipients. In contrast, EBV DNA monitoring and pre-emptive therapy is widely accepted as the current standard of care in the allo-HSCT setting. Thus, several retrospective studies have shown this approach to be effective, resulting in lower rates of PTLD than in historic patient cohorts[498-501]. Reflecting this, guidelines from the Second European Conference on Infections in Leukemia have advocated EBV qPCR monitoring for all patients undergoing high risk allo-HSCT (principally defined as unrelated, HLA-mismatched or T-cell

deplete transplants), comprising weekly testing for at least 3 months after transplant[496]. It is advised that patients who develop high-level EBV DNAemia should receive pre-emptive treatment including RI and Rituximab therapy.

Despite the above recommendations regarding post-transplant EBV qPCR monitoring, it should be noted that there is currently no consensus as to optimal qPCR methodology. Thus, assays measuring EBV DNA within whole blood, plasma and PBMCs have all been employed[384]. PBMC-based assays are generally impractical for routine clinical purposes, due to the time required for cell separation. However whole blood and plasma assays are both widely used; there is some evidence to suggest that whole blood assays may be more sensitive, whereas plasma assays may be more specific for the diagnosis of PTLD[384]. Furthermore, there is no standardised definition as to what constitutes a raised EBV load; results produced by qPCR assays in different laboratories may vary by several logs[502,503]. These limitations have been acknowledged in current guidelines, which state that PCR thresholds for intervention should be determined locally[496]. Notably, the WHO have recently endorsed a whole virus EBV B95.8 preparation to be used in the standardisation of EBV qPCR assays[504].

Interestingly, it has also been suggested that the predictive value of post-transplant monitoring could be improved by combining EBV qPCR with measurement of T-cell responses. Thus, Clave et al. reported that patients who spontaneously settle EBV DNAemia after allo-HSCT had a significantly higher proportion of EBV tetramer-positive $CD8^+$ T-cells than those requiring Rituximab[505]. Furthermore, Annels et al. showed that 6 of 8 patients treated with Rituximab for EBV DNAemia after allo-HSCT developed T-cell responses, comprising

increased $CD3^+$ T-cell counts and EBV-specific tetramer-positive cells[506]. Given these findings, pre-emptive Rituximab therapy was successfully withheld from 2 of 3 prospectively monitored patients who developed EBV DNAemia. More recently, Worth et al. reported a monitoring strategy in which $CD3^+$ T-cell counts were considered when deciding whether to pre-emptively treat paediatric recipients of allo-HSCT[507]. All patients who developed significant EBV DNA within the first 3 months after -transplant were treated, whereas those reactivating after 3 months were only treated if their $CD3^+$ T-cell count was less than 0.3 $x10^9$/L. Consequently, Rituximab was successfully withheld from 6 patients who would normally have been treated. Although such strategies may prove valuable, they carry implications in terms of financial costs and practicality, and require validation in large prospective studies.

Management of Established PTLD

In the solid organ transplant setting, the treatment of $CD20^+$ B-cell PTLD typically involves RI, followed by chemo-immunotherapy[508]. Unfortunately, the scope for RI is often limited by the potential for triggering alloreactive responses, which can lead to organ rejection and death. Although overall response rates to RI when used alone are reportedly as high as 45% in retrospective studies[509,510], the only prospective study to examine this showed response in only 1/16 (6%) cases[511]. Notably, surgery and/or radiotherapy may be curative where disease is localised to a single site[509,510]. No role for antiviral therapies is currently supported by existing data[508].

Most patients who remain unresponsive to RI are treated with Rituximab, with or without cytotoxic chemotherapy. A large body of evidence has demonstrated the benefit of Rituximab

in the treatment of $CD20^+$ NHL developing in immunocompetent patients. Meanwhile, 3 prospective studies have examined the use of Rituximab monotherapy (R-mono) for PTLD arising after solid organ transplant[512-514]. These have shown it to be well tolerated, and have reported complete remission rates of around 20 – 50% following 4 weekly infusions. However, early disease progression is common after R-mono, with around 60% of patients progressing within 12 months of treatment. As a consequence, Rituximab has often been used in combination with anthracycline based cytotoxic chemotherapy (R-chemo), the commonest regimen being CHOP (cyclophosphamide, doxorubicin, vincristine and prednisolone). Several retrospective studies have shown that increasing the intensity of PTLD treatment by using R-chemo leads to improved response rates of up to 100%, with overall survival rates of around 60% at 12 months[515-518]. However, this appears to be at the cost of toxicity, and treatment-related mortality up to 31% has been reported.

Deciding whether to initiate treatment with R-mono or R-chemo is challenging, not least because of a lack of robust data facilitating prognostication. Indeed, there is currently no universally agreed prognostic scoring system for PTLD[388]. Notably, British Committee for Standards in Haematology guidelines recommended R-mono for patients with low risk PTLD, and R-chemo for patients with aggressive disease[508]. Here, low risk disease has been defined as PTLD arising in patients aged less than 60 years, with normal LDH and good performance status, based on the study by Choquet et al., which included only 43 patients[513]. Interestingly, an alternative approach of 'sequential therapy' has been proposed by Trappe et al., in which all patients with $CD20^+$ PTLD are initially treated with 4 weekly infusions of R-mono, followed by a 4 week break from therapy, after which 4 (3 weekly) cycles of CHOP chemotherapy are delivered[519]. The aim of this strategy is to reduce toxicity by using R-mono

to initially debulk disease, leading to improved performance status and thus tolerability for R-CHOP. This was evaluated in 70 patients in the prospective phase II study PTLD-I, the largest prospective study on PTLD to date, showing an overall response rate of 60% after R-mono, rising to 90% after R-CHOP (CR rate of 67%), with a median overall survival of 79 months[519]. A treatment-related mortality of 10.6% was associated with the delivery of CHOP.

In the allo-HSCT setting, first line treatment for established PTLD is R-mono in combination with RI, where feasible. Reported response rates to such therapy are around 70%[520,521]. However, the management of patients who fail to respond to Rituximab is often challenging. In contrast to the SOT setting, outcomes following cytotoxic chemotherapy are extremely disappointing, with up to 100% mortality[520,521]. This is likely to be a consequence of increased toxicity in this patient group, such that allo-HSCT recipients are invariably unable to tolerate cytotoxic chemotherapy.

Cellular Therapy for PTLD

In recent years, a growing body of evidence has demonstrated an important role for adoptive cell therapy in the treatment of PTLD[522]. These therapies aim to treat, or prevent, PTLD by infusing EBV-specific T-cells in order to reconstitute virus-specific immunity and generate anti-tumour responses. Thus, patients with PTLD arising after allo-HSCT have been treated with DLI, which contain EBV-specific T-cells whenever the donor is EBV-seropositive, with response rates of around 70%[523-526]. However, because DLI contain unselected $CD8^+$ T-cells their use may be complicated by potentially life threatening GvHD; in the largest study of outcomes following DLI, Doubrovina et al. reported a rate of DLI-related acute GvHD of 17% amongst 32 patients treated[525].

Given the limitations of unselected T-cell therapy, preparations of EBV-specific cytotoxic T-lymphocytes (EBV CTLs) have been developed for clinical use. These are generated *in vitro* by repeatedly stimulating PBMCs from EBV-seropositive donors with irradiated autologous or HLA-matched LCLs, in the presence of IL2, for a period of 2-3 months. EBV CTLs generated from transplant donors have been shown to provide highly effective prophylaxis against PTLD amongst individuals undergoing allo-HSCT; Heslop et al. reported that none of 101 patients treated prophylactically developed PTLD[527,528]. Furthermore, EBV CTLs have been successfully used as pre-emptive therapy or as treatment for established PTLD in solid allograft and allo-HSCT settings[525,527-530].

Notably, one important limitation of EBV-specific CTLs are the long periods of time required to generate them in sufficient quantities *in vitro*. However, to circumvent this problem, cryopreserved banks of EBV CTLs have been generated from third party donors, and these cells have been used to treat partially HLA-matched recipients[531,532]. This approach was evaluated by Haque at al. in a prospective phase 2 study, in which 33 patients with progressive PTLD (31 of whom were solid allograft recipients) were treated with cryopreserved third party EBV CTLs[531]. No hypersensitivity or alloreactive responses were observed and an overall response rate of 52% at 6 months was observed. In a long term follow-up report, 12 of 14 patients who achieved CR remained alive and free of disease after 4 – 9 years[533]. Based on this experience a new third party EBV CTL bank has recently begun operating in the UK, led by Prof Mark Vickers from the University of Aberdeen.

In recent years, new innovations have contributed to the advancement of adoptive immunotherapy. These include methods for the rapid generation of EBV-specific CTLs. Thus

Moosmann et al. have developed an approach in which donor PBMCs are stimulated overnight with pools of EBV antigen-derived peptides, after which EBV-specific cells are selected by IFN-γ surface capture and immunomagnetic bead separation[534]. Infusion of the selected EBV-specific T-cells produced lasting responses in 3 of 6 patients with PTLD (3 patients had very advanced disease at the time of administration and therefore may have had limited potential to respond). Meanwhile, similar techniques have been used to select T-cells specific to just the EBNA1 antigen, infusion of which led to responses in 7 of 10 patents with EBV DNAemia or PTLD after allo-HSCT[535]. Notably, CTLs preparations containing cells specific to multiple viruses have also recently been developed[536,537]. Simultaneously targeting EBV, CMV and adenovirus, these multi-virus specific CTLs are designed to provide effective prophylaxis to some of the most serious viral complications affecting transplant recipients.

1.8 Aims of Current Work

A series of independent but complementary studies related to a central theme of EBV-associated PTLD were undertaken with the aim of extending our understanding in the following areas:

Retrospective Clinical Studies (Chapters 3 and 4)

In order to define the current clinical problem posed by PTLD, and to provide important context for the subsequent studies presented in this thesis, 2 retrospective clinical studies related to PTLD were undertaken. Thus, Chapter 3 presents the results of a multicentre United Kingdom study carried out to explore Rituximab era outcomes and prognostic factors for PTLD arising after solid organ transplant. Meanwhile, Chapter 4 presents the results of a study to characterise incidence, risk factors and outcomes for EBV reactivation and PTLD

arising in patients after T-cell deplete allo-HSCT.

Studies on the Persistence of EBV Following Allo-HSCT (Chapter 5)

The pathophysiology of EBV reactivation and PTLD following allo-HSCT remains imperfectly characterised. In particular, the nature of EBV persistence during the course of allo-HSCT, and how the reconstituting B-cell system might be altered during EBV reactivation, has not been explored in any detail. In healthy individuals, EBV is normally carried at low frequency within the memory B-cell compartment. Therefore, it is intriguing that EBV DNAemia typically occurs around 2 to 3 months following allo-HSCT, when the B-cell system is characterised by a predominance of $CD27^{-}IgD^{+}$ naive B-cells and a marked deficiency of $CD27^{+}$ memory B-cells. To explore this apparent paradox, blood samples collected from a cohort of patients undergoing allo-HSCT were analysed to determine the properties of circulating EBV-infected cells.

Modelling the Clonal Evolution of PTLD *in Vitro* (Chapter 6)

Previous studies in this and other laboratories have demonstrated that *in vitro* B-cell transformation by EBV is accompanied by clonal outgrowth of LCLs, such that over a period of several weeks polyclonal cultures tend towards oligoclonality and thereafter to monoclonality. This has been proposed as a possible model for PTLD. As such, factors which may influence the clonal outgrowth of LCLs *in vitro* might also be relevant to the hypothesised progression of early polyclonal B-cell proliferations to monoclonal lymphomas. In this chapter some of the processes which may influence clonal outgrowth are explored. In particular, the role of DNA damage response signalling and the acquisition of AID-associated mutations will be assessed as possible contributing factors.

DLI for Rituximab-Refractory PTLD (Chapter 7)

The introduction of Rituximab has led to a marked improvement in outcomes for patients developing PTLD following allo-HSCT. However, a proportion of patients remain refractory to Rituximab and are at significant risk of mortality. For such individuals, adoptive cellular therapy with DLI or EBV CTLs is increasingly being used. In this chapter, we describe 2 patients with Rituximab-refractory PTLD who were successfully treated with DLI. For both, detailed analysis of EBV antigen epitope-specific T-cell responses following DLI infusion was undertaken, yielding insights relevant to the future optimisation of cellular therapy.

2. Materials and Methods

2.1 Retrospective Study of PTLD Arising After Solid Organ Transplantation

This retrospective study invited participating centres to submit data on patients over 16 years of age with biopsy-proven PTLD diagnosed between 2000 and 2012. Data was collected from 4 clinical centres: University Hospital Birmingham, Birmingham, UK; The Royal Free Hospital, London, UK; St James's University Hospital, Leeds, UK.; The Freeman Hospital, Newcastle-upon-Tyne, UK. Due to case-finding and data retrieval limitations, submitted cases represent a proportion of total incident PTLD cases. All clinical, radiological and pathological data were critically reviewed and cases were excluded where they failed to meet inclusion criteria or where a minimal data set was not available. The study was conducted in line with National Research Ethics Service guidance for Service Evaluation and was registered with NHS Research and Development departments at each centre. Dr Sridhar Chaganti, Consultant Haematologist at University Hospital Birmingham, was the study lead.

Histopathology reports were used to categorise cases into pathological subtypes in accordance with the WHO classification system for PTLD[421] (Table 2). Cases were considered to be EBV-associated if EBV EBER *in situ* hybridisation and/or LMP1 immunohistochemistry were positive, or if significant EBV DNAemia was detected by EBV qPCR; negative staining for LMP1 in the absence of EBER *in situ* hybridisation was not considered sufficient to exclude EBV-association and such cases were classified as equivocal. Disease stage was determined from available clinical, bone marrow and radiological data, the latter comprising computed tomography (CT) and/or positron emission tomography (PET), in accordance with the Ann Arbor staging system[538,539], including the Lugano classification[540] for primary

gastrointestinal lesions.

Response to therapy was evaluated on the basis of submitted clinical and radiological data and was categorised into complete remission (CR), partial remission (PR) or no remission (NR), in line with the Cheson criteria.[541] Owing to the nature of the study, the timing and modality of response evaluation were determined clinically. Overall survival was calculated from the date of diagnosis to the date of death or last follow-up. Event-free survival was calculated from date of diagnosis to date of discontinuation of treatment for any reason, initiation of new treatment, disease progression, or death from any cause. Progression-free survival was calculated from date of diagnosis to date of disease progression or death from any cause. Factors influencing selection of R-mono versus R-CHOP were analysed using univariate and multivariate logistic regression. Predictors of overall survival were analysed using univariate and multivariate Cox proportional hazards modelling.

2.2 Retrospective Study of EBV Reactivation and PTLD Following Allo-HSCT

This retrospective study examined adult patients undergoing consecutive T-cell deplete allo-HSCT at University Hospital Birmingham between May 2009 and September 2012. All participants provided written consent for clinical data collection and the study was registered with the University Hospital Birmingham's Research and Development department. All patients received myeloablative or RIC preparative conditioning according to institutional protocols, followed by PBSC grafts. T-cell depletion was with *in vivo* Alemtuzumab, typically comprising 10mg daily intravenously from day -7 to day -3 before stem cell infusion, or with ATG. GvHD prophylaxis comprised cyclosporin, with or without methotrexate, or mycophenolate mofetil. All patients received aciclovir prophylaxis for a

minimum of 3 months following transplant.

Patients were monitored with EBV qPCR whole blood assay, with testing scheduled every 1 - 2 weeks for the first 6 months post-transplant and intermittently thereafter[542]. For the purpose of this study, EBV reactivation was defined as a single positive EBV qPCR result exceeding the assay limit of sensitivity of 500 genomes/ml, whist high-level EBV reactivation was defined as a single result ≥20,000 genomes/ml. Patients exceeding the high-level EBV threshold were assessed for possible PTLD and received pre-emptive treatment with up to 4 weekly infusions of Rituximab 375 mg/m^2. Cases of PTLD were diagnosed in accordance with recently published definitions for biopsy-proven or probable disease arising after allo-HSCT, the latter including radiologic evidence of disease in association with EBV DNAemia[496].

Cumulative incidence of EBV reactivation following allo-HSCT was estimated, taking the competing risk of death into account. Cumulative incidence curves were compared using the Log Rank test. Univariate and multivariate analysis of risk factors for EBV reactivation were performed using Cox proportional hazards modelling. Acute GvHD was treated as a time-dependent covariate. Overall survival was calculated from transplant to the time of death from any cause; surviving patients were censored at last follow-up. Non-relapse mortality was calculated from transplant to the time of death without relapse, which was considered a competing event. The effect of post-transplant (pre-emptive) Rituximab therapy on overall survival or non-relapse mortality was analysed using Cox testing, considering Rituximab as a time-dependent covariate; patients who died from PTLD were excluded from this analysis to eliminate the effect of PTLD-related mortality. The effect of pre-transplant Rituximab therapy

on overall survival or non-relapse mortality was analysed using Cox testing. All analyses were carried out in Stata 12.

2.3 Biological Samples

Work presented in Chapters 5, 6, and 7 made use of the following donor materials:

Patients Undergoing Allo-HSCT

Blood samples (and clinical data) were collected from patients undergoing allo-HSCT at University Hospital Birmingham, UK under the National Research Ethics Service (NRES) committee approved 'Study of immune reconstitution following stem cell transplantation,' (Chief Investigator, Prof Paul Moss, University of Birmingham). Additional samples (and clinical data) were collected from Nottingham University Hospital, UK under the NRES approved 'Study of Epstein-Barr virus after transplantation' (Chief Investigator, Dr David Burns, University of Birmingham).

Healthy Adult Donors

Blood samples were obtained from healthy laboratory donors under the NRES committee approved study 'Epstein-Barr virus infection of human lymphocytes and the pathogenesis of virus associated lymphomas' (Chief Investigator, Dr Andrew Bell, University of Birmingham). Apheresis cones (buffy coats) from healthy adult donors were also obtained via NHS Blood and Transplant (NHSBT) under the same ethics.

Umbilical Cord Blood

Samples of umbilical cord blood were collected from Birmingham Women's Hospital via the

University of Birmingham Human Biomaterials Resource Centre, with appropriate ethical approval.

Cell Lines

Namalwa-BL is a Latency III EBV-positive BL line with 2 stably integrated copies of the EBV genome[543]. AKBM cells are a derivative of the EBV-positive Japanese BL cell line Akata, stably transfected with a GFP reporter (pHEBO-BMRF1p-rCD2/GFP) under the control of the promoter for the EBV lytic cycle BMRF1 gene[544]. Kem-BL and Rael-BL are endemic EBV-positive Latency I BL lines[100,545]. Kem-BL clone h10 is an EBV-negative subclone of Kem-BL. HEK293 is a human embryonic kidney cell line immortalised by the adenoviral early region[546]. The HEK293-2089 cell line is a derivative of HEK293, stably transfected with a bacterial artificial chromosome (2089) containing the genome of the standard laboratory EBV strain B95-8 and a hygromycin resistance gene[547]. The HEK293-BZLF1-KO cell line is a derivative of HEK293, stably transfected with a recombinant EBV BAC in which the IE gene BZLF1 gene has been inactivated[548]. The CD40L mouse L-cell line is the LTK^- mouse fibroblast cell line stably expressing human CD40L[549].

2.4 Maintenance of Cell Lines

EBV-transformed LCLs and BL cell lines were maintained in RPMI 1640 medium (Gibco or Sigma) supplemented with 10% v/v foetal calf serum (BioSera), 2mM L-glutamine (Gibco) and 500 U/ml penicillin and streptomycin (Gibco), known henceforth as standard B-cell medium. Mitogen-stimulated blasts were maintained as described below. HEK293-2089 and HEK293-BZLF1-KO cells were maintained in standard B-cell medium, supplemented with 100μg/ml hygromycin. CD40L L-cells and LTK^- cells were maintained in DMEM medium

(Gibco) supplemented with 10% v/v FCS, 2mM L-glutamine (Gibco) and 500 U/ml penicillin and streptomycin (Gibco). All cells were cultured at 37°C with 5% CO_2.

2.5 Isolation and Storage of Peripheral Blood Mononuclear Cells

Blood samples were diluted 1:1 in phosphate buffered saline (PBS) and then overlaid onto 15ml Lymphoprep (Axis-Shield) in 50ml tubes. Samples were then centrifuged at 1800rpm (without brake) for 30 minutes at room temperature. The top layer containing serum and platelets was then removed with a transfer pipette and discarded, after which the buffy coat layer was collected. The cells were then washed twice in PBS or RPMI 1640 and either used immediately, transferred to 1.5ml microcentrifuge tubes and frozen as pellets at -20°C, or transferred to cryovials in RPMI 1640 medium supplemented with 20% FCS and 10% v/v dimethylsulphoxide (DMSO) and cryopreserved in liquid nitrogen. Cryopreserved cells were subsequently thawed by incubating cryovials in a 37°C water bath for approximately 1 minute before adding them drop-wise to RPMI 1640 medium or MACS buffer supplemented with 10% FCS, after which they were washed at least once according to requirement.

2.6 Surface Immunophenotyping of PBMCs with Flow Cytometry

Immunophenotyping of allo-HSCT patient and healthy adult donor PBMCs was performed by staining thawed PBMCs with up to 8-colour combinations of the antibodies listed in Table 3. 2.5 $x10^5$ – 1.0 $x10^6$ PBMCs were washed in MACS buffer before resuspending them in 50µl of MACS buffer containing a mixture of fluorochrome-conjugated antibodies at predetermined concentrations. The cells were incubated on ice in the dark for 30 minutes before washing in cold MACS buffer, after which they were resuspended in MACS buffer for analysis. Samples were stored at 4°C in the dark and analysed within 2 hours of staining.

Marker	Fluorochrome	Clone	Manufacturer	No.
CD3	eFluor 450	UCHT1	eBioscience	48-0038
CD3	APC-eFluor 780	UCHT1	eBioscience	47-0038
CD4	APC	SK3	eBioscience	17-0047
CD8	PerCP-Cy5.5	SK1	Biolegend	344709
CD10	PerCP-eFluor 710	SN5c	eBioscience	46-0108
CD14	Pacific Blue	M5E2	Biolegend	301828
CD14	APC	MEM-15	Abcam	ab60901
CD19	PE-Cy7	HIB19	eBioscience	25-0199
CD20	Alexa Fluor 700	2H7	Biolegend	56-0209
CD23	APC-Cy7	EBVCS-5	Biolegend	338520
CD24	APC-eFluor 780	SN3	eBioscience	47-0247
CD27	PE	M-T271	BD	555441
CD30	APC	BerH8	BD	563500
CD38	APC	HIT2	Biolegend	303510
CD45	Alexa Fluor 700	HI30	Biolegend	304023
CD56	Pacific Blue	MEM-188	Biolegend	304629
CD56	PE	HCD56	Biolegend	318306
EBNA-LP*	Unconjugated	JF186[147]	In house	NA
IgA	APC	IS11-8E10	Miltenyi	130-093-113
IgD	FITC	IA6-2	Biolegend	348206
IgD	PerCP-Cy5.5	IA6-2	Biolegend	348208
IgG	FITC	G18-145	BD	555786
IgM	APC-Cy7	MHM-88	Biolegend	314519
Kappa	PE	MHK-49	Biolegend	316508
Kappa	APC	MHK-49	Biolegend	316510
Ki-67*	FITC	B56	BD	556026
Lambda	FITC	MHL-38	Biolegend	316606
Phospho-H2AX*	eFluor 660	CR55T33	eBioscience	50-9865
TCR αβ	Alexa Fluor 488	IP26	Biolegend	306711

Table 3. Antibodies for Flow Cytometry

Up to 8-colour combinations of the mouse anti-human monoclonal antibodies shown here were used to stain PBMCs and cell lines during the course of these studies. *Intracellular staining.

Sytox Blue (Invitrogen) was added to the samples around 5 minutes before analysis to facilitate dead cell discrimination. Stained cells were acquired on an LSRII (BD Biosciences) and a minimum of 30,000 lymphocyte and/or 2500 $CD19^+$ events were recorded. Data was analysed using FacsDIVA software (BD Biosciences). In all flow cytometry panels, lymphocytes were gated on forward (FSC) and side scatter (SSC), after which doublets, dead cells, $CD14^+$ monocytes and/or $CD3^+$ and/or $CD56^+$ events were excluded as appropriate. Lymphocyte counts determined by analysis of blood using automated haematology analysers (performed in clinical laboratories) were used to derive lymphocyte subset cell counts.

2.7 Flow Cytometric Cell Sorting

Cell sorting was performed using a MoFlo Cell Sorter (Beckman Coulter). When sorting PBMCs isolated from allo-HSCT patients or healthy adults, 0.5-1.0 $x10^7$ PBMCs were stained in MACS buffer on ice for 30 minutes using the following mix of fluorochrome-conjugated antibodies at predetermined concentrations: CD27 PE, IgD PerCp-Cy5.5, CD19 PE-Cy7, CD14 APC and CD3 APC-efluor 780 (Table 3). After gating lymphocytes on FSC and SSC, doublets and $CD14^+$ monocytes were excluded before sorting $CD19^+IgD^+CD27^-$ naive B-cells, $CD19^+CD27^+$ memory B-cells and $CD19^-$ non-B-cells into tubes containing 250 µl FCS. Reanalysis confirmed that the purity of sorted cells was typically >98%.

In order to assay EBV genomes in single cells, a proportion of sorted naive and memory B-cells were subsequently re-sorted into 96-well plates containing 5µl of lysis buffer (see Section 2.8), depositing 1 cell per well. As a comparator, AKBM cells were induced to enter lytic cycle by exposure to 100µg/ml F(ab')2 goat anti-human IgG antibody (Cappel) for 48 hours before sorting single GFP-positive cells as above. The reliability of single cell sorting

was confirmed by visual inspection of 96-well plates under a light microscope, and also by sorting EBV-positive and EBV-negative Kem-BL cells mixed in known proportions, which were subsequently assayed using EBV qPCR (as shown in Section 5.10).

2.8 Extraction and Purification of DNA

Genomic DNA was extracted from pellets of 0.25 - 5.0 $x10^6$ cells using the DNeasy Blood and Tissue kit (Qiagen), according to the manufacturer's instructions. DNA was eluted in 50 – 100µl DEPC treated PCR grade water (Ambion) as appropriate to cell input. DNA concentration was determined using a NanoDrop™ spectrophotometer and samples were stored at -20 °C. Where cell input was <0.25 $x10^6$, including when cells were FACS-sorted into 96-well pates, DNA was extracted *in situ* by incubating cells in lysis buffer (50 mM KCl, 10 mM Tris-HCl, pH 8.3, 2 mM $MgCl_2$, 0.5% Tween-20, 0.4 mg/mL Proteinase K) at 55°C for 2 hours followed by 95°C for 15 minutes to inactivate the Proteinase K.

2.9 TaqMan qPCR to Estimate EBV DNA Load

EBV qPCR Assay

To quantitate EBV genomes, real time quantitative PCR (qPCR) amplification of the EBV polymerase gene BALF5 (EBV pol) and of the cellular gene beta-2-microglobulin (β2M) gene was performed in a multiplex assay, using the primers (Alta Bioscience, University of Birmingham) and probes (Eurogentec) shown in Table 4. PCR amplification was performed using TaqMan Universal PCR Master Mix (ABI Applied Biosystems) which contains PCR buffer, $MgCl_2$, AmpliTaq Gold, dNTPs and ROX (a passive reference dye). For each reaction, 20µl of a mix containing 1x TaqMan Universal PCR Master Mix, primers and probes at the final concentrations given in Table 4 and PCR grade water (Ambion) to make up the final

Target	Primer / Probe	Primer Sequence	Final conc.	Conditions
EBV Pol	Forward	5'AGTCCTTCTTGGCTAGTCTGTTGAC3'	200µM	95°C for 10 min to activate AmpliTaq Gold 40 cycles of: Denaturation at 95°C for 15 sec Annealing and extension at 60°C for 1 min
	Reverse	5'CTTTGGCGCGGATCCTC3'	200µM	
	Probe	5'FAM-CATCAAGAAGCTGCTGGCGGCC-TAMRA3'	200nM	
β2M	Forward	5'GGAATTGATTTGGGAGAGCATC3'	60nM	
	Reverse	5’CAGGTCCTGGCTCTACAATTTACTAA3'	80nM	
	Probe	5'VIC-AGTGTGACTGGGCAGATCATCCACCTTC-TAMRA3'	100nM	

Table 4. Primers, Probes and Conditions for EBV qPCR

volume, was added to wells of a 96-well PCR plate. To each well, 5µl of DNA was then added in duplicate or triplicate. On each plate, alongside test samples, standards consisting of DNA from the Namalwa-BL cell line (known to contain 2 integrated copies of the EBV genome) serially diluted in PCR-grade water to generate a set of 8 concentrations ranging from 4 $x10^4$ copies/µl to 1 copy/µl were included, as well as a no-template control. Wells were sealed with Microamp Optical Caps (Applied Biosystems) and the plates were shaken to mix the reagents before centrifuging at 1000rpm. The plates were then analysed in an ABI Prism 7500 Sequence Detection System (Applied Biosystems), using the thermal cycling conditions shown in Table 4.

Analysis of EBV qPCR Data

qPCR data was analysed using Applied Biosystems 7500 software version 2.0.5. Namalwa standards were used to generate pol and β2M calibration curves, from which test sample copy number values were determined. EBV loads were calculated as the number of pol copies per 10^6 cells (assuming 2 β2M copies per diploid cell).

2.10 Determination of EBV Gene Expression Using RT-PCR

EBV gene expression was measured using a panel of TaqMan PCR assays designed to detect selected latent and lytic cycle transcripts. Due to the small of amounts of RNA available, a modified version of our existing method[550] was used which employed a pre-amplification step and a high throughput 48:48 Dynamic Array Integrated Fluidics Circuit (Fluidigm). In addition, a reference plasmid containing a single copy of each target amplicon was designed such that absolute numbers of each transcript could be determined[551].

TaqMan PCR Assays

Forty-five EBV-specific TaqMan PCR assays, each consisting of a forward and reverse primer and a FAM/TAMRA-labelled probe, were designed to detect a range of EBV latent and lytic transcripts; full sequence details are provided in the Appendix (Table 26). Endogenous control assays to detect glyceraldehyde-3-phosphate dehydrogenase (GAPDH, assay ID hs99999905.m1), β2M (assay ID hs00187842) and phosphoglycerate kinase 1 (PGK1, assay ID hs99999906.m1) were obtained from Life Technologies.

Plasmid for Absolute Quantitation

To perform absolute rather than relative quantitation of transcript levels, a 4951bp DNA sequence containing each of the 45 EBV target amplicons and 3 cellular target amplicons was designed[551]. This sequence was commercially synthesised and cloned into pUC57 by GenScript. The resulting plasmid (AQ-plasmid) was diluted in PCR-grade water to generate a range of 10-fold serial dilutions containing 10^5 to 10^1 copies/µl.

RNA Isolation and DNA Synthesis

Total RNA was extracted from approximately 5 x10^4 $CD27^+$ sorted memory B-cells from allo-HSCT patients, using the RNeasy Micro kit (Qiagen), or up to 5 x10^6 cells from EBV-positive reference cell lines using the Nucleospin RNA kit II (Macherey Nagel); both kits include a DNAse I step. Total RNA was then reverse transcribed into cDNA using qScript cDNA SuperMix (Quanta Biosciences), including approximately 5ng RNA in a final reaction volume of 3µl for transplant samples or 400ng RNA in a final reaction volume of 20µl for cell lines.

Specific Target Amplification

An aliquot of cDNA (1.25 µl) was subsequently pre-amplified for 12 (cell lines) or 14 (transplant patient samples) cycles using 2.5µl TaqMan® PreAmp Master Mix (Life Technologies) and 1.25µl 2x primer mix containing 45 EBV and 3 cellular 20 x Taqman assays diluted in DNA suspension buffer (10 mM Tris, pH 8.0, 0.1 mM EDTA) according to the manufacturer's protocol. These pre-amplified samples were then diluted 1:5 in DNA suspension buffer prior to loading on a 48:48 Dynamic Array IFC (Fluidigm) alongside the PCR assays, according to the manufacturer's protocol. To enable absolute quantitation, the 48:48 array also included dilutions of the AQ-plasmid (corresponding to 10^5, 10^4, 10^3, 10^2 and 10^1 copies per µl input sample) which had been subjected to the appropriate number of pre-amplification cycles. Once assembled, the 48:48 array was loaded into a Biomark HD system (Fluidigm) and the PCR amplification performed using the standard v1 protocol. The data was analysed using the Biomark Real Time PCR Analysis Software v2.0.

2.11 Determination of Chimerism Using Microsatellite Analysis

To determine recipient or donor origin of $CD27^+$ B-cells from allo-HSCT patients, DNA extracted from approximately 1.0 $x10^4$ FACS-sorted $CD27^+$ memory B-cells was sent for microsatellite marker analysis, performed by the Clinical Pathology Accredited West Midlands Regional Genetics Laboratory, Birmingham, UK. Samples were compared to pre-transplant recipient and donor samples using at least 2 polymorphic microsatellite markers. The results were reported as percentage of donor or recipient origin.

2.12 Determination of EBV Strains in Allo-HSCT Patients and Donors

PCRs for EBNA3B and EBNA3C

To identify EBV strains in allo-HSCT patients and donors, DNA extracted from PBMCs was subjected to nested and semi-nested PCR amplification of polymorphic regions of EBNA3B and EBNA3C using published primers[552] shown in (Table 5). PCR was performed using the Expand High Fidelity PCR System (Roche) which contains a mixture of Taq DNA polymerase and a second DNA polymerase possessing a 3'-5' exonuclease proofreading activity to improve fidelity. This system reportedly has 3-fold better DNA synthesis fidelity compared to standard Taq DNA polymerase, with an estimated error rate of 8.3 $x10^{-6}$ bp compared to 2.6 $x10^{-5}$ bp[553]. Care was taken to avoid cross contamination, including the use of a dedicated PCR room with an ultraviolet (UV) irradiation facility to set up assay mixes, and alternative set-up areas when handling first and second round PCR products. Non-template controls were included for all assays.

Reactions were performed in 0.5 ml PCR tubes, each of which contained 5 µl of template DNA, a final concentration of 1x Expand High Fidelity Buffer containing 1.5 mM $MgCl_2$, 2.6 units of Expand High Fidelity Enzyme mix (containing Taq DNA polymerase), 200 µM each of dATP, dGTP, dTTP and dCTP, 1 µM each of forward and reverse primers, in a final volume of 50 µl made up with PCR grade water (Ambion). PCR amplification was performed in an Eppendorf Thermocycler using the conditions shown in Table 5. Completed PCR reactions were stored at -20°C.

Identification and Purification of the PCR Products

Second round PCR products were separated by electrophoresis in 1.5% agarose gels in 1x

Target	Round	Direction	Primer Sequence	Size (bp)	Conditions	
EBNA3B	Round 1	Forward	5'AAGAAGGACCACACTCATATACG3'	665	Denaturation	94ºC 5 min
					Denaturation	94ºC 30 sec
					Annealing	55ºC 1 min
		Reverse	5'TTTTCAAGAAGGTCTAGCAT3'		Extension	72ºC 1 min x 40 cycles
					Extension	72ºC 5 min
	Round 2	Forward	5'CGCCAGTGCACCGGGAGACCC3'	543	Denaturation	94ºC 5 min
					Denaturation	94ºC 30 sec
					Annealing	70ºC 1 min
		Reverse	5'CAAAGGTTGCCATGGCTCCAG3'		Extension	72ºC 1 min x 40 cycles
					Extension	72ºC 5 min
EBNA3C	Round 1	Forward	5'CACAAAGCACCCCTGAAAGG3'	314	Denaturation	94ºC 5 min
					Denaturation	94ºC 30 sec
					Annealing	60ºC 1 min
		Reverse	5'GGCTCGTTTTTGACGTCGGC3'		Extension	72ºC 1 min x 40 cycles
					Extension	72ºC 5 min
	Round 2	Forward	Same as round 1 forward primer	277	Denaturation	94ºC 5 min
					Denaturation	94ºC 30 sec
					Annealing	60ºC 1 min
		Reverse	5'GTCTTGATGTTTCCGATGTGGCTTA3'		Extension	72ºC 1 min x 40 cycles
					Extension	72ºC 5 min

Table 5. Primers and Conditions for EBNA3B and EBNA3C PCRs

TBE running buffer (89 mM Tris-borate, 2 mM EDTA, pH 8.3), alongside 1kb DNA ladder (Invitrogen). Care was taken to avoid cross contamination by using alternate lanes. Gels were stained with ethidium bromide and bands visualised using a UV transilluminator (Geneflow). Appropriately sized bands were cut out of gels using a new scalpel blade each time and placed into 1.5 ml microcentrifuge tubes. PCR products were extracted using the Qiaquick Gel Extraction Kit (Qiagen) according to the manufacturer's instructions, eluted in 30µl of PCR grade water (Ambion) and stored at -20°C.

Sanger Sequencing of PCR Products

The purified second round EBNA3B and EBNA3C PCR products were Sanger sequenced, using the EBNA3B reverse primer and EBNA3C forward primer (Table 5). Each sequencing reaction contained approximately 200-500ng DNA and 3.2 pmol of primer, made up to a final volume of 10µl with PCR grade water (Ambion). Sequencing was performed using the 'Plasmid to Profile' DNA sequencing service provided by the Functional Genomics Laboratory, University of Birmingham, UK.

Analysis of Sequence Data

Sequence data was analysed using the BioEdit software package version 7.2.0 (Ibis Therapeutics; http://www.mbio.ncsu.edu/bioedit/bioedit.html). Sequences were aligned to the corresponding regions of the reference B95-8 genome (Accession number NC_007605.1) using the ClustalW Multiple Alignment tool. Each chromatogram trace was manually inspected to verify any base changes relative to the EBNA3B and EBNA3C reference sequences..

2.13 Intracellular Flow Cytometry for Ki-67

To stain FACS-sorted $CD27^+$ memory B-cells or LCLs for intracellular Ki-67, cells were first fixed in ice cold 70% ethanol and stored at -20°C for between 1 and 7 days. After washing twice in MACS buffer the cells were resuspended in 100 µl of MACS buffer plus 20 µl of anti-human Ki-67 FITC antibody or isotype control (BD Biosciences). After incubating for 1 hour at room temperature in the dark, the cells were washed with several volumes of MACS buffer and then resuspended in a small volume for analysis. Cells were acquired on an Accuri flow cytometer (BD biosciences) and data was analysed using FlowJo version 7.6.5 software.

2.14 Purification of $CD19^+$ B-Cells

$CD19^+$ Dynabead Selection

B-cells were positively selected from PBMCs isolated from apheresis cones and umbilical cord blood samples using pan-CD19 Dynabeads (Life Technologies) according to the manufacturer's instructions. PBMCs were mixed with Dynabeads at a ratio of 4 beads per B-cell (assuming B-cells comprise 5% of PBMCs), adjusted to a final concentration of 1 $x10^7$ beads/ml in cold RPMI 1640 with 1% FCS. Following incubation at 4°C for 30 minutes with gentle mixing, bead-bound cells were collected by attaching to a magnet for 2 minutes and then washing with 10 ml RPMI 1640 with 1% FCS; a total of 5 magnet/wash procedures were performed to ensure high purity of isolated B-cells. The Dynabeads were subsequently detached by incubating bead-bound B-cells with 10 µl DETACHaBEAD for every 25 µl of Dynabeads used, at a final concentration of 100 µl DETACHaBEAD per ml, at room temperature with gentle mixing for 45 minutes. Bead-free B-cells were finally recovered by making the mixture up to 10 ml with RPMI 1640 with 1% FCS before allowing the Dynabeads to attach to the magnet for 2 minutes, after which the supernatant containing free

$CD19^+$ B-cells was recovered; the magnet/wash procedure was repeated to achieve maximal recovery of the B-cells. Purified cells were counted and stored at 4°C in standard B-cell medium for a maximum of 24 hours before usage. Purity of the recovered B-cells was typically >98%, as confirmed by flow cytometry for CD19 surface antigen.

Flow Cytometric Cell Sorting

As required, Dynabead-selected B-cells were FACS-sorted using a MoFlo cell sorter (Beckman Coulter). Up to 4 $x10^7$ B-cells were stained in MACS buffer on ice for 30 minutes using predetermined concentrations of fluorochrome-conjugated antibodies against CD27 and IgD (Table 3). Subsequently, after excluding debris and doublets, $CD27^-IgD^+$ naive, $CD27^+IgD^-$ CSM and $CD27^+$ IgD^+ NSM B-cell subsets were sorted into tubes containing 250 µl of FCS. Reanalysis confirmed that the purity of sorted cells was typically >98%.

2.15 Generation of LCLs

Preparation of EBV Supernatant

2089 and BZLF1-knock out (BZKO) virus supernatants were prepared from HEK293-2089 and HEK293-BZLF1-KO cell lines induced into lytic cycle by transfection with plasmids containing the BZLF1 viral transactivator (p509) and BALF4 (pRA) in the presence of lipofectamine. Supernatants were harvested 3 - 5 days following lytic induction, filtered with a 0.45µm membrane filter and then stored at -80^oC until use. To determine the concentration of viral genomes present in the recovered supernatant, a DNA lysate was prepared from an aliquot by incubating with 2x lysis buffer (2x PCR buffer, 2% Tween20, and 0.2 mg/ml Proteinase K) at 55 ^oC for 1 hour, followed by 95 ^oC for 5 minutes to inactivate the Proteinase K. The prepared lysate was then tested using EBV qPCR. Viral supernatants used in this

study typically contained 1.0 $x10^8$ – 2.5 $x10^8$ genomes/ml.

B-Cell Infections

2089 and BZKO LCLs were generated by incubating purified B-cells with virus supernatant at a multiplicity of infection (MOI; the ratio of virus particles to target cells) of 50 for 1 – 2 hours at 37 ^oC. Following centrifugation at 1600 rpm for 5 minutes, cells were re-suspended in standard B-cell medium, and then 0.5 – 4.0 $x10^6$ cells were added to either 48-, 24- or 12-well plate wells as appropriate to give an optimal cell density for transformation. Cultures were inspected daily and fed with fresh medium at least every 3 - 4 days. As cell numbers increased the cultures were transferred to larger size wells or flasks in order to maintain optimal seeding density.

2.16 Generation of B-Cell Blasts

B-cell blasts were generated from primary $CD19^+$ B-cells by culturing them on mouse L-cell fibroblasts stably transfected with human CD40L, in the presence of human interleukin-4 (IL4)[554]. L-cells were irradiated with 100 Gray and then plated into 6cm tissue culture plates at 0.5 $x10^6$ per well and allowed to adhere overnight. 0.5 – 4.0 $x10^6$ B-cells were then transferred onto the L-cell coated wells in 3 ml of Iscove's Modified Dulbecco's Medium supplemented with 10% human serum, 2 mM L-glutamine (Gibco), 500 U/ml penicillin and streptomycin (Gibco) and 50 ng/ml IL4 (Biolegend or Prospec). The blasts were maintained for up to 8 weeks by transferring them onto new L-cell coated wells in fresh media every 3-4 days. In some cases, larger scale cultures were maintained by transferring up to 10 $x10^6$ B-cell blasts onto 10 cm plates prepared with 2.5 $x10^6$ irradiated L-cells per plate in 10 ml of medium.

2.17 Cell Counts in LCLs and B-Cell Blasts

For experiments comparing growth rates of LCLs and B-cell blasts, cell counts were performed using a TC20 Automated Cell Counter with trypan blue dead cell exclusion. At each passage known cell numbers were re-cultured and increases recorded at the following passage were used to calculate growth rates, according to the exponential growth equation:

$$N_T = N_0 \times e^{RT}$$

where N_T is the number of cells at time T, N_0 is the initial number of cells, and R is the growth rate. Cells counts in early EBV-infected and B-cell blast cultures were performed using an Accuri flow cytometer (BD Biosciences). Aliquots of cell culture were analysed to determine events per µl of media after excluding debris. Non-viable, non-blastoid and blastoid subsets were identified as discussed in Section 6.2. Propidium iodide was added to culture medium 5 minutes before analysis for dead cell discrimination in selected experiments.

2.18 Intracellular Flow Cytometry for EBNA-LP

To stain LCLs for EBNA-LP, cells were washed in PBS and then fixed by resuspending them in 4% paraformaldehyde in PBS (pH 7.0) with vortexing. After incubating them at 37°C for 10 minutes, the cells were centrifuged and resuspended in ice cold 90% methanol with vortexing, before storing them at -20 °C. The cells were subsequently washed twice in MACS buffer and then resuspended in 50 µl of MACS containing a 1/10 dilution of the anti-EBNA-LP antibody JF186[147]. After incubating for 1 hour at room temperature, the cells were washed twice in MACS buffer and then resuspended in 50 µl of MACS containing a 1/1000 dilution of Alexa Fluor-488-conjugated goat anti-mouse secondary antibody (Invitrogen). After

incubating for 1 hour in the dark, the cells were washed twice in MACS buffer before being resuspended in a small volume for analysis. Cells were acquired on an Accuri flow cytometer (BD biosciences) and data was analysed using FlowJo version 7.6.5 software.

2.19 Analysis of Proliferation with CFSE Labelling

Proliferation kinetics in early LCLs and B-cell blasts were also assayed by labelling B-cells with CFSE, prior to infection or mitogen-stimulation. Labelling was performed by first washing purified B-cells 3 times with PBS (without FCS), and then thoroughly resuspending them at 1 - 2 $x10^7$/ml in PBS. The cell suspension was then vortexed 1:1 with PBS containing CFSE to give a final concentration of 1.25μM. After incubating at 37°C for 10 minutes, 4-5 volumes of RPMI 1640 containing 10% FCS was added to stop the labelling process, after which the cells were washed 3 further times in RPMI 1640 containing 10% FCS. Labelled cells were used to generate LCLs and B-blast cultures as described, and aliquots were analysed daily for up to 10 days using an Accuri flow cytometer (BD Biosciences). Data were analysed with FlowJo version 7.6.5 software (TreeStar). After excluding doublets and dead cells based on FSC and SSC profile, events within viable non-blastoid and blastoid gates were analysed to determine the number of events in each generation. CFSE data were subsequently analysed using 2 alternative methods. The first used the methodology of the FlowJo Proliferation Tool to calculate 'Proliferation Index' as the average number of divisions of responding cells (cells that have undergone at least 1 division)[555,556]. The second was that of Hawkins et al., which determines 'Mean Division Number' by fitting the number of cells in each cell division to a Gaussian distribution[557]. Illustrative examples are given in Section 6.2 (Figures 52 and 54).

2.20 Intracellular Flow Cytometry for Phospho-H2AX

To stain EBV-infected cultures and B-cell blasts for intracellular phospho-H2AX, cells were fixed and permeabilised in 4% paraformaldehyde and 90% methanol, as described in Section 2.18. Prior to fixation, cells were labelled with the Fixable Viability Dye eFluor® 520 (eBioscience) to allow dead cell discrimination, according to manufacturer's instructions. For the comparison of phospho-H2AX in EBV-infected and B-cell blast cultures, B-cells were also labelled with Proliferation Dye eFluor® 450 (eBioscience) using a method similar to that for CFSE labelling, and mouse L-cells were labelled with CFSE, to aid discrimination of B-cell blasts from contaminating L-cells. Fixed cells were subsequently washed twice in MACS buffer and then resuspended in 50 µl of MACS containing eFluor 660-conjugated mouse anti-human phoso-H2AX antibody or isotype control (eBioscience) at predetermined concentrations. After incubation for 1 hour at room temperature in the dark, the cells were washed twice in MACS buffer before being resuspended in a small volume for analysis. Cells were acquired on an LSRII flow cytometer (BD biosciences) and data was analysed using FlowJo version 7.6.5 software.

2.21 Determination of Clonality by IgVH CDR3 Spectratyping

To determine the clonality of LCL and B-cell blasts cultures, IgVH spectratyping was performed by the West Midlands Genetics Laboratory using the IgH Gene Clonality Assay kit (Invivoscribe). Briefly, genomic DNA was amplified using PCR primers spanning the unique hypervariable CDR3 region of the IgH gene, with a forward PCR primer located in conserved framework region 1 (FR1) and a reverse primer in the J region. Fluorescently labelled PCR products (ranging in size from 270-350 bp) were subsequently separated on an ABI capillary gel electrophoresis platform and analysed using the Genemapper version 4.0 software

package (Applied Biosystems). Samples were tested alongside polyclonal and monoclonal controls supplied with the kit.

2.22 Analysis of IgVH rearrangements

IgVH PCR

PCR amplification of the IgVH region (IgVH PCR) was performed using published primers[460,558]. These comprised a forward primer corresponding to a consensus sequence for the framework 1 (FR1c) region, and a mix of reverse primers including a consensus primer for JH1, JH2, JH4 and JH5 regions, and separate primers for JH3 and JH6 (Table 6). PCR reactions were set up in a dedicated room, and non-template and Namalwa DNA positive controls were included for all assays. Reactions were performed in 0.5 ml PCR tubes, each of which contained 5 µl of template DNA, a final concentration of 1x Expand High Fidelity reaction buffer with 1.5mM $MgCl_2$ (Roche), 3.5 units of Expand High Fidelity enzyme mix (Roche), 200µM each of dATP, dGTP, dTTP and dCTP, 0.8µM of forward primer and 0.26µM of each reverse primer, in a final volume of 50 µl made up with PCR grade water (Ambion). PCR amplification was performed in an Eppendorf Thermocycler using the conditions shown in Table 6. Completed PCR reactions were stored at -20°C until analysis.

Identification and Recovery of the PCR Product

Since analysis of the PCR products demanded better resolution than that provided by an agarose gel, non-denaturing polyacrylamide gels were used. 13µl of gel loading dye (1.25 mg/ml bromophenol blue, 1.25 mg/ml xylene cyanol, 30% v/v glycerol) was added to 50µl of PCR product. Aliquots of 5µl and 50µl of sample were loaded in adjacent wells of a gel comprised of 8% acrylamide solution (BioRad), 0.07% w/v ammonium persulphate and

Primer	Primer Sequence	Conditions	
Forward	5'AGGTGCAGCTGSWGSAGTCDGG3' (FR1c)	Denaturation	94ºC 5 min (hot start)
		Denaturation Annealing Extension	94ºC 30 sec 61ºC 1 min 72ºC 1 min x 29 cycles
Reverse	5'ACCTGAGGAGACGGTGACCAGGGT3' (JH1, JH2, JH4 and JH5) 5'TACCTGAAGAGACGGTGACCATTGT3' (JH3) 5'ACCTGAGGAGACGGTGACCGTGGT3' (JH6)	Extension	72ºC 10 min

Table 6. Primers and Conditions for IgVH PCR

0.02% v/v N, N, N', N'- tetramethylenediamine (TEMED, Sigma) in 1x TBE running buffer (89 mM Tris-borate, 2 mM EDTA pH 8.3). The 5µl aliquot was used to improve discrimination of the bands of interest. The size of the expected PCR products (~360bp) was determined by comparison to a 1kb DNA ladder (Invitrogen), which was run in parallel. Electrophoresis was carried out at 180V for ~2 hours. The gel was stained with ethidium bromide, and the bands were visualised by UV light using a transilluminator. The desired bands were sliced from the gel using a scalpel blade and placed in a 1.5ml microcentrifuge tube. The gel fragments were mashed using a 1000µl filter tip, before adding 350µl 2.5M ammonium acetate. The mixture was left shaking overnight at 37°C. The following day, the eluate was transferred to a fresh 1.5ml tube and the DNA precipitated by addition of 2.5 volumes of 99% ethanol together with 2µg glycogen DNA carrier (Roche) in order to help visualise the pellet. The sample was incubated for 30 minutes at -70°C, and then pelleted by centrifugation at 13000 rpm for 30 minutes at 4°C. The DNA pellet was washed twice more in 70% v/v ethanol, air-dried and resuspended in 25µl PCR grade water. To estimate the quantity of the PCR product, a 3µl aliquot of DNA was analysed on a 2% agarose gel (1x TBE as running buffer), with comparison against a 1kb DNA ladder.

TA Cloning in E. coli

The purified PCR products were cloned using the TA cloning system, pGEM®-T Easy Vector System I (Promega). This system uses a linearised pGEM-T vector with a single 3′ deoxythymidine overhang present at both ends, which prevents recircularisation of the vector and provides an overhang compatible with non-template directed deoxyadenosine bases frequently added to the 3′ end of PCR products by DNA polymerases. Several features of the pGEM-T vector facilitate selection of bacteria successfully transformed with insert-containing

vector. Firstly, the pGEM-T plasmid carries an ampicillin resistance gene which allows transformed bacteria to be selected by growing in media containing ampicillin. Secondly, the vector carries a coding region for the α-peptide subunit of the β-galactosidase enzyme (lacZ gene) under the control of an IPTG promoter and spanning the cloning site. This allows blue/white colony selection when DH5α E.coli, which carry a deletion of the endogenous α-peptide, are transformed and cultured on X-gal and IPTG-treated indicator plates. Thus, when vector without an insert is transformed into the bacteria, IPTG induces expression of the α-peptide which restores β-galactosidase enzyme activity and results in hydrolysis of X-gal to a blue compound which colours the bacterial colonies. However, in a vector containing an insert successfully ligated into the cloning site the α-peptide coding region in disrupted, such that transformed colonies will appear white. Finally, the pGEM-T vector carries EcoRI restriction enzyme recognition sites, flanking the cloning site. These facilitate a straightforward method for confirming the presence of an appropriately sized insert by subjecting purified plasmid DNA to EcoRI digestion, followed by DNA electrophoresis. Notably, the pGEM-T vector also contains an M13 primer sequence adjacent to the cloning site which can be used to sequence the insert.

Ligation of PCR Products into pGEM-T Vector

For each PCR product, 3.5µl DNA was combined with 0.5 µl pGEM®-T Easy vector, 5 µl 2x Rapid Ligation Buffer and 1 µl T4 DNA ligase (Promega) in a 1.5 ml microcentrifuge tube. After mixing, tubes were incubated overnight (or for up to 72 hours) at 4°C. A positive control using supplied insert DNA, and a vector-only control, were also set up.

E.coli Transformation

DH5α competent cells (prepared as below) were thawed on ice and 50 µl added to each 10 µl ligation mix in a 1.5 ml microcentrifuge tube. After incubating on ice for at least 5 minutes, the cells were heat-shocked by transferring the tubes to a 42°C water-bath for 2 minutes before returning to ice for 1 minute. 1 ml L-broth (without ampicillin) was added to the tubes, which were then incubated at 37°C for 1 hour in a heating block with gentle mixing. The tubes were then centrifuged at 8,0000 rpm for 3 minutes in a microcentrifuge, after which the supernatant was tipped off to leave approximately 100 µl which was used to re-suspend the bacterial pellet by gentle pipetting. The cell suspension was then spread onto freshly prepared LB agar plates supplemented with 100 µg/ml ampicillin and coated with 80 µl 2% Xgal (Calbiochem) and 20 µl 100mM IPTG (Promega) and the plates were incubated at 37°C overnight. The following day, white colonies (corresponding to bacterial clones carrying inserts) were picked and inoculated into 2ml L-broth supplemented with 100 µg/ml ampicillin in 15ml tubes. These were then grown up by incubation at 37°C overnight in an orbital shaker.

Analysis of Recombinant Plasmids

Plasmid DNA was purified from the bacterial cultures using the QIAprep Spin Miniprep Kit (Qiagen), according to the manufacturer's instructions and DNA was eluted in 50µl PCR grade water. In order to confirm the presence of appropriately sized PCR products in the recombinants, an aliquot of each plasmid preparation was digested using FastDigest EcoRI restriction endonuclease (Thermo Scientific). 2 µl plasmid DNA was mixed with 2 µl 10x FastDigest Green Buffer, 1 µl FastDigest EcoRI enzyme and 15 µl PCR grade water (Ambion). After incubating at 37°C for 15 minutes, the samples were separated by

electrophoresis in 1.5% agarose gels in 1x TBE alongside 1kb DNA ladder (Invitrogen). The gel was stained with ethidium bromide and bands visualised using a UV transilluminator. Plasmid preparations containing inserts of appropriate size were subsequently analysed by DNA sequencing.

Preparation of Competent Cells

DH5α competent-cells were prepared based on the method described by Inoue et al.[559] Approximately 10-12 DH5α colonies were added to 250 ml SOB media (containing 20 g bacto-tryptone, 5 g yeast extract, 10 ml 250 mM KCl, 0.5 g NaCl, pH 7, plus 20 mM Mg salts in each litre) and grown at room temperature to an optical density of A600 = 0.6. The culture was then split, and following incubation on ice for 10 minutes, the cells were centrifuged at 2500xg (3000rpm in Beckmann J-6B) for 10 minutes at 4°C. The cell pellet was resuspended in ice-cold TB (containing 10 mM Pipes, 15mM CaCl2, 260 mM KCl adjusted to pH 6.7 with KOH, before addition of 55 mM $MnCl_2$) and, following incubation on ice for a further 10 minutes, was centrifuged again at 2500xg for 10 minutes. The pellet was then resuspended in 20 ml ice-cold TB to which 1.5 ml of DMSO was added. Finally, after incubation on ice for a further 10 minutes, aliquots of the DH5α cells in sterile 1.5ml microcentrifuge tubes were flash-frozen in liquid nitrogen and stored at -80°C.

Sequencing IgVH Products

Plasmid clones (at least 20 per sample) were Sanger sequenced by priming from the M13 sequence present on the pGEM-T vector. Each sequencing reaction contained 200-500 ng plasmid DNA and 3.2 pmol M13 forward primer, made up to a final volume of 10 µl with PCR grade water (Ambion). Sequencing was performed using the 'Plasmid to Profile' DNA

sequencing service provided by the Functional Genomics Laboratory, University of Birmingham, UK.

Analysis of IgVH Sequences

Sequence data was analysed using the BioEdit software package version 7.2.0 (Ibis Therapeutics). Each chromatogram trace was manually inspected and ambiguous bases were corrected if required. Sequences were subsequently analysed with the IMGT/V-QUEST database[560] (http://www. IMGT.org) in order to identify the V, D and J segments used in each IgVH rearrangement, the number of SHM mutations present in the V segment and the amino acid sequence of the CDR3 region.

2.23 Analysis of BCL6 and p53 Mutations in LCL Cultures

PCR for BCL6 and p53 Sequences

Selected regions of the cellular BCL6 and p53 genes were PCR amplified using published primers (Table 7). Non-template controls were included for all assays. Reactions were performed in 0.5 ml PCR tubes, each of which contained 0.5 - 1.0 μg of template DNA, a final concentration of 1x Expand High Fidelity Buffer containing 1.5 mM $MgCl_2$, 3.5 units of Expand High Fidelity Enzyme mix (containing Taq DNA polymerase), 200μM each of dATP, dGTP, dTTP and dCTP, 2 μM each of forward and reverse primers, in a final volume of 50 μl made up with PCR grade water (Ambion). PCR amplification was performed in an Eppendorf Thermocycler using the conditions shown in Table 7. Completed PCR reactions were stored at -20°C.

Target	Direction	Primer Sequence	Size (bp)	Conditions	
BCL6	Forward	5'ATGCTTTGGCTCCAAGTT3'	750	Denaturation Denaturation Annealing Extension Extension	95ºC 2 min (hot start) 95ºC 30 sec 58ºC 1 min 72ºC 1 min x 40 cycles 72ºC 10 min
	Reverse	5'CACGATACTTCATCTCATC3'			
P53	Forward	5'GTTTCTTTGCTGCCGTGTTC3'	522	Denaturation Denaturation Annealing Extension Extension	95ºC 2 min (hot start) 95ºC 30 sec 58ºC 30 sec 72ºC 30 sec x 35 cycles 72ºC 10 min
	Reverse	5'GGAGGGCCACTGACAACCA3'			

Table 7. Primers and Conditions for BCL6 and p53 PCRs

TA Cloning in E. coli

BCL6 and p53 PCR products were separated by electrophoresis on agarose gels and purified, as described in Section 2.12. Subsequently, the purified PCR products were cloned using the pGEM® Easy Vector System I (Promega) and sequenced as described in Section 2.22. A total of 10 plasmid clones were analysed for each sample time point.

Analysis of BCL6 and p53 sequences

Sequence data was analysed using the BioEdit software package version 7.2.0 (Ibis Therapeutics). Sequences were aligned to the BCL6 intron 1 (accession number AY189709) and complete p53 gene (accession number HSU94788) sequences using the ClustalW Multiple Alignment tool. Each chromatogram trace was manually inspected and any base changes relative to the BCL6 and p53 reference sequences were individually verified. The number of mutated sequences and total number of mutations were scored for each time point.

2.24 Interferon Gamma Elispot

To enumerate EBV-specific T-cells in PBMCs or donor lymphocytes for Patients A and B (Chapter 7) interferon-gamma (IFN-γ) release Elispot assays were performed on cells stimulated with $CD8^+$ and $CD4^+$ T-cell EBV epitope peptides, as listed in Tables 8 and 9. As described previously[325], 96-well polyvinylidene difluoride-backed plates were first coated with a 15 μg/ml concentration of the anti-IFN-γ monoclonal antibody 1-DIK (Mabtech) and then blocked with RPMI 1640 containing 10% FCS. 1 $x10^5$ or 2 $x10^5$ cells were then added to wells, in duplicate or triplicate where numbers allowed, alongside peptides at a final concentration of 5 μg/ml. Wells containing an equivalent volume of DMSO without peptide were used as a negative control. Plates were incubated overnight at 37°C in 5% CO_2

Peptide	HLA restriction	Protein	Amino acid coordinates	Latent or lytic
VEI	B44:02	EBNA3B	657-666	Lat
EEN	B44:02	EBNA3C	281-290	Lat
KEH	B44:02	EBNA3C	335-343	Lat
CLG	A02:01	LMP2	426-434	Lat
FLY	A02:01	LMP2	356-364	Lat
LLW	A02:01	LMP2	329-337	Lat
YLL	A02:01	LMP1	125-133	Lat
YVL	A02:01	BRLF1	109-117	Lyt
GLC	A02:01	BMLF1	280-288	Lyt
FLD	A02:01	BALF4	276-284	Lyt
TSL*	DRB1 01:01	EBNA1	515-528	Lat
GPW*	DRB1 01:01	EBNA3A	780-799	Lat
MVF*	DRB1 05:01	EBNA1	563-577	Lat
EDL*	DRB1 05:01	EBNA3A	364-383	Lat
LDL**	DRB1 05:01	BLLF1	61-81	Lyt
TDA**	DRB1 05:01	BNRF1	1238-1252	Lyt
SNP*	DRB5 01:01	EBNA1	474-489	Lat
LEK**	DRB5 01:01	BXLF2	126-140	Lyt
SDD*	DQB1 06:02	EBNA3C	386-400	Lat

Table 8. IFN-γ Elispot Assay Peptides for Patient A

Individual or combined pools of peptides corresponding to HLA antigen-specific EBV epitopes were used to stimulate PBMCs from Patient A. *$CD4^+$ T-cell latent antigen pool, **$CD4^+$ T-cell lytic antigen pool.

Peptide	HLA Restriction	Protein	Amino acid coordinates	Latent or lytic
RYS	A24:01	EBNA3A	246-253	Lat
TYS	A24:01	EBNA3B	217-225	Lat
TYG	A24:01	LMP2	419-427	Lat
RPGK	B07:02	EBNA1	72-80	Lat
IPQ	B07:02	EBNA1	528-536	Lat
RPP	B07:02	EBNA3A	379-387	Lat
QPR	B07:02	EBNA3C	881-889	Lat
YPR*	B07:02	BNRF1	1247-1257	Lyt
TPS*	B07:02	BFRF3	127-137	Lyt
SRL*	B14:01	BMLF1	435-444	Lyt
LQH*	Cw08	BZLF1	101-115	Lyt
VYG	DRB1 07:01	EBNA1	509-528	Lat
PRS	DRB1 07:01	EBNA2	276-295	Lat
SRD**	DRB1 07:01	BARF1	185-199	Lyt
MVF	DRB1 15:01	EBNA1	563-577	Lat
EDL	DRB1 15:01	EBNA3A	364-383	Lat
LDL**	DRB1 15:01	BLLF1	61-81	Lyt
TDA**	DRB1 15:01	BNRF1	1238-1252	Lyt
SNP	DRB5 01:01	EBNA1	474-489	Lat
LEK**	DRB5 01:01	BXLF2	126-140	Lyt
ILR**	DRB4 01:01	EBNA3C	771-790	Lat

Table 9. IFN-γ Elispot Assay Peptides for Patient B

Individual or combined pools of peptides corresponding to HLA antigen-specific EBV epitopes were used to stimulate PBMCs from Patient B. *$CD8^+$ T-cell pool, **$CD4^+$ T-cell pool.

and the cells were then discarded. A biotinylated anti-IFN-γ monoclonal antibody, 7-B6-1 (Mabtech), was then added at 1 μg/ml and incubated for 2 hours at room temperature, followed by streptavidin-conjugated alkaline phosphatase (Mabtech) for an additional 1 hour. Washes were performed between all steps of the assay with PBS, PBS-Tween or RPMI 1640 as appropriate. Individual cytokine-producing cells were finally detected using an alkaline phosphatase-conjugated substrate kit (BioRad). Spots were counted using an automated Elispot plate reader. Results are expressed as spot-forming cells (SFC) per 2 $x10^5$ cells.

2.25 Tetramer Staining

Further analysis of EBV-specific T-cells in Patient A (Chapter 7) was performed using MHC class I tetramer staining. Thawed PBMCs were incubated at 37°C for 15 min with pre-titrated volumes of APC-conjugated HLA A*0201 tetramers for EBV epitopes YVLDHLIVV (BRLF1 aa 109-117), GLCTLVAML (BMLF1 aa 280-288) and CLGGLLTMV (LMP2 aa 426-434).[296,326] After washing in PBS, the cells were stained with LIVE/DEAD fixable violet dead cell stain (Life Technologies) according to the manufacturer's instructions, before surface markers were stained with pre-determined concentrations of CD3-AmCyan and CD8-PE antibodies (BD Biosciences) as described in Section 2.6. After washing, the cells were acquired on an LSRII flow cytometer, excluding doublets and dead cells. Data were processed using FlowJo software version 7.6.5 (Tree Star). Absolute numbers of tetramer-specific T-cells were calculated from lymphocyte subset frequencies, determined as described in Section 2.6.

2.26 Immunohistochemistry and EBER *in situ* Hybridisation

For immunohistochemistry, sections from paraffin-embedded biopsy material were first

dewaxed in Histoclear for 10 min, rehydrated and then quenched in 0.3% hydrogen peroxide for 15 minutes. The slides were subsequently boiled in citrate buffer pH 6.0 for 10 minutes for antigen retrieval (40 minutes for BZLF1 staining). After blocking with casein, the slides were incubated overnight at 4°C with primary antibodies against the following antigens diluted in PBS with 0.5% Tween20: EBNA1 (1:1000), EBNA2 (1:2), LMP1 CS1-4 (Dako; 1:25), LMP2A 15F9 (Santa Cruz; 1:100), BZLF1 (neat) and gp350 (1:1000). After 3 washes in PBS/Tween20, slides were incubated for 30 minutes at room temperature with appropriate peroxidase-conjugated secondary antibodies (Dako). After 3 washes with PBS/Tween20, 100µl diaminobenzidine (Dako) was applied to each slide for visualisation, counter-staining with Meyer's Haematoxylin. EBER *in situ* hybridisation (EBER ISH) was performed with a Leica automated Bond system, using an EBER probe in combination with an anti-fluorescein antibody and Bond Polymer Refine Detection (Leica Biosystems), according to manufacturer's instructions.

3. PTLD Arising after Solid Organ Transplant: A UK Multicentre Study of Outcomes with Rituximab Monotherapy versus R-CHOP

PTLD occurs in up to 10% of solid allograft recipients and carries a high risk of mortality. Many cases of PTLD are associated with EBV, in which the virus is thought to play a key pathogenic role. Thus, whereas immunocompetent individuals possess effective $CD8^+$ and $CD4^+$ T-cell responses that maintain long-term control over chronic EBV infection, in transplant recipients iatrogenic T-cell compromise may trigger opportunistic accumulation of EBV-transformed B-cells, leading to PTLD. Regarding the management of these patients, RI on its own is often insufficient to produce sustained disease remission[511]. Consequently, first line therapy for $CD20^+$ B-cell PTLD usually comprises R-mono, or Rituximab in combination with CHOP chemotherapy (R-CHOP). However, deciding between these therapies may be challenging. Although studies have shown that R-mono is safe and can produce satisfactory response rates, concerns have been raised regarding a lack of durable remissions[519,561]. Whereas CHOP chemotherapy can deliver long-term remissions, high levels of toxicity have been reported[376,509]. Optimal selection between these initial therapies is also complicated by the lack of an accepted prognostic scoring system for PTLD[388]. Given these issues, a retrospective study was undertaken to gather data from solid allograft recipients from the UK diagnosed with PTLD. The principal aim was to characterise outcomes and prognostic factors for patients managed in the Rituximab era.

3.1 Patient Characteristics

This retrospective study invited 4 UK centres to submit data on patients aged over 16 years with biopsy-proven PTLD diagnosed between 2000 and 2012. A total of 72 cases meeting the

inclusion criteria were identified and median follow-up was 38 months. Patient characteristics are summarised in Table 10. These included 34 liver, 32 renal and 6 cardiothoracic transplant recipients. The median age at histological diagnosis was 47 years (range 16 - 72 years) and 68% were male. The median time from transplant to diagnosis of PTLD was 93 months (range 2 – 302 months), with 83% of cases occurring after 1 year. Disease staging, assigned using the Ann Arbor staging system, revealed that 51% of patients had stage ≥2 disease at presentation. Notably, extranodal disease was common, with 69% of patients exhibiting involvement of at least 1 extranodal site and 17% exhibiting 2 or more sites. Of these, the gastrointestinal tract was the most commonly involved, in 39% of cases.

3.2 Histopathology

Histopathology reports were used to categorise cases according to pathological subtype, using the WHO classification system for PTLD[421] (Figure 10A). This identified 14 polymorphic lesions, 45 B-cell monomorphic lesions (including 35 DLBCL, 3 plasmacytoma-like and 2 plasmablastic lymphoma subtypes), 8 cases of B-cell PTLD of unspecified subtype, 1 monomorphic T-cell lymphoma and 4 HL types. EBV-association, defined as positivity for EBER *in situ* hybridisation and/or LMP1 immunohistochemistry, or concurrent high-level EBV DNAemia, was noted in 54% of cases (Figure 10B); this is likely to be an underestimate because adequate assessment of EBV status was not available for 17 cases. Notably, EBV-association was found to be significantly associated with disease presenting within a year of transplant (χ^2 P = 0.004) and polymorphic disease (χ^2 P = 0.07; borderline significance). Furthermore, for 16 cases where EBV and CD30 status were both known, positivity was significantly associated (χ^2 P = 0.04).

	N	%
Age at diagnosis of PTLD		
Median years (range)	47 (16-52)	
Sex		
Male	49 / 72	68
Female	23 / 72	32
Transplant Type		
Liver	34 / 72	47
Renal	32 / 72	44
Cardiothoracic	6 / 72	8
Onset		
Early (<1 year)	12 / 72	17
Late (≥1 year)	60 / 72	83
B Symptoms		
Yes	27 / 51	53
No. of Extranodal Sites		
0	20 / 70	29
1	38 / 70	54
≥2	12 / 70	17
Extranodal Sites		
Gut	27 / 70	39
Liver	13 / 70	19
Lung	7 / 70	10
Spleen	7 / 70	10
CNS	5 / 70	7
Marrow	4 / 62	6
Subcutaneous	3 / 70	4
Skeletal	3 / 70	4
Renal	2 / 70	3
Stage		
I	25 / 70	36
II	9 / 70	13
III	10 / 70	14
IV	26 / 70	37
ECOG PS		
0-1	44 / 69	64
2-4	25 / 69	36
Serum LDH		
Elevated	30 / 59	51

Table 10. Patients with PTLD Arising after Solid Organ Transplant

Baseline characteristics for 72 adult patients with biopsy-proven PTLD arising after solid organ transplant included in the study.

A. Pathology

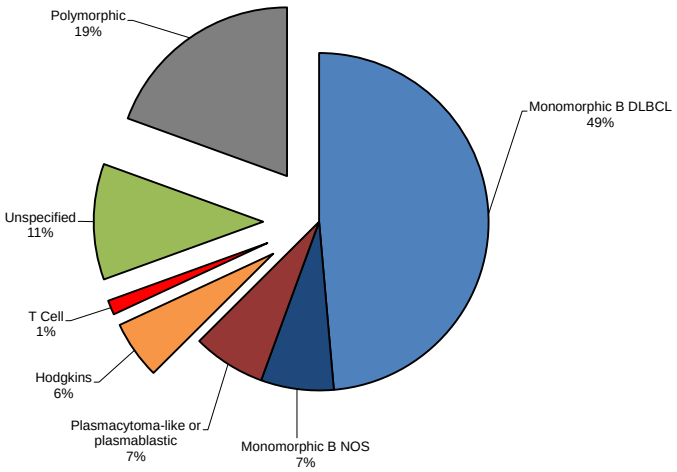

B. EBV Association

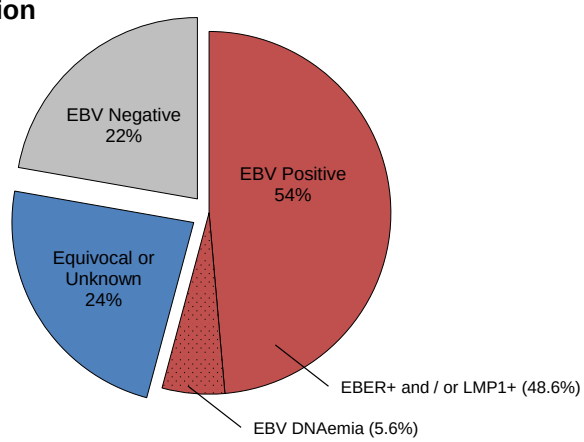

Figure 10. Pathology of PTLD Cases Arising after Solid Organ Transplant

A. PTLD cases categorised according to the WHO Classification for PTLD 2008[421]. B. Cases were identified as EBV-associated if EBER in situ hybridisation and/or LMP1 immunohistochemistry were positive, or if significant EBV DNAemia was detected by EBV qPCR; negative staining for LMP1 in the absence of EBER in situ hybridisation was not considered sufficient to exclude EBV-association and such cases were classified as equivocal

3.3 Treatment

Table 11 summarises the first line therapy used for all study patients. In 4 patients, this comprised RI in the absence of immuno-chemotherapy; all patients had undergone radical surgery and had no evidence of disease on subsequent imaging. Three patients received palliative treatment from diagnosis because they were moribund. For the remaining 65 individuals, first line treatment comprised RI in combination with Rituximab and/or chemotherapy. Initial therapy was with R-mono in 16/72 (22%) and R-CHOP in 34/72 (47%).

In order to understand how baseline characteristics influenced the selection of R-CHOP versus R-mono, statistical analysis was performed using logistic regression (Table 12). This statistical test generates odds ratios (OR), which express the strength association between independent and dependent variables – it is the odds of an outcome occurring in one group divided by the odds of the outcome occurring in the other group. This revealed that R-CHOP was more likely to be used in cases with advanced stage (OR 6.7, P = 0.01), onset more than 1 year after transplant (OR 7.3, P = 0.03), lack of EBV association (OR 0.1, P = 0.002) and monomorphic versus polymorphic histology (OR 14.5, P = 0.003). In a multivariate logistic model, advanced stage (OR 10.7, P = 0.06) and monomorphic histology (OR 8.8, P = 0.03) retained significance as variables favouring the selection of R-CHOP.

3.4 Treatment Tolerability and Outcomes

Due to the retrospective nature of the study, detailed information on treatment-related toxicity was not available. However, of those treated with R-mono, 15/16 (94%) completed at least 4 infusions, with no treatment-related mortality (Table 13). Of these, 4 patients subsequently received R-CHOP for consolidation of response (2 patients) or for relapsed and/or refractory

Initial Treatment	N	%
R-Monotherapy	16 / 72	22
R-CHOP	34 / 72	47
Other Therapy	22 / 72	31
Surgery + RI	4	
Palliation	3	
ABVD	3	
CHOP (no R)	3	
CTD	3	
Other chemo	6	

Table 11. Initial Treatment

Reduction of immunosuppression (RI) in combination with R-Mono or R-CHOP comprised initial therapy for the majority of patients with PTLD arising after solid organ transplant.

Univariate Analysis	Odds Ratio	P
Age	1.0	0.13
Male Sex	2.0	0.31
Transplant Type	-	0.91
Late Onset (≥1 year)	7.3	**0.03**
B Monomorphic Pathology	14.5	**0.003**
EBV-association	0.1	**0.002**
Stage ≥3	6.7	**0.01**
Extranodal Disease	1.2	0.77
≥2 Extranodal sites	All R-CHOP	-
Elevated LDH	1.4	0.59
ECOG PS ≥ 2	1.3	0.70

Multivariate Analysis	Odds Ratio	P
Late Onset (≥1 year)	6.1	0.17
B Monomorphic Pathology	8.8	**0.03**
EBV-association	0.3	0.22
Stage ≥3	10.7	**0.06**

Table 12. Factors Influencing Selection of R-CHOP versus R-Mono

Factors associated with the selection of R-CHOP as first line therapy for PTLD arising after solid organ transplant were analysed using univariate logistic regression. Significant factors ($P < 0.05$) were subsequently analysed in a multivariate logistic regression model, in which monomorphic pathology and advanced stage (borderline P value) retained significance.

Regimen	N	Treatment Completed	Deaths on Treatment	Response	
		≥ 4 Infusions:			
R-Mono	16	15 / 16 (94%)	0 / 16 (0%)	ORR	13 / 16 (81%)
				CR	10 / 16 (63%)
				PR	3 / 16 (19%)
				NR	3 / 16 (19%)
		≥ 6 Cycles:			
R-CHOP	34	23 / 34 (68%)	4 / 34 (12%)	ORR	25 / 30 (83%)
				CR	19 / 34 (56%)
				PR	6 / 34 (18%)
				NR	5 / 34 (15%)
				n/a	4 / 34 (12%)

Table 13. Treatment Tolerability and Response

The number of infusions of Rituximab or cycles of R-CHOP delivered to patients with PTLD arising after solid organ transplant are shown, as are deaths observed on treatment and response to therapy. CR indicates complete response; PR, partial response; NR, no response; ORR, overall response rate (CR + PR); n/a, not available.

disease (2 patients). One patient was changed to R-CHOP due to poor response. Of those who received R-CHOP as initial therapy, 23/34 (68%) completed at least 6 cycles, and 4 patients died whilst on treatment.

Response to therapy was evaluated on the basis of submitted clinical and radiological data and was categorised into complete remission (CR), partial remission (PR) or no remission (NR), in line with the Cheson criteria[541]. The overall response rate (ORR) to R-mono was 81% (10 CR, 3 PR and 3 NR; Table 13). This was similar to that of R-CHOP at 83% (19 CR, 6 PR, 5 NR and 4 undetermined; χ^2 P = 0.67). Of those who received R-mono as initial therapy, 1 patient subsequently received R-CHOP for consolidation and remained in long term remission, whereas 4 patients exhibited NR or subsequently progressed and died despite further chemotherapy in 3 cases. Survival outcomes for R-mono and R-CHOP were 2 year event-free survival of 62% and 54% (P = 0.77), 2 year progression-free survival of 67% and 58% (P = 0.47) and 2 year overall survival of 74% and 59% (P =0.52) respectively (Figure 11).

3.5 Predictors of Outcome

Predictors for overall survival were assessed using Cox analysis (Table 14). This statistical test generates hazard ratios (HR), which express the risk of an event occurring in relation to an independent variable - it is the ratio of the hazard rates (the chance of an event occurring over time) in one group compared to another group. Amongst all study patients, significant baseline predictors of (inferior) survival were age ≥50 years (HR 2.9, P = 0.006), stage ≥2 disease (HR 4.0, P = 0.01), ECOG performance status ≥2 (HR 2.1, P = 0.05), and elevated LDH (HR 2.2, P = 0.08 borderline significance). Extranodal disease, histology, EBV-

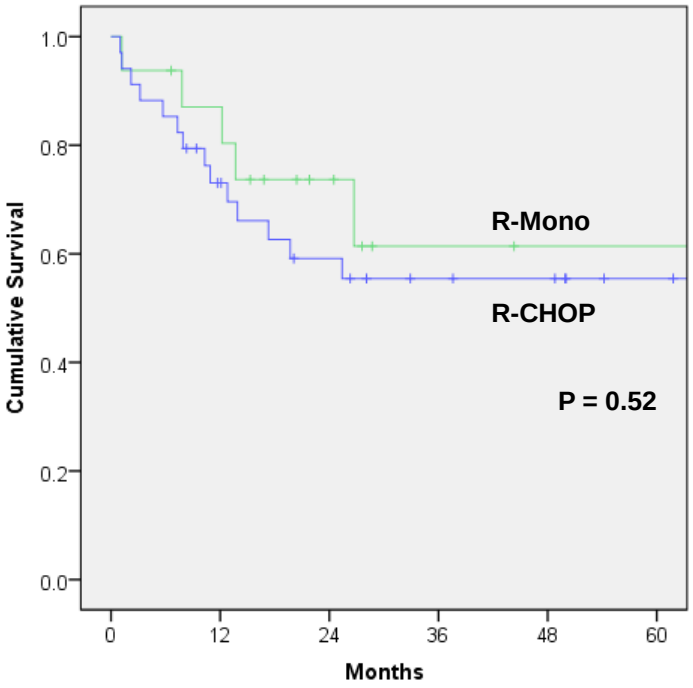

Figure 11. Overall Survival by Initial Therapy

Overall survival amongst patients with PTLD arising after solid organ transplant initially treated with R-Mono or R-CHOP chemotherapy. Kaplan-Meier curves were compared with the Log Rank test. A significant difference was not observed.

Univariate Analysis	**HR**	**95% CI**	**P**
Age ≥ 50 years	2.9	1.4 – 6.2	**0.006**
Male sex	0.9	0.4 – 1.9	0.75
Late onset	0.6	0.3 – 1.4	0.24
B Monomorphic pathology	1.1	0.4 – 2.9	0.85
EBV association	1.1	0.5 – 2.2	0.88
Stage ≥ 2	4.0	1.4 – 11.4	**0.01**
Stage ≥ 3	2.2	1.0 - 4.9	**0.05**
Extranodal disease	1.0	0.5 – 2.2	0.96
≥2 Extranodal sites	1.6	0.7 – 3.8	0.28
Elevated LDH	2.2	0.9 – 5.6	**0.08**
ECOG PS ≥ 2	2.1	1.0 – 4.5	**0.05**

Multivariate Analysis	**HR**	**95% CI**	**P**
Age ≥ 50 years	3.5	1.4 – 8.7	0.008
Stage ≥ 2	3.5	1.1 – 10.7	0.03
Elevated LDH	1.1	0.4 – 3.2	0.80
ECOG PS ≥ 2	2.0	0.8 – 5.0	0.15

Table 14. Predictors of Overall Survival

Factors predicting for overall survival amongst patients treated with either R-mono or R-CHOP as first line therapy for PTLD were analysed using Cox regression. Factors significant in univariate analysis were subsequently analysed in a multivariate Cox proportional hazards model. In this, age ≥50 years and stage ≥2 disease retained significance as predictors of inferior survival. HR indicates hazard ratio; CI, confidence interval.

association and time from transplant were not predictive. In multivariate analysis, age>50 years (HR 3.5, P = 0.008) and advanced stage (HR 3.5, P = 0.03) retained significance. Importantly, amongst those treated with R-mono or R-CHOP, response to initial therapy was highly predictive of overall survival (overall response, HR 0.2, P < 0.0001; complete response, HR 0.1, P < 0.0001).

Sufficient data was available to apply the well validated 5 point international prognostic index (IPI) for *de novo* DLBCL to patients treated with R-CHOP or R-mono. This showed that those with 3 or more points had significantly inferior overall survival (78% vs 48% at 2 years; P = 0.046). However, a 4-point modified prognostic index (MPI) comprising age>50 years, stage ≥2 disease, ECOG performance status ≥2 and elevated LDH was found to be superior for the current dataset (Figure 12). Using this, patients treated with R-mono or R-CHOP with low risk disease (<2 points) had significantly improved survival compared to those with high risk disease (≥2 points), with 2 year overall survival of 90% versus 43% (P = 0.001;). Notably, comparison of outcomes for R-mono versus R-CHOP within high risk or low risk groups revealed no significant differences in survival (. However, there was a trend towards inferior response amongst patients with high risk disease treated with R-mono compared to R-CHOP (CR rate 1/6 [17%] versus 9/16 [56%]; χ^2 P = 0.16), which was not observed for low risk disease.

3.6 Discussion

There is currently a paucity of data to inform the management of PTLD arising after solid organ transplant. In seeking to address this problem we collected data from several leading UK clinical haematology centres, resulting in one of the largest case series of its kind.

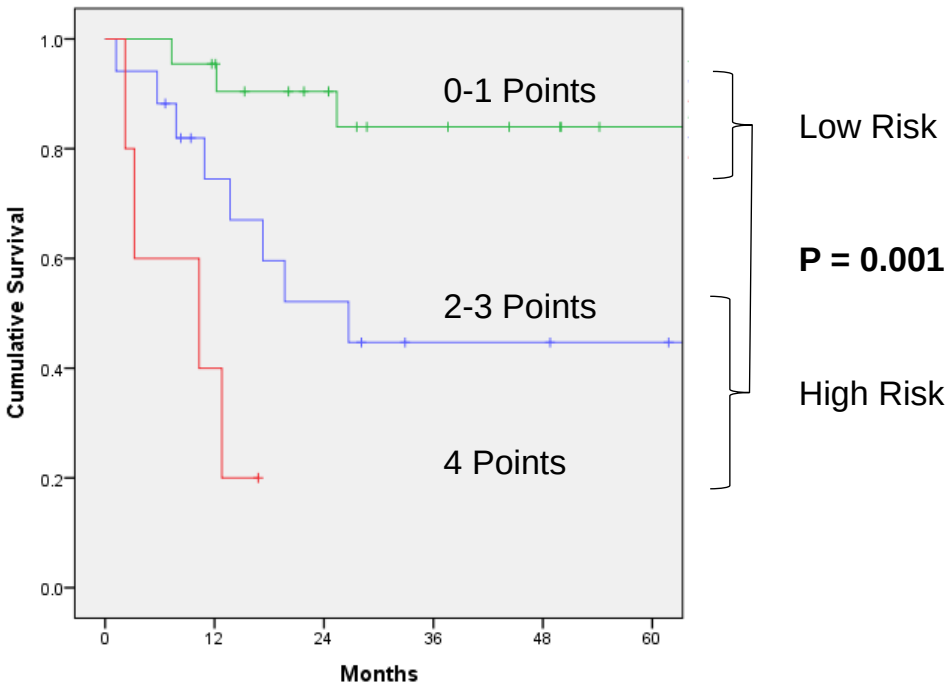

Figure 12. Survival by 4-Point Modified Prognostic Index

Overall survival amongst patients initially treated with R-mono or R-CHOP was determined according to a 4-point modified IPI scoring system, in which 1 point was assigned for each of the following baseline factors: age >50 years, stage ≥2 disease, ECOG performance status ≥2, elevated LDH. Patients with high risk disease (scoring ≥2 points) had significantly (P = 0.001) inferior survival compared to those with low risk disease (scoring 0-1 points). Curves were compared with the Log Rank test.

Consistent with the heterogeneous nature of PTLD, considerable variability was observed in baseline pathological and clinical characteristics of included patients. Thus, although the majority of cases were monomorphic B-cell PTLD of DLBCL type or polymorphic PTLD, each of the principal WHO pathological categories of PTLD were encountered. At least 54% of cases were found to be EBV-associated, although this is likely to be an underestimate for the reasons detailed above. The majority (83%) of cases were late onset, perhaps explained by the exclusion of children from the study. Extranodal disease was very common, occurring in 71% of patients, and it was particularly striking how frequently PTLD involved the gastrointestinal tract, apparent in 39% of patients. Whilst this may reflect the relatively large amount of nodal tissue found occupying the gastrointestinal tract within Peyer's patches, it also suggests that the gut microenvironment may be important for the development of PTLD.

The principal focus of the study was to examine outcomes with R-mono versus R-CHOP as initial therapy for $CD20^{+}$ B-cell PTLD. Importantly, it should be stressed that due to the retrospective nature of the study this comparison was biased by the lack of randomisation between R-mono and R-CHOP treatments; such a randomisation would almost certainly be unethical in the context of a prospective RCT. However, in order to mitigate for this limitation, we examined differences in the baseline factors that may have influenced selection of treatment between the groups. Thus, patients who received R-CHOP were found to exhibit more advanced stage, later onset disease, lack of EBV-association and monomorphic histology. Because these factors have variously been associated with inferior outcomes, it is apparent that R-mono was generally reserved for a prognostically favourable group.

Acknowledging these differences, outcomes were found to be similar with both initial

therapies. Thus, overall response rates to R-mono and R-CHOP were 81% and 83% respectively. Although overall survival at 2 years was marginally better for those treated with R-mono, at 74% versus 69%, this difference was not statistically significant and the survival curve for both groups subsequently plateaued at around 60% (Figure 11). These results compare favourably with those reported in previous studies[512-519]. However, caution should be exercised in seeking to draw such comparisons due to the significant variation between cohorts in different studies. Furthermore, prior studies have typically applied a single form of therapy to all patients[512-514], rather than selecting between therapies according to baseline factors, as occurs in routine clinical practice. Importantly, concerns have previously been raised about relatively high rates of relapse, despite initial responses, when R-mono is used as initial therapy. However, the finding in the present study that 11/16 (69%) patients treated with R-mono exhibited durable remissions without the need for further therapy, confirms that R-mono *can* be efficacious when used for selected patients with favourable disease.

Patients with PTLD are at particular risk of treatment-related toxicity, often due to significant co-morbidities associated with the primary indication for transplant and co-existing complications. With regard to treatment tolerability, it was unfortunate that detailed information on the toxicities encountered was not available for the present study. However, we did find that all but one of the patients treated with R-mono completed at least 4 infusions; the only patient not doing so changed therapy due to poor response rather than toxicity. In contrast, considerably fewer patients completed a minimum of 6 cycles of R-CHOP, and 4 patients died on treatment. As such, our data are consistent with that of other studies, confirming that R-CHOP is associated with significantly greater toxicity that R-mono[515-518]. However, the rate of toxicity compared favourably with that found in other studies, where

treatment-related mortality as high as 31 % has been reported[562]. Notably, in the PTLD-1 trial, mortality associated with CHOP chemotherapy was 11%[519]. This is almost identical to the level of toxicity found in our study (12%), and therefore it arguably remains an open question as to whether sequential therapy, as evaluated in the PTLD-1 trial, is indeed superior to treating from the outset according to baseline risk stratification.

Several previous studies have sought to characterise prognostic factors for PTLD arising after solid allograft, variously reporting that advanced age, late onset disease, advanced stage, extranodal disease, number of disease sites, poor performance status, LDH, hypoalbuminaemia, monomorphic disease and EBV negativity may predict for inferior outcome[513,563-566]. However, there is a noticeable lack of concordance between these studies, presumably due to the limited size of their cohorts and heterogeneity of patient characteristics. Consistent with this, a validated and universally agreed prognostic scoring system does not currently exist for PTLD[388], contributing to the challenge of selecting appropriate initial therapy. In the present study, we found that older age, advanced stage, poor performance status and raised serum LDH were associated with significantly inferior overall survival. Response to therapy was also significantly associated with overall survival. However, we failed to demonstrate prognostic associations for factors including EBV association, polymorphic versus monomorphic disease, late onset disease and extranodal disease. It may be that the study was too underpowered to detect some associations. However, it is notable that other large retrospective studies of PTLD have also failed to show that EBV association is prognostic[564,566]. Using these factors we designed a modified 4 point IPI that modelled our data very well. This principally differs from the standard *de novo* DLBCL IPI due to the exclusion of extranodal disease as a variable, because this was not prognostic for our series;

probably as a consequence of the high rates of extranodal disease identified in all patients. It remains to be seen how well our scoring system will apply to other PTLD series. Ultimately, large prospective studies, undertaken on well-defined patient cohorts, will be required to refine prognostication amongst patients with PTLD.

Some patients exhibit very poor outcomes, irrespective of initial treatment. Indeed, individuals with a modified IPI score of 4/4 had a median survival of only 10 months. It is therefore clear that R-mono or R-CHOP are inadequate for such patients, and that novel treatment strategies, with low toxicity, are urgently required. Regarding this, several emerging therapies are yet to be evaluated in the setting of PTLD. These include novel therapeutic monoclonal antibodies targeting CD20, such as Ofatumumab and Obinutuzumab[567]. Similarly, Brentuximab-vedotin is an anti-CD30 antibody linked to a cytotoxic molecule that has shown efficacy for refractory HL[568], and which is currently being evaluated in a phase II study for PTLD[569]. Meanwhile, a number of novel small molecule inhibitors have shown promising results in other B-cell malignancies and may also prove efficacious for PTLD. Amongst these is the BTK inhibitor Ibrutinib which has delivered excellent preliminary results for the treatment of chronic lymphocytic leukaemia (CLL) and Mantle-cell lymphoma, and is currently being evaluated for the treatment of DLBCL in the immunocompetent setting[570]. A range of other small molecule inhibitors are either currently available or in development. Importantly, access to large cohorts of clinically annotated PTLD tumour material will benefit the development of targeted therapy, and will aid in the design of new agents; it is hoped that the data collected in the present study may support such efforts. Finally, although adoptive immunotherapy with EBV CTLs has proved to be effective rescue therapy for PTLD[531], this approach is yet to be assessed as standard treatment for PTLD. To

address this important issue, an RCT designed to evaluate third party derived EBV CTLs as first-line treatment for PTLD arising after solid organ transplantation is currently being developed by Dr Chaganti of University Hospital Birmingham.

4. EBV Reactivation and PTLD after Allo-HSCT: Greatly Reduced Risk in Patients with Non-Hodgkin Lymphoma Previously Treated with Rituximab

PTLD is also a life threatening complication of allo-HSCT[520,571,572]. In this setting, almost all cases arise from donor-derived EBV-transformed B-cells. These opportunistically expand in the state of T-cell immunocompromise resulting from preparative conditioning and immunosuppressive therapy. The incidence of PTLD arising after allo-HSCT varies significantly in relation to graft T-cell depletion (TCD), ranging from <1% without TCD, to >10% with TCD in some series[392,407-419420]. Other important risks factors include the use of unrelated and/or HLA-antigen mismatched donors, the occurrence of severe GvHD and older age.

Of the alternative forms of TCD available, several studies have reported significantly elevated rates of PTLD (or EBV reactivation) following ATG[392,416,419,420]. Meanwhile, the anti-CD52 monoclonal antibody Campath has been associated with a lower incidence of disease, reportedly 0.4-1.3% in initial studies[392,407]. Unlike ATG, which selectively depletes T-cells, Campath targets all lymphocytes. Therefore, the risk associated with using Campath to deplete T-cells may be offset by it simultaneous depletion of B-cells. However, it is notable that initial studies examining the risks associated with Campath involved first and second generation rat antibodies (Campath-1M and -1G), whereas relatively few studies have examined the third generation humanised antibody Campath-1H (Alemtuzumab), which has now superseded the other antibodies in routine clinical practice[573]. Alemtuzumab has a much longer half-life than Campath-1G (15-21 days, compared to less than 24 hours) and is known to cause prolonged delays in the reconstitution of both general[521,522] and EBV-specific

immunity[383]. Consequently, it might contribute to an increased risk of PTLD compared to the earlier antibodies. In the largest series to specifically explore the risk of EBV reactivation and PTLD in Alemtuzumab-treated patients, Carpenter et al. reported a relatively high incidence of EBV reactivation, in 40.3% at 2 years post-transplant amongst 111 patients, although only 1 case of PTLD (0.9%) was observed[409]. Meanwhile, smaller series have reported the incidence of PTLD following Alemtuzumab to be between 2.3% and 9.5%[412,414,415,500].

The introduction of Rituximab has significantly improved PTLD-related mortality following allo-HSCT[521]. In particular, the pre-emptive administration of Rituximab to individuals developing raised levels of circulating EBV DNA, an indicator of emergent PTLD identified by EBV qPCR monitoring, has led to a marked reduction in mortality relative to historic cohorts[498,499,501,506,507]. However, there remains marked inter-centre variation in EBV qPCR methodology and a lack of consensus as to the optimal virus load thresholds to trigger intervention[384,502,503]. Alternative strategies for the prevention of PTLD include the prophylactic infusion of donor-derived EBV CTLs[527]. However, although efficacious, this approach has not been widely adopted, probably due to the significant logistical burdens and financial costs. Alternatively, it has been proposed that peri-transplant Rituximab (Rituximab delivered shortly before or after transplant) might be an effective method of prophylaxis[574].

In order to explore these issues, and to provide important context for the studies described later in this thesis, work was undertaken to define the incidence, kinetics and risk factors for EBV reactivation and PTLD amongst a large cohort of adult patients undergoing Alemtuzumab or ATG-conditioned TCD allo-HSCT.

4.1 Incidence and Kinetics of EBV Reactivation and PTLD

This study includes 196 adult patients undergoing first TCD allo-HSCT at University Hospital Birmingham, UK. Median follow-up was 28 months, and overall survival was 72% at 1 year post-transplant, with non-relapse mortality of 4.6% at 100 days and 15.0% at 1 year. Patient characteristics are summarised in Table 15. *In vivo* Alemtuzumab was used in 186 (95%) patients, whilst 10 (5%) received ATG. Reduced intensity conditioning was used in 159 (81%) of patients.

All allo-HSCT recipients were monitored with EBV qPCR whole blood assay, with testing scheduled every 1-2 weeks for the first 6 months post-transplant and intermittently thereafter. Monitoring revealed a cumulative incidence of EBV reactivation (defined as a single positive EBV qPCR test above the threshold of sensitivity of 500 genomes/ml) of 48% (CI 41 - 55%) at 1 year for Alemtuzumab-conditioned transplants and 80% (41% - 95%) for ATG-treated transplants (Figure 13A). More importantly, cumulative incidence of high-level EBV reactivation (defined as a single test ≥ 20,000 genomes/ml) was 18% (CI 13 - 24%) and 30% (CI 7% - 58%) respectively (Figure 13B).

The distribution of EBV reactivation and high-level EBV reactivation events are shown in Figure 14, revealing that both occurred most frequently between 8 and 16 weeks after transplant. Notably, no cases of high-level EBV reactivation occurred in the first 4 weeks after transplant, whilst 3 (7%) were observed more than a year afterwards. All 3 high-level EBV reactivations following ATG-conditioned transplants occurred within the first 8 weeks, earlier than those after Alemtuzumab. Furthermore, analysis of the interval between initial EBV qPCR positivity and high-level reactivation (Figure 14C) revealed rapid progression in

		N	%
Age	Median years (range)	51 (16 – 71)	
Sex	Male	126	64
	Female	70	36
Diagnosis	AML/MDS	104	53
	NHL	29	15
	ALL	18	9
	HL	11	6
	CLL	12	6
	MPD	11	6
	Other	11	6
Donor	Unrelated	133	68
	Sibling	63	32
HLA antigen mismatches	None	155	80
	1 or more	38	20
Stem-cell source	PBSC	196	100
Intensity	Reduced intensity	159	81
	Myeloablative	37	19
Conditioning	Flu Mel	129	66
	Cy TBI	37	19
	BEAM $^{+}$/- Flu	15	8
	Other	15	8
T-cell depletion	Alemtuzumab	186	95
	ATG	10	5
Acute GvHD	Grade ≥2	67	34

Table 15. Characteristics of Patients Undergoing T-Cell Deplete Allo-HSCT

Incidence and risk factors for EBV reactivation were analysed in 196 patients undergoing T-cell deplete allo-HSCT.

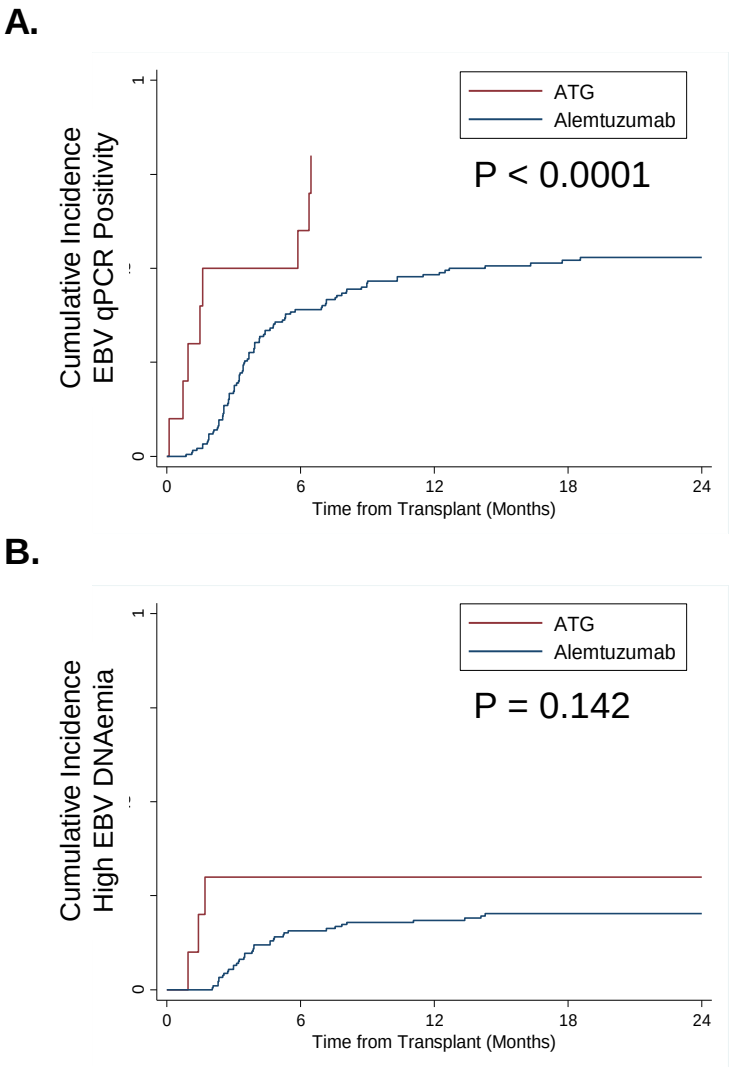

Figure 13. Incidence of EBV Reactivation after T-Cell Deplete Allo-HSCT

Cumulative incidence of EBV DNAemia was determined for patients receiving either ATG or Alemtuzumab T-cell depletion. A. Incidence of EBV qPCR positivity (>500 genomes/ml). B. Incidence of high-level EBV DNAemia (>20,000 genomes/ml). Cumulative incidence curves were compared with the Log Rank test.

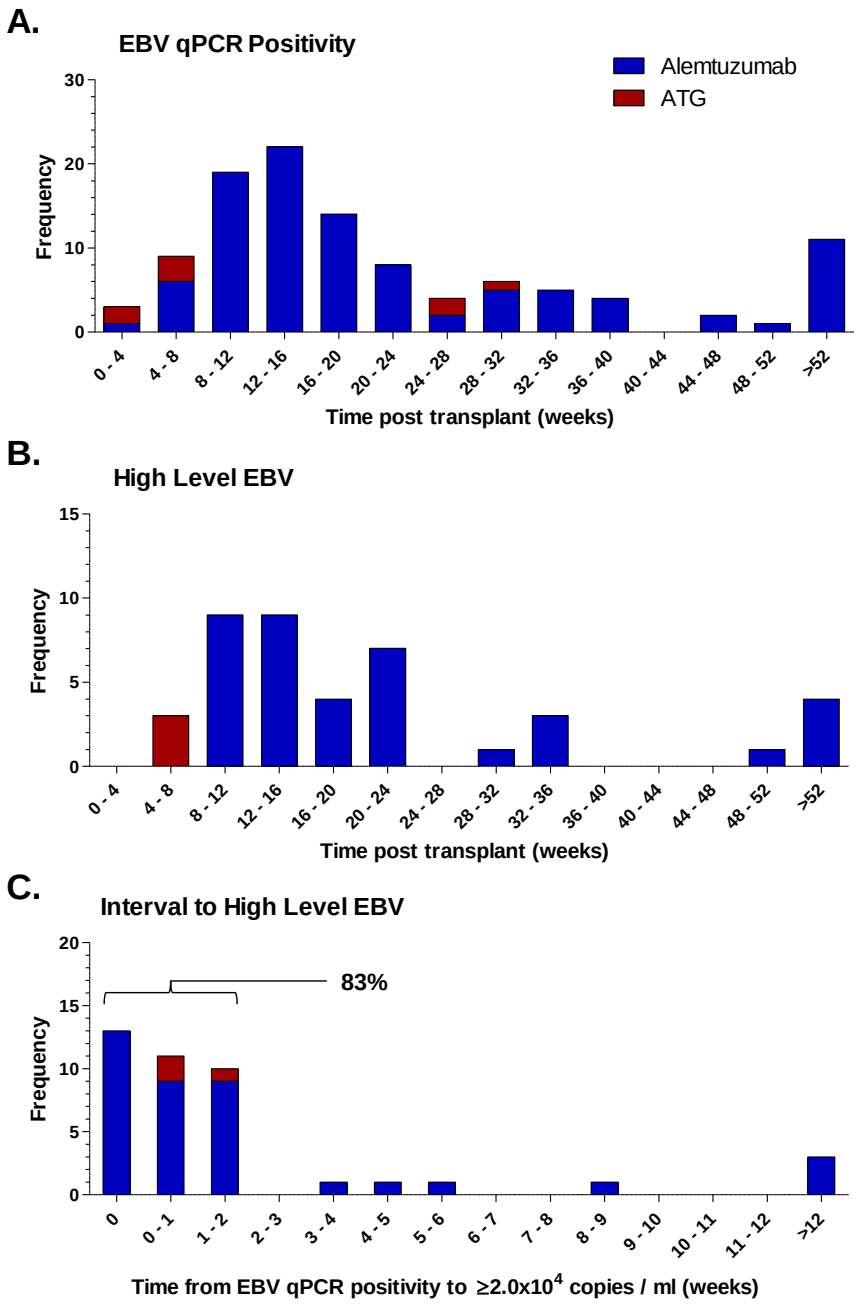

Figure 14. Kinetics of EBV Reactivation after Allo-HSCT

A. Interval from transplant to first EBV qPCR-positive test (≥500 genomes/ml). B. Interval from transplant to high-level EBV reactivation (≥20,000 copies/ml). C. Interval from first EBV qPCR-positive test to high-level EBV DNAemia. The proportion of patients exhibiting high-level EBV reactivation within 2 weeks of initial EBV qPCR positivity is indicated.

many patients, such that in 34 (83%) the interval was less than 2 weeks, and 13 (32%) patients already exhibited high-level reactivation at first EBV qPCR positivity.

In total, 41 patients developed high-level EBV reactivation. Of these, 11 were concurrently diagnosed with PTLD (Table 16), 3 of whom had received ATG-conditioned transplants. The median interval between first EBV load ≥20,000 copies/ml and radiographically documented disease, comprising CT or PET-CT imaging in all cases, was only 7 days (range 0 – 16 days). Biopsy material was subsequently obtained in 4 patients, with confirmation of PTLD in all cases. Histology comprised 2 cases of EBV-positive polymorphic PTLD (one patient also had early PTLD of IM subtype documented in a separate lesion), 1 case of EBV-positive monomorphic PTLD of DLBCL subtype and 1 case of PTLD of unspecified subtype. Of these, 7/11 (64%) had B symptoms documented at presentation and 9/11 (82%) had stage ≥3 disease.

4.2 Pre-Emptive Management

Figure 15 summarises the management of all patients who developed EBV reactivation ≥20,000 copies/ml. A total of 41 patients with high-level EBV reactivation, including 11 diagnosed with PTLD as described above, were treated pre-emptively with up to 4 weekly infusions of Rituximab. Of these, all 30 without evidence of PTLD, and 8/11 (73%) of those with PTLD, had complete responses (defined as sustained resolution of EBV loads to undetectable levels and complete radiological remission of disease where present). Three patients with PTLD showed refractoriness to Rituximab (Figure 16). Patients 6 and 9, who both had nodal PTLD, exhibited initial resolution of EBV DNAemia in response to Rituximab but this recrudesced shortly afterwards. Patient 5, who had nodal PTLD with probable EBV

No.	Diagnosis	Age (years)	Sex	Conditioning	TCD	Donor	Onset of High EBV DNAemia (days)	Interval to diagnosis (days)	Peak EBV load (copies/ml)	B symptoms	Stage	Histology	Outcome, cause of death	Follow-up (months)
1	AA	16	M	Cy	ATG	Sibling	29	16	930,000	N	IE		Alive	48
2	AML	34	M	Cy TBI	Alemtuzumab	Unrelated	119	16	4,346,790	Y	III		Died, Relapse	13
3	AML	56	F	FLAMSA	ATG	Unrelated	52	3	1,081,930	Y	III	PTLD NOS	Died, Relapse	11
4	ALL	63	M	Flu Mel	Alemtuzumab	Sibling	71	7	2,704,380	Y	III		Alive	29
5	AML	57	M	Flu Mel	Alemtuzumab	Unrelated	119	9	2,150,650	Y	IV	DLBCL	Died, PTLD	5
6	HL	43	M	Flu Mel	Alemtuzumab	Unrelated	84	1	57,039	N	III		Died, PTLD	8
7	AML	29	F	Cy TBI	Alemtuzumab	Unrelated	71	7	329,542	N	III		Alive	34
8	MDS	64	M	Flu Mel	Alemtuzumab	Unrelated	56	2	1,805,490	Y	IV	Polymorphic	Died, PTLD	6
9	AML	57	M	Flu Mel	Alemtuzumab	Sibling	91	1	94,945	Y	II	Polymorphic	Died, Relapse	15
10	CLL	54	M	Flu Cy	ATG	Unrelated	43	2	94,789	Y	III		Alive	12
11	ALL	42	F	Flu Mel	Alemtuzumab	Unrelated	70	7	494,794	N	III		Alive	13

Table 16. Patients with PTLD Arising after Allo-HSCT

PTLD was diagnosed in 11 of 196 patients undergoing T-cell deplete allo-HSCT. Of these, 3 had received T-cell depletion with ATG and 8 with Alemtuzumab.

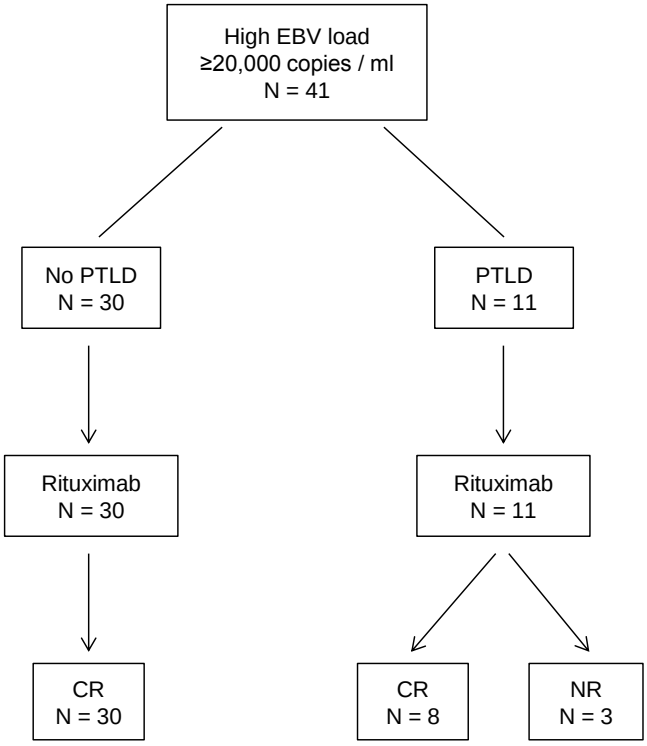

Figure 15. Pre-Emptive Management of EBV Reactivation after allo-HSCT

All patients with EBV DNAemia exceeding 20,000 copies/ml were treated with up to 4 weekly infusions of Rituximab 375mg/m2. 11 patients were diagnosed with PTLD at initiation of therapy. Complete response (CR) was defined as sustained resolution of EBV DNAemia, and disease where evident.

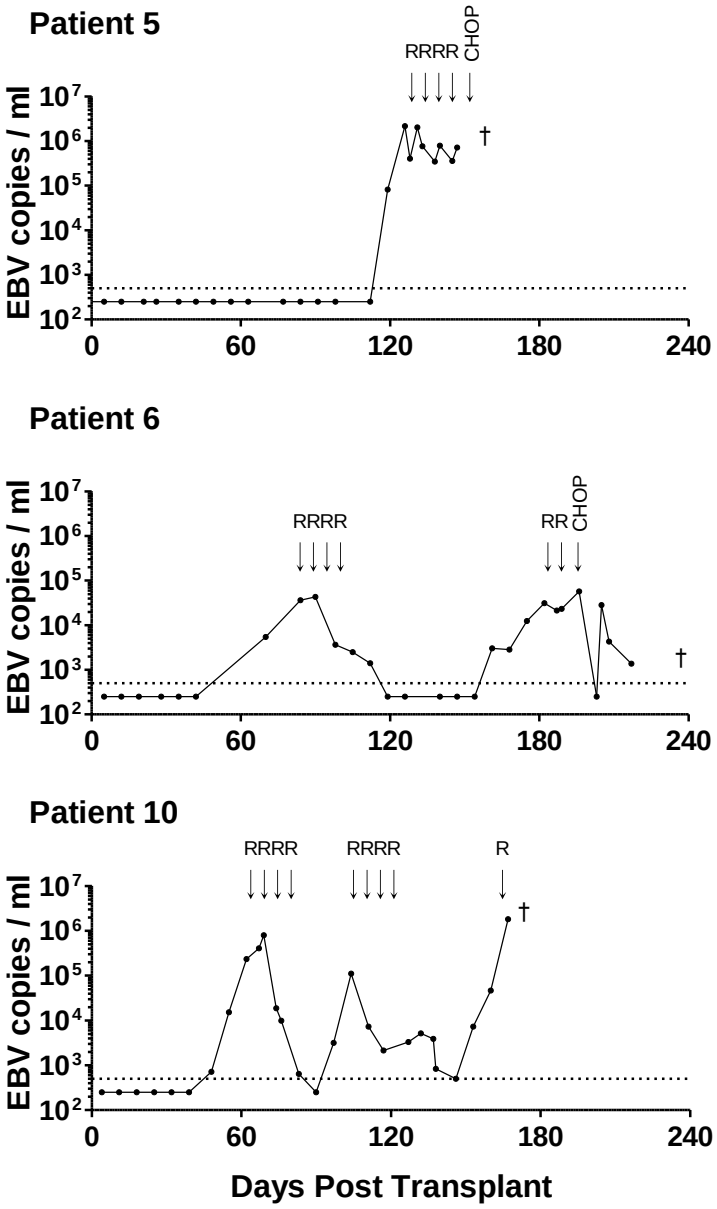

Figure 16. Patients with Rituximab-Refractory PTLD after Allo-HSCT

Serial whole blood EBV loads for patients with PTLD in whom Rituximab therapy failed. All 3 patients died despite use of cytotoxic chemotherapy in 2 of them. R indicates Rituximab; CHOP, cyclophosphamide / doxorubicin / vincristine/ prednisolone.

encephalitis showed no response in EBV load. All 3 patients died with progressive PTLD despite further treatment including CHOP chemotherapy in 2 cases.

Given that some concerns have been raised about the safety of Rituximab use in patients after allo-HSCT[575,576], the impact of pre-emptive Rituximab therapy on survival was analysed using Cox regression; 3 patients who died from PTLD were excluded from this analysis to eliminate the effect of PTLD-related mortality. This revealed no significant deleterious effect from pre-emptive Rituximab on overall survival (HR 1.45, CI 0.81 – 2.60; P = 0.211) or non-relapse mortality (HR 1.44, CI 0.57 – 3.61; P = 0.44).

4.3 Factors Predicting for EBV Reactivation

Baseline predictors for EBV reactivation were analysed using univariate Cox regression (Table 17 and Figure 17). Of these, ATG versus Alemtuzumab was a highly significant risk factor for EBV reactivation (HR 4.6, CI 2.2 – 9.6; P < 0.0001). Age >50 years at transplant was also significantly associated with increased risk (HR 1.6, CI 1.1 - 2.3; P = 0.024). Notably, unrelated or HLA-antigen-mismatched donor status were not identified as risk factors. Although intensity of transplant conditioning was not significantly predictive overall, Flu Mel conditioning was associated with increased risk relative to Cy TBI (borderline significance) and other conditioning regimens. Analysis of these risk factors for high-level EBV reactivation did not reveal significant differences in this small dataset, probably due to lack of statistical power. However, a significant association between acute GvHD grade ≥2 and risk of high-level EBV reactivation was observed (HR 2.54, CI 1.12 – 5.78; P = 0.026).

Importantly, a diagnosis of NHL was associated with a highly significant reduction in the risk

	EBV ≥ 500 copies/ml			EBV ≥ 20,000 copies/ml		
	HR	**95% CI**	**P**	**HR**	**95% CI**	**P**
Age						
> 50 Years	1.57	1.06 – 2.33	**0.024**	1.48	0.76 – 2.90	0.252
Sex						
Male vs Female	1.23	0.81 – 1.85	0.328	1.43	0.72 – 2.86	0.309
Diagnosis						
AML/MDS	1.00	-	Ref	1.00	-	Ref
NHL	0.10	0.03 – 0.32	**0.0001**	-	-	No Events
ALL	0.77	0.40 – 1.51	0.449	0.67	0.20 – 2.20	0.505
HL	0.76	0.33 – 1.76	0.519	1.83	0.70 – 4.78	0.216
CLL	1.08	0.54 – 2.18	0.828	1.25	0.44 – 3.58	0.679
MPD	0.91	0.42 – 2.00	0.820	0.30	0.04 – 2.24	0.242
Other	1.59	0.79 – 3.20	0.197	0.63	0.15 – 2.65	0.526
Donor						
Sibling vs Unrelated	1.27	0.86 – 1.87	0.233	0.64	0.32 – 1.28	0.208
HLA Mismatch						
≥1 Antigens	1.03	0.63 – 1.68	0.903	0.96	0.42 – 2.18	0.921
Intensity						
Myeloablative vs RIC	0.71	0.42 – 1.21	0.210	0.78	0.33 – 1.86	0.578
Conditioning						
Flu Mel	1.00	-	Ref	1.00	-	Ref
Cy TBI	0.64	0.37 – 1.09	0.099	0.69	0.29 – 1.65	0.403
$BEAM^{+}$/- Flu	No Events	-	-	No Events	-	-
Other	1.87	0.99 – 3.52	0.054	0.39	0.12 – 1.27	0.117
T Cell Depletion						
ATG vs Alemtuzumab	4.60	2.21 – 9.57	**<0.0001**	2.35	0.72 – 7.63	0.155
Acute GvHD						
Grade ≥2	1.50	0.91 – 2.50	0.115	2.54	1.12 – 5.78	**0.026**
Prior Rituximab						
Within 6 months	0.17	0.06 – 0.46	**0.0005**	0.16	0.02 – 1.13	0.066
Ever	0.35	0.19 – 0.64	**0.0007**	0.40	0.14 – 1.12	0.081

Table 17. Univariate Analysis of Risk Factors for EBV Reactivation after Allo-HSCT

Risk factors for EBV reactivation ≥ 500 copies/ml or high-level EBV reactivation ≥ 20,000 copies/ml were analysed using univariate Cox testing. Hazard ratios (HR) with 95% confidence intervals (95% CI) were determined for categories within each variable, relative to a reference category (Ref).

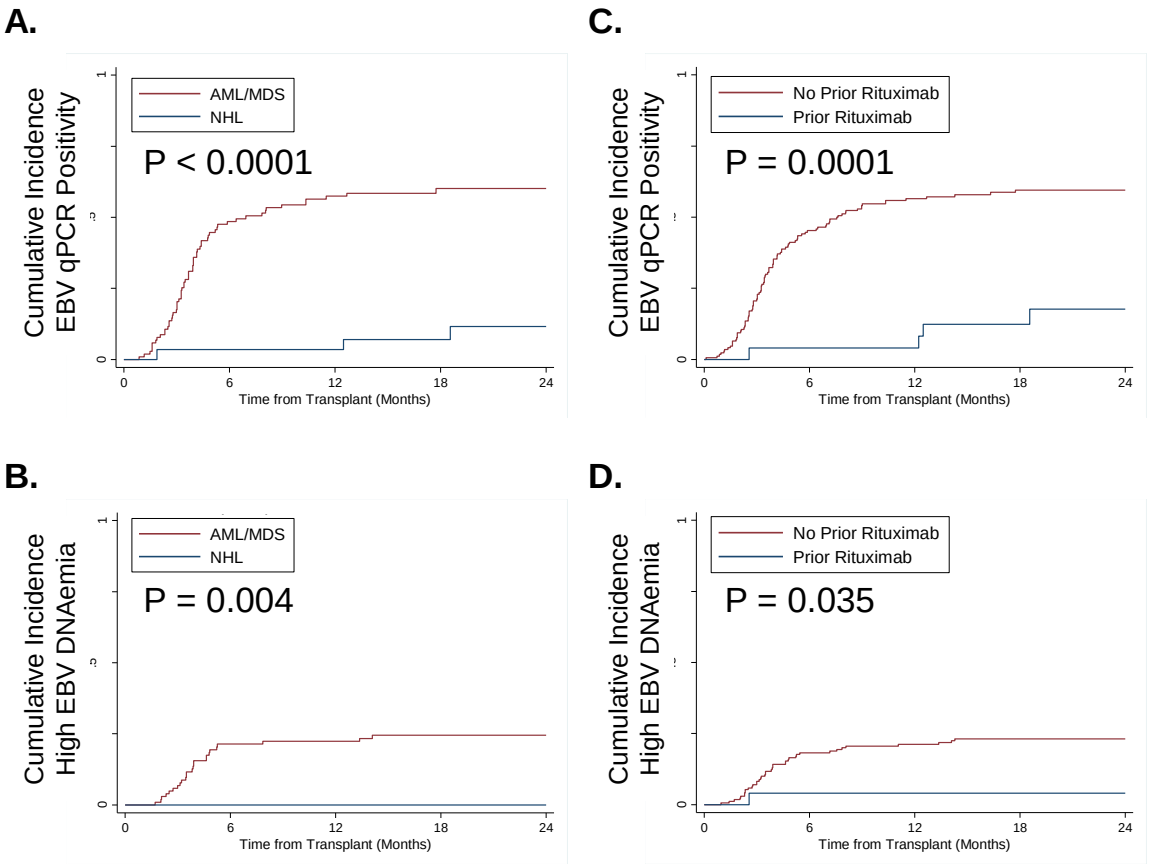

Figure 17. Incidence of EBV Reactivation by Diagnosis and Prior Rituximab Exposure

Cumulative incidence of EBV reactivation or high-level EBV reactivation was determined for patients with AML/MDS or NHL (A and C), or patients who had received Rituximab within 6 months prior to transplant or not (B and D). Cumulative incidence curves are compared with the Log Rank test.

of EBV reactivation (HR 0.10, 0.03 - 0.32; P < 0.0001). Thus, of 29 patients with NHL, only 3 became EBV qPCR-positive (on days 57, 380 and 565 days post-transplant). Furthermore, no cases of high-level EBV reactivation were observed for those with NHL in the 2 years after transplant. This was apparent despite equivalent frequency and duration of EBV monitoring in comparison to other patients. Notably, the markedly reduced risk of EBV reactivation observed for patients with NHL was not similarly noted for those with HL; 6/11 (55%) patients with HL exhibited EBV qPCR positivity, including 5 cases of high-level EBV DNAemia.

In order to establish whether lack of EBV reactivation observed amongst patients with NHL was independent of other baseline factors, multivariate testing was performed using a Cox proportional hazards model including baseline factors age, diagnosis, type of TCD and transplant conditioning (Table 18). Within this analysis, a diagnosis of NHL remained highly predictive for lack of EBV reactivation (HR 0.16, CI 0.05 – 0.51; P = 0.002).

4.4 Pre-Transplant Rituximab

Given that a highly significant reduction in risk of EBV reactivation had been observed amongst patients with NHL, pre-transplant use of Rituximab was examined as a possible factor (Table 19). Thus, Rituximab use was documented in 28/29 (97%) patients with NHL, with the last infusion administered a median 3 months (IQR 2 – 5 months) before transplant. Prior Rituximab was also recorded in 11/12 (92%) patients with CLL but the last infusion of Rituximab was delivered substantially longer before transplant, at median 14 months (IQR 8 – 23 months). Importantly, only 1/25 (4%) patients who received Rituximab less than 6 months before transplant reactivated EBV in the first year - a patient with CLL who received

	EBV ≥ 500 copies/ml		
	HR	**95% CI**	**P**
Age			
> 50 Years	1.46	0.85 – 2.50	0.168
Diagnosis			
AML/MDS	1.00	-	Ref
NHL	0.18	0.06 – 0.58	0.004
ALL	0.90	0.46 – 1.77	0.762
HL	1.77	0.69 – 4.53	0.236
CLL	0.98	0.48 – 2.00	0.955
MPD	0.97	0.44 – 2.15	0.940
Other	2.50	0.94 - 6.64	0.067
Conditioning			
Flu Mel	1.00	-	Ref
Cy TBI	0.77	0.39 – 1.52	0.452
$BEAM^{+}$/- Flu	No Events	-	-
Other	0.35	0.08 – 1.51	0.159
T Cell Depletion			
ATG vs Alemtuzumab	7.36	1.75 – 30.9	0.006

Table 18. Multivariate Analysis of Risk Factors for EBV Reactivation after Allo-HSCT

In a multivariate Cox proportional hazards model including the age, diagnosis, conditioning and T-cell depletion, NHL was a highly significant predictor for lack of EBV reactivation. Prior Rituximab therapy was also a highly significant predictor for lack of EBV reactivation in a separate model that excluded diagnosis. Significance for prior Rituximab was eliminated when diagnosis was included in this model. However, severe confounding between prior Rituximab therapy and diagnostic category was apparent. Hazard ratios (HR) with 95% confidence intervals (95% CI) were determined for categories within each variable, relative to a reference category (Ref).

Diagnosis	Rituximab: Months prior to transplant	Day EBV qPCR positive	Day EBV >20,000 copies/ml
NHL	1	.	.
NHL	2	.	.
NHL	2	.	.
NHL	2	.	.
NHL	2	.	.
NHL	2	.	.
NHL	2	.	.
NHL	2	.	.
NHL	2	565	.
NHL	2	.	.
NHL	2	.	.
NHL	2	.	.
NHL	2	.	.
NHL	2	.	.
CLL	2	372	.
NHL	3	.	.
NHL	3	380	.
NHL	4	.	.
NHL	4	.	.
NHL	4	.	.
NHL	4	.	.
NHL	5	.	.
CLL	5	78	78
NHL	6	.	.
NHL	6	.	.
NHL	7	.	.
CLL	7	.	.
CLL	9	29	43
CLL	10	104	.
CLL	14	.	.
CLL	15	273	.
CLL	15	217	.
NHL	17	.	.
NHL	24	57	.
NHL	29	.	.
CLL	30	41	.
NHL	31	.	.
CLL	37	218	337
CLL	47	85	99
NHL	None	.	.
CLL	None	.	.

EBV DNAemia within 1 year

EBV DNAemia after 1 year

Table 19. Prior Rituximab Therapy and EBV Reactivation after Allo-HSCT

The interval (months) between the last infusion of pre-transplant Rituximab and day 0 of the transplant is given for all study patients with NHL and CLL. The corresponding day of EBV reactivation or high-level EBV reactivation post-transplant is shown. EBV reactivation events occurring within 1 year after transplant appear in red, whilst those occurring after 1 year appear in blue. Only 1 patient who received Rituximab within 6 months prior to transplant reactivated EBV in the first year after transplant.

Rituximab 5 months prior to transplant and who developed high-level EBV reactivation on day 78. In contrast, 8/14 (57%) patients who received Rituximab more than 6 months before transplant developed EBV reactivation, including 3 patients with high-level EBV reactivation.

In univariate Cox analysis, there was a highly significant association between pre-transplant Rituximab therapy and lack of EBV reactivation, using definitions of pre-transplant Rituximab of either 'prior Rituximab ever' (HR 0.35, CI 0.19 – 0.64; P = 0.0007) or a cut-off of 6 months prior to transplant (HR 0.17, CI 0.06-0.46; P = 0.0005). These differences did not persist in multivariate testing but this analysis was complicated for several reasons. Firstly, there was strong confounding between diagnostic category and prior use of Rituximab, such that almost all patients with NHL and CLL received Rituximab at some time before transplant. Secondly, there was uncertainty regarding what constitutes an appropriate cut-off (months before transplant) to use to define pre-transplant Rituximab. Finally, few patients with NHL reactivated EBV, even if they received Rituximab more than 6 months before transplant, unlike patients with CLL (Table 19).

Regarding the safety of pre-transplant Rituximab, testing revealed no significant difference in overall survival for patients treated with Rituximab at any time before transplant (HR 0.72, CI 0.41 – 1.28; P = 0.262) or within 6 months before transplant (HR 0.75, CI 0.38 – 1.5; P = 0.420). Similarly no significant differences were seen for non-relapse mortality for Rituximab given at any time before transplant (HR 0.93 CI 0.43 – 2.02; P = 0.856) or using a 6 month cut-off (HR 0.91, CI 0.36 – 2.33; P = 0.845). An association between pre-transplant Rituximab (defined as any time before transplant or using a 6 month cut-off) and risk of either Grade ≥I or Grade ≥2 acute GvHD was also not observed.

4.5 Discussion

This study reports incidence and risk factors for EBV reactivation and PTLD amongst patients undergoing TCD allo-HSCT at a major UK transplant centre, and includes the largest number of transplants using Alemtuzumab reported thus far. A relatively high overall incidence of EBV DNAemia was observed amongst Alemtuzumab-treated patients, with 48% of individuals exhibiting EBV qPCR positivity by 12 months post-transplant and 18% developing high-level EBV reactivation. This incidence was significantly higher amongst ATG-treated patients, with 80% exhibiting EBV qPCR positivity and 30% developing high-level reactivation. Importantly, PTLD was diagnosed, coincident with high-level EBV reactivation, in 11 patients. Three of these had received ATG, whilst Alemtuzumab had been used in 8, giving a crude incidence of PTLD amongst Alemtuzumab-treated patients of 4.3%. This is greater than that reported in the study by Carpenter et al., in which only 0.9% of Alemtuzumab-treated patients developed PTLD[409], although it is within the range report by other studies[412,414,415,500]. However, it is notable that around a third of patients in the Carpenter study received Alemtuzumab 'in the bag' (in which the drug is used to treat the stem cell graft *in vitro*, before it is infused into the recipient) rather than *in vivo*, whereas the latter was used for all patients in the present study. Higher peak concentrations and persistence of Alemtuzumab have been reported when it is used *in vivo*[577], and this is also associated with delayed reconstitution of EBV-specific immunity[383]. These alternative approaches to TCD may account for at least some of the variation observed in PTLD incidence between these studies.

Regarding the kinetics of EBV DNAemia, most cases of EBV reactivation occurred between 2 and 4 months after transplant, with reactivations in ATG-treated patients typically occurring

earlier than in those treated with Alemtuzumab. However, some instances were documented up to and beyond 12 months. Given this, it is notable that recent guidelines have advised that high risk patients should be monitored for 3 months after allo-HSCT[496]. The current study supports extending this recommendation to 6 months, at least for Alemtuzumab-treated patients. Furthermore, given that over 80% of high-level reactivations were seen to occur within 2 weeks of initial EBV qPCR positivity, particular scrutiny should be exercised in the first weeks following initial EBV qPCR positivity.

Amongst patients who developed high-level EBV reactivation, with or without PTLD, excellent response rates to pre-emptive Rituximab therapy were observed, with 38/41 (93%) patients exhibiting complete resolution of EBV DNAemia. However, 3 patients developed Rituximab-refractory PTLD and died from progressive disease, despite the use of cytotoxic chemotherapy in 2 of them. Unfortunately, although chemotherapy such as CHOP may achieve good outcomes for Rituximab-refractory disease in the setting of solid organ transplantation, this has not been the case for PTLD arising after allo-HSCT, where very poor outcomes are likely to be a consequence of increased toxicity in this patient group[520,572]. In light of these experiences we now recommend that all patients developing Rituximab-refractory PTLD are treated with EBV CTLs. Notably, some studies have recently raised concerns about the safety of Rituximab in recipients of allo-HSCT, demonstrating a possible excess of infectious complications, although an effect on survival has not been established[507,575,576]. Given this, it is notable that the use of pre-emptive Rituximab was not associated with an increase in mortality in the present study, although this analysis was based on a relatively small number of events and it may have lacked statistical power.

Of possible predictors for EBV reactivation we found that ATG treatment, older age at transplant and the occurrence of acute GvHD were all significant risk factors. In this respect, our data agree with previous studies on risks associated with EBV reactivation and PTLD after allo-HSCT[392]. However, the most striking finding was a dramatically reduced incidence of EBV reactivation and PTLD amongst patients with a diagnosis of NHL. Therefore, individuals with NHL exhibited a highly significant reduction in the risk of EBV reactivation in both univariate and multivariate analyses, and no patients with NHL exhibited high-level reactivation. Whilst our data should be treated with some caution due to the retrospective nature of the study, our observation is intriguing because it raises the possibility that Rituximab therapy delivered prior to transplant might be responsible for this effect. In support of this we found that individuals with HL *did* frequently experience EBV reactivation - patients with HL do not routinely receive treatment with Rituximab. Furthermore, our observations are consistent with the anecdotal description by Savani et al. of an absence of EBV reactivation after allo-HSCT in 38 patients who received Rituximab prior to, or concurrent with, transplantation[574]. Although our findings have not been observed in other studies of EBV reactivation and PTLD after allo-HSCT, this may be because these studies pre-date the routine use of Rituximab for patients with NHL[392,407], or because they have not specifically analysed the risks associated with NHL[408,410,411,416-419]. Notably, in the study by Carpenter et al., NHL showed a trend towards lower incidence of EBV reactivation (HR 0.68; CI 0.25–1.85) but this was not statistically significant (P = 0.45); however it is unknown what type of NHL these patients had, or indeed whether they had ever received Rituximab[501].

It light of the above, it is possible that Rituximab delivered shortly before transplant might be a highly effective alternative to pre-emptive strategies for managing PTLD. Conceivably,

Rituximab might prevent EBV reactivation through 1 of 2 alternative mechanisms. Firstly, it has a half-life of up to 18 days, with levels remaining detectable in the serum for up to 3 months after administration, and it is known to deplete circulating B-cells for around 6 months[497]. As such, prior Rituximab might contribute to a delay in the recovery of B-cells post-transplant. Indeed, van Dorp et al. demonstrated a significantly reduced rate of B-cell reconstitution in patients who had received Rituximab within 6 months prior to transplant[578]. Alternatively, Rituximab may act by reducing recipient pre-transplant virus burden. Interestingly, the latter supposes that it is predominantly recipient-derived virus that most commonly leads to EBV reactivation. With regard to this, a small number of (largely anecdotal) studies have demonstrated that patients with EBV reactivation or PTLD arising after allo-HSCT acquire a donor or third party EBV strain in approximately 50% of cases[579-582]. However, it is notable that all such studies have been conducted in the setting of myeloablative transplantation; it is possible that RIC transplantation may increase the likelihood that recipient-derived virus is important for the pathogenesis of EBV reactivation and PTLD post allo-HSCT.

To conclude, in this study we have examined EBV reactivation and PTLD amongst a large cohort of adult patients undergoing TCD allo-HSCT. Importantly, we describe the novel finding that risk of EBV reactivation appears to be greatly reduced amongst recipients with NHL. This suggests that Rituximab could be used as effective prophylaxis for PTLD arising after allo-HSCT. Ultimately, our data make a strong case for prospectively evaluating the role of Rituximab in allograft conditioning.

5. Studies on the Persistence of EBV in Patients Undergoing Allo-HSCT

As we have seen, EBV reactivation is a relatively common event following allo-HSCT. Nevertheless, much of the pathophysiology of this process remains poorly characterised. Given that healthy individuals, and immunocompromised solid allograft recipients with raised circulating EBV loads, are thought to selectively harbour EBV in resting $CD27^+$ memory B-cells[315-317,386], we were intrigued by the fact that most patients who reactivate EBV following allo-HSCT typically do so between 2 - 3 months after transplant, when the reconstituting B-cell system usually contains few memory B-cells[363-365]. In order to investigate this apparent paradox, studies were undertaken to characterise the relationship between EBV reactivation and B-cell reconstitution in a cohort of patients undergoing allo-HSCT.

5.1 Patients

Study patients were recruited from those undergoing allo-HSCT at University Hospital Birmingham, UK (the same cohort as analysed in Chapter 4). As mentioned previously, all patients undergoing T deplete allo-HSCT at this centre (who are thus considered to be at increased risk of developing PTLD) are monitored using EBV qPCR analysis of whole blood samples, with testing performed every 1 - 2 weeks for at least 6 months post-transplant. This clinical EBV qPCR monitoring system was used to identify patients exhibiting high-level EBV reactivation who were subsequently approached and asked to provide a blood sample, prior to the routine administration of Rituximab to treat the EBV reactivation.

Using this strategy, 13 patients who had undergone consecutive allo-HSCT and subsequently developed high-level EBV reactivation (defined here as an EBV load $\geq 2 \times 10^4$ EBV copies/ml)

within 6 months of transplant were identified. Blood samples obtained from this 'High EBV' group were processed to isolate PBMCs which were then cryopreserved. In addition, samples were obtained for an age- and sex- matched control group of 16 allo-HSCT patients who did not develop high-level EBV reactivation at any time post-transplant; known as the 'No/Low EBV' group. Table 20 shows the characteristics of all study patients.

High EBV Group

For those in the 'High EBV' group, the age at transplant was median 57 years (range 34 – 67) and 10/13 (77%) patients were male. All patients had undergone reduced intensity preparative conditioning with FMC, apart from Patient 1 who underwent myeloablative conditioning with Cyclophosphamide/TBI. The indication for transplant was treatment of AML or myelodysplasia in 11/13 (85%) patients, with 1 patient undergoing transplantation for HL and another for CLL. None of the patients had evidence of primary disease relapse at the time of high-level EBV reactivation.

Figure 18 shows plots of serial whole blood EBV qPCR testing for each patient in the High EBV group, indicating the time point at which each was bled during the EBV reactivation. Importantly, these plots demonstrate that each patient was bled at or near to the point of maximal EBV load during the reactivation. The kinetics of viral DNAemia were similar amongst these patients, with a median interval from transplant to first EBV qPCR positivity (defined as a single EBV qPCR test ≥500 genomes/ml) of 99 days (IQR 84 – 119 days). All patients showed a rapid expansion in EBV load, with a median interval from first EBV qPCR positivity to high-level EBV DNAemia of only 7 days (IQR 0 – 14 days). The EBV load at first EBV qPCR positivity was median 2.9 $x10^3$ genomes/ml, whilst the EBV load at the time

High EBV Group								
No.	**Age**	**Sex**	**Diagnosis**	**Donor**	**Regimen**	**Acute GvHD (grade)**	**Peak EBV (copies/ml)**	**PTLD**
1	34	M	AML	MUD	Cy TBI C	II+	4,346,790	+
2	57	M	AML	MUD	FMC	II+	216,452	
3	57	M	AML	MUD	FMC	I	160,389	
4	55	M	AML	MUD	FMC	II+	33,051	
5	64	M	MDS	MUD	FMC	II+	1,805,490	+
6	51	M	AML	MUD	FMC	I	141,098	
7	61	M	AML	MUD	FMC		97,302	
8	48	M	HL	MUD	FMC	II+	26,897	
9	57	F	CLL	MUD	FMC	II+	154,0170	
10	57	M	AML	Sibling	FMC	I	94,945	+
11	67	F	MDS	MUD	FMC		1,670,830	
12	61	M	AML	MUD	FMC	II+	535,988	
13	50	F	AML	Sibling	FMC	I	249,749	
No/Low EBV Group								
No.	Age	**Sex**	**Diagnosis**	**Donor**	**Regimen**	**Acute GvHD (grade)**	**Peak EBV (copies/ml)**	**PTLD**
14	55	M	AML	MUD	FMC		966	
15	61	M	AML	MUD	FMC		1,798	
16	65	M	AML	Sibling	FMC	II+	3,203	
17	51	F	ALL	Sibling	FMC	I	3,648	
18	57	M	MDS	MUD	FMC	I	<500	
19	54	M	ALL	MUD	FMC	I	3,291	
20	54	F	HL	Sibling	FMC	II+	4,241	
21	58	M	T-PLL	Sibling	FMC		3,800	
22	62	M	AML	MUD	FMC		1,339	
23	64	M	AML	MUD	FMC	I	1,230	
24	70	F	AML	MUD	FMC		<500	
25	66	M	AML	MUD	FMC	II+	1,370	
26	53	M	AML	Sibling	FMC		<500	
27	61	M	MDS	Sibling	FMC		550	
28	44	M	MF	MUD	FMC		<500	
29	47	F	AML	MUD	FMC	I	<500	

Table 20. High EBV and No/Low EBV Allo-HSCT Patients

Characteristics for the High EBV (≥20,000 EBV copies/ml) and No/Low EBV (<5000 EBV copies/ml) groups of allo-HSCT patients are shown.

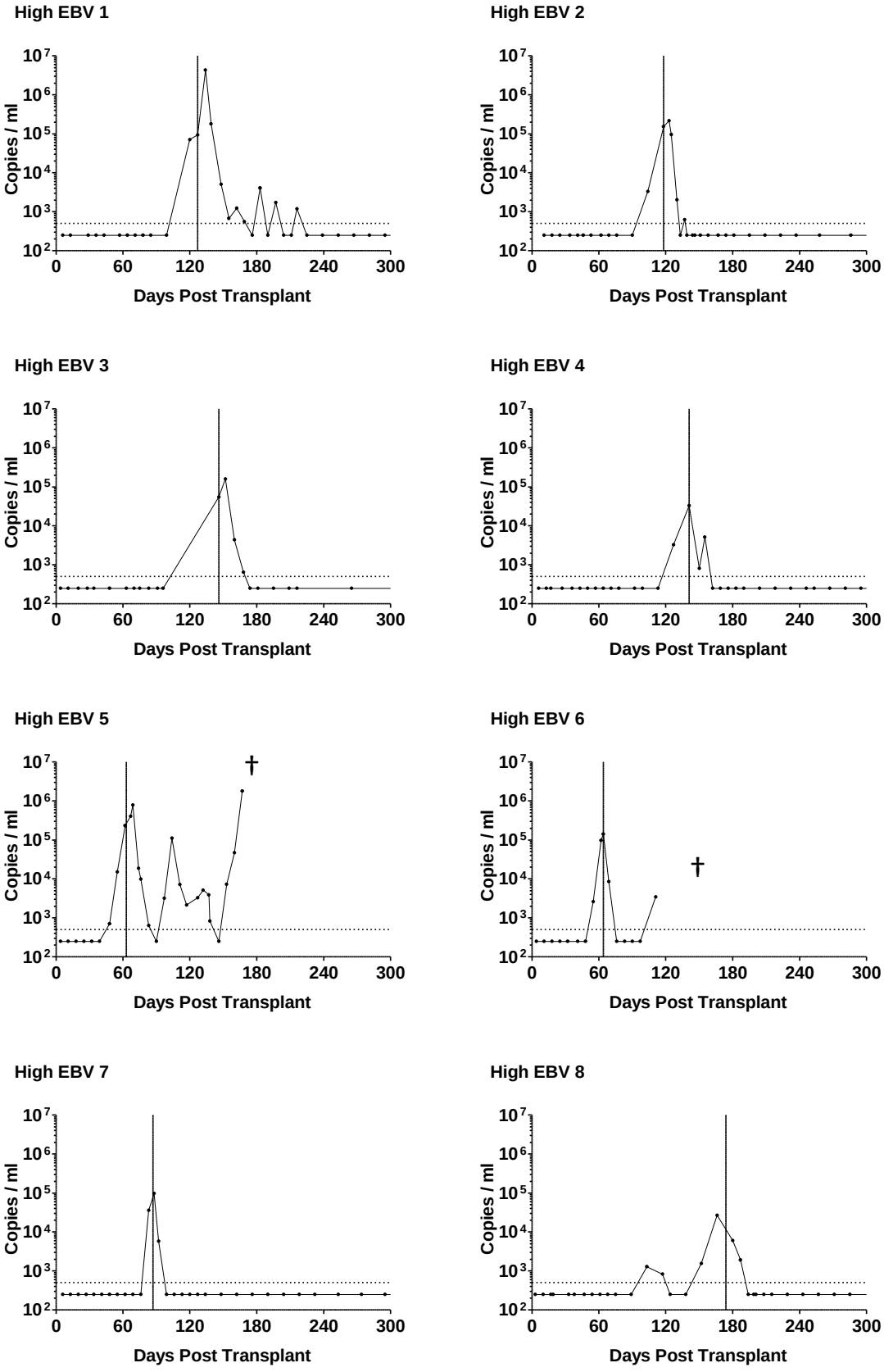
High EBV 1
High EBV 2
High EBV 3
High EBV 4
High EBV 5
High EBV 6
High EBV 7
High EBV 8
Copies / ml
Days Post Transplant
†

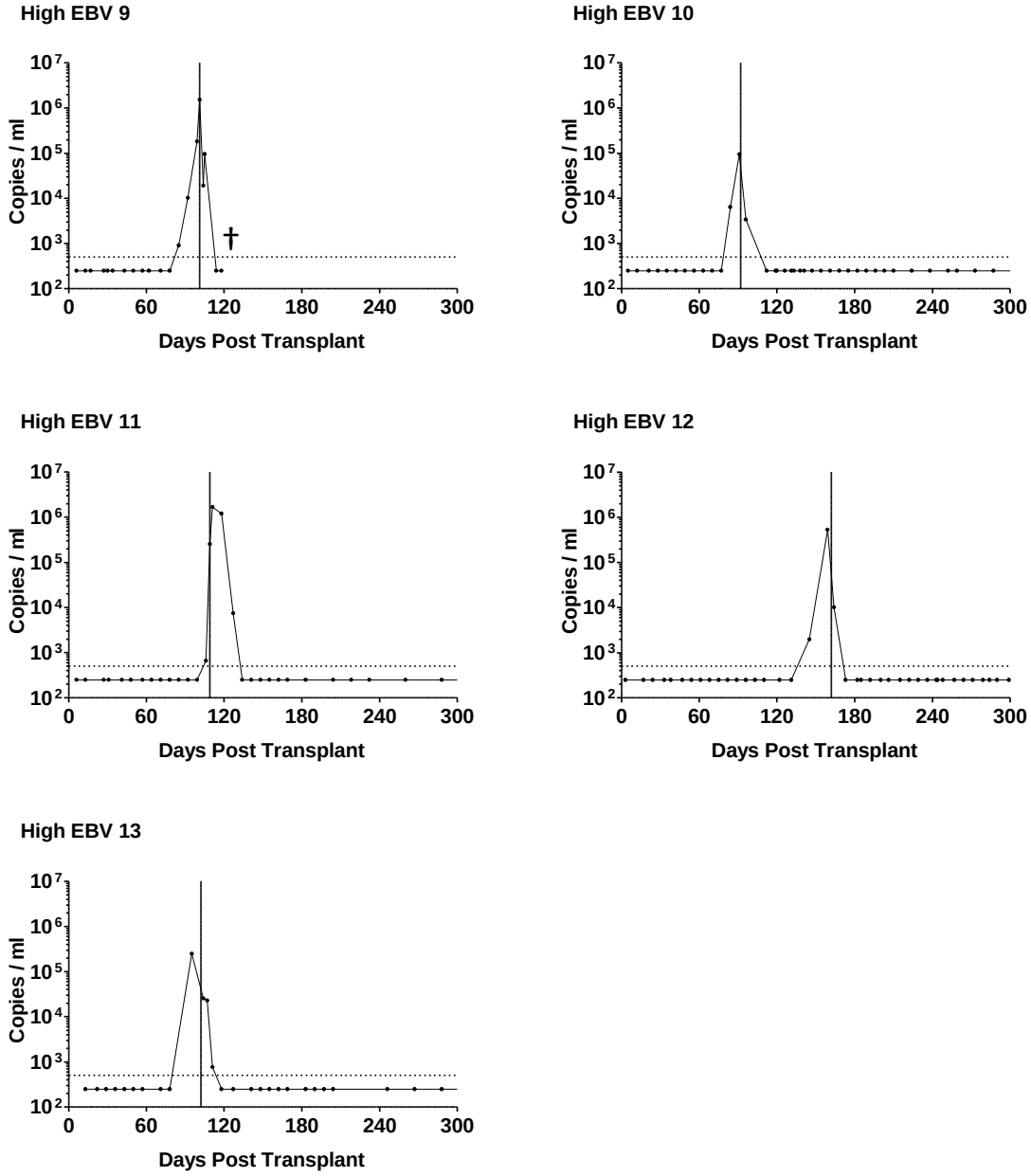

Figure 18. Serial Whole Blood EBV Loads for High EBV Allo-HSCT Patients

Patients with high-level EBV DNAemia were identified by routine clinical EBV qPCR monitoring. Blood samples were collected prior to the initiation of Rituximab, as indicated by the vertical lines. Values below the 500 EBV genome copies/ml sensitivity of the assay are displayed as 250 copies/ml.† indicates death of the patient within the first 300 days; Patient 5 died from PTLD, Patient 6 from relapsed AML and Patient 9 from pneumonia.

of first high-level DNAemia was median 9.8 $x10^4$ genomes/ml. Peak EBV load was median 1.9 $x10^5$ genomes/ml.

Of those with high-level EBV reactivation, Patients 1, 5 and 10 were diagnosed with PTLD. For these, radiographic evidence of disease was documented at 16, 9 and 1 day(s) after first detection of the high EBV load respectively. All exhibited B symptoms at presentation and Ann-Arbor stage was III, IV and II respectively. A lymph node biopsy was performed for Patient 10, confirming $EBER^+$ polymorphic PTLD. A tissue biopsy was not obtained for Patients 1 and 5 and therefore a diagnosis of probable PTLD was made.

All patients with high-level EBV DNAemia were treated pre-emptively with up to 4 infusions of Rituximab 375mg/m^2. Twelve of the 13 patients had a complete response to Rituximab, with durable resolution of EBV DNAemia and disease where present (Figure 18). Although Patient 5 showed an initial response to Rituximab, with a reduction in EBV load to an undetectable level, this rapidly relapsed and the patient subsequently died from progressive PTLD.

No/Low EBV Group

For patients in the No/Low EBV group, median age at transplant was 57 years (44 – 70 years) and 12/16 (75%) were male. All patients had undergone reduced intensity transplantation with FMC conditioning. Notably, all had been recruited to the study prior to transplant and had been bled prospectively, such that cryopreserved PBMCs were available from them at time points around 3, 6 and 12 months post-transplant. Despite EBV qPCR monitoring with the same frequency and duration as those who developed high-level EBV reactivation, 5/16

(31%) of these patients remained EBV qPCR-negative after transplant, whilst the others exhibited only low-level EBV reactivation, with a maximal EBV load of only 4.2 $x10^3$ genomes/ml.

Statistical Comparisons between High EBV and No/Low EBV Groups

Samples from the High EBV group were collected at a median of 109 days post-transplant (IQR 92 – 141 days). For the purpose of statistical analysis, all comparisons were made to No/Low EBV group samples combined from 3 and 6 month time points, collected at a median of 112 days post-transplant (IQR 84 – 169 days). No statistical difference was observed for the distributions of post-transplant collection times (P = 0.624) for these groups. All statistical comparisons were made using the Mann-Whitney U test.

5.2 Total Lymphocyte Counts

Simultaneous with the collection of study blood samples, an automated haematology analyser was used to determine absolute lymphocyte counts (Figure 19). The No/Low EBV patients had lymphocyte numbers at 3, 6 and 12 months post-transplant of median 0.6 $x10^9$ cells/L (IQR 0.6 – 0.9 $x10^9$ cells/L), 1.4 $x10^9$ cells/L (IQR 1.0 – 1.9 $x10^9$ cells/L) and 1.5 $x10^9$ cells/L (1.1 – 2.3 $x10^9$ cells/L) respectively. These values were noticeably lower than those of a control group of 10 healthy adult donors who had a median lymphocyte count of 1.9 $x10^9$ cells/L (IQR 1.4 – 2.3 $x10^9$ cells/L), which was within the reference range of the assay of 1.0 – 4.0 $x10^9$ cells/L. The finding of marked lymphopenia which gradually recovered over several months is characteristic of lymphocyte reconstitution following allo-HSCT. Notably,

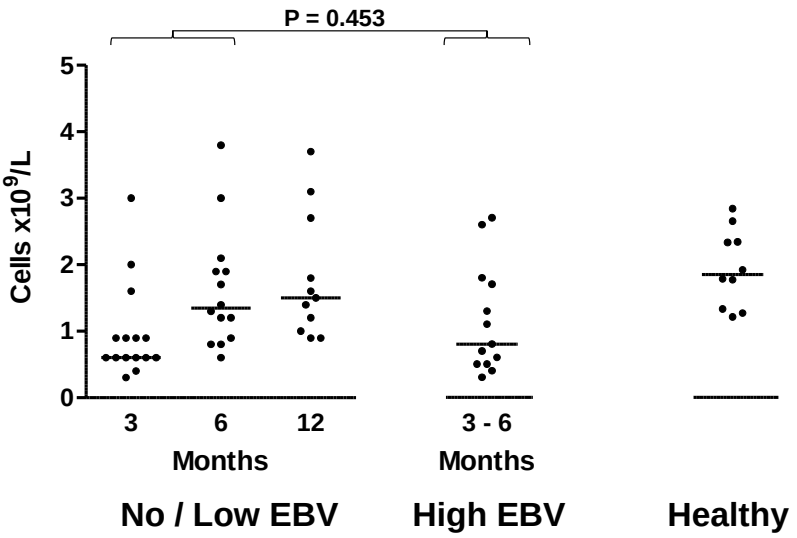

Figure 19. Lymphocyte Counts after Allo-HSCT

Total lymphocyte counts were determined for No/Low EBV, High EBV and healthy adult donors using an automated haematology analyser. Median values are shown by the horizontal bars. No significant difference was observed between the High EBV and No/Low EBV groups.

patients with high-level EBV DNAemia had a median lymphocyte count of 1.0 $x10^9$ cells/L (IQR 0.6 - 1.6 $x10^9$ cells/L), which was not significantly different to those of the No/Low EBV group, matching for time post-transplant (P = 0.453).

5.3 EBV Loads in PBMCs from Patients after Allo-HSCT

Circulating EBV DNA (as measured by whole blood PCR) can either be cell-associated or extracellular; in the latter it is thought to exist either as fragments of DNA released from dying cells or encapsulated viral DNA[385]. With the aim of quantitating EBV genome load in the cellular compartment, DNA was extracted from PBMCs and then analysed using a highly sensitive in-house EBV qPCR assay. This quantitates both EBV genome copy number and equivalent cell number by simultaneously amplifying regions of EBV DNA polymerase and cellular β2M genes. Thus, the assay is able to determine average EBV genome copies per cell within a given population of cells; by convention values are reported as EBV copies per 10^6 cells.

The in-house EBV qPCR assay was used to test PBMCs collected from all study patients and those from 27 healthy adult donors (Figure 20). Of the healthy adult controls, 19/27 (70%) had detectable EBV loads, amongst whom there was a median of 73 copies per 10^6 PBMCs (IQR 19 – 187 copies per 10^6 PBMCs). These values are typical of a healthy adult population analysed with this assay[299,331,338]. Of the No/Low EBV group 47%, 64% and 73% had detectable EBV loads at around 3, 6 and 12 months after transplant, with median EBV loads amongst the positive patients of 6.0 $x10^2$ copies per 10^6 PBMCs (IQR 1.3 $x10^2$ – 1.3 $x10^3$ copies per 10^6 PBMCs), 1.8 $x10^3$ copies per 10^6 PBMCs (IQR 7.8 $x10^2$ – 1.1 $x10^4$ copies per 10^6 PBMCs) and 2.7 $x10^3$ copies per 10^6 PBMCs (IQR 2.4 $x10^2$ - 9.8 $x10^3$ copies per 10^6

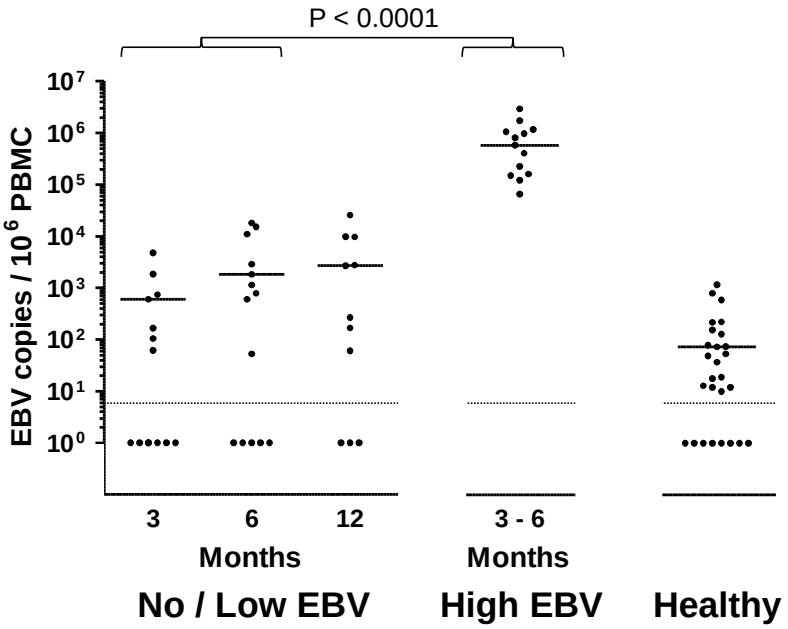

Figure 20. PBMC EBV Loads after Allo-HSCT

EBV loads within PBMC preparations were determined for No/Low EBV, High EBV and healthy adult donors using EBV qPCR. The medians of positive values are shown by the horizontal bars. The dotted line represents the level of sensitivity of 10 copies/10^6 PBMCs and undetected values are shown as having a value of 1. Loads in the High EBV group were significantly higher ($P < 0.0001$) than those of the No/Low EBV group for 3 – 6 month time points.

PBMCs) respectively. As expected, the samples for patients with high-level EBV reactivation contained significantly ($P < 0.0001$) higher EBV loads, with a median of 5.9 $x10^5$ copies per 10^6 PBMCs (IQR 1.6 $x10^5$ – 1.1 $x10^6$ copies per 10^6 PBMCs). These values are amongst the highest ever detected from *ex vivo* samples in this laboratory. Comparison of the EBV loads generated by the whole blood and PBMC EBV qPCR assays showed a relatively poor correlation amongst High EBV patients (Appendix, Figure 67). Overall, these findings confirmed that the samples collected from High EBV patients contained very high cell-associated EBV loads.

5.4 Analysis of Main Lymphocyte Subsets

A flow cytometry panel was designed to distinguish main lymphocyte subsets present within PBMCs from healthy adult donors (Figure 21). In this panel, a gate was set to include lymphocytes and monocytes on the basis of FSC/SSC profile, after which doublets, $CD14^+$ monocytes and non-viable cells were excluded. Events positive for the pan-lymphocyte marker CD45 were then gated to exclude, amongst other contaminating subsets, nucleated erythrocytes which may be increased in patients with haematological disease and which often possess a FSC/SSC profile similar to lymphocytes. Subsequently, the proportion of $CD3^+$ T-cells, CD3-$CD56^+$ NK-cells and $CD19^+$ B-cells were quantitated as a proportion of $CD45^+$ lymphocytes. Additional T-cell subsets were also identified, including $CD4^+$ and $CD8^+$ T-cells (from which CD4/8 ratios could be determined), as well as $CD3^+CD56^+$ NK/T-cells. Furthermore, inclusion of an anti-T-cell receptor α/β antibody made it possible to distinguish TCR α/β positive and negative subsets, the latter allowing estimation of TCR γ/δ T-cells. Absolute numbers were subsequently calculated from corresponding lymphocyte counts.

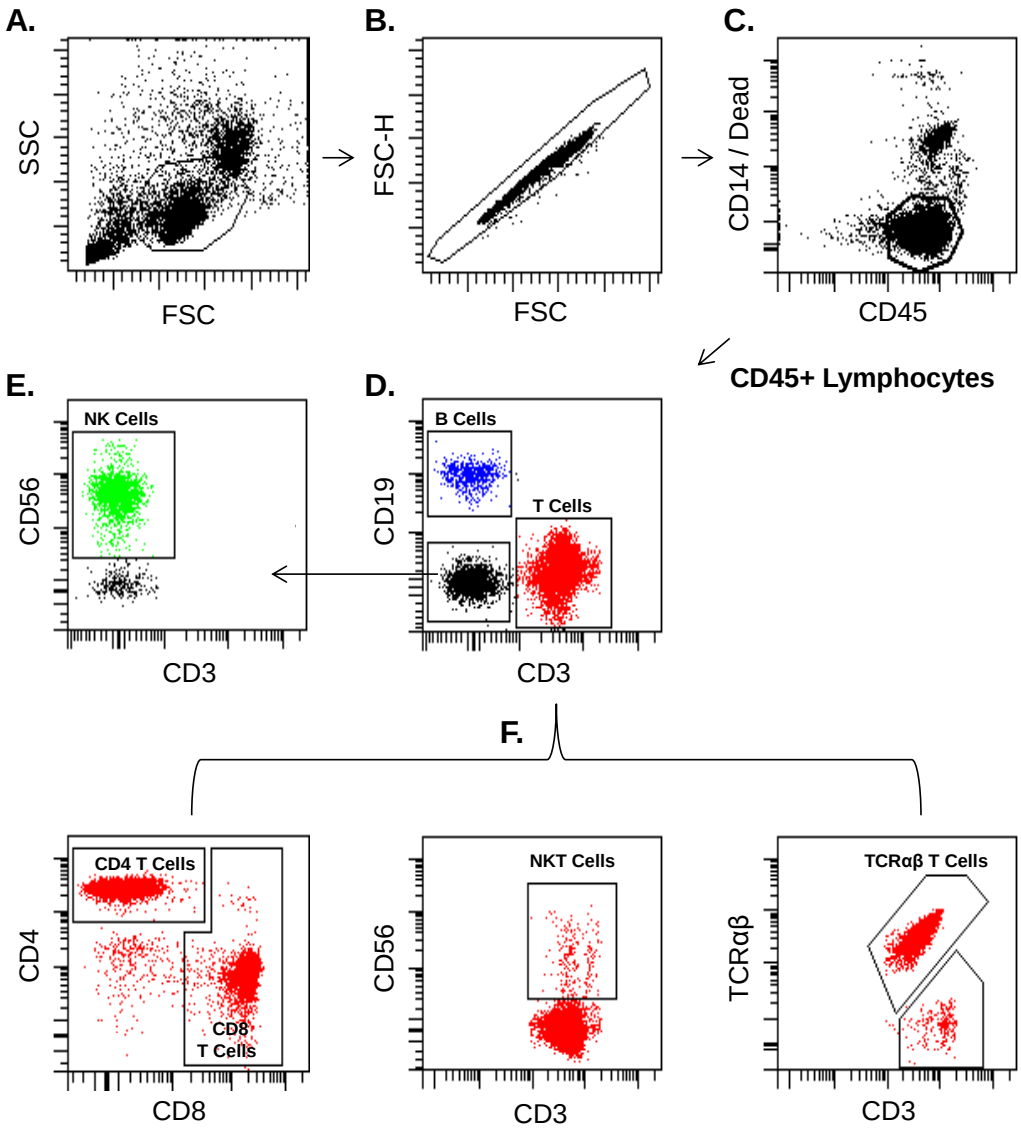

Figure 21. Flow Cytometry Panel for Main Lymphocyte Subsets

PBMCs were analysed with multicolour flow cytometry to identify lymphocyte subsets. Staining of a representative healthy donor is depicted. After (A) gating on lymphocytes and (B) excluding doublets, (C) $CD14^+$ monocytes and non-viable cells were excluded and $CD45^+$ lymphocytes were gated. Thereafter, (D) $CD19^+$ B-cells, $CD3^+$ T-cells and (E) CD3-$CD56^+$ NK-cells were identified. (F) $CD3^+$ T-cells were further analysed to identify $CD4^+$ T-cells, $CD8^+$ T-cells, $CD3^+CD56^+$ NK/T-cells and $TCR\alpha\beta^+$ T-cells.

Using this flow cytometry panel, PBMCs from the No/Low EBV and High EBV groups were analysed in order to characterise immune reconstitution after allo-HSCT in the absence, or presence, of high-level EBV DNAemia (Figures 22 and 23). PBMCs from 10 healthy controls were also tested.

T-Cells and NK-cells

Analysis of the healthy controls revealed T-cells, as expected, to be the most frequent subset, comprising a median 71% (IQR 68 – 75%) of $CD45^+$ lymphocytes (Figure 22). Meanwhile NK-cells made up 20% (IQR 16 – 22%) of cells. Within the $CD3^+$ T-cell subset, a median CD4/8 ratio of 2.0 was observed and 4.3% were NK/T-cells (Figure 23). Furthermore, 96% of $CD3^+$ T-cells were positive for TCR α/β, suggesting that up 4% of cells were TCR γ/δ^+.

In comparison to healthy donors, analysis of PBMCs from the No/Low EBV control group revealed a marked numerical deficiency of all subsets. Notably, NK-cells were the first lymphocytes to reconstitute after transplant, comprising 51% (IQR 43 – 59%) of all circulating lymphocytes at 3 months. Thereafter, T-cells replaced these as the most common subset by 6 months. Further analysis of T-cell subsets revealed a similar proportion of $CD8^+$ and $CD4^+$ T-cells to that found within healthy individuals at the 3 month time point, although a disproportionate increase in $CD8^+$ T-cells at later time points resulted in reversal of the normal CD4:8 ratio (Figure 23).

Comparison of data from the High EBV and No/Low EBV groups (matching for time post-transplant) revealed no significant differences in either the proportion or absolute frequency of T-cells (including $CD8^+$, $CD4^+$ and NK/T T-cell subsets) or NK-cells (Figures 22 and 23).

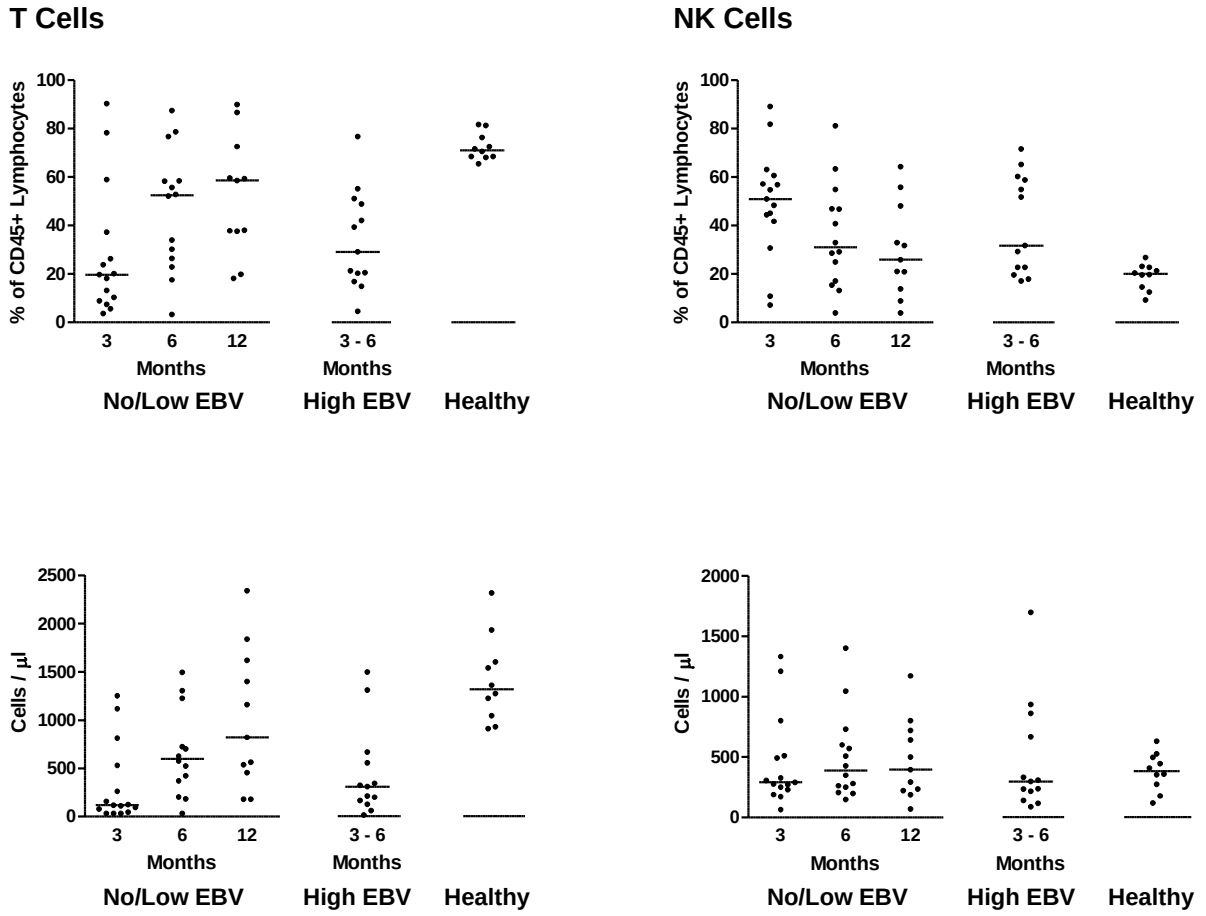

Figure 22. T-Cells and NK-Cells after Allo-HSCT

T- and NK-cell subsets were determined for No/Low EBV, High EBV and healthy adult donors. Upper plots show values as a percentage of $CD45^+$ lymphocytes, whilst the lower plots show cell numbers. Median values are depicted by the horizontal bars. No significant differences were observed between High EBV and No/Low EBV groups.

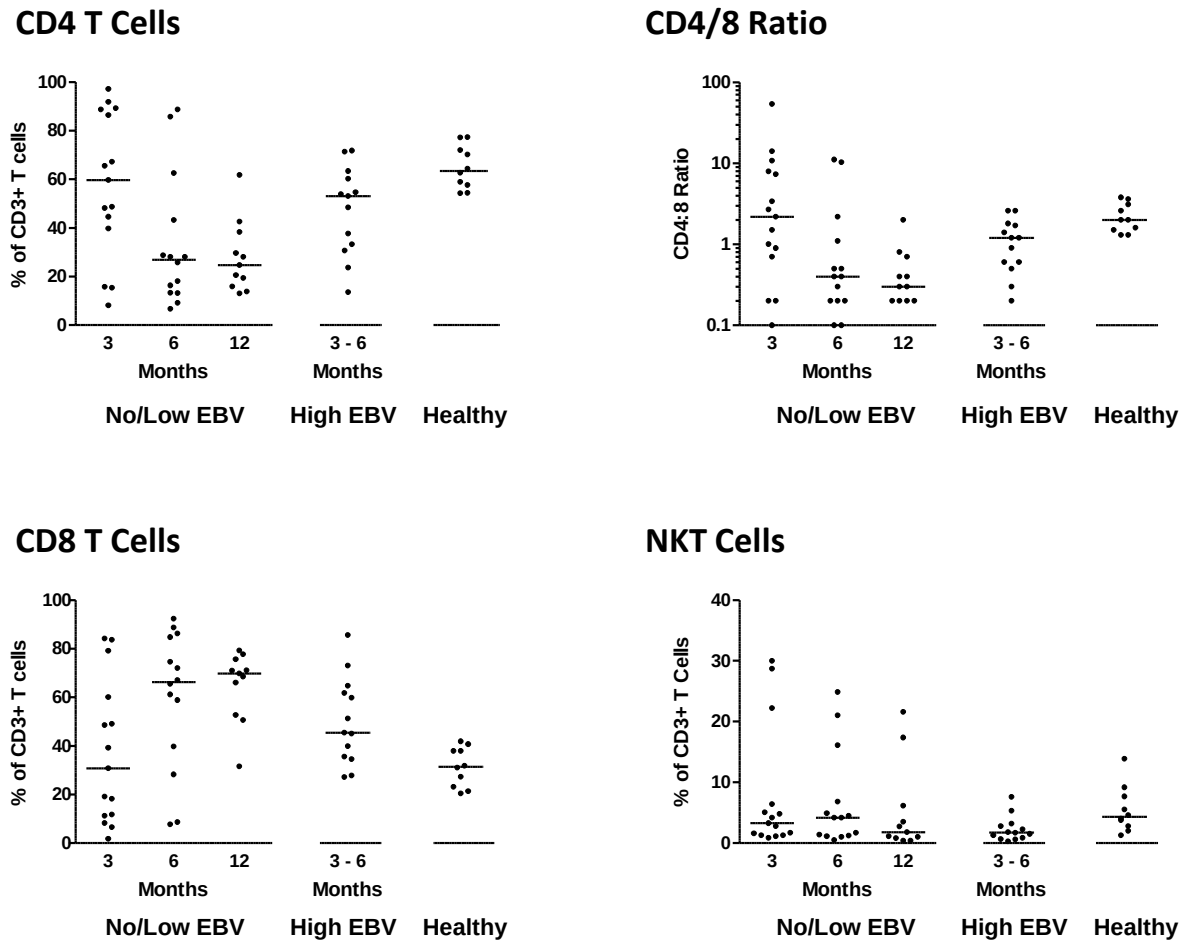

Figure 23. CD4$^+$, CD8$^+$ and NK/T-Cell Subsets after Allo-HSCT

CD4$^+$ T-cell, CD8$^+$ T-cell, CD4:8 ratios and NK/T-cell subsets were determined for No/Low EBV, High EBV and healthy adult donors. Except for CD4:8 ratios, all values are a percentage of CD3$^+$ T-cells. Median values are depicted by the horizontal bars. No significant differences were observed between High EBV and No/Low EBV groups.

B-cells

In the healthy controls, B-cells comprised a median 6.1% (IQR 5.1 – 6.2%) of $CD45^+$ lymphocytes, with median 116 cells/μl (IQR 86 – 123 cells/μl; Figure 24). In comparison, in the No/Low EBV group, the median percentage of B-cells was 9% at 3 months post-transplant (IQR 4 – 16%), exceeding that found in the healthy donors, although absolute cell numbers were considerably lower at 57 cells/μl (IQR 31-169 cells/μl). However, by 6 months approximately normal B-cell frequency was observed, with a median of 109 cells/μl (IQR 80 – 227 cells/μl). Furthermore, by 12 months post-transplant, B-cell numbers were supranormal, comprising 10% (IQR 8 – 14%) of circulating lymphocytes, with median 162 cells/μl (IQR 100 – 263 cells/μl).

Importantly, the proportion of B-cells was increased in the High EBV group compared to the No/Low EBV group (matching for time post-transplant) at 17% (IQR 7 – 24%) versus 8% (IQR 5% - 15%), with borderline significance (P = 0.079; Figure 24). The absolute number of B-cells was also increased with median 168 cells/μl (96 – 182 cells/μl) compared to 92 cells/μl (IQR 49 – 188 cells/μl) although this analysis lacked statistical significance (P = 0.178).

5.5 Characterisation of B-Cell Subsets

A second multicolour flow cytometry panel was designed to analyse B-cell subsets (Figure 25). In this panel, a gate was set to include lymphocytes and monocytes on the basis of FSC/SSC profile, after which doublets, $CD14^+$, $CD3^+$, $CD56^+$ and non-viable cells were all excluded before gating on $CD19^+$ B-cells. In this way, great care was taken to exclude non-B-cell contaminants; $CD3^+$ T-cells present after HSCT often exhibit CD27 positivity and thus

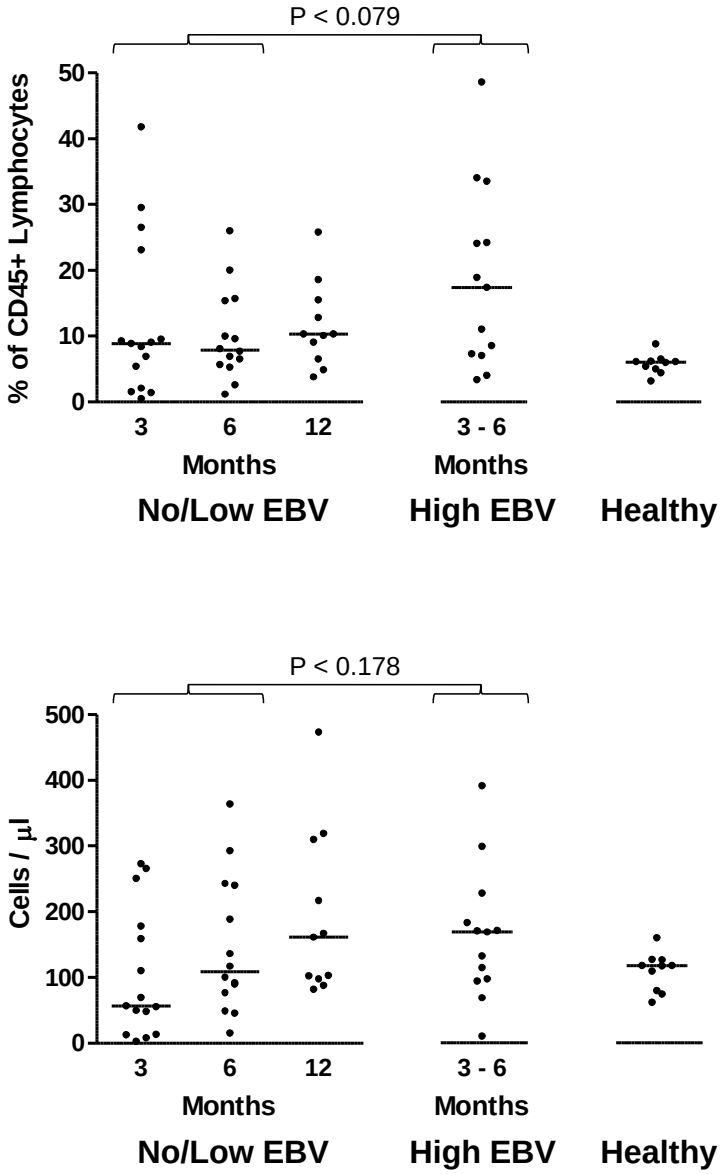

Figure 24. B-Cells after Allo-HSCT

B-cells were enumerated in No/Low EBV, High EBV and healthy adult donors. The upper plot shows values as a percentage of $CD45^+$ lymphocytes, and the lower plot shows cell numbers. Median values are depicted by the horizontal bars. The proportion of B-cells in the High EBV group was higher than that of the No/Low EBV group with borderline significance (P = 0.079). A non-significant (P = 0.178) increase in cell number was also observed.

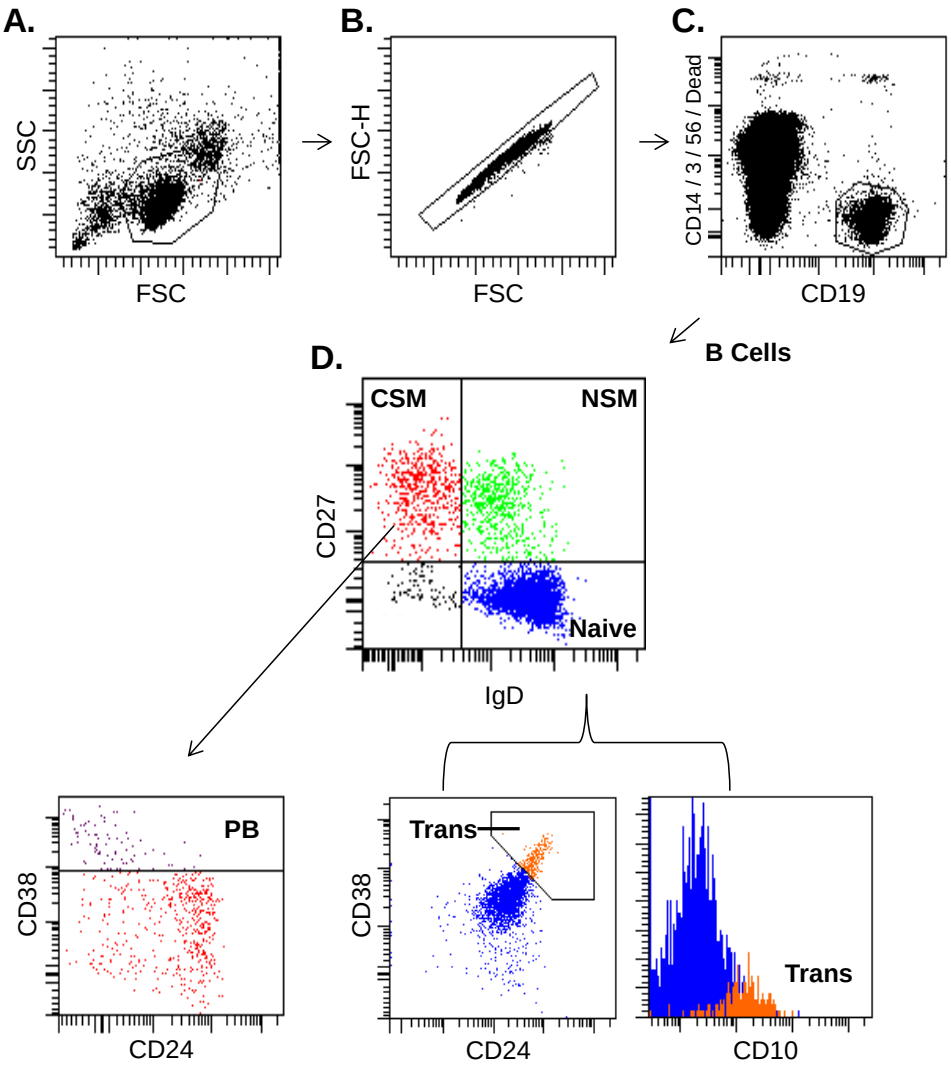

Figure 25. Flow Cytometry Panel for B-Cell Subsets

PBMCs were analysed with multicolour flow cytometry to identify B-cell subsets. Staining of a representative healthy donor is depicted. After (A) gating on lymphocytes (B) doublets were excluded after which (C) $CD14^{+}$ monocytes, $CD3^{+}$ T-cells, $CD56^{+}$ NK-cells and non-viable cells were excluded, and $CD19^{+}$ B-cells were gated. Thereafter (D) $CD27^{-}IgD^{+}$ naive, $CD27^{+}IgD^{-}$ CSM, $CD27^{+}IgD^{+}$ NSM and $CD27^{-}IgD^{-}$ other B-cell subsets were identified. Plasmablasts (PB) were identified as a $CD38^{++}$ subset of CSM cells. Transitional B-cells (Trans) were identified as a $CD38^{++}CD24^{++}$ and $CD10^{+}$ subset of naive B-cells.

can be misinterpreted as $CD27^+$ memory B-cells unless care is taken to exclude them from the $CD19^+$ population. $CD19^+$ B-cells were then separated on the basis of surface IgD and CD27 staining into $CD27^-IgD^+$ naive B-cells, $CD27^+IgD^-$ CSM B-cells, $CD27^+IgD^+$ NSM B-cells and $CD27^-IgD^-$ B-cells. This panel was also designed to identify additional subsets by co-staining for CD24, CD38, CD10 and CD20. As such, transitional B-cells could be identified as a subset of the naive B-cells on the basis of $CD38^{++}CD24^{++}$ staining, with additional phenotypic confirmation provided by $CD10^+$ surface expression. Furthermore, plasmablasts could be identified as a $CD38^{++}$ subset of $CD19^+CD27^+$ B-cells.

Using this panel, PBMCs from No/Low EBV and High EBV groups were compared to each other and those from 10 healthy donors. Representative staining data is shown in Figure 26, and a summary for all patients is shown in Figure 27. This revealed notable differences in the balance of naive and memory B-cells in these groups. In healthy donors, naive B-cells were shown to be the most common subset, comprising 68% (IQR 59 – 75%) of all B-cells, of which only a small proportion exhibited a transitional cell phenotype, at a median 7% (IQR 5 – 8%; Figure 28). Meanwhile $CD27^+$ B-cells comprised median 29% of B-cells (IQR 22 – 40%; Figure 27).

Unlike in the healthy controls, almost all B-cells in the No/Low EBV patients were found to exhibit a naive phenotype, and this pattern persisted that for at least 12 months post-transplant (Figure 27). Furthermore, these naive B-cells showed a predominantly transitional cell phenotype that gradually declined over time (Figure 28). Consistent with these findings, a marked delay in the reconstitution of $CD27^+$ memory B-cells was observed (Figure 27). Even at 12 months post-transplant, memory B-cells were only median 9% (IQR 4 – 12%) of total

	No / Low EBV	High EBV	Healthy
Day post transplant	98	101	-
EBV load (copies/ml)	<500	1,540,170	-
CD19 (%)	5.4	7.3	6.1

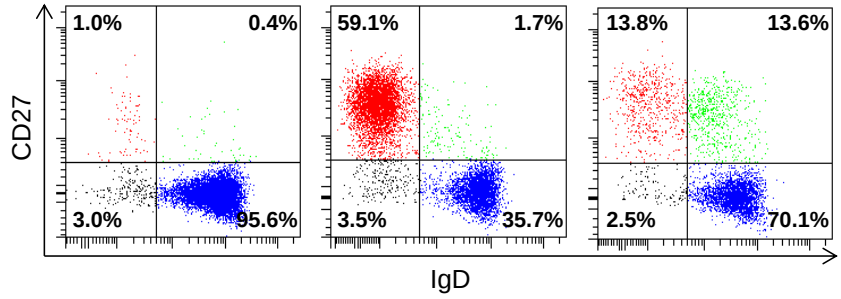

Figure 26. Memory B-Cell Expansion in Patients with EBV DNAemia after Allo-HSCT
Staining for B-cell subsets is shown for representative No/Low EBV, High EBV and healthy adult donors. The No/Low EBV patient (Patient 17) was bled 98 days post-transplant when EBV load was undetectable by the clinical whole blood EBV qPCR assay. The High EBV patient (Patient 9) was bled 101 days post-transplant during a high-level EBV reactivation when EBV load was 1.54 $x10^6$ copies/ml. $CD27^+$ B-cells are scarce in the No/Low EBV patient compared to the healthy individual. A striking increase in the proportion of $CD27^+$ B-cells is observed in the High EBV patient.

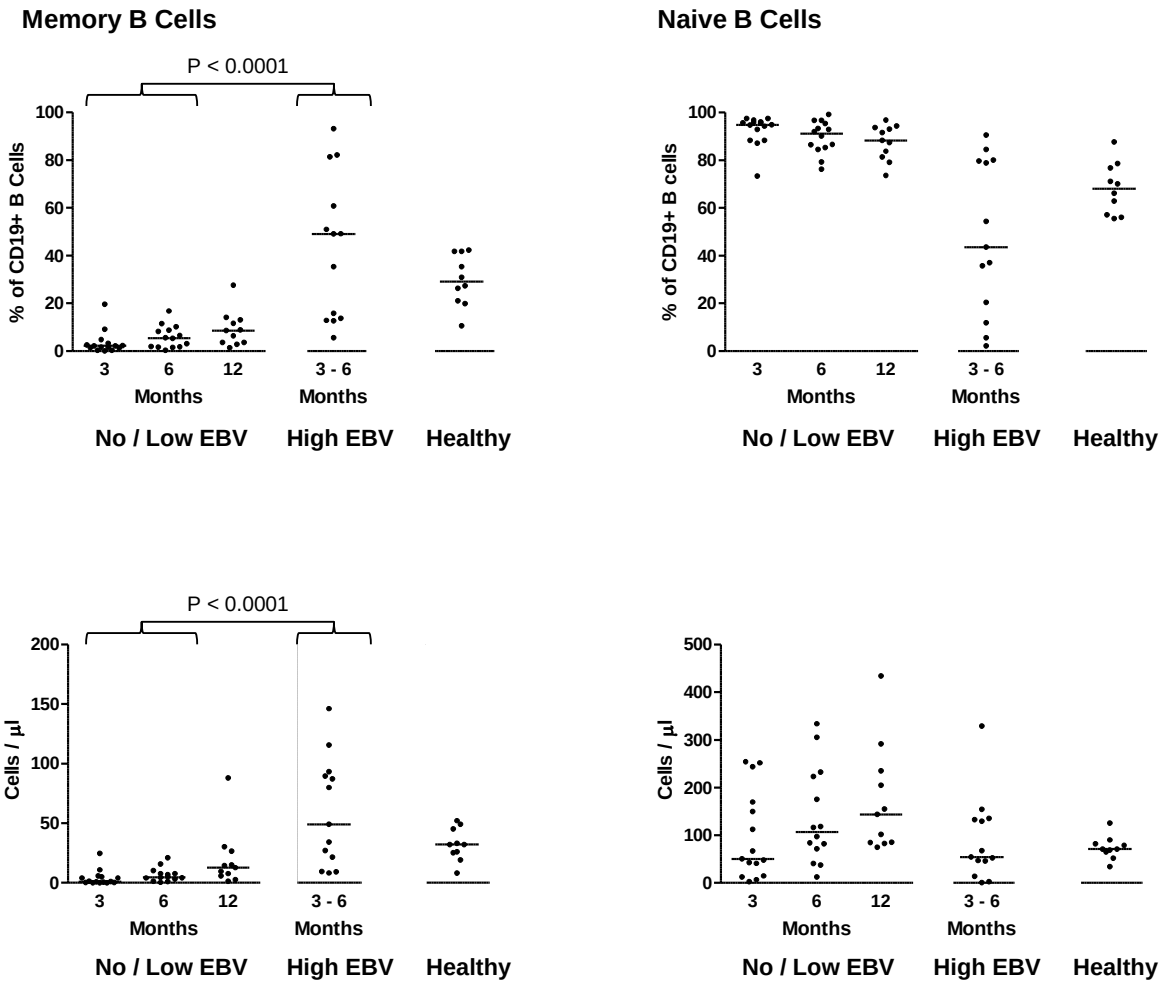

Figure 27. Variation in Memory and Naive B-Cells with EBV Load after Allo-HSCT

Memory ($CD27^{+)}$ and naive ($CD27^{-}IgD^{+)}$ B-cell subsets were determined for No/Low EBV, High EBV and healthy adult donors. The upper plots show values as a percentage of $CD19^{+}$ B-cells and the lower plots show cell numbers. Median values are depicted by the horizontal bars. A highly significant increase in both the percentage ($P < 0.0001$) and number ($P < 0.0001$) of memory B-cells was seen in the High EBV group in comparison to the No/Low EBV group.

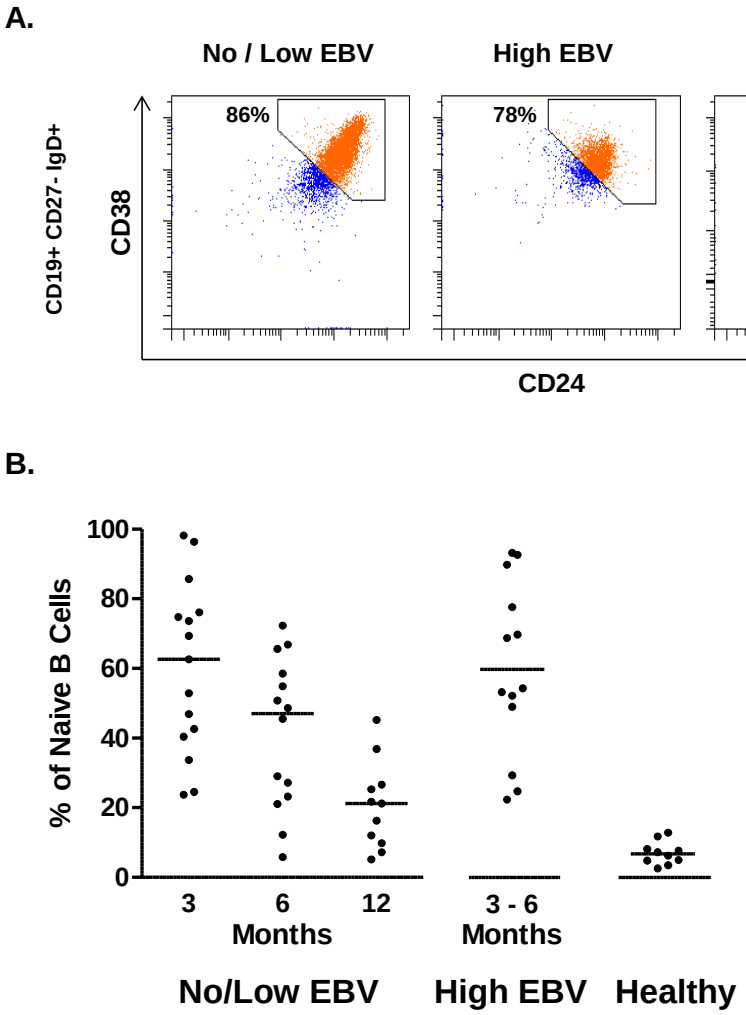

Figure 28. Transitional B-Cells after Allo-HSCT

Transitional B-cells ($CD27^{-}IgD^{+}CD38^{++}CD24^{++}$) were determined for No/Low EBV, High EBV and healthy adult donors. A. Representative flow cytometry plots for each group showing the gate used to identify transitional B-cells. B. Summary of data for all donors. Values are shown as a percentage of naive ($CD27^{-}IgD^{+}$) B-cells. Median values are depicted by the horizontal bars. Naive B-cells exhibit a predominantly transitional B-cell phenotype following allo-HSCT that resolves over time. No significant difference was observed between High EBV and No/Low EBV groups.

B-cells, and a corresponding delay in the recovery of absolute memory B-cell numbers was found.

However, analysis of B-cell phenotypes in the High EBV group revealed a striking difference to the No/Low EBV group, with marked increases in both the proportion and number of $CD27^+$ memory B-cells. Thus, in the High EBV group, $CD27^+$ B-cells were found to make up median 49.1% (IQR 13.7 – 60.8%) of total B-cells. This was a highly significant ($P < 0.0001$) increase compared to No/Low EBV patients (matching for time post-transplant), in whom memory B-cells were only median 2.3% (IQR 1.5 – 6.5%). Furthermore, a highly significant ($P < 0.0001$) increase was observed in the absolute number of memory B-cells, with median 49 cells/μl (IQR 21.6 – 89.4 cells/μl) in the High EBV group compared to 4.1 cells/μl (IQR 0.7 – 6.9 cells/μl) for No/Low EBV patients. These findings are highly suggestive that memory B-cell expansions are associated with high-level EBV DNAemia following allo-HSCT.

Data were also analysed to characterise the proportion of B-cells with CSM and NSM phenotypes (Figure 29). In healthy donors, CSM were shown to comprise median 13% (IQR 9 – 15%) of B-cells, whereas NSM made up median 15% (IQR 13 – 18%). Importantly, in High EBV patients almost all of the expanded memory B-cell population was seen to exhibit a CSM phenotype, with very few NSM cells apparent (Figure 29).

The proportion of $CD27^+$ memory B-cells exhibiting plasmablastic phenotype ($CD38^{++}$) was also determined (Figure 30). As expected, in the healthy controls these comprised only a small proportion of memory B-cells, at median 5% (IQR 3 – 9%). However, analysis of High

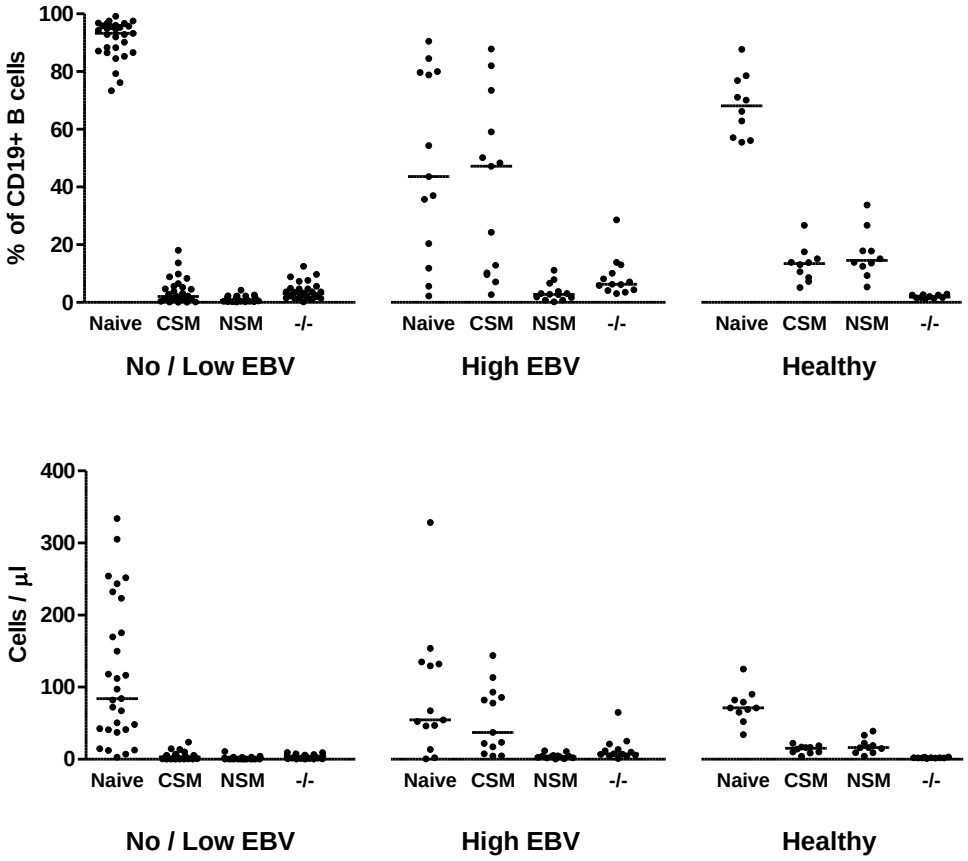

Figure 29. Variation in B-Cell Subsets with EBV Load after Allo-HSCT

Naive ($CD27^-IgD^+$), CSM ($CD27^+IgD^-$), NSM ($CD27^+IgD^+$) and -/- ($CD27^-IgD^-$) B-cell subsets were determined for No/Low EBV and High EBV groups at 3 - 6 months post-transplant, as well as for healthy donors. The upper plot shows values as a percentage of $CD19^+$ B-cells, and the lower plot shows cell numbers. Median values are depicted by the horizontal bars.

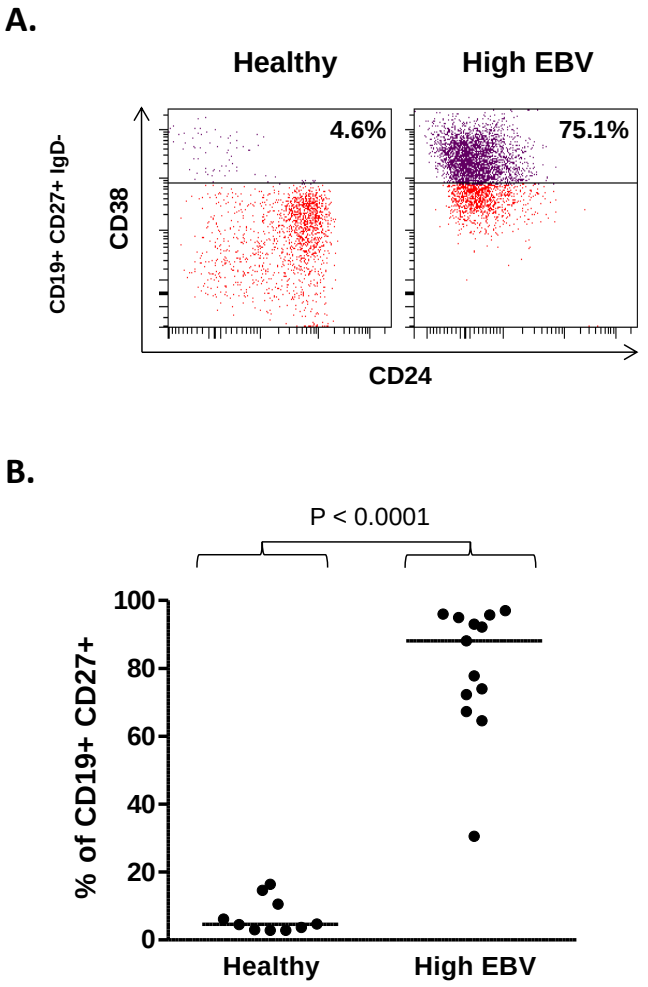

Figure 30. Plasmablastic Phenotype of Memory B-Cells after Allo-HSCT

The proportion of $CD27^{+}$ memory B-cells exhibiting a plasmablastic phenotype ($CD38^{++}$) was determined for the High EBV group and healthy donors. A. Representative healthy and High EBV donors. B. Summary of data for healthy and High EBV donors. All values are a percentage of $CD19^{+}CD27^{+}IgD^{-}$ memory B-cells. Median values are depicted by the horizontal bars. A highly significant increase in the proportion of plasmablasts was observed in the High EBV group ($P < 0.0001$).

EBV patients revealed, remarkably, that the majority of $CD27^+$ B-cells possessed plasmablastic phenotype, comprising median 88% (IQR 72% - 95%).

5.6 Surface Immunoglobulin Expression

An additional flow cytometry panel was designed to analyse B-cell surface Ig expression (Figure 31). After gating to identify $CD19^+$ B-cells (in the same way as for the B-cell flow cytometry panel; Figure 25), cell-subsets were determined according to surface Ig-M, -D, -G or -A expression. Figure 32 shows data for 9 of the High EBV patients with the greatest proportion of $CD27^+$ B-cells, and 3 healthy controls. This revealed that a substantial proportion of the $CD27^+$ B-cells present in each patient were positive for surface IgG, and to a lesser extent surface IgA. This confirms that the majority of $CD27^+$ B-cells found in patients with EBV DNAemia after allo-HSCT have undergone class switch recombination and can therefore be considered as true memory B-cells.

5.7 $CD27^+$ B-Cell Expansions are Coincident with EBV Reactivation

Further investigation was undertaken to ascertain if the $CD27^+$ B-cells expansions detected in patients with high-level EBV DNAemia appear co-incident with EBV reactivation or whether they are pre-existing (Figure 33). For 6 High EBV patients, cryopreserved PBMCs were available from time points preceding the EBV reactivation. From these, samples were selected that had been collected a median of 32 days (range 16-73 days) before those at the point of high-level EBV DNAemia. DNA extracted from these cells was analysed using the in-house EBV qPCR assay, and this confirmed that the EBV loads in these were significantly (<0.0001) lower than in the corresponding high-level EBV reactivation samples; they were similar to those from the No/Low EBV patients. The PBMCs were then analysed using the

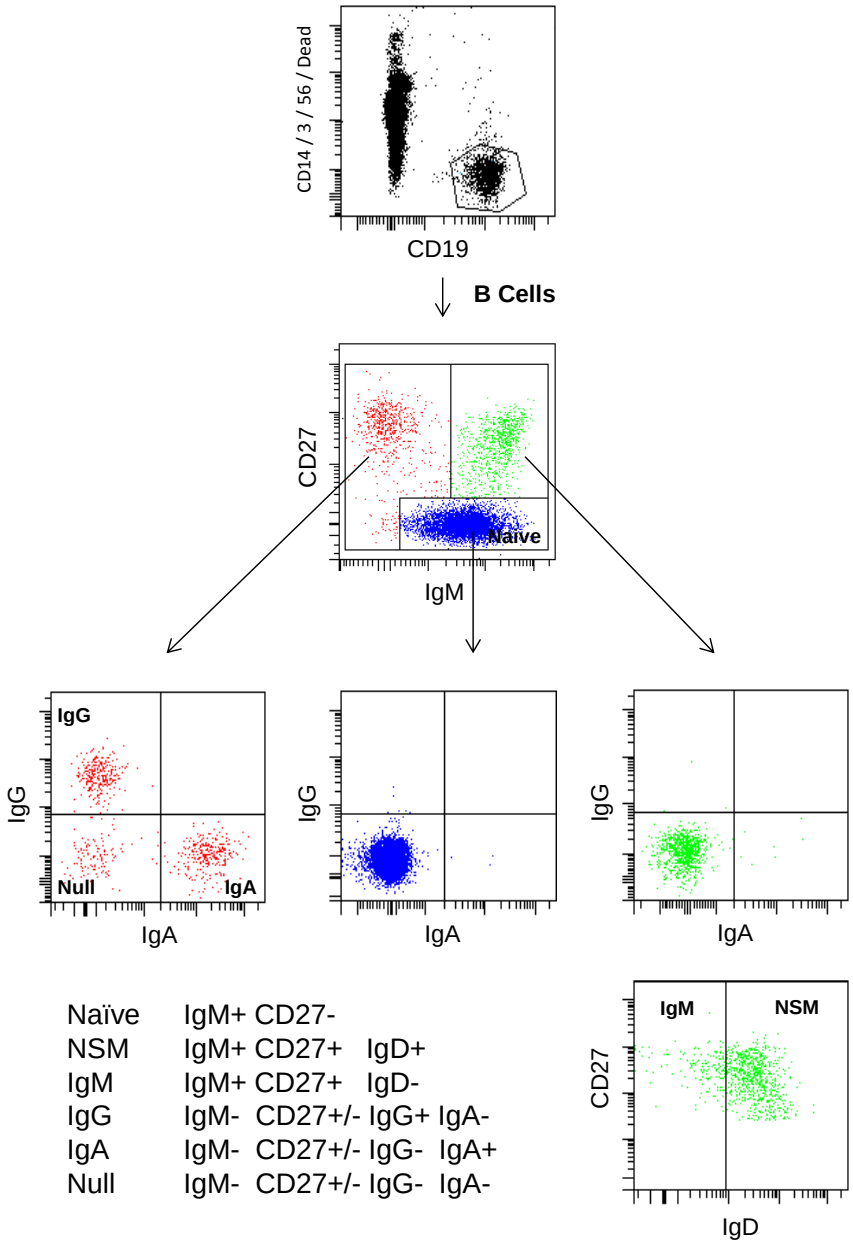

Figure 31. Flow Cytometry Panel for Surface Immunoglobulins

PBMCs were analysed with multicolour flow cytometry to analyse surface Ig expression. Staining of a representative healthy donor is shown. $CD19^+$ B-cells were first gated using the same method as for Figure 25. Thereafter, CD27 and IgM staining was used to identify naive ($CD27\text{-}IgM^+$), IgM^- memory ($CD27^{+/-}IgM^-$) and IgM^+ memory ($CD27^+IgM^+$) subsets. Each of these subsets was co-stained with IgG and IgA, showing that only the IgM^- memory subset was positive for either. IgD staining of the IgM^+ memory subset was used to distinguish NSM (IgD^+) and IgM only (IgD^-) subsets.

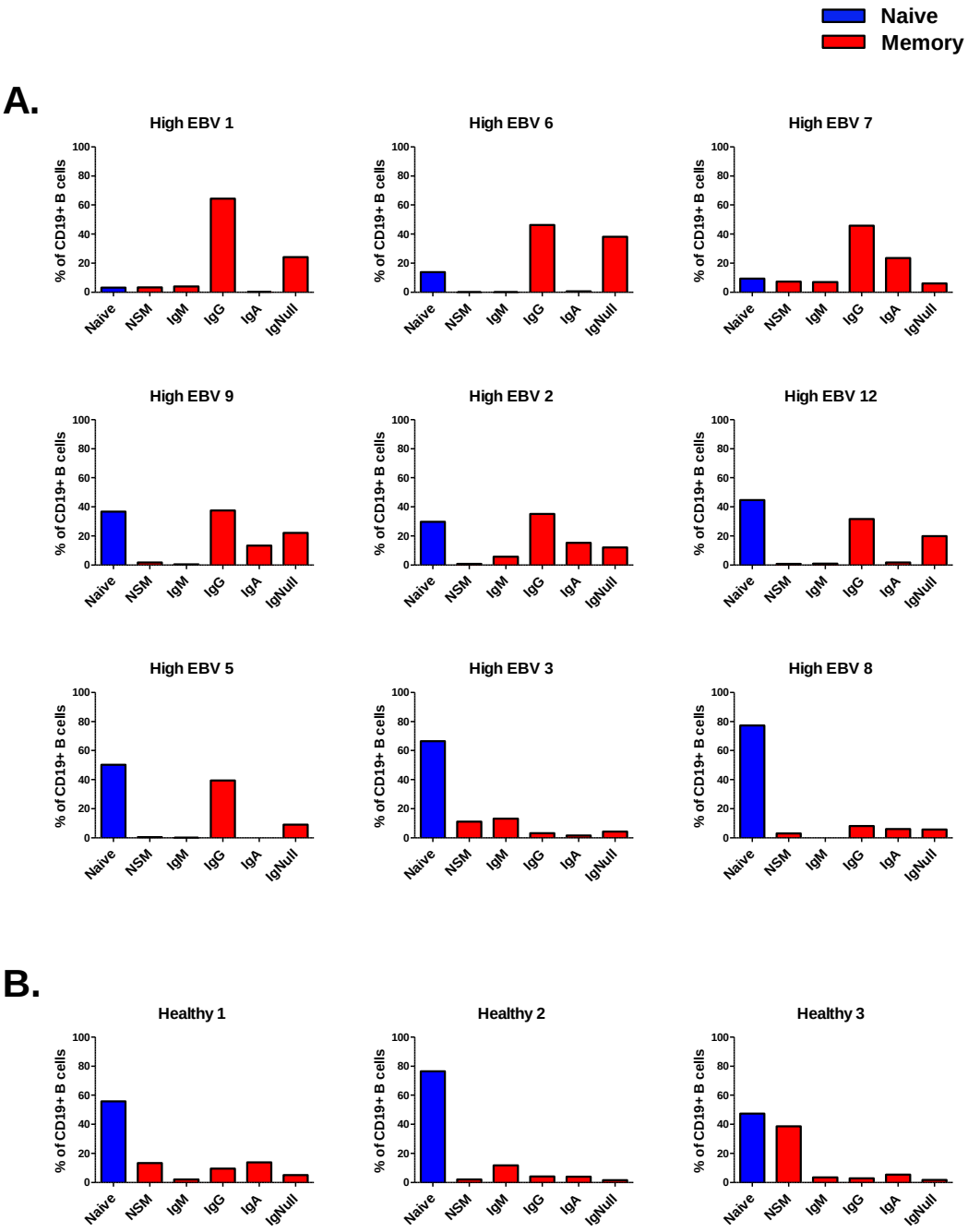

Figure 32. Surface Immunoglobulin Expression on B-Cells after Allo-HSCT

B-cell surface Ig expression was analysed for High EBV patients and healthy controls. A. 9 High EBV patients, ordered from greatest to lowest proportion of memory B-cells. B. 3 healthy donors. All values are a percentage of $CD19^+$ B-cells. The following B-cell subsets were identified: Naive ($CD27^-IgM^+$), NSM ($CD27^+IgM^+IgD^+$), IgM only ($CD27^{+/-}IgM^+IgD^-$), IgG CSM ($CD27^{+/-}IgG^+$), IgA CSM ($CD27^{+/-}IgA^+$), Ig Null ($CD27^{+/-}IgG^-IgA^-$).

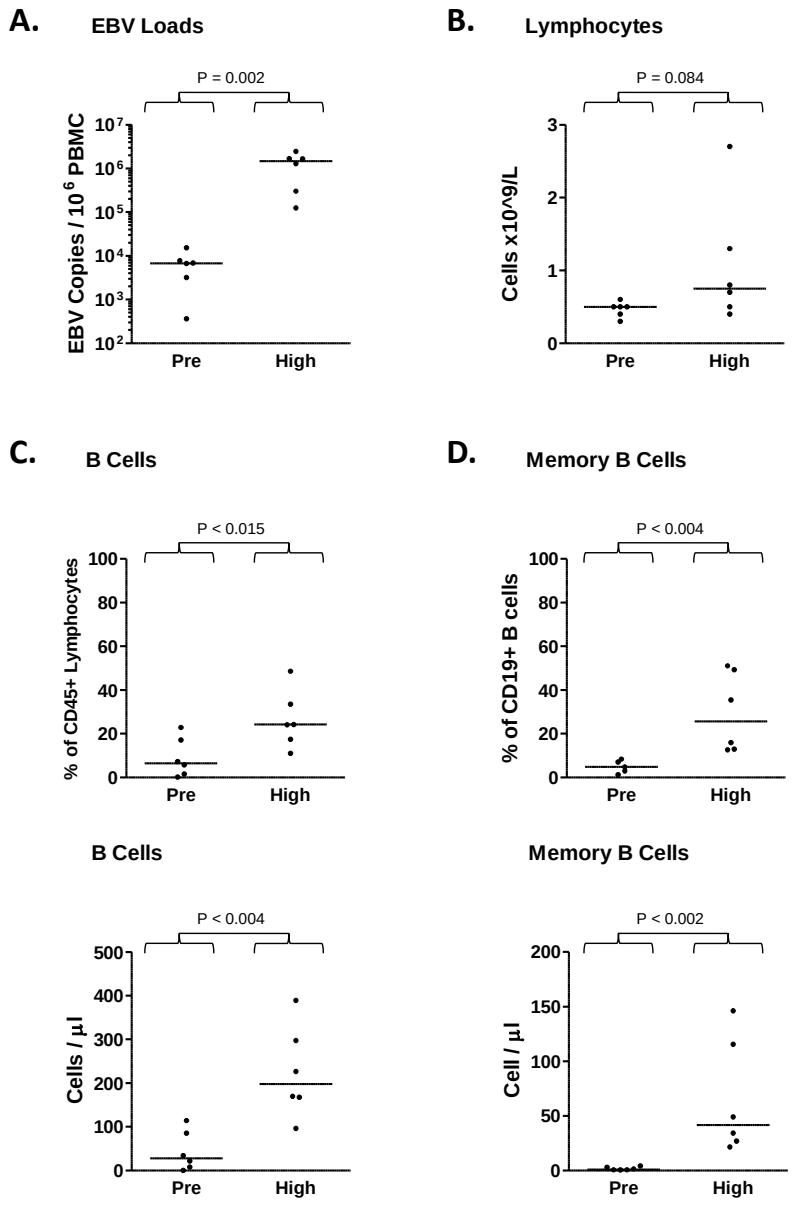

Figure 33. Analysis of Samples Preceding EBV Reactivation

For 6 High EBV patients, samples collected a median of 32 days (range 16-73 days) prior to those at the point of high-level EBV DNAemia were analysed. A. EBV load in PBMCs. B. Lymphocyte count. C. $CD19^+$ B-cells (upper plot, proportion of $CD45^+$ lymphocytes; lower plot, cell number). D. $CD27^+$ memory B-cells (upper plot, proportion of $CD19^+$ B-cells; lower plot, cell number). The samples preceding EBV reactivation were significantly different ($P < 0.05$) from those at the time of EBV reactivation for all variables except lymphocyte count.

main lymphocyte and B-cell subset flow cytometry panels. These analyses showed that both the proportion and frequency of $CD19^+$ and $CD27^+$ memory B-cells in the earlier time points were significantly ($P < 0.05$ in all cases) lower than in the EBV reactivation samples. Furthermore, these were similar to those found in the No/Low EBV controls at corresponding time points. Overall, it was concluded that the $CD27^+$ memory B-cell expansions found in patients at the point of high-level EBV DNAemia are not pre-existing, and are probably the result of *de novo* expansion associated with EBV DNAemia.

5.8 Correlation of EBV Loads with Lymphocyte Subset Frequency

Noting that $CD27^+$ B-cells are expanded in patients with EBV DNAemia following allo-HSCT, further analysis was undertaken to more fully characterise the relationship between EBV load and the absolute number of different lymphocyte subsets in these patients. Therefore, EBV loads detected in PBMCs were correlated against T-cell, NK-cell, total B-cell and $CD27^+$ B-cell numbers for all study patients (Figure 34). No significant correlations between EBV load and T-cell, NK-cell or total B-cells were observed. However, a highly significant correlation was observed between EBV load and the $CD27^+$ B-cell subset ($P < 0.0001$). This provided good evidence to suggest that $CD27^+$ B-cells are the main site of EBV persistence in patients with EBV DNAemia following allo-HSCT.

5.9 Analysis of Bulk Sorted Subsets

We went on to seek direct evidence that EBV is predominantly found in the expanded $CD27^+$ memory B-cell subset in patients following allo-HSCT, by using EBV qPCR to analyse FACS-sorted lymphocyte subsets. This was performed by staining 5 – 10 $x10^6$ PBMCS on each occasion, which were then sorted using a MoFlo cell sorter (Figure 35) to isolate $CD27^-$

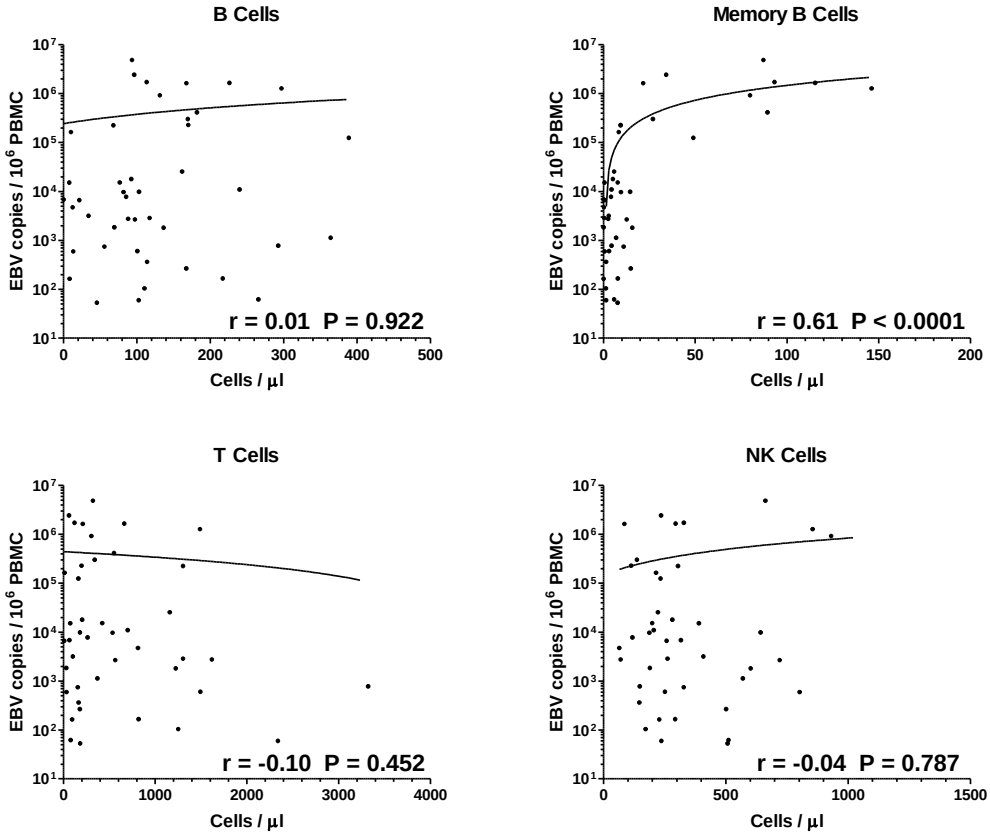

Figure 34. Correlation of EBV Load with Lymphocyte Subsets after Allo-HSCT

EBV load in PBMCs was correlated against the number of T-cells, NK-cells, B-cells and $CD27^+$ memory B-cells for all study patients, using Pearson correlation. A highly significant (positive) correlation was only seen for the memory B-cell subset ($r = 0.61$; $P < 0.0001$).

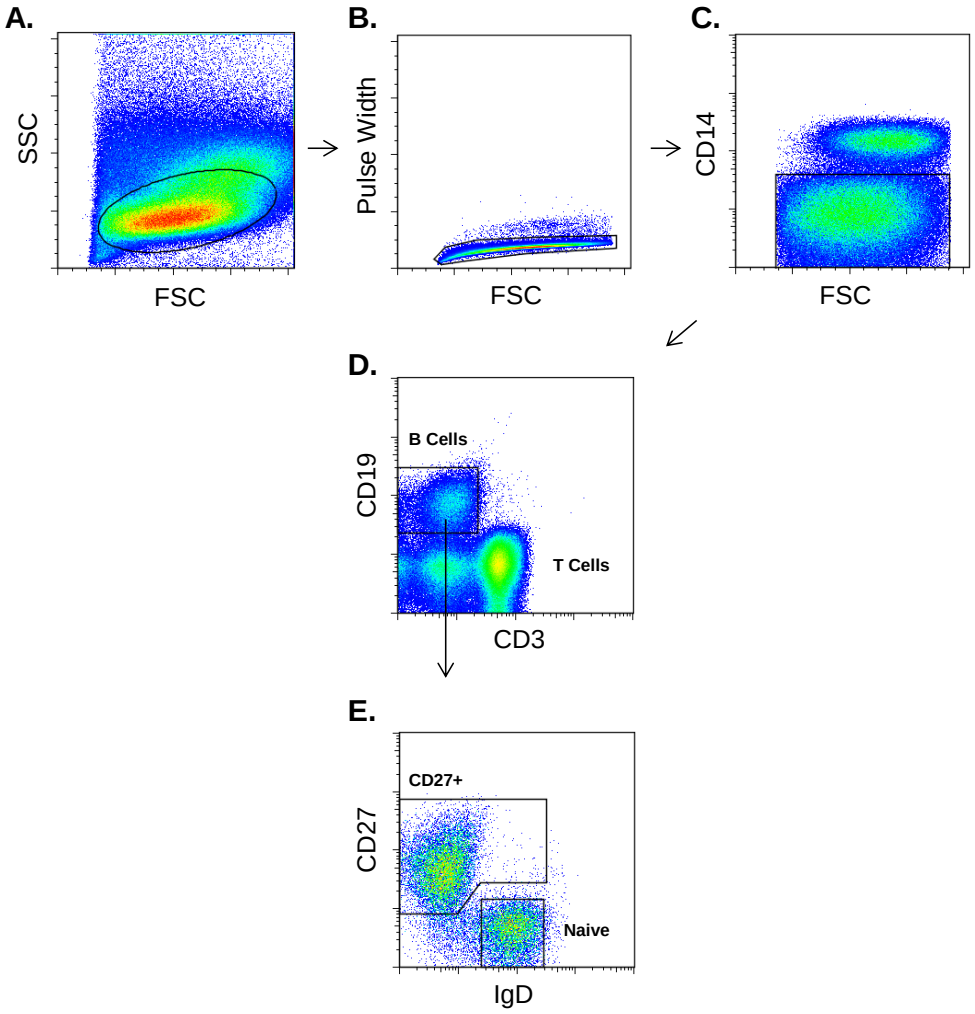

Figure 35. FACS-Sorting of Lymphocyte Subsets from Patients after Allo-HSCT

PBMCs were FACS-sorted on a MoFlo cell sorter. Representative sorting for High EBV Patient 12 is depicted. A. Lymphocytes and monocytes were gated. B. Doublets were excluded C. $CD14^+$ monocytes were excluded D. $CD19^+$ B-cells were gated, excluding $CD3^+$ T-cells. E. Staining with CD27 and IgD was used to identify B-cell subsets. In this way 3 subsets were isolated: $CD27^+$ memory B-cells, $CD27^-IgD^+$ naive B-cells, and non-B-cells comprising all $CD19^-$ lymphocytes and monocytes.

IgD^+ naive, $CD27^+$ memory and $CD19^-$ non-B-cell subsets. DNA was extracted from the sorted populations and analysed, alongside DNA from unsorted PBMCs, using EBV qPCR.

Figure 36 shows the result of analyses for High EBV Patients 6, 9, 11 and 12. For each patient, EBV genomes were found to be highly enriched in the $CD27^+$ B-cell subset, as they are in healthy individuals. Therefore, median 1.2 $x10^7$ genomes per 10^6 cells was recorded for the $CD27^+$ B-cell subset. In comparison, few genomes (on average <1% of the load found in the $CD27^+$ subset) were detected in either the naive-B-cell or non-B-cell subsets, comprising median 7.8 $x10^4$ genomes per 10^6 naive B-cells, and median 1.1 $x10^5$ genomes per 10^6 non-B-cells.

5.10 Single Cell Sorting Studies

Having confirmed that EBV genomes are selectively present within the $CD27^+$ B-cell subset in High EBV patients, single cell FACS-sorting was then undertaken to determine what proportion of these cells carry EBV. This involved FACS-sorting cells into $CD27^-IgD^+$ and $CD27^+$ B-cells subsets, as described previously, before depositing single cells into individual wells of a 96-well plate containing lysis buffer. In total 48 individual cells of each type were tested using the in-house EBV qPCR assay. This approach was initially validated in 2 ways. Firstly, single cells were FACS-sorted into individual wells of a 96-well plate and then the cells were counted using a light microscope. This confirmed that a single cell was present in (almost) all wells (data not shown). Secondly, cells from an EBV-positive and EBV-negative BL cell line were mixed in known proportions before depositing single cells into 96 well plates, which were then tested using EBV qPCR (Figure 37A). This revealed a proportion of EBV-positive wells that closely approximated the known proportion of EBV-positive and

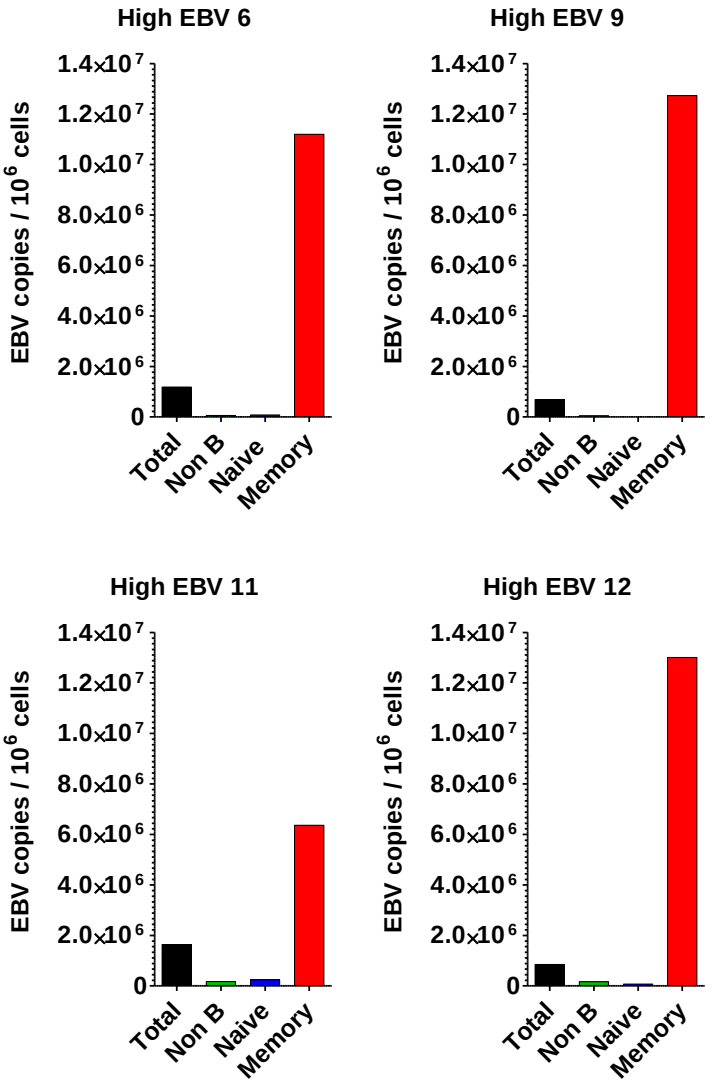

Figure 36. EBV Loads in FACS-Sorted Lymphocyte Subsets from Allo-HSCT Patients

FACS-sorted lymphocyte subsets isolated from High EBV patients 6, 9, 11 and 12 were analysed using EBV qPCR. In each patient, a highly significant enrichment of viral genomes was seen in the $CD27^+$ memory B-cell subset. Relatively low levels of EBV DNA were detected in naive B-cell and non-B-cell subsets.

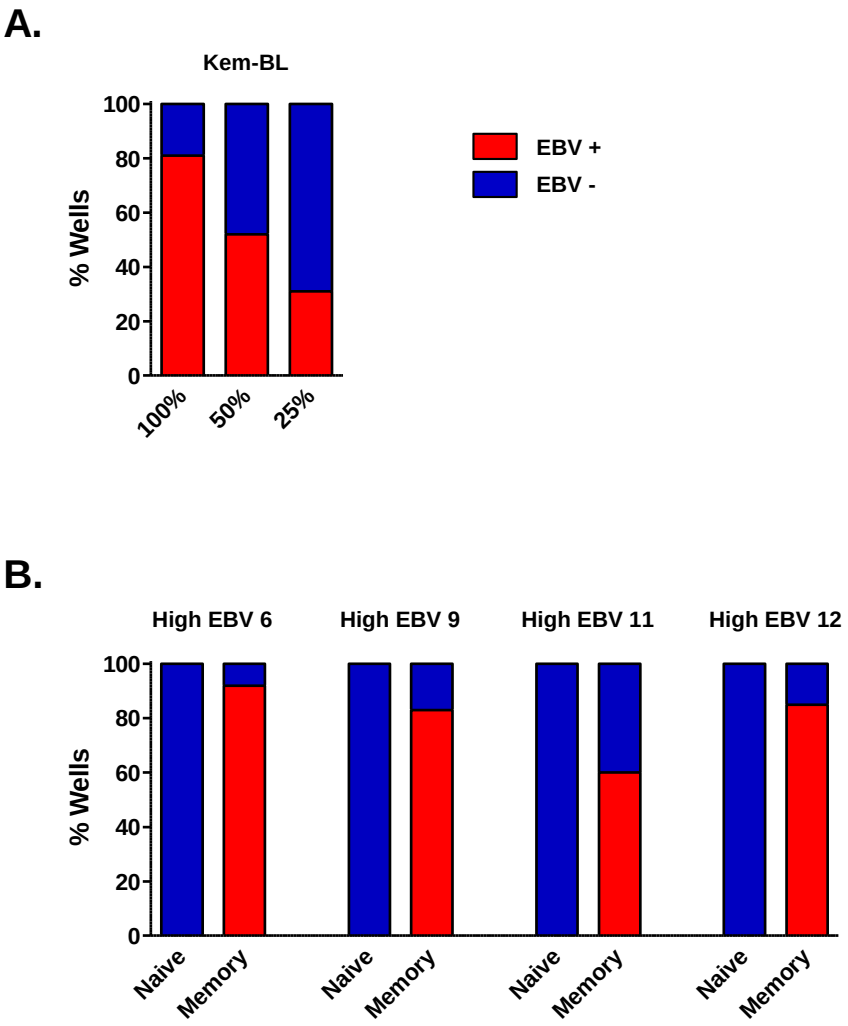

Figure 37. EBV qPCR Analysis of Single FACS-Sorted B-Cells

To determine the proportion of EBV-positive cells, single cells (N = 48) were FACS-sorted into individual wells of a 96-well plate and then tested with EBV qPCR. A. The assay was first validated by FACS-sorting mixtures of EBV-positive and EBV-negative Kem-BL cells comprising 100%, 50% or 25% EBV-positive cells. The proportion of EBV qPCR-positive wells was similar to that expected. B. FACS-sorted naive ($CD27^{-}IgD^{+}$) and memory ($CD27^{+}$) B-cells from High EBV patients 6, 9, 11 and 12 were tested, demonstrating that up to 92% of memory B-cells were positive for EBV DNA.

EBV-negative BL cells in the sorted mixtures.

Having validated the approach, single $CD27^{-}IgD^{+}$ naive and $CD27^{+}$ memory B-cells from Patients 6, 9, 11 and 12 were FACS-sorted into 96 well plates which were then tested with EBV qPCR (Figure 37B). Overall this showed that approximately 80% of the $CD27^{+}$ memory B-cells present in these patients harbour EBV genomes. Furthermore, none of the naive B-cells from any of the 4 patients tested positive for EBV genomes. This supports our other data to confirm that EBV is selectively carried within the $CD27^{+}$ B-cell subset in these patients.

Using this single cell sorting approach, it was also possible to estimate the genome copy number within individual $CD27^{+}$ B-cells (Figure 38). Thus, a median of 19 genomes per cell (IQR 10 – 29 genomes per cell) were detected amongst EBV-positive cells from the 4 High EBV patients. Importantly, the relatively narrow copy number distribution provides a strong indication that most of the circulating EBV genomes in these patients exist in the context of a latent viral infection. By contrast, the median cellular EBV copy number in a productively infected cell (EBV-positive Akata BL cells induced into lytic cycle by IgG crosslinking) was 2.4×10^{4} genomes per cell (IQR 2.5×10^{3} - 5.7×10^{4} genomes per cell), reflecting the massive genome amplification that occurs during virus replication (Figure 38). Overall, these data suggest that high-level EBV DNAemia following allo-HSCT is predominantly an accumulation of latently infected $CD27^{+}$ B-cells.

5.11 Quantitative Analysis of EBV Gene Expression in $CD27^{+}$ B-cells

We speculated that EBV might be driving the expansion of $CD27^{+}$ B-cells in patients with EBV DNAemia through a growth transforming infection. Therefore, further investigation was

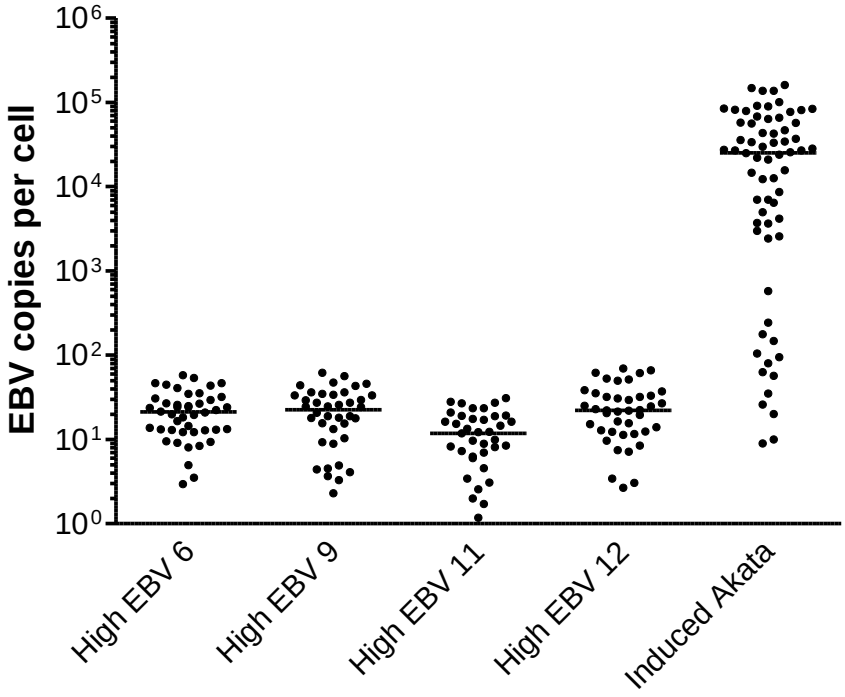

Figure 38. EBV Copy Number in Single Memory B-Cells after Allo-HSCT

EBV genome copy number/cell was determined by analysing single FACS-sorted $CD27^+$ memory B-cells with EBV qPCR. The distribution of EBV copies in individual cells from High EBV patients 6, 9, 11 and 12 is shown. Only cells positive for EBV DNA are displayed. Medians are depicted by the horizontal bars. As a comparator, AKBM cells induced into virus lytic cycle were also analysed. AKBM cells are a derivative of the EBV-positive Akata-BL cell line stably transfected with a GFP reporter under control of the BMRF1 EBV lytic cycle gene promoter. Single GFP^+ cells in lytic cycle were FACS-sorted and then tested with EBV qPCR. EBV copy number distributions for the High-EBV patients were consistent with latently, rather than lytically, infected cells; lytic cells contain a substantially greater number of genomes. Notably, a small proportion of AKBM cells had a lower number of EBV copies; these cells are likely to be in the early stages of replication, such that they are expressing the IE gene BZLF1 but are yet to replicate their viral DNA. Data for sorted AKBM cells courtesy of Dr A. Bell, University of Birmingham.

undertaken to determine viral gene expression in these cells using RT-PCR. Importantly, whereas previous studies have examined virus gene expression in *ex vivo* samples using non-quantitative RT-PCR methods[315,319,320,386,583,584], quantitative RT-PCR was employed. This was performed using a novel technique recently established in our laboratory, involving a Fluidigm gene expression array chip with the capacity to simultaneously analyse up to 48 different transcripts from very small amounts of RNA[551]. These were quantified relative to a specifically designed plasmid standard, carrying all of the target sequences. In this way, target transcripts could be properly quantitated relative to one another.

To perform this analysis, PBMCS from Patients 6, 9 and 12 were first FACS-sorted to isolate $CD27^+$ B-cells, from which total RNA was extracted and then converted to cDNA. This was then analysed using the Fluidigm gene expression array to quantify target EBV latent and lytic transcripts, and cellular transcripts used as normalisation controls. Data was compared to that from EBV-positive cell lines including LCLs expressing the Latency III pattern of gene expression, the Rael-BL cell line expressing Latency I, and the Akata-BL cell line induced into lytic cycle.

Initially, viral transcripts levels were analysed by expressing them relative to those of the cellular housekeeping gene PGK1 (Figure 39A). This revealed similar, albeit marginally lower, levels of the EBER1 transcript compared to that found in LCLs. This provided good evidence to confirm that EBV is indeed harboured at high frequency in the $CD27^+$ B-cell subset in these patients. However, this finding was not reproduced for other viral transcripts, which were seen to be several logs lower than in the LCLs; representative data for EBNA1 transcripts are shown in Figure 39A. This suggests that the EBV genomes found in most

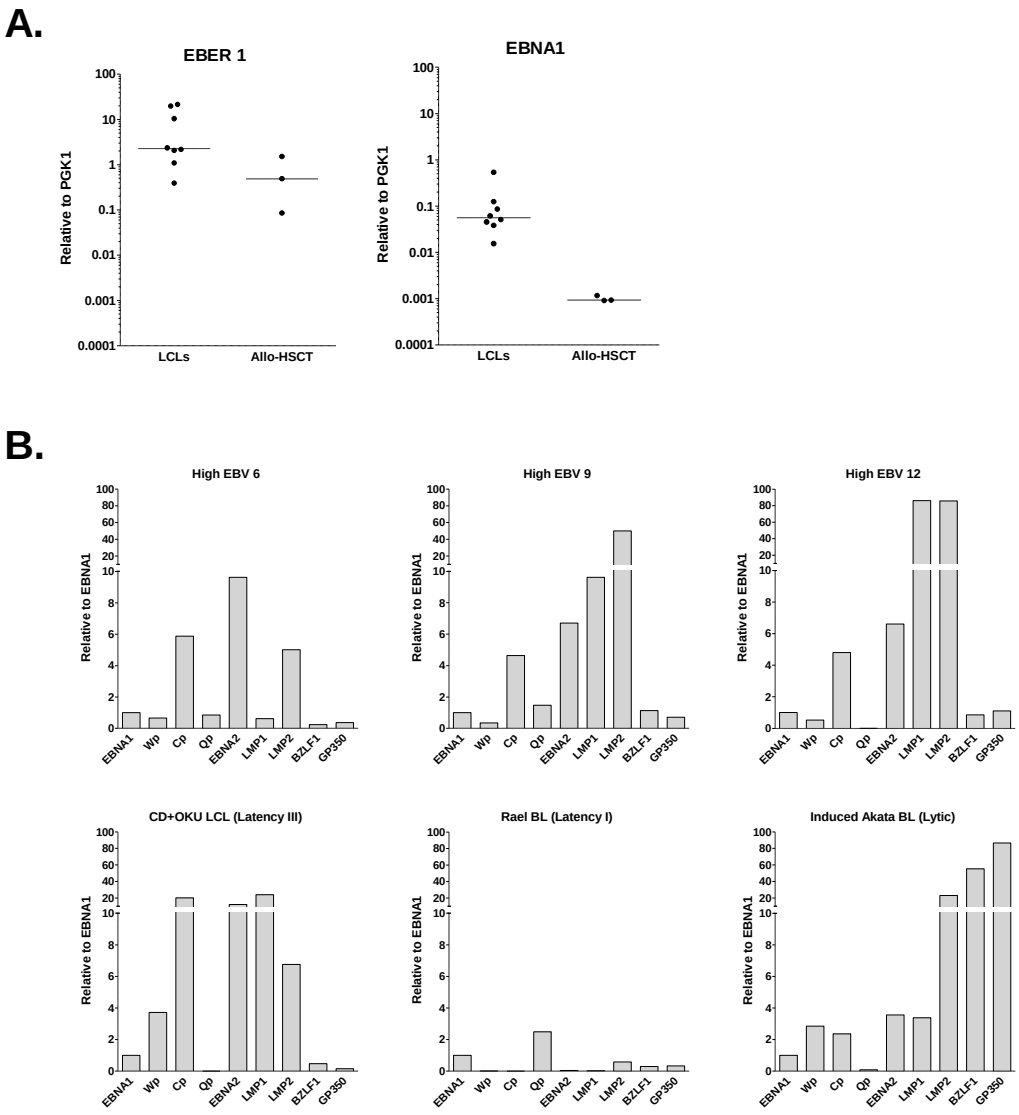

Figure 39. EBV Gene Expression in FACS-Sorted CD27$^+$ B-Cells

Quantitative RT-PCR analysis was used to determine EBV gene expression in FACS-sorted memory (CD27$^+$) B-cells from High EBV patients 6, 9 and 12, and EBV-positive cell lines. A. Expression of EBER1 and EBNA1 normalised to the cellular transcript PGK1 in patient samples and LCLs. Median values are shown by the horizontal bars. Patient samples contained similar levels of EBER1 as found in LCLs but much lower levels of EBNA1 B. Patterns of EBV gene expression normalised to EBNA1. Patient samples showed a Latency III pattern similar to the Latency III cell line CD$^+$OKU LCL and unlike the Latency I cell line Rael-BL. Patient samples contained low levels of BZLF1 and gp350 lytic transcripts, unlike the high levels seen in AKBM cells induced into lytic cycle.

$CD27^+$ B-cells in these patients express EBERs but are otherwise transcriptionally silent.

However, in a secondary analysis, viral transcript levels were then expressed relative to those of the EBNA1 gene, which is expressed in all forms of latency (Figure 39B). Doing so revealed a common transcriptional pattern for the patient samples that closely resembled that of the Latency III LCLs, characterised by high levels of Cp-initiated EBNA transcripts, EBNA2 and LMPs. Notably, this was clearly different from that of Latency I Rael-BL. Furthermore, unlike the induced Akata-BL cells, there were only low levels of the EBV lytic cycle genes BZLF1 and Gp350. Overall, these data suggest that the majority of $CD27^+$ B-cells isolated from patients with high-level EBV DNAemia after allo-HCT carry EBV genomes expressing a highly restricted pattern of latent gene expression, but a minority of cells do appear to exhibit Latency III expression (with little evidence of lytic cycle expression).

5.12 Activation and Proliferation Status of $CD27^+$ Cells

Cell Size

Data presented in Section 5.5 (Figure 30) shows that many of the $CD27^+$ memory cells found in High EBV patients exhibit a plasmablastic phenotype. Given this, further investigations were undertaken to explore the activation and proliferation status of these cells. Thus, given that lymphocytes are known to increase in size as they transition from an inactive resting state into their activated forms, cell size measurements collected during flow cytometry were analysed. Thus, values for FSC (forward scatter; a flow cytometric parameter which is primarily a measure of cell size) were compared for different B-cell subsets (Figure 40). In order to control for day-to-day variation in baseline FSC voltages, these values were corrected by expressing them relative to the total lymphocyte population for each sample. Using this

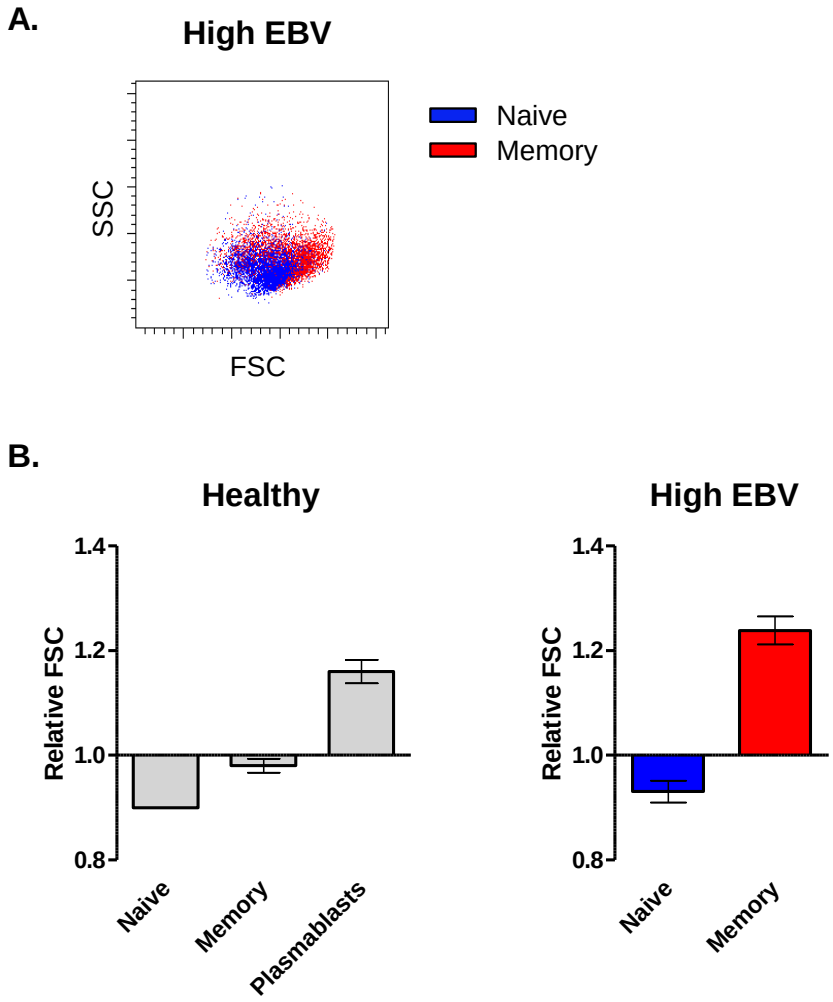

Figure 40. Analysis of Cell Size in B-Cell Subsets after Allo-HSCT

Cell size was analysed as an indicator of activation status. A. The FSC and SSC profile of naive ($CD27^{-}IgD^{+}$) and memory ($CD27^{+}$) B-cells from a representative High EBV patient, demonstrating the larger size (higher FSC) of the memory B-cells. B. Cell size was analysed for naive ($CD27^{-}IgD^{+}$), memory ($CD27^{+}IgD^{-}$) and plasmablastic ($CD27^{+}CD38^{++}$) B-cells in healthy donors (N=10), and naive and memory subsets from High EBV patients (N=13). FSC is expressed relative to the size of the total lymphocyte population for each sample. Memory B-cells from High EBV patients had a similar size ratio to that of plasmablasts in healthy donors, suggesting a state of activation.

approach, the size of $CD27^{-}IgD^{+}$ naive, $CD27^{+}$ memory and $CD27^{+}CD38^{++}$ plasmablast B-cells from healthy individuals was found to differ, as expected. Thus, naive B-cells were the smallest cells (average size ratio of 0.90; smaller than the average lymphocyte), whilst $CD27^{+}$ B-cells were larger (average size ratio 0.98; similar to the average lymphocyte) and plasmablasts were the largest cells (size ratio 1.16; larger than the average lymphocyte). Subsequently, analysis of B-cell subsets in High EBV patients revealed that the $CD27^{+}$ B-cells had a positive size ratio (average size ratio of 1.24) similar to that of plasmablasts from healthy individuals (Figure 40). This supports the view that the $CD27^{+}$ B-cells are in a state of activation.

Ki-67 Staining

To investigate further, flow cytometric measurement of Ki-67 was then performed to determine the proliferation status of the $CD27^{+}$ B-cell expansions; Ki-67 is a marker known to be expressed exclusively in proliferating cells[585]. To do so, FACS-sorted naive ($CD27^{-}IgD^{+}$) and memory ($CD27^{+}$) B-cells were first fixed and permeabilised in ethanol before performing intracellular staining with a FITC-conjugated anti-Ki-67 antibody or isotype control, after which the cells were analysed with flow cytometry (Figure 41). Two LCL lines were stained as positive controls, and these exhibited an average of 68% $Ki\text{-}67^{High}$ events, in keeping with a state of proliferation. In comparison, as expected, both naive and memory B-cells from a healthy individual showed <1% $Ki\text{-}67^{High}$ events, confirming that they are almost entirely resting. Meanwhile, naive B-cells from High EBV patients 6, 9 and 12 showed an average of only 5% $Ki\text{-}67^{High}$ events, confirming that they are also predominantly resting. However, in marked contrast, the $CD27^{+}$ memory B-cell subset from these patients contained an average of 50% $Ki\text{-}67^{High}$ cells. This suggests that a proportion of the memory B-cells present in

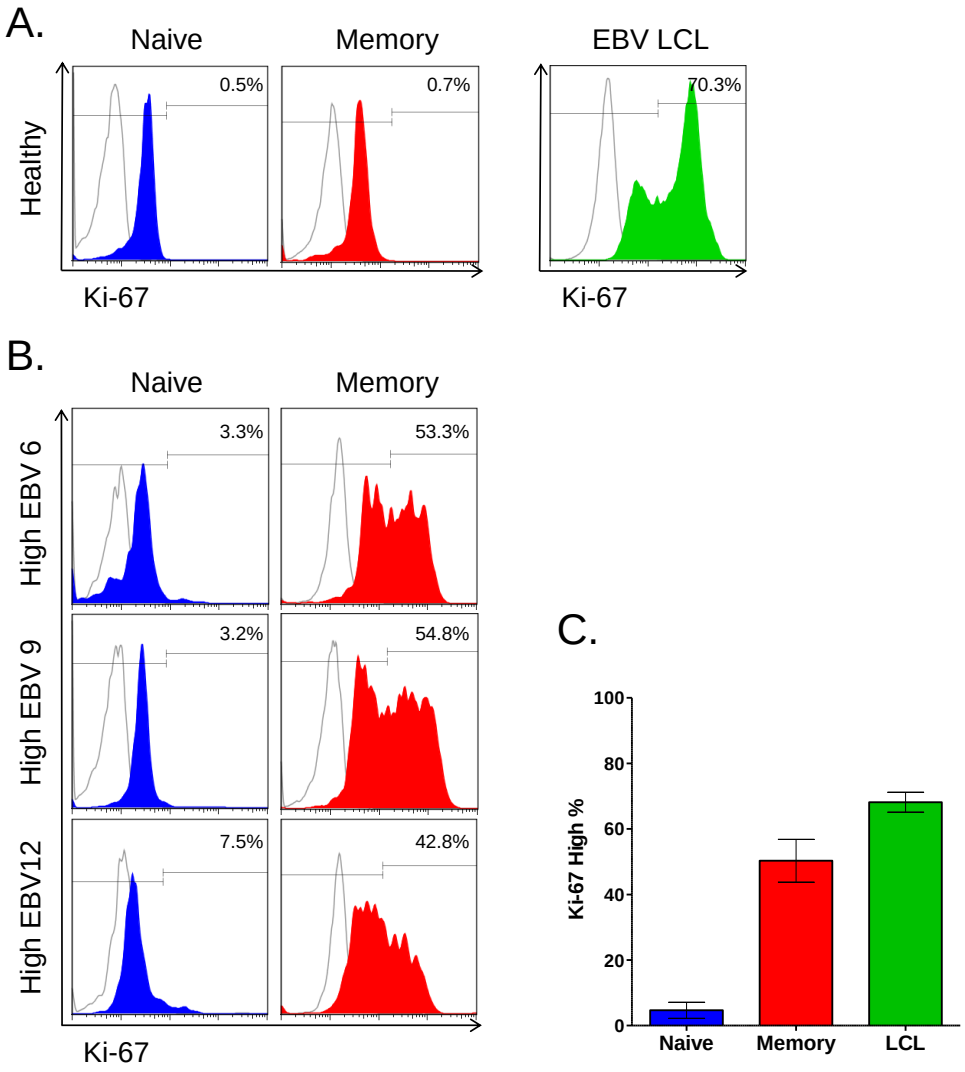

Figure 41. Expression of Ki-67 in Memory B-Cells after Allo-HSCT

Ki-67 expression was determined using intracellular flow cytometry. A. FACS-sorted naive ($CD27^{-}IgD^{+}$) and memory ($CD27^{+}$) B-cells from a healthy individual and an (unsorted) LCL positive control were stained with an anti-Ki-67 antibody (filled histogram) or isotype control (unfilled histogram). B. FACS-sorted naive and memory B-cells from High EBV patients 6, 9 and 12 were analysed. C. Summary of data for 3 High EBV patients and 2 LCLs (N=2). A high proportion of FACS-sorted memory, but not naive, B-cells from the High EBV patients were positive for Ki-67.

patients with high-level EBV DNAemia after allo-HSCT may be actively proliferating.

5.13 Determination of Surface Immunoglobulin Light-Chain Status

To assess the clonality of $CD19^+$ B-cells and $CD27^+$ memory B-cells in High EBV patients, cells were stained for surface κ and λ IgL and analysed with flow cytometry (Figure 42). The B-cells from healthy individuals showed polytypic IgL, with κ/λ ratios ranging from 1.3 - 1.9 and 1.3 – 2.0 for total B-cells and $CD27^+$ B-cells respectively. For the 13 High EBV patients, analysis of total B-cells also revealed polytypic IgL, albeit with more variability, with κ/λ ratios of 0.4 - 6.9. However, analysis of the $CD27^+$ memory B-cells showed evidence of IgL restriction (defined as a κ/λ ratio <0.1 or >10) in 4 patients, 2 of whom had PTLD. Thus High EBV Patients 3 and 10 showed moderate κ restriction, with κ/λ ratios of 11.0 and 11.7 respectively, whilst Patient 5 showed clear κ restriction with a ratio of 134. Meanwhile, Patient 12 showed clear λ restriction with a κ/λ ratio of 0.01.

5.14 Donor or Recipient Origin of $CD27^+$ B-cells

To investigate whether the $CD27^+$ memory B-cells observed in patients with high-level EBV reactivation were of donor or recipient origin, DNA extracted from FACS-sorted $CD27^+$ B-cells was analysed using microsatellite analysis, performed by the West Midlands Genetics Laboratory. This approach is routinely used to monitor the proportion of transplant donor-derived total lymphocytes or T-cells in patients following allo-HSCT, in order to determine the degree of donor chimerism. Comparing to previously determined recipient and donor microsatellite marker profiles, using at least 2 informative markers in each case, the $CD27^+$ B-cells derived from patients 6, 9 and 12 were all shown to be of 100% donor origin (data not shown).

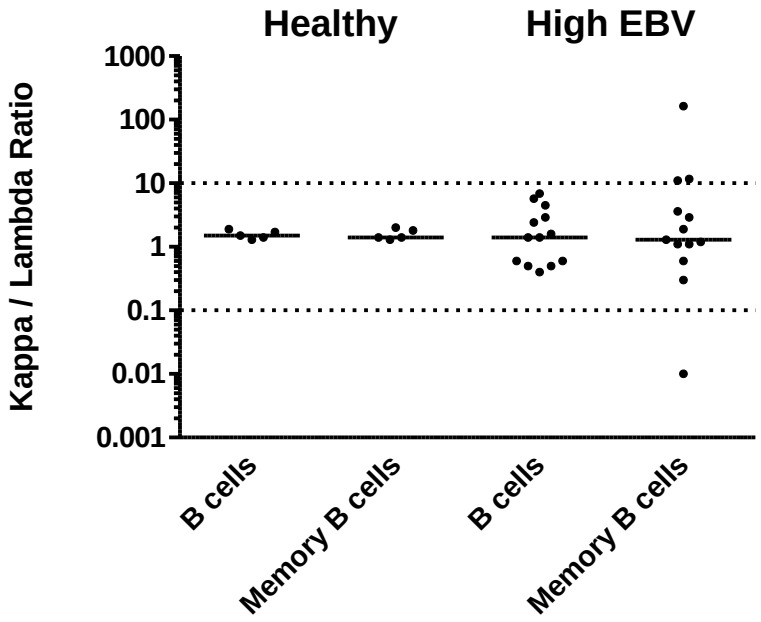

Figure 42. Immunoglobulin Light Chain Expression on B-Cells after Allo-HSCT

Surface κ and λ IgL status was determined for total $CD19^+$ B-cells and $CD27^+$ memory B-cells from High EBV patients and healthy controls. Medians are indicated by the solid horizontal lines. Dotted horizontal lines mark kappa/lambda ratios of 0.1 and 10. Of 13 High EBV patients analysed, 4 had memory B-cells which showed evidence of IgL restriction, as determined by a ratios of <0.1 or >10.

5.15 Origin of Virus Strains after Allo-HSCT

Work was also undertaken to investigate the origin (recipient or donor) of EBV strains present in patients with EBV reactivation after allo-HSCT. To do so, PCR was used to amplify sections of the EBNA3B and EBNA3C virus genes known to exhibit high levels of polymorphism. These were then sequenced and compared to a B95.8 reference sequence. This approach was used to analyse a series of patients for whom DNA was available from a) the recipient at the point of EBV reactivation, b) the recipient before transplant, and/or c) the donor. Notably, the PCR reactions were either nested (EBNA3B) or semi-nested (EBNA3C) to achieve the high levels of sensitivity necessary for successful amplification from samples containing little EBV DNA. All PCR reactions were carried out using high-fidelity DNA polymerase to minimise the risk of artefactual base changes, and all efforts were made to avoid cross contamination.

Unfortunately, only a limited number of samples were available to screen, and of these several could not be used because it proved impossible to amplify sequences from either the pre-transplant or donor samples. Nevertheless EBNA3B and EBNA3C sequences were successfully amplified for 8 patients (Table 21). These included 3 of the High EBV patients studied in preceding sections of this chapter, whilst the remaining 5 were other allo-HSCT patients for whom DNA was available. In interpreting the results, it is important to recognise several caveats. Firstly, the degree of confidence with which conclusions can be drawn regarding the origin of EBV strains varies depending on the samples available for each patient. Secondly, multiple EBV strains may simultaneously persist in one individual, and therefore the sequences identified may belong to the dominant strain of several present. Finally, third party infections should also be considered.

Patient	Donor Type	Sample	EBNA-3B				EBNA-3C				Interpretation
			417	444	702	827	821	910	940	1001	
			C	C	G	T	A	T	G	C	
A	Unrelated	Recipient	C	C	G	C	A	T	G	C	Donor
		Donor	C	T	T	C	C	T	G	C	
		Reactivation	C	T	T	C	C	T	G	C	
B	Unrelated	Recipient	C	T	G	C	C	T	G	T	Donor
		Donor	.	.	.	.	A	C	T	C	
		Reactivation	C	T	T	C	A	C	T	C	
C	Sibling	Donor	C	T	T	C	A	C	T	C	Equivocal
		Reactivation	C	T	T	C	A	C	T	C	
D	Unrelated	Donor	C	T	G	C	.	.	.	.	Donor
		Reactivation	C	T	G	C	A	T	G	T	
E	Unrelated	Recipient	T	T	T	C	A	C	T	C	Not Recipient
		Reactivation	C	T	G	C	C	T	G	T	
F	Unrelated	Recipient	C	T	G	C	C	T	G	T	Recipient
		Reactivation	C	T	G	C	C	T	G	T	
G	Sibling	Recipient	.	.	.	.	C	T	G	C	Equivocal
		Reactivation	.	.	.	.	C	T	G	C	
H	Unrelated	Donor	C	C	G	T	A	T	G	C	Not Donor
		Reactivation	C	T	T	C	A	C	T	C	

Table 21. Origin of EBV Strains in Patients with EBV Reactivation after Allo-HSCT

The origin of EBV strains present in patients with EBV DNAemia after allo-HCT was analysed by comparing EBNA3B and EBNA3C sequences in the recipient post-transplant with those in the recipient pre-transplant or the donor, where samples were available and could be successfully amplified. Sequences are aligned to the reference EBV strain B95.8. Red boxes highlight informative polymorphisms. Patient A is High EBV Patient 8; Patient E is High EBV Patient 12; Patient H is High EBV Patient 9.

The results for individual patients were interpreted as follows:

- In patients A and B, where all 3 samples were available, donor origin of the reactivation strain could be determined with a high degree of confidence because reactivation and donor sequences were identical, and there were several informative differences compared to the recipient pre-transplant strain.

- In patient C, the reactivation strain was identical to that of the donor for both amplicons. However, the strain could not be determined from the pre-transplant recipient strain. Furthermore, it is notable that in this case the donor was a sibling, which increases the likelihood that donor and recipient shared a common strain of virus. Given this the result remains equivocal.

- In patient D, donor origin was suggested by identical matching between reactivation and donor strains, although in the absence of a recipient pre-transplant sample it cannot be excluded that this strain was also present in the recipient originally

- In patient E, donor origin was suggested by multiple differences between the reactivation sample and that of the recipient pre-transplant strain, although alternative explanations include that this was a minor strain in the recipient prior to transplant, or that a third party infection occurred

- In patient F recipient origin was suggested by identical matching between reactivation and recipient pre-transplant samples, although in the absence of a donor sample it cannot be excluded that this strain was also present in the donor.

- In patient G, sequences were only available for EBNA3C for the reactivation and recipient pre-transplant samples, which were identical. Whilst this may imply recipient origin of the reactivation strain, noting that the donor was sibling from who sequence information was not available, the result is equivocal.

- In patient H, recipient origin was suggested by multiple differences between the reactivation sample and that of the donor, although alternative explanations are that this was a minor strain in the donor, or that third party infection occurred

Overall, despite the caveats mentioned above, these data suggest that EBV strains present during reactivation originate from *either* donor or recipient.

5.16 Discussion

Studies exploring EBV infection in immunocompromised transplant patients have generally focussed on recipients of solid organ allografts. Given this, several aspects pertaining to the pathophysiology of EBV reactivation complicating allo-HSCT have remained poorly characterised. As EBV is known to selectively colonise the circulating $CD27^+$ resting memory B-cell pool in healthy individuals[315-317], as well as in solid allograft recipients[386,387], we were particularly intrigued by the apparent paradox that EBV most commonly reactivates around 2-3 months post allo-HSCT, when the reconstituting B-cell compartment normally contains scarce quantities of $CD27^+$ B-cell memory[363-365]. Speculating as to possible explanations for this, we first considered that EBV genomes might be detected in the naive B-cell pool after allo-HSCT. Earlier work has suggested that EBV infects naive B-cells in the tonsils of healthy individuals[321,330]. Finding such cells in the circulation of allo-HSCT patients would therefore be remarkable. However, the alternative possibility, that EBV maintains selectivity for circulating B-cell memory after allo-HSCT, would be equally noteworthy. This would raise important questions as to how this exclusivity is mediated in the context of the reconstituting immune system following allo-HSCT.

Study Patients and Sample Collection

We successfully collected blood samples from 13 patients with high-level EBV reactivation, 3 of whom were concurrently diagnosed with PTLD. Importantly, these samples were all collected at, or near to, the time of peak EBV reactivation, and prior to pre-emptive Rituximab therapy. This challenging task was achieved through an innovative approach that made use of routine post-transplant EBV qPCR monitoring. Thus, patients were followed prospectively, and those who developed significantly elevated EBV DNA were bled as soon as possible afterwards.

Our approach to sample collection is remarkable, because it differs substantially from that employed by most previous studies of EBV persistence following transplantation. Thus, Babcock et al.[386] and other authors have typically collected samples from patients after solid organ allograft, sampling at arbitrary time points without the benefit of prospective EBV qPCR monitoring. This is potentially problematic because solid allograft patients often exhibit only modestly elevated EBV loads, and these are often chronically raised[384,495,586-588]. However, as elegantly demonstrated by the serial whole blood EBV qPCR plots displayed in Figure 18, allo-HSCT patients typically exhibit a very rapid and vigorous expansion in EBV load that frequently reaches extremely high levels, and which usually occurs during the first few months after transplant. Consequently, our approach allowed us to collect blood samples containing exceptionally high levels of EBV DNA which, *crucially*, contained cells that had only just appeared in the circulation. Therefore, we were able to study the earliest events during EBV reactivation.

EBV Loads

The EBV qPCR assay was used to show that PBMCs isolated from High EBV patients did indeed possess extremely high levels of EBV DNA. This is important because it confirms that much of the EBV DNA present in patients experiencing EBV reactivation following allo-HSCT is cell-associated. Such information is not provided by the clinical whole blood EBV qPCR assay, which is unable to distinguish EBV DNA present in plasma from that in the cellular compartment. Notably, comparison of the EBV loads generated by the whole blood and PBMC EBV qPCR assays showed a poor correlation. Although this could reflect measurement errors in either assay, it is considerably more likely to indicate variability in the proportion of EBV DNA found in cellular versus extracellular compartments.

Interestingly, as shown in Figure 20, it was also apparent that many patients in the No/Low EBV group also had somewhat elevated EBV loads in comparison to healthy controls; these were around the upper limit of normal observed in the healthy controls. This demonstrates that the in house EBV qPCR assay, when used to test PBMCs, is a considerably more sensitive technique than the clinical whole blood EBV qPCR assay. More importantly, it provides evidence that many patients maintain low levels of circulating EBV during the course of allo-HSCT. This is in agreement with previous data that immunocompromised transplants patients often have generally increased levels of EBV DNA, and also highlights that the presence of circulating EBV DNA *per se* is insufficient to trigger EBV reactivation.

T-Cell and NK-Cell Reconstitution

Considerable effort was made to characterise immune reconstitution following allo-HSCT in study patients. This revealed patterns of cell recovery amongst the No/Low EBV group that

closely resembled those reported by previous studies of immune reconstitution[342,354]. Thus, NK-cells were the first lymphocyte subset to recover, predominating in the first months following transplant, after which T-cells gradually became the most frequent cell type, with reversal of the CD4/CD8 T-cell ratio also apparent. We had speculated that High EBV patients might display delayed or otherwise altered levels of T- or NK-cells, which might account for the occurrence of EBV DNAemia in these patients. However, this was not the case and no significant differences were identified when the No/Low EBV and High EBV groups were compared, matching for time after transplant.

These data are interesting when they are considered in the context of proposals that T-cell monitoring might be introduced as an adjunct to EBV qPCR monitoring, to better predict which patients should be treated pre-emptively with Rituximab. Thus, Annels et al.[506] and Worth et al.[507] have both suggested that total $CD3^+$ T-cell counts in excess of 300 cells/μl at the time of EBV reactivation may identify patients who will spontaneously resolve EBV DNAemia, without the need for Rituximab. Meanwhile, other work has suggested that detection of EBV-specific T-cell responses at the time of EBV-reactivation is useful in identifying those at risk of progressing to PTLD[505,506,589]. Given these findings, it is notable that 7/13 patients in our series had $CD3^+$ T-cell counts over 300 cells/μl at the time of high-level EBV reactivation, although it is unknown whether these included EBV-specific T-cell responses. Clearly, in the absence of serial T-cell counts or data on EBV-specific immunity it is impossible to predict the outcome for High EBV patients if Rituximab had not been delivered. Nevertheless it is intriguing to consider whether these patients might have settled their EBV reactivation spontaneously.

$CD27^+$ Memory B-Cell Expansion

Analysis of B-cell reconstitution in the No/Low EBV patients revealed prolonged deficiency of $CD27^+$ memory B-cells that persisted up to and beyond 12 months after transplant. As such, our data agree with previous studies of B-cells after allo-HSCT[363-365], and support the interpretation that B-cells reconstitute primarily from newly engrafted donor-derived stem cells, rather than by expansion of mature cells transferred across with the graft.

However, a strikingly different pattern was found in High EBV patients, most of whom were found to have significant expansions in both the proportion and absolute number of circulating $CD27^+$ B-cells. Indeed, several patients had $CD27^+$ B-cell levels that were supra-normal in comparison to healthy donors. These data were interpreted as strong circumstantial evidence that EBV DNAemia is accompanied by the accumulation of B-cells exhibiting a memory B-cell phenotype. Subsequently, this was confirmed by using EBV qPCR to analyse FACS-sorted B-cell subsets. For all 4 patients tested this showed enrichment of genomes within the $CD27^+$ B-cell population, yielding some of the highest EBV loads recorded in *ex vivo* samples in our laboratory, and importantly relatively few (<1%) genomes were found within the naive B-cell and non-B-cell subsets. Although it was not possible to confirm the memory status of these $CD27^+$ cells by molecular means (Ig sequencing was attempted but proved impossible due to the small quantities of DNA available) we were able to demonstrate surface expression of IgG or IgA on these $CD27^+$ B-cell expansions, consistent with them being genuine B-cell memory.

These data clearly show that EBV maintains selectivity for the memory B-cell pool following allo-HSCT. In this respect our findings agree with Babcock et al. and others who have

explored EBV persistence in the solid organ transplant setting[386,387]. Furthermore, they show that EBV reactivation can drive the peripheral expansion of these memory B-cells to remarkably high levels, even when these cells are normally scarce following allo-HSCT. Notably, using single cell sorting experiments we showed that up to 90% of $CD27^+$ B-cells in patients with EBV DNAemia after allo-HSCT carried EBV genomes (whereas no genomes were present in $CD27^-IgD^+$ naive B-cells). This contrasts with the study by Babcock et al. in which the highest frequency of EBV-infected cells detected was around 1 in 60 B-cells[386], and even more starkly with the healthy carrier state in which only around 0.001% of memory B-cells are thought to carry EBV.

Having demonstrated a clear relationship between EBV and B-cell memory following allo-HSCT, it is nevertheless important to note that we cannot fully exclude the possibility of at least some low level carriage of EBV genomes within the naive B-cell compartment. Thus, although cell sorting experiments showed enrichment of EBV DNA within the $CD27^+$ B-cell subset, viral genomes were still detected within sorted naive B and non-B-cell subsets at relatively high levels compared to those expected for total B-cells from healthy donors; although even a small amount of contamination from the $CD27^+$ B-cell subset during FACS-sorting could explain these findings. In addition, the single sorting experiments only sampled 48 individual cells, and thus EBV-positive naive B-cells may have been missed by sampling error. Furthermore, not every High EBV group patient had particularly raised levels of $CD27^+$ B-cells. In accounting for this, it is notable that there was a relatively wide distribution of EBV loads amongst patients with high-level EBV DNAemia, and those with lower loads typically had lower $CD27^+$ cell frequencies, as one might expect. It is possible that the $CD27^+$ B-cells in these patients may have contained increased EBV genome copies/cell compared to

patients with higher $CD27^+$ B-cell levels. However, this might also be taken as evidence of EBV carriage within $CD27^-$ B-cells, or even non-B-cell subsets. The significance of these findings remains to be tested, as lack of $CD27^+$ B-cells in these patients meant they were not investigated further in the present studies.

EBV Copy Number Per Cell

Single cell sorting experiments were also used to show that EBV-positive $CD27^+$ cells from the High EBV patients carried an average of 19 EBV genome copies/cell (Figure 38). Importantly, the distribution of EBV copies/cell in the allo-HSCT patients was found to be several logs lower than that seen for a cell line stimulated *in vitro* to enter lytic cycle. This provided good evidence that the bulk of cell-associated EBV genomes occur in the context of latent, rather than lytic, infection in these patients.

Interestingly, our estimate of EBV genome copy number/cell is similar to those provided by other studies which have examined transplant patients. Thus, Rose at al. used fluorescence *in situ* hybridisation (FISH) to demonstrate that EBV-infected cells in the circulation of paediatric solid allograft recipients carry 1 - 30 EBV copies/cell; interestingly, those with lower EBV loads were found to carry 1 - 2 copies/cell, whereas those with higher EBV loads carried some cells with a low number (1 - 2) of copies and other cells with a higher number (20-30) of copies[590]. Similarly, Calattini et al. used FISH to show 3 - 35 EBV copies/cell in B-cells isolated from patients with EBV DNAemia after allo-HSCT[591]. These values contrast with estimates for healthy individuals of 2 - 5 copies/cell[313,592,593], although higher estimates averaging around 50 copies/cell have also been made[331]. Meanwhile, although EBV copy number in established LCLs was originally reported to range from 5 – 800 copies/cell[594], a

more recent study used FISH to show around 50 copies/cell[595]. Interestingly, the latter study found only 1 - 2 copies/cell in newly infected B-cells but copy number was found to amplify to around 20 copies/cell by 3-4 weeks after infection[595]. This intriguing observation leads us to speculate that this process may also occur *in vivo*, and therefore the $CD27^+$ B-cells from High EBV patients which were found to carry fewer copies/cell (Figure 38) might have been infected more recently and/or undergone fewer cell divisions.

EBV Gene Expression

EBV gene expression was analysed using a novel quantitative RT-PCR method that used standardisation against a plasmid containing target EBV sequences, such that different transcript levels could be directly compared to each other. For all 3 High EBV patients analysed, a complete range of EBV Latency III gene targets were detected in FACS-sorted $CD27^+$ B-cells. Furthermore, when normalised to EBNA1 transcript levels, the expression patterns were easily distinguished from those present in a Latency I BL cell line, or Akata BL triggered to exhibit lytic cycle expression. However, normalisation of transcript levels to the cellular gene PGK1 revealed EBERs to be expressed at reasonably similar levels to those in an LCL but all other viral transcripts were found at disproportionately low levels. This probably indicates that only a minority of circulating EBV genomes express the Latency III programme in these patients, whilst the bulk of genomes are transcriptionally inactive, except for EBERs. However, it could also indicate that levels of Latency III RNAs *in vivo* are considerably lower than those seen in EBV transformed LCLs established *in vitro*.

Our data are notable in the context of prior studies of EBV gene expression. Thus, RT-PCR analysis of circulating lymphocytes from healthy individuals has shown the only consistently

detectable EBV transcripts, other than the EBERs and BARTs, to be LMP2A and in some studies EBNA1[314,318,319]. These findings have been used to postulate that a highly restricted pattern of expression defines the normal carrier state, contrasting with the Latency III expression pattern found in PTLD tumours and LCLs. Meanwhile, attempts to analyse EBV gene expression in circulating lymphocytes from immunocompromised transplant patients have shown mixed results. Thus, Babcock et al. demonstrated only LMP2A expression in 1 of 4 solid organ transplant patients analysed. Whereas, Qu et al. showed LMP2A expression in several solid organ transplant patients, with additional LMP1 transcripts in patients with higher EBV loads[584]. Furthermore, Hopwood et al. showed that healthy cardiothoracic transplant patients often exhibit either LMP2A expression alone, or alongside one or more additional transcripts including EBNA3C, LMP1 or lytic genes, whilst patients with PTLD often exhibited a pattern consistent with Latency III including lytic transcripts[583]. This demonstrates a notable degree of heterogeneity in the currently available data. However, it should be noted that these studies have all used non-quantitative nested RT-PCR methods, which give no indication of the relative abundance of transcripts, and therefore they should be interpreted with caution.

Activation and Proliferation Status of CD27$^+$ B-cells

Since Babcock et al. have previously demonstrated that EBV-infected B-cells isolated from the blood of solid allograft patients are in a resting state[386], like those of healthy donors, we were surprised to find data contrary to this for patients after allo-HSCT. Thus, CD27$^+$ memory B-cells from High EBV patients were found to be strongly positive for CD38, suggesting plasmablastic phenotype. They were also considerably larger than resting naive and memory B-cells from healthy individuals. Most importantly, a significant proportion

(around 50% versus 90% in LCLs) were Ki-67$^+$ by flow cytometry. Unfortunately, application of the techniques used by Babcock et al. was precluded by limited amounts of patient material in the current study. Nevertheless, taken together these data are highly suggestive that these CD27$^+$ B-cells are activated and that at least a proportion of them are proliferating.

These findings are particularly intriguing in light of our EBV gene expression data, which showed only low levels of growth transforming EBV Latency III transcripts in the CD27$^+$ memory B-cells from High EBV patients. Reconciling these apparently contradictory findings, we propose that circulating CD27$^+$ B-cells may have recently exited nodal tissues, in which Latency III driven expansion is occurring in the majority of cells, as it does in PTLD. We suggest that down-regulation of EBV latent gene expression, from Latency III to more restricted patterns, may accompany egress into the circulation, and that progressive exit from cell cycle may follow this as a consequence. Indeed, EBV latent proteins typically have half-lives greater than 24 hours, which might mean that the cells could continue to proliferate for 1 - 2 divisions after transcription has ceased. Notably, successful identification of cells still exhibiting an activated and proliferating is likely to reflect collection of blood samples so soon after initiation of EBV reactivation in this study.

Origin of the CD27$^+$ B-cells

In order to further define the pathophysiology of EBV reactivation in study patients, we also sought to identify the origin of circulating CD27$^+$ B-cells in High EBV patients. Thus, in what to our knowledge is the first analysis of its kind, we demonstrated using microsatellite analysis that FACS-sorted CD27$^+$ B-cells were of 100% donor origin in 3 patients tested. This

result is in keeping with the observation that most PTLD tumours arising after allo-HSCT are donor-derived.

Despite this finding, uncertainty still remains as to whether circulating EBV-infected $CD27^+$ B-cells in High EBV patients originate from mature B-cells transferred across with the donor stem cell graft, or from naive B-cells which have newly differentiated from engrafted donor stem cells. At present, we can only speculate as to the exact mechanism. However, the former of these possibilities is supported by evidence that mature donor memory B-cells which remain responsive to stimulation *have* been detected in allo-HSCT recipients[596,597]. Furthermore, this mechanism is favoured by studies suggesting that graft T-cell depletion with ATG, which spares B-cells, leads to increased rates of EBV reactivation and PTLD than Alemtuzumab, which also depletes B-cells[392,407,409,415]. Alternatively, this effect may simply be a consequence of more profound T-cell depletion with ATG than with Alemtuzumab. On the other hand, the observation that EBV reactivation is often delayed until 2-3 months after transplant, which is typically when new B-lymphopoiesis begins, supports the competing possibility that EBV-infected B-cells usually originate from new naive B-cells. Of course, it may be that both phenomena occur, and that transplant conditioning may influence which mechanism predominates.

Assuming that EBV-infected B-cells *do* originate from mature B-cells transferred across with the graft, a further consideration is whether EBV-infected resting memory B-cells from the donor undergo spontaneous outgrowth in the recipient. Against this, it has been shown that when PBMCs from a healthy EBV-infected donor are used to generate spontaneous LCLs *in vitro*, this does not occur by direct outgrowth of EBV-infected B-cells but rather occurs via a

2-step process in which EBV-infected B-cells first initiate viral replication, yielding new virions that subsequently infect other cells[598].

Origin of Virus Strains

Work was also undertaken to determine the origin of EBV strains present in patients undergoing EBV reactivation, by comparing EBV sequence polymorphisms in transplant recipients, before and after transplant, with those in the donor where available. Bearing in mind the caveat that transplant patients may carry multiple virus strains[105], this nevertheless revealed that the dominant post-transplant EBV strain may be of donor *or* recipient origin. Thus, our data agree with a limited number of case reports and small series which have previously shown that the post-transplant viral strain is identical to the recipient pre-transplant strain in only about half of cases[579-582]. However, it is notable that unlike previous studies, which have all been undertaken in patients receiving myeloablative conditioning, our data were generated from patients who had undergone RIC transplantation, which conceivably might have favoured retention of recipient viral strain post-transplant.

These observations have potentially important implications for our understanding of the pathophysiology of EBV infection. Thus, the fact that both donor and recipient strains are found after transplant is evidence against spontaneous outgrowth of donor-derived resting memory B-cells, as this would invariably lead to acquisition of donor-derived virus strains. Furthermore, it also informs the debate as to whether B-cell depletion prior to allo-HSCT (as discussed in Chapter 4) operates by reducing levels of recipient-derived virus. Thus, the finding that patients often acquire the donor strain is evidence against this possibility. Finally, it also provides additional evidence that B-cells, rather than oropharyngeal epithelium, are the

principal reservoir of EBV infection. Indeed, if epithelial cells were a site of chronic EBV persistence, it could be expected that the pre-transplant strain would invariably be maintained.

A Model for EBV Reactivation after Allo-HSCT

In a synthesis of the data generated by this and previous studies, we can now propose a model for the events of EBV reactivation following allo-HSCT (Figure 43). As such, we suggest that underlying all instances of EBV DNAemia is a Latency III growth transforming infection which arises in nodal tissues as a consequence of immune compromise. This drives the proliferation of EBV-infected cells with a $CD27^+$ memory B-cell phenotype, which subsequently transit into the circulation. Co-incident with this, there is probably down-regulation of EBV gene expression and progressive exit from cell cycle, such that a proportion of cells temporarily remain $Ki\text{-}67^+$. The source of the B-cells that contribute to the Latency III reactivation may be mature B-cells transferred across with the graft, or newly emergent B-cells. Similarly, the virus infecting these cells may derive from either the recipient or the donor. These mechanisms may be dictated by the type of transplant conditioning used, and the form of T-cell depletion, and/or the time taken for B-cells to reconstitute and thus appear as targets for transformation. Although this process is usually subclinical, it may progress to established PTLD in some patients if the Latency III-driven proliferation in nodal tissues continues, due to a lack of emergent EBV-specific T-cell responses or pre-emptive Rituximab therapy.

Significance for Models of EBV Persistence

Importantly, our finding that EBV maintains selectively for the $CD27^+$ memory B-cell compartment after allo-HSCT also carries significance for our understanding of how EBV

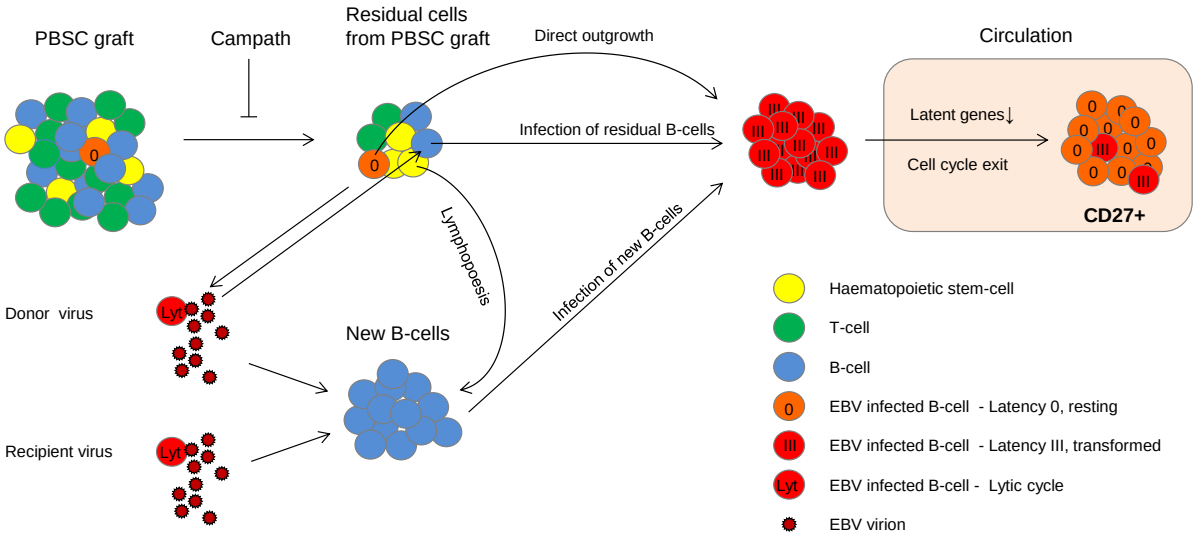

Figure 43. Model of EBV Reactivation Following Allo-HSCT

CD27$^+$ memory B-cells of transplant donor origin accumulate in the circulation of patients with EBV reactivation following allo-HSCT. Many of these cells are Ki-67$^+$ and display an activated phenotype, although only a minority of Latency III transcripts are detected. We propose that these cells originate from a Latency III growth transforming infection taking place in the secondary lymphoid tissues (which may progress to PTLD if it is uncontrolled). Departure of virally infected cells into the circulation seems to be accompanied by down-regulation of latent viral gene expression and progressive exit from cell cycle, such that a proportion of circulating cells remain Ki-67$^+$ for some time. The events preceding this are less certain. EBV is found almost entirely within donor derived B-cells in this setting but it is unclear whether these are usually mature B-cells which have been carried across with the PBSC graft, or whether they derive from new naive B-cells which develop from recently engrafted donor haematopoietic stem cells. Although EBV-infected donor B-cells carried across with the graft might undergo direct outgrowth, this is not supported by in vitro evidence598. It is therefore more likely that uninfected donor B-cells are infected by EBV in the transplant recipient. The infecting virus may originate from infected donor B-cells which undergo productive lytic cycle following transfer, or from infected host cells (B-cells or epithelial cells) that have survived transplant conditioning.

achieves this selective colonisation, in this and other settings. Thus, as mentioned previously, competing GC-dependent[329] and -independent models[41,272,331] have been proposed to explain the route by which EBV enters the B-cell memory reservoir. Considering these in relation to allo-HSCT, it is impossible to ignore the likelihood that GCs are significantly disrupted or even abolished by the process of allo-HSCT. Indeed, this is likely to be a consequence of the destruction of nodal tissues by conditioning therapy, and due to delays in the reconstitution of key cell types required for GC activity, including $CD4^+$ T-cells. Notably, acute GvHD is well recognised to precede EBV reactivation, and it is known to significantly disrupt GC formation[377-379]. Consequently, it seems improbable that the circulating $CD27^+$ B-cells which accumulate in patients with EBV DNAemia after allo-HSCT originate exclusively from naive B-cells of donor origin which have been driven through a GC reaction by EBV.

Relevant to these issues, is the interesting finding that $CD27^+$ B-cells found in High EBV patients were almost entirely confined to the $CD27^+IgD^-$ CSM subset, whereas few, if any, had a $CD27^+IgD^+$ NSM phenotype. This is remarkable because previous studies have shown that EBV can be found within the NSM subset; both in healthy individuals[331], albeit at lower frequency than in the CSM subset, and in patients with genetic disorders that abolish normal GC physiology, such as XLP[338]. As discussed previously, the origin of the NSM subset remains controversial, although they may arise via GC-independent pathways principally located in the spleen[18,72,599,600]. Given these observations, it is challenging to explain why the $CD27^+$ B-cells found in High EBV patients were almost entirely of CSM phenotype. In one interpretation, EBV may preferentially drive naive B-cells to differentiate into memory B-cells with an exclusively CSM phenotype, in keeping with the GC-dependent model of EBV persistence. However, it is notable that our data showed the NSM subset to be impaired

relative to CSM cell in *all* allo-HSCT patients, including those from No/Low EBV patients. Thus, NSM cells probably recover at an even slower pace than CSM cells during normal B-cell reconstitution. Given this, a more likely interpretation may be that EBV simply colonises the B-cell subsets available to it, operating via GC- independent pathways.

6. Modelling the Clonal Evolution of PTLD *in Vitro*

Previous studies in this and other laboratories have demonstrated that EBV-transformed B-cell cultures exhibit clonal outgrowth, such that over a period of several weeks polyclonal cultures tend towards oligoclonality and thereafter to monoclonality[236,238,239]. In contrast mitogen-stimulated B-cell blasts remain polyclonal for several weeks in culture[236]. Importantly, this process of clonal outgrowth in EBV transformed cultures may be a useful model to explore the pathogenesis of PTLD. Indeed, factors which may influence clonal outgrowth of LCLs *in vitro* might also be relevant to the progression of early polyclonal B-cell proliferations to monoclonal lymphomas, reflecting the diversity observed in PTLD pathological subtypes.

Much uncertainty remains regarding the processes which might underlie clonal selection and outgrowth. Among potential determinants of the contrasting results observed for EBV-transformed versus B-cell blast cultures, are differences in proliferation and cell survival. Furthermore, recent evidence has suggested that DNA damage signalling and/or genomic instability may also be important. Thus, Nikitin et al. have described that early EBV-infected B-cells exhibit a period of hyperproliferation, causing genomic instability which triggers DNA damage response signalling and inhibition of outgrowth for some cells[158]. In order to explore these factors as possible determinants of clonal outgrowth, a series of investigations were undertaken to compare cell death, proliferation and DNA damage signalling in early EBV cultures with those present in mitogen-stimulated B-cell blasts.

It is also possible that cellular mutations caused by EBV might act as an important

determinant of clonal selection, by promoting cell survival or proliferation. Indeed, EBV is known to induce expression of AID in LCLs[219,227-229]; as discussed previously this enzyme is responsible for the mutagenic processes SHM and CSR during B-cell development and has been implicated in tumourigenesis. Notably, this laboratory has previously shown that dominant clonotypes arising in EBV-infected naive B-cells cultures often contain AID-induced Ig gene mutations, and these appear to undergo sequence diversification *in vitro*[601]. Furthermore, Epeldegui *et al.* have demonstrated that following EBV infection of total B-cells, AID-associated mutations accumulate in non-Ig genes such as BCL6 and p53[244]. However, from this earlier study it remains uncertain to what extent these BCL6 mutations are *de novo* events, or whether pre-existing mutations are simply selected during the course of clonal outgrowth. To investigate this further, we also sought to characterise BCL6 and other 'off target' AID-associated mutations in EBV cultures established from a range of alternative B-cell types, including naive and umbilical cord blood B-cells which do not contain pre-existing mutations.

6.1 Clonal Outgrowth in EBV and B-Cell Blast Cultures

Generation of EBV and B-Cell Blast Cultures

All of the experiments described in this chapter were conducted on EBV-infected or mitogen-stimulated B-cell cultures. B-cells were isolated from healthy adult donors, or in some experiments from umbilical cord samples, using CD19 Dynabead separation. This resulted in highly purified B-cell populations (typically >98%), as demonstrated by flow cytometric evaluation for CD19 in Figure 44A. For several of the experiments, isolated B-cells were subsequently FACS-sorted into $CD27^{-}IgD^{+}$ naive, $CD27^{+}IgD^{-}$ CSM and $CD27^{+}IgD^{+}$ NSM B-cell subsets as shown in Figure 44B. The 2089 strain of EBV was used to infect B-cells at an

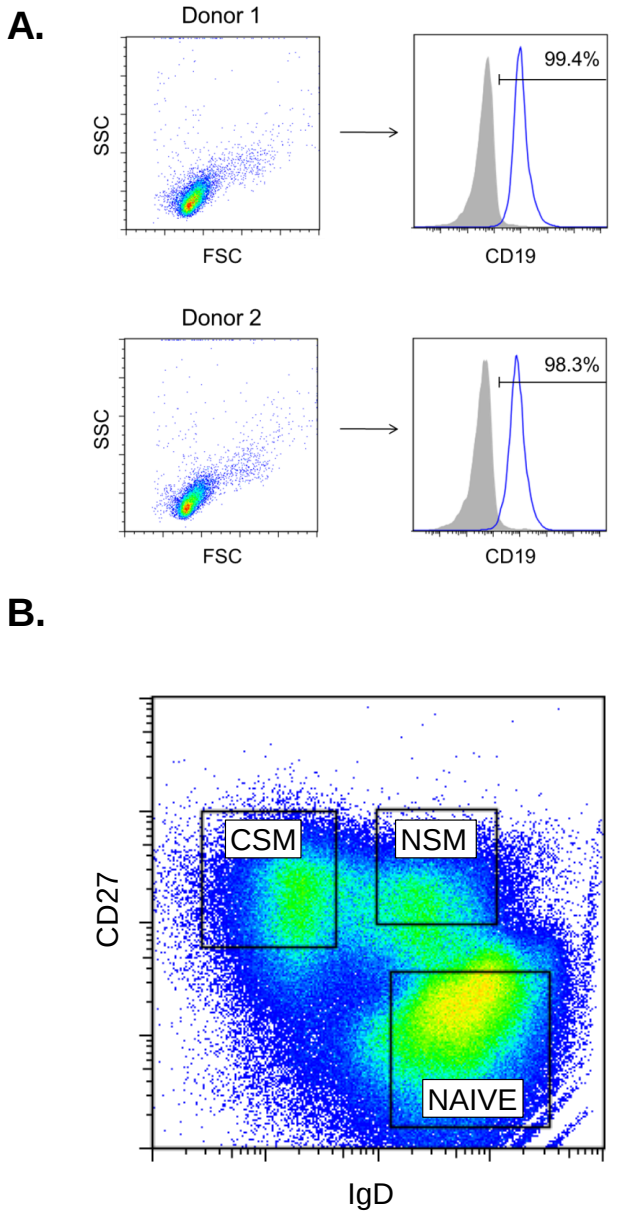

Figure 44. Purification of B-Cells from Apheresis Cones and Umbilical Cord Blood

B-cells were isolated using CD19 Dynabead magnetic separation. When required, they were then FACS-sorted into B-cell subsets using a MoFlo cell sorter. A. The purity of B-cells isolated with CD19 Dynabeads was confirmed by staining for surface CD19, typically revealing purities >98%. This is exemplified here by analysis of purified B-cells from 2 donors stained with an anti-CD19 antibody (blue histograms) or isotype control (filled grey histograms). B. Dynabead purified B-cells were FACS-sorted into $CD27^{-}IgD^{+}$ naive, $CD27^{+}$ IgD^{-} CSM and $CD27^{+}$ IgD^{-} NSM subsets using the gates depicted.

MOI of 50 to generate all EBV-infected cultures unless otherwise indicated. In parallel, mitogen-stimulated B-cell blasts were generated by culturing B-cells on irradiated mouse fibroblasts stably transfected with human CD40L in the presence of soluble human IL4[554].

Measurement of Clonal Outgrowth with IgH CDR3 Spectratyping

Clonal outgrowth in EBV-transformed B-cell cultures was analysed using IgH CDR3 spectratyping. Previous studies in this laboratory have primarily analysed B-cell clonality by sequencing across the VDJ region of the rearranged IgH chain in multiple PCR-generated clones; detection of multiple unique IgVH sequences provides evidence of polyclonality, whilst detection of identical sequences suggests monoclonality or oligoclonality. However, IgH CDR3 spectratyping provides an alternative measure of clonality, using a standardised set of primers in a multiplex PCR reaction, to amplify across the IgH CDR3 region[602]. This generates multiple fragments which differ in length according to VDJ usage, which are subsequently separated on a capillary gel electrophoresis platform to produce a spectratype. CDR3 spectratyping has the advantage that many thousands of VDJ rearrangements can be analysed in a single experiment, thus providing a greater depth of sampling. In polyclonal samples the spectratype approximates a standard distribution curve, whilst in oligoclonal or monoclonal samples certain peaks are enriched while others are reduced or absent.

The IgH CDR3 spectratyping technique was initially used to confirm the earlier observation of clonal outgrowth within EBV transformed B-cell cultures (Figure 45). Thus LCLs generated from either total B-cells or naive B-cells were sampled at intervals following infection, and DNA prepared from these was tested to produce serial IgH CDR3 spectratypes. As expected, at 2 weeks following infection the spectratypes were entirely polyclonal.

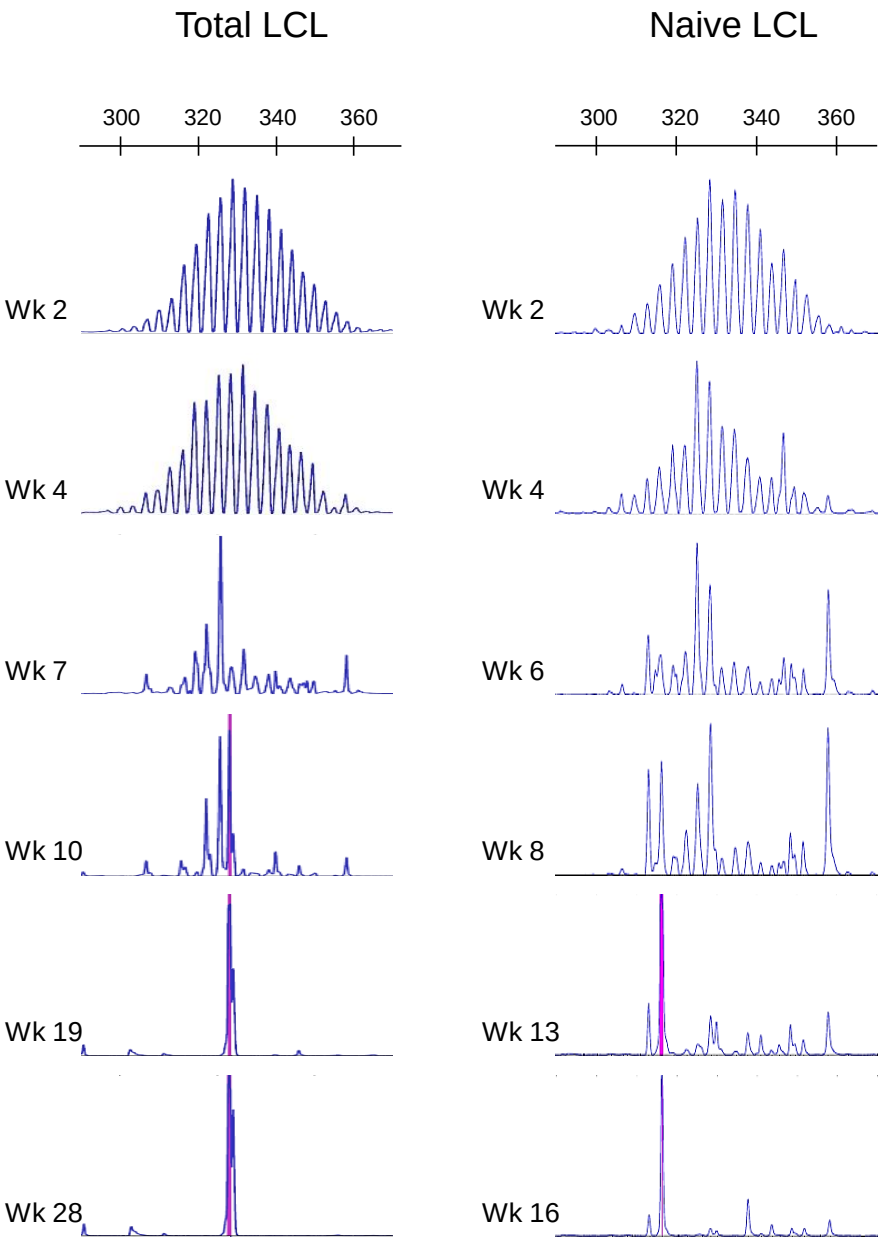

Figure 45. IgH CDR3 Spectratype Analysis of Clonal Outgrowth in LCLs

The clonality of LCLs established from adult total B-cells or naive B-cells was analysed using IgH CDR3 spectratyping. This technique uses a set of primers to amplify across the IgH CDR3 region in a multiplex reaction, generating multiple fragments which differ in length (bp) according to VDJ usage. As shown, both cultures are polyclonal at the 2 week time point, as evidenced by spectratypes approximating a normal distribution. Thereafter the cultures demonstrate clonal outgrowth to oligoclonality and ultimately monoclonality, as apparent from the appearance of dominant peaks.

However, from 4 weeks there was emergence of dominant clonotypes, leading to readily apparent oligoclonality by 6 - 8 weeks after infection. Thereafter, progression to a single dominant clonotype was observed in both cases.

As an independent validation of the spectratyping technique, multiple IgVH sequences were also obtained from the naive B-cell culture at 8 and 16 week time points (Table 22). As expected, this showed evidence of repeated IgH sequences with identical VDJ usage and CDR3 junctions at both time points, consistent with the emergence of oligoclonality. Notably, this also confirmed that infection with EBV can lead to the acquisition of AID-associated SHM events in naive B-cells.

Comparison of Clonal Outgrowth in Alternative Cultures

Previous studies have only examined clonal outgrowth in cultures generated by infecting mature total B-cells, or naive B-cells, with a wild type EBV strain. However, preliminary evidence from 2 prior experiments had suggested that EBV-infected cultures generated from umbilical cord blood B-cells may remain polyclonal, similar to the situation with mitogen-stimulated B-cell blasts. Furthermore, since a small proportion of B-cells in EBV-infected cultures may spontaneously support virus replication, we speculated that EBV lytic cycle entry might also contribute to clonal outgrowth, possibly by triggering the secretion of soluble factors.

Work was therefore undertaken to compare clonal outgrowth in cultures generated from 2 healthy adults or 2 umbilical cord bloods, under the following conditions: (1) adult B-cells stimulated with CD40L and IL4 to form blasts, (2) adult B-cells infected with a wild type

	V	D	J	V Mutations	CDR3 Translation	Spectra Size
Week 8	IGHV3-74*01	IGHD3-10*01	IGHJ6*03	8	CVRRGEYMDVW	316
	IGHV3-74*01	IGHD3-10*01	IGHJ6*03	8	CVRRGEYMDVW	315
	IGHV3-74*01	IGHD3-10*01	IGHJ6*03	9	CVRRGEYMDVW	315
	IGHV3-74*01	IGHD3-10*01	IGHJ6*03	9	CVRRGEYMDVW	315
	IGHV3-74*01	IGHD3-10*01	IGHJ6*03	9	CVRRGEYMDVW	315
	IGHV1-46*01	IGHD4-17*01	IGHJ4*02	5	CARDYGDRSSFDYW	324
	IGHV3-53*01	IGHD4-11*01	IGHJ5*02	7	CAKDYSNSGWFDLW	321
	IGHV4-31*03	IGHD1-20*01	IGHJ5*02	8	CARDNNWLHNWFDPW	330
	IGHV4-31*03	IGHD1-20*01	IGHJ5*02	8	CARDNNWLHNWFDPW	330
	IGHV4-59*01	IGHD6-13*01	IGHJ5*02	5	CARAAGSITQFWFDPW	327
	IGHV1-02*02	IGHD1-1*01	IGHJ6*02	2	CARRLDADYYYFMDVW	329
	IGHV3-07*01	IGHD3-3*01	IGHJ6*02	6	CARDLEQQLGYGMDVW	330
	IGHV5-51*01	IGHD2-2*01	IGHJ5*01	4	CARQRDRVVVPAGGWFDSW	333
	IGHV1-18*01	IGHD3-22*01	IGHJ6*03	3	CARDPYYDSRGYYYYYMDVW	342
Week 16	IGHV3-74*01	IGHD3-10*01	IGHJ6*03	8	CVRRGEYMDVW	314
	IGHV3-74*01	IGHD3-10*01	IGHJ6*03	8	CVRRGEYMDVW	315
	IGHV3-74*02	IGHD3-10*01	IGHJ6*03	8	CVRRGEYMDVW	315
	IGHV4-31*03	IGHD2-15*01	IGHJ4*02	12	CAKWEGGSGDYW	321
	IGHV3-23*04	IGHD6-6*01	IGHJ4*02	20	CAKAAESPFDYW	318
	IGHV3-30*01	IGHD3-3*01	IGHJ4*02	11	CARVVFPRSSGGLDSW	330
	IGHV1-02*01	IGHD2-2*01	IGHJ4*02	14	CARDLSALVAAAFSDHW	333
	IGHV3-11*01	IGHD3-3*01	IGHJ6*03	7	CARTIFGVIPTYSYHMDAW	339
	IGHV3-11*01	IGHD3-3*01	IGHJ6*03	7	CARTIFGVIPTYSYHMDAW	339
	IGHV3-23*04	IGHD1-26*01	IGHJ3*02	9	CAKILPYRGSSLIVSEAFDIW	346
	IGHV3-30*03	IGHD2-15*01	IGHJ4*03	10	CAKDNIGYCSGVSCPGGGFGMDVW	354
	IGHV3-30*03	IGHD2-15*01	IGHJ4*03	10	CAKDNIGYCSGVSCPGGGFGMDVW	354

Table 22. IgVH Rearrangements for the Naive LCL

IgVH rearrangements from 8 and 16 week time points for the naive LCL analysed by spectratyping in Figure 45 were cloned and sequenced. By aligning to germline sequences present in the IMGT database, individual V, D and J segments used in each rearrangement were identified, as were the number of SHM mutations present in the V segment (V Mutations) and the amino acid sequence of the CDR3 region (CDR3 Translation). The occurrence of identical CDR3 regions (highlighted with different colours) is consistent with the emergence of clonality in these cultures. Specific IgVH sequences could be matched to spectratype peaks based on fragment size, as indicated in the right hand column (Spectra Size). Notably, the appearance of V region mutations in an LCL derived from naive B-cells indicates that EBV infection can lead to the acquisition of AID-associated SHM mutations. Data courtesy of Dr A. Bell, University of Birmingham.

(2089) EBV strain, (3) adult B-cells infected with a mutant EBV strain (BZLF1-KO), which is defective in virus lytic cycle entry due to lack of the IE gene BZLF1, and (4) umbilical cord blood B-cells infected with a wild type (2089) EBV strain.

For each culture, IgH CDR3 spectratypes were determined for the 8 week time point, because all EBV cultures previously analysed have exhibited oligoclonality by this time. Figure 46 shows the resulting spectratypes. Firstly, these data confirm that B-cell blast cultures remain polyclonal in comparison to 2089 EBV-infected LCLs generated from total adult B-cells, which show clear evidence of oligoclonal outgrowth. Furthermore, adult total B-cell cultures were seen to exhibit oligoclonal outgrowth, irrespective of whether they were infected with 2089 EBV or the BZLF1-KO EBV strain. This suggests that lytic cycle EBV gene expression is not important in determining clonal outgrowth. Finally, it was apparent that cultures generated from immature umbilical cord blood B-cells also exhibit a similar degree of clonal outgrowth to those of mature adult B-cells.

6.2 Assessment of Proliferation Rates and Cell Death in EBV and Blast Cultures

Growth Rates in EBV-Infected and Blast Cultures

Although the above results confirm that EBV-infected LCLs, but not mitogen-stimulated B-cell blast cultures, develop oligoclonality within a few weeks, it is possible that this difference may result from differences in growth rates between these 2 culture types, rather than a specific effect of EBV infection. Therefore, additional work was carried out to compare growth kinetics in the first few weeks for EBV-infected LCLs versus mitogen-stimulated B-cell blasts. For this, cell counts were determined with an automated cell counter, using trypan blue to identify dead cells. At each passage, identical numbers of cells were re-cultured, and

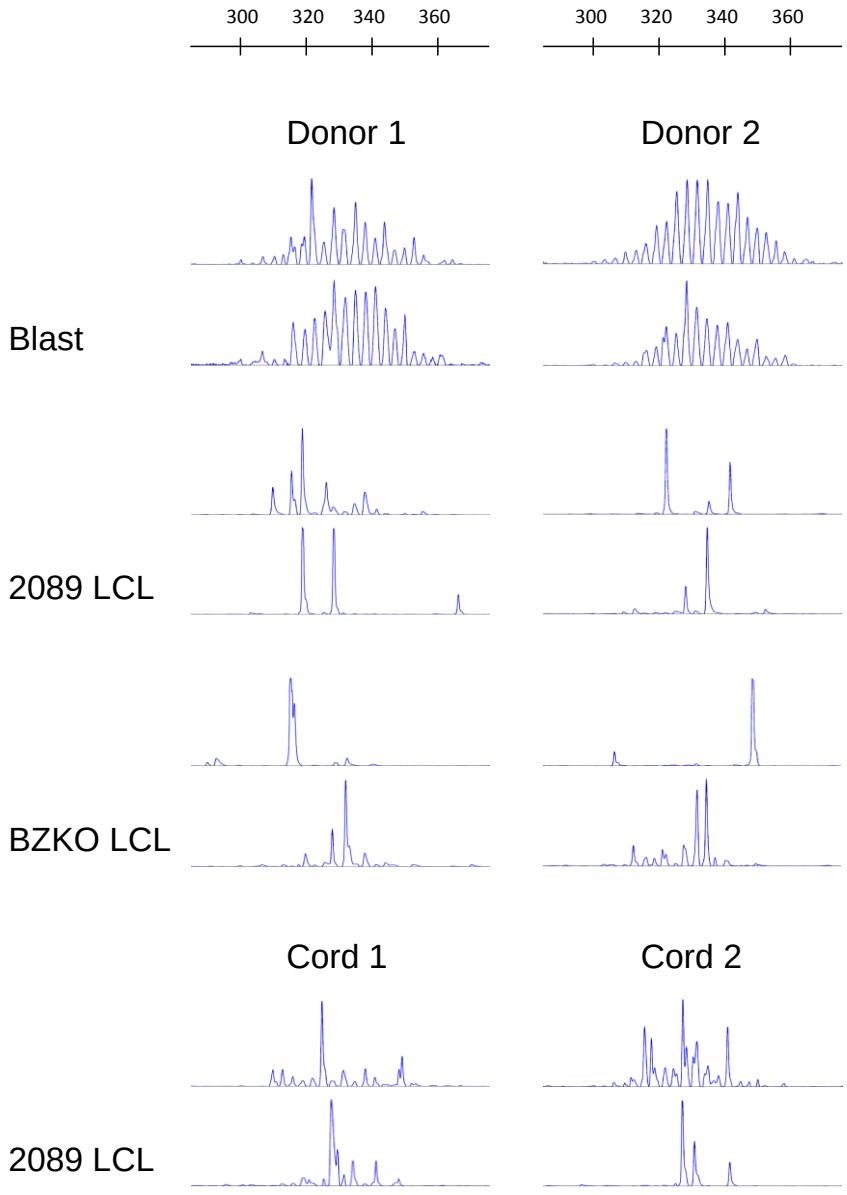

Figure 46. CDR3 Spectratype Analysis of Clonal Outgrowth in Different Cultures

B-cell blasts and LCLs infected with either 2089 or BZLF1-KO (BZKO) EBV strains were generated from total B-cells isolated from 2 adult donors. LCLs infected with 2089 EBV were also generated from umbilical cord blood B-cells from 2 donors. Duplicate cultures of each type were analysed with CDR3 spectratyping to determine clonality at the 8 week time point. All LCL cultures exhibited clonal outgrowth whereas the blasts remained polyclonal.

cell counts recorded at the following passage were used to calculate growth rates, according to the following equation:

$$N_T = N_0 \times e^{RT}$$

where N_T is the number of cells at time T, N_0 is the initial number of cells, and R is the growth rate (it should be noted this equation assumes exponential growth in these cultures).

As shown in Figure 47, after an initial lag period, LCLs were seen to exhibit a reasonably stable rate of proliferation. In contrast, following a lag period, the blasts exhibited a substantially increased rate of proliferation over the first 3 weeks, after which the rate decreased to a level similar to that found in the LCLs. Notably, cultures generated from different donors had differing overall growth rates, with those from donor 1 showing the fastest growth, demonstrating evidence of donor-dependent influences on proliferation. Similar patterns were observed in multiple other LCL and blast cultures generated during the course of this work (data not shown). In each case, the blast cultures were typically exhausted by around 8 weeks after initiation.

Cell Survival and Growth in Early EBV and Blast Cultures

Having compared growth rates in LCLs and mitogen-stimulated B-cell blast cultures over several weeks, we then sought to analyse cell survival and proliferation in the first few days. In the first instance, this was undertaken using flow cytometric FSC and SSC profiles to identify 3 informative subsets in early cultures: non-viable cells, viable non-blastoid cells and viable blastoid cells (Figure 48). By using a flow cytometer with the capacity to undertake

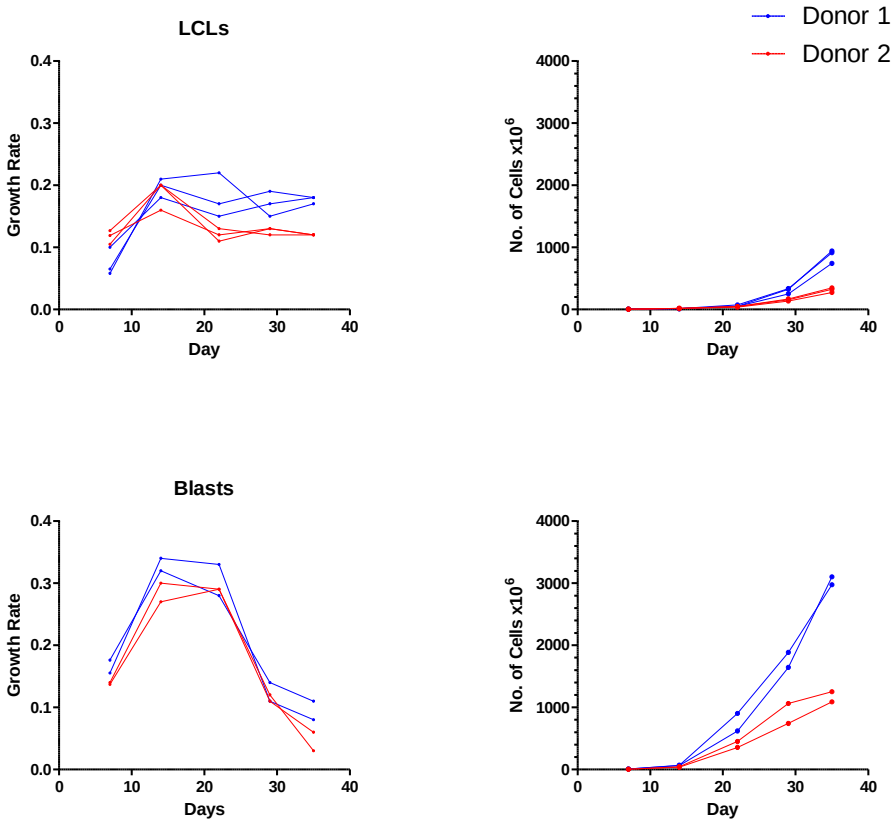

Figure 47. Growth Rates in LCLs and B-Cell Blasts

Growth rates (plots on the left) and projected cell numbers (plots on the right) were determined for LCLs and mitogen-stimulated B-cell blasts generated from total B-cells from 2 adult donors (3 LCL and 2 blast cultures from each). After an initial lag period, LCLs maintained a relatively stable growth rate. In contrast, the blasts exhibited a period of rapid growth before slowing. Resulting cell numbers were greater in the B-cell blast cultures than in LCLs.

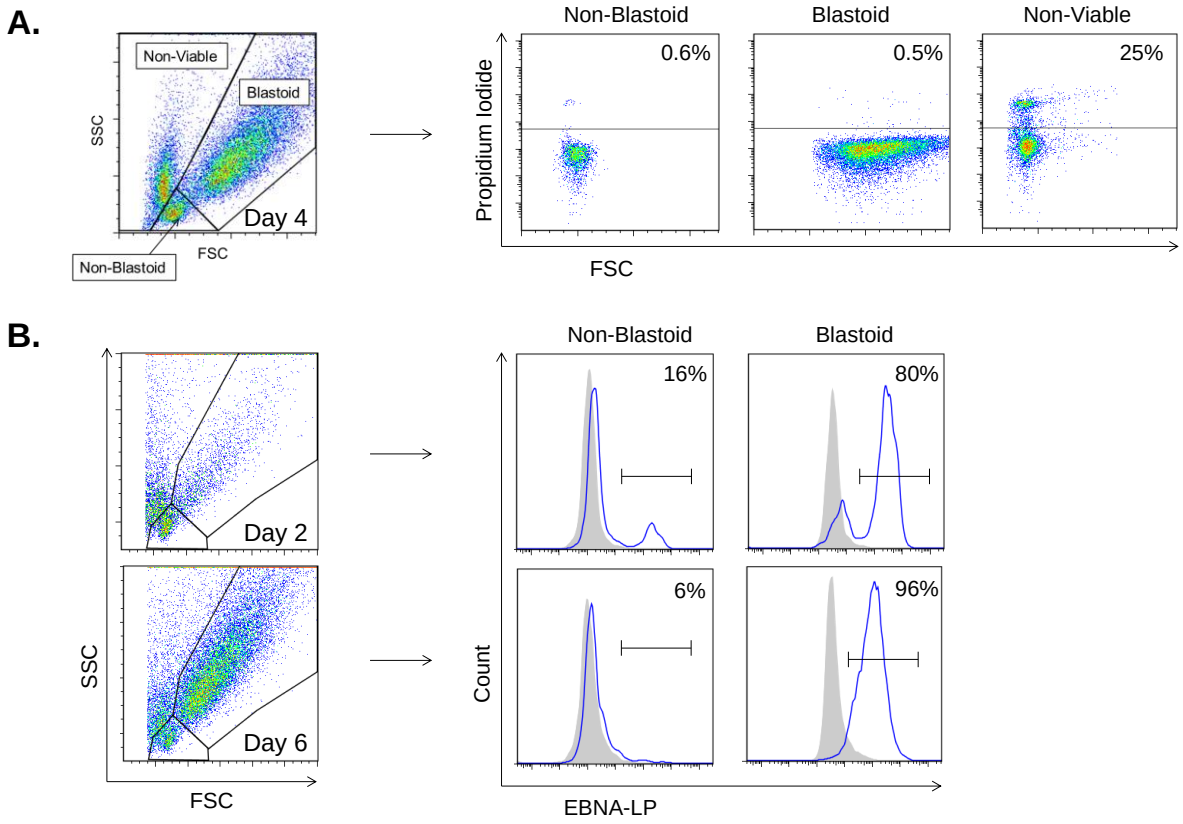

Figure 48. Gating to Identify Non-Viable, Non-Blastoid and Blastoid Cell Subsets

Flow cytometry was used to identify non-blastoid, blastoid and non-viable cell subsets in early EBV-infected cultures, on the basis of FSC and SSC profile. A. Propidium iodide staining on day 4 confirmed that non-blastoid and blastoid cells were almost all viable, whilst a high proportion of non-viable cells stained positive for this late marker of cell death. B. Day 2 and day 6 cultures were subjected to intracellular staining with an anti-EBNA-LP monoclonal antibody (blue histograms) or secondary only control (filled grey histograms). Blastoid cells were predominantly positive for EBNA-LP at both time points

precise volume measurements, it was also possible to generate absolute cell counts for these 3 subsets, by analysing aliquots of cell culture media without prior dilution or washing. Total cell counts were calculated by measuring the total volume of each culture.

The validity of this '3 subset' approach was firstly confirmed by showing that very few cells in the viable gates stained positive with propidium iodide, a marker of dead cells, whereas a significantly higher proportion of cells in the non-viable gate showed positive staining (Figure 48A). Secondly, intracellular staining for EBNA-LP, the earliest protein reliably detected after EBV-infection of B-cells, was used to show that almost all cells falling within the blastoid gate are indeed EBV-positive (Figure 48B).

Figure 49 illustrates data from a representative experiment in which this approach was used to compare changes in non-viable and viable subsets over the first few days in EBV-infected and B-cell blast cultures. Importantly, markedly different patterns of cell death and blastoid transformation were observed. Thus, whereas almost all cells occupied the non-blastoid gate in both cultures at day 0, by day 2 there was a striking increase in the proportion of non-viable cells in the EBV culture that was not apparent in the blast culture. Consistent with this, the proportion of cells occupying the blastoid gate was considerably higher in the blast culture until around day 6. Therefore, it appears that a high proportion of B-cells used to generate EBV cultures undergo cell death, whereas almost all cells used to generate a blast culture successfully undergo blastoid transformation.

Examination of absolute cell counts also revealed notable differences between the EBV-infected and B-cell blast cultures. Thus, Figure 50 shows comparison of viable (non-blastoid

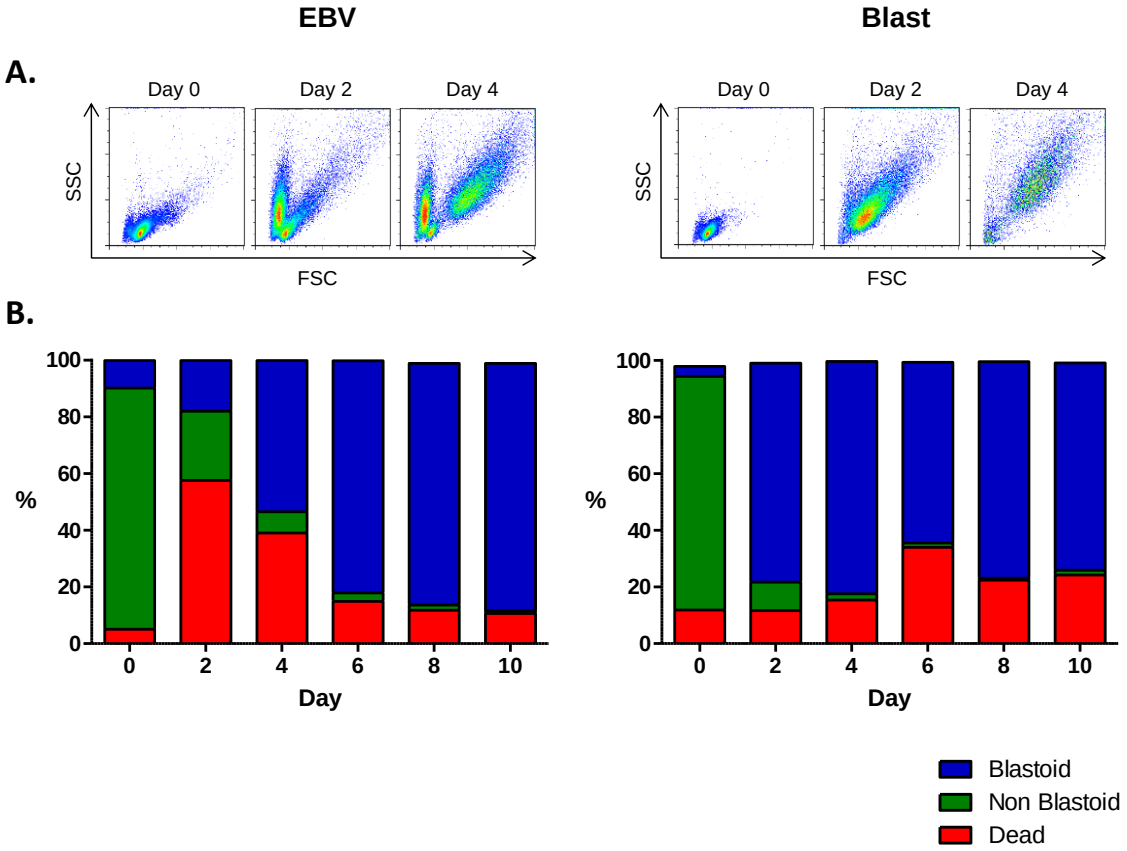

Figure 49. Non-Viable, Non-Blastoid and Blastoid Cell Subsets in Early Cultures

Flow cytometry was used to determine the proportion of non-viable, non-blastoid and blastoid cell subsets in EBV-infected and B-cell blast cultures. Data from a paired EBV-infected and B-cell blast culture is depicted, which is representative of several separate analyses. A. FSC and SSC plots for cultures on days 0, 2 and 4. B. Stacked columns summarise the proportions of the subsets on days 0 - 10. A marked increase in cell death was observed in day 2 EBV-infected cultures, which was not apparent in the B-cell blasts. The proportion of blastoid cells was very different at this time point. An increase in non-viable cells was also observed on day 6 in the blast culture; this is likely to reflect contamination from L-cell fibroblasts because the blast cells had been re-plated on the previous day.

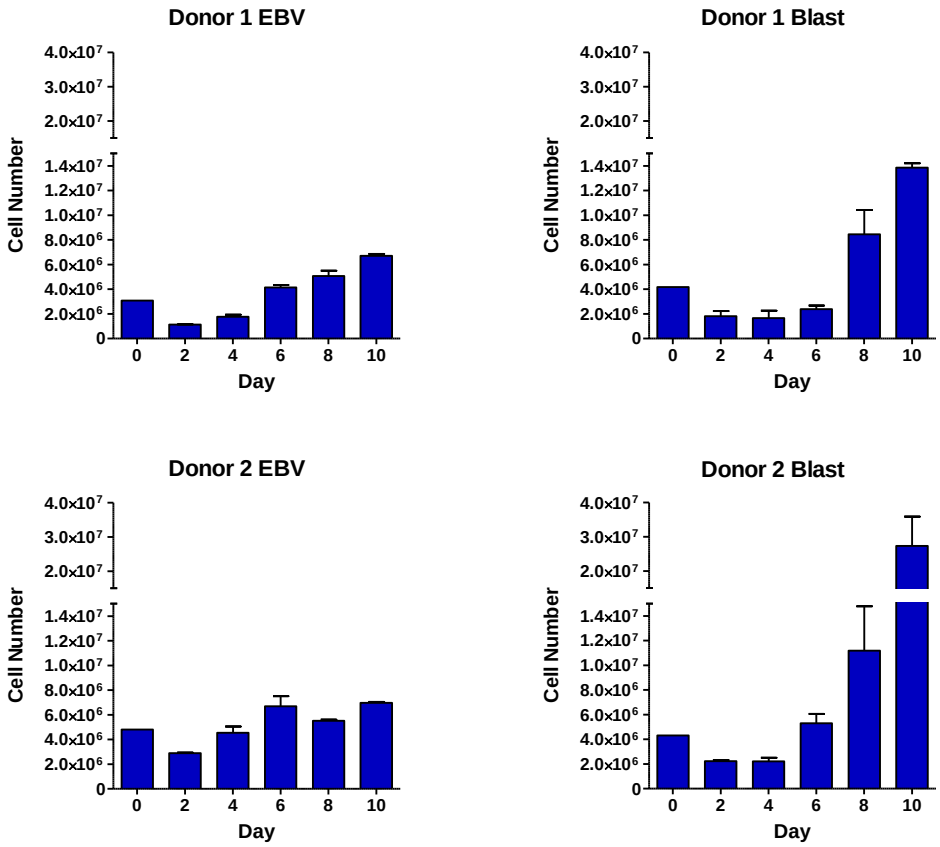

Figure 50. Cell Counts in EBV-Infected and B-Cell Blast Cultures

Cell counts for EBV-infected or mitogen-stimulated B-cell blast cultures generated from 2 adult donors were determined using flow cytometry over the first 10 days. Columns show the mean number of viable (non-blastoid + blastoid) cells from 2 independent counts per time point; error bars show standard deviation. Although an identical input cell number was used to generate the cultures, by day 10 the B-cell blast cultures contained a greater number of cells than the paired EBV-infected cultures.

+ blastoid) cell numbers for EBV-infected and mitogen-stimulated blast cultures generated from 2 donors. After 10 days the B-cell blast counts were much higher than those of the EBV culture. Together these results suggest key differences in early survival and proliferation between these cultures types that might be important for understanding clonal outgrowth.

Assessment of Proliferation Using CFSE Labelling

We went on to characterise proliferation in early EBV-infected and mitogen-stimulated B-cell blasts cultures using the fluorescent dye CFSE. CFSE-labelling allows cell division to be traced because each division leads to an approximately 50% reduction in fluorescent signal, which can be readily monitored by flow cytometry. Purified total B-cells were labelled with CFSE prior to establishing cultures, and daily flow cytometric measurements were performed.

Figure 51 shows CFSE plots for paired EBV-infected and mitogen-stimulated B-cell blast cultures generated from the same donor, representative of several experiments. Visual inspection of these data suggested that EBV cultures exhibit shorter times to initial proliferation and possibly more rapid proliferation rates compared to B-cell blasts. However, given that visual inspection of CFSE profiles can be misleading[556], we went on to analyse 4 paired EBV and blast cultures in more detail. To do so, we first used the FlowJo Proliferation Tool methodology for analysing CFSE data. This calculates a Proliferation Index (PI) i.e. the average number of divisions undergone by cells that have divided at least once[555,556] (Figure 52). Using this method, EBV-infected cells appear to divide earlier than B-cell blasts, which exhibit a more notable lag period (Figure 53A). However, both cultures exhibit relatively linear expansion at similar rates once division has commenced.

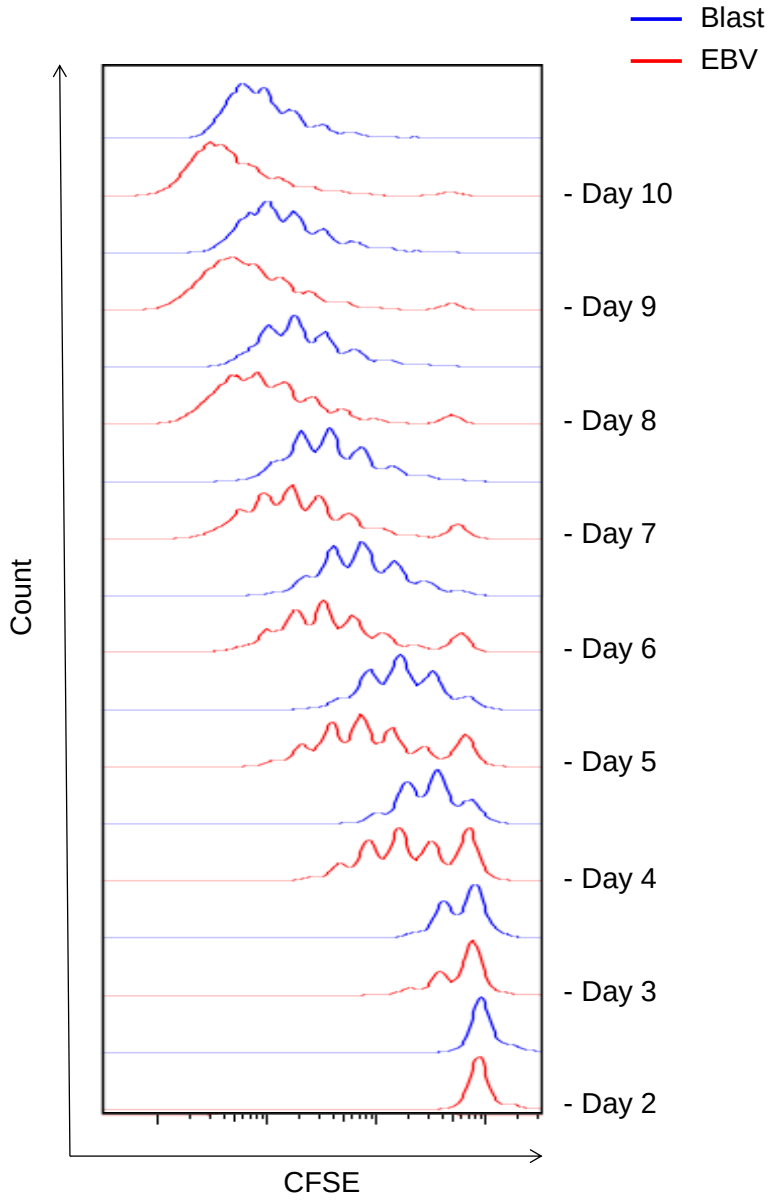

Figure 51. CFSE Proliferation Profiles in EBV-Infected and B-Cell Blast Cultures

To analyse proliferation in early cultures, B-cells stained with the fluorescent dye CFSE were used to establish EBV-infected or B-cell blast cultures, which were then analysed daily using flow cytometry. As each CFSE-labelled cell divides, the fluorescent signal is reduced by approximately 50%, so each new peak to the left corresponds to a single division. Here, the EBV-infected culture appears to be proliferating more quickly than the paired B-cell blast.

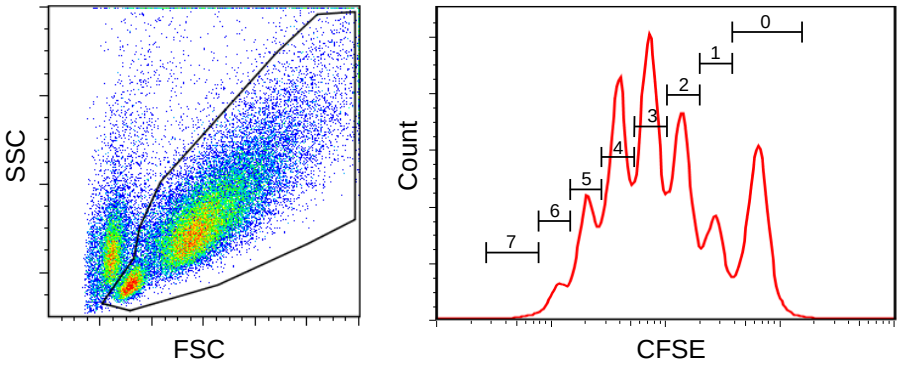

Generation (i)	Events	Precursors = Events / 2^i	Divisions = Precursors x i
0	4817	4817.0	0.0
1	2579	1289.5	1289.5
2	5146	1286.5	2573.0
3	6802	850.3	2550.9
4	5769	360.6	1442.4
5	2780	86.9	434.5
6	811	12.7	76.2
7	107	0.8	5.6
		Total = 8704.3	**Total = 8372.1**

Dividing cells = Total precursors – undivided cells

= 8704.3 – 4817.0

= 3887.3

Proliferation index = Total divisions / dividing cells

= 8372.1 / 3887.3

= **2.15**

Figure 52 Analysis of CFSE Data: FlowJo Method

CFSE-labelled cultures were analysed with flow cytometry to determine the number of cells in each generation, as exemplified here by analysis of a day 5 EBV-infected culture. Thereafter, data were analysed using the FlowJo (TreeStar) Proliferation Tool method. Thus, cell number in each generation was used to estimate precursor frequency, e.g. 64 cells in generation 6 correspond to 1 precursor cell. 'Proliferation Index' was then calculated as a measure of the average number of divisions for responding cells i.e. cells which have undergone at least 1 division.

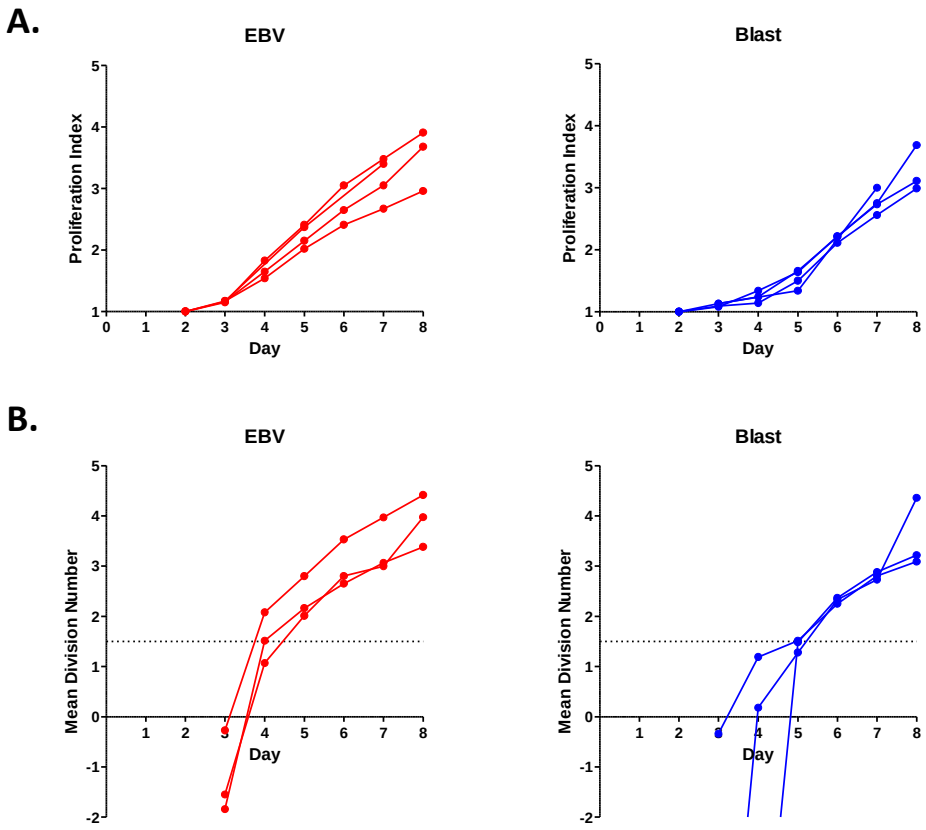

Figure 53. CFSE Proliferation Data for EBV-Infected and B-Cell Blast Cultures

EBV-infected and B-cell blast cultures, established in parallel from CFSE-labelled total B-cells from 4 adult donors, were used to generate proliferation data which were analysed using 2 alternative methods. A. 'Proliferation index' was calculated using the FlowJo Proliferation Tool method. B. 'Mean division number' was calculated using the method of Hawkins et al.; results with a mean division number lower than 1.5 (dotted line) are considered unreliable according to the authors of this method.

In light of these data, we conclude that the reason B-cell blast numbers are greater than EBV-infected cells after 7-10 days is not because B-cell blasts proliferate more rapidly. Instead, it is likely to be a consequence of higher death rates amongst B-cells used to generate EBV-infected cultures, whereas a higher proportion of cells are successfully transformed in B-cell blast cultures.

Hyperproliferation: An Artefact of CFSE Data Analysis?

We were surprised by our finding that EBV cultures exhibit linear expansion once they enter division (Figure 53A) because Nikitin et al. have reported that EBV-infected cultures exhibit a period of hyperproliferation around 3 to 5 days after infection[158], but this was not apparent from our analysis. Given this discrepancy, we decided to reanalyse our CFSE data using the same method employed by Nikitin et al.[557] This approach, developed by Hawkins et al., is a modification of previous methods which determines 'Mean Division Number', by fitting the number of cells in each cell division to a Gaussian distribution[557] (Figure 54). This new analysis (Figure 53B) now revealed a period of apparent hyperproliferation for the EBV-infected cultures, similar to that reported by Nikitin et al. However, it is our opinion that this data should be treated with a great deal of caution because, as stated by Hawkins et al., data points with a mean division number less than 1.5 should be regarded as unreliable[557].

Comparison of Clonal Outgrowth with Alternative Culture Conditions

Given our results demonstrating different patterns of proliferation and cell survival in EBV-infected and B-cell blast cultures, we hypothesised that differences observed in clonal outgrowth might be related to either the feeder layer used to support the blasts cells, or CD40L/IL4 signals provided by them. In order to test this, we undertook an experiment to

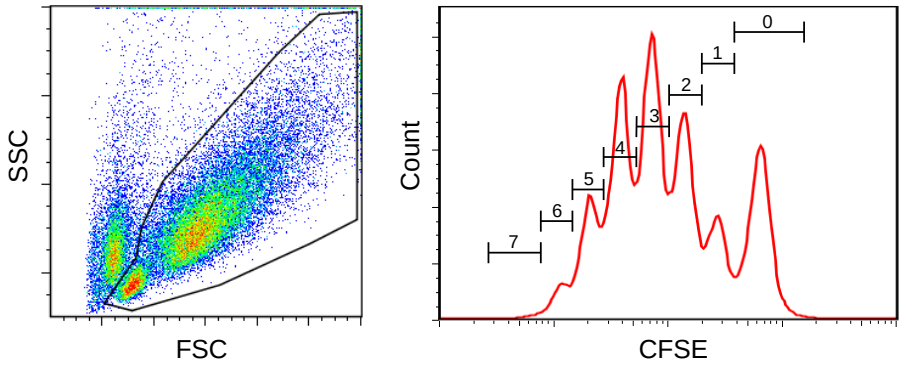

Generation (i)	Events	Precursors = Events / $2^{i+0.5}$
0	4817	3406.1
1	2579	911.8
2	5146	909.7
3	6802	601.2
4	5769	255.0
5	2780	61.4
6	811	9.0
7	107	0.6

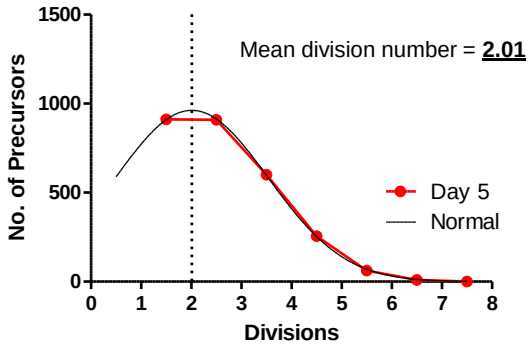

Figure 54. Analysis of CFSE Data: The Hawkins Method

CFSE data were also analysed according to the method proposed by Hawkins et al557, as exemplified here using the same data as in Figure 52. Thus, the number of cells in each generation was used to estimate precursor cell frequency, using i+0.5 in the equation to account for cells that have entered cell cycle but which are yet to divide. Thereafter, division number was plotted against the number of precursors for generations ≥1, and 'Mean Division Number' was estimated by fitting a normal distribution using Prism 5 software (Graphpad).

determine clonal outgrowth in EBV-infected B-cell cultures maintained on irradiated mouse fibroblast L-cells transfected with CD40L and supplemented with IL4 added, or control irradiated mouse fibroblasts lacking CD40L in the absence of IL4; as a comparator, EBV-infected cells were also grown in normal media as before. Again, samples harvested at the 8 week time point were analysed using IgH CDR3 spectratyping. However, this only revealed a similar degree of oligoclonality for each of the cultures (data not shown). This suggests that feeder layer support and/or CD40L/IL4 signalling probably does not play a significant role in determining clonal outgrowth.

In conclusion, although we have demonstrated marked differences in proliferation rates and cell survival between EBV-infected and mitogen-stimulated B-cell blast cultures, we have been unable to demonstrate whether these factors contribute to differences observed in clonal outgrowth.

6.3 Assessment of Genomic Instability in Early EBV and Blast Cultures

Having characterised proliferation and cell survival in early EBV-infected and B-cell blast cultures, work was then undertaken to explore the role of genomic instability and DNA damage response signalling in clonal outgrowth. As discussed previously, Nikitin et al. have shown that EBV-infection leads to a period of genomic instability, maximal between days 3 and 7 post-infection[158], as evidenced by the accumulation of phospho-H2AX (a marker of double-stranded DNA breaks which is thought to trigger ATM/Chk2-mediated DNA damage response signalling). However, it is notable that in this study cultures were generated by infecting PBMCs rather than purified B-cells, and furthermore no comparison was made with mitogen-stimulated B-cell blasts.

Initially, Western blotting was used to analyse DNA damage response signalling in early EBV-infected B-cell cultures (data not shown). However, it rapidly became apparent that this strategy was inappropriate as a method to compare DNA damage responses in EBV-infected versus B-cell blast cultures. This is because the proportion of non-viable, non-blastoid and blastoid cells are substantially different between these cultures, as previously shown in Figure 49. Furthermore, blasts are maintained on an irradiated fibroblast layer which express high levels of DNA damage-induced proteins and which often contaminate harvested B-cell blasts.

Given the limitations of Western blotting, we instead elected to measure genomic instability using intracellular flow cytometry to stain for phospo-H2AX. Thus, previous studies have demonstrated that flow cytometry is a robust and quantitative method for measuring phospho-H2AX[603-607]. Furthermore, and of crucial importance to the current application, this technique has the advantage of facilitating measurement of phospho-H2AX levels specifically within the viable blastoid cell population. The intracellular phospho-H2AX staining technique was first validated by analysing an established LCL which had been irradiated with 0 – 16 Gray (Figure 55). Plotting radiation dose against median fluorescence intensity (MFI) for phospho-H2AX staining revealed an excellent dose-response curve, and confirmed the specificity of the phospho-H2AX antibody.

Having validated the phopho-H2AX assay, EBV-infected B-cells harvested between 0 and 12 days after infection were analysed (Figure 56 shows data representative of 2 separate experiments). Importantly, this showed that the MFI of phospho-H2AX staining was never above that of a control LCL irradiated with 1 Gray. Furthermore, phospho-H2AX levels were similar to those detected in 3 established LCLs included as controls. Whilst there was a small

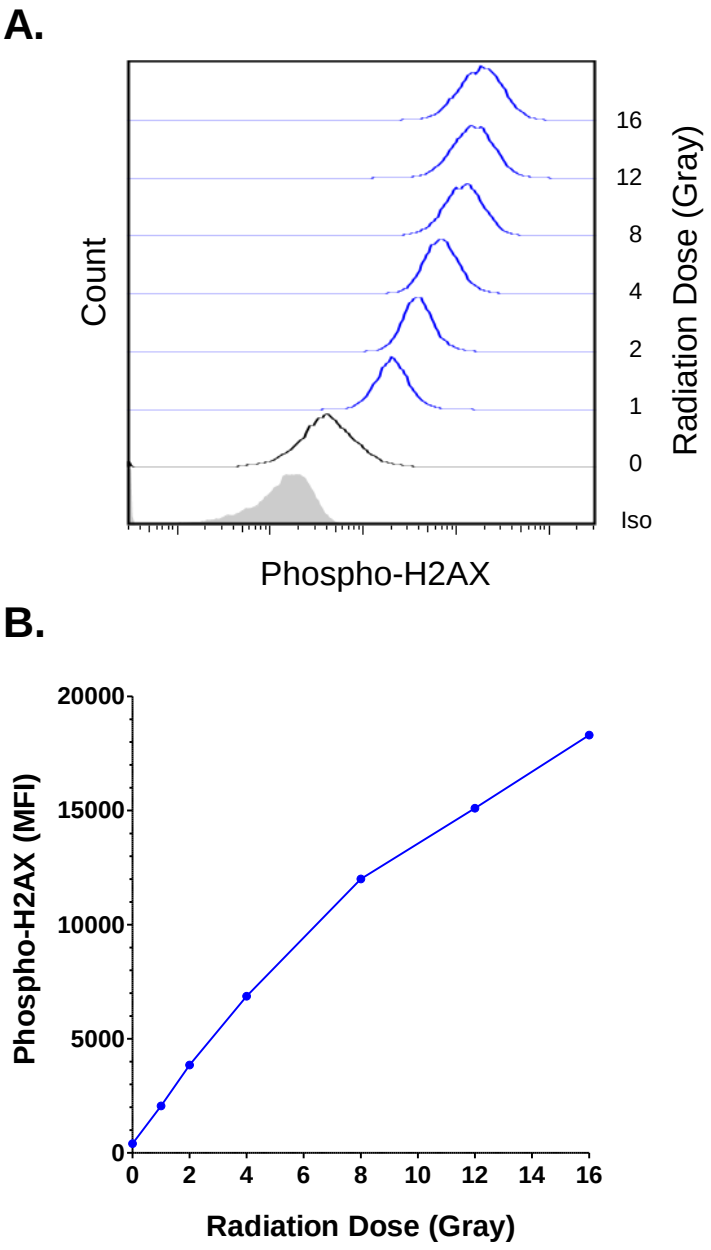

Figure 55. Intracellular Flow Cytometry for Phospho-H2AX

Intracellular flow cytometry was used to quantify levels of phospho-H2AX as a measure of genomic instability. To validate the assay, an established LCL was mock-irradiated or irradiated with 1 - 16 Gray, incubated for 1 hour and then fixed before being stained. A. Histograms for an LCL stained with anti-phospho-H2AX antibody or isotype control (filled grey histogram). B. Plot of radiation dose against phospho-H2AX median fluorescence intensity (MFI). An excellent dose-response curve was observed.

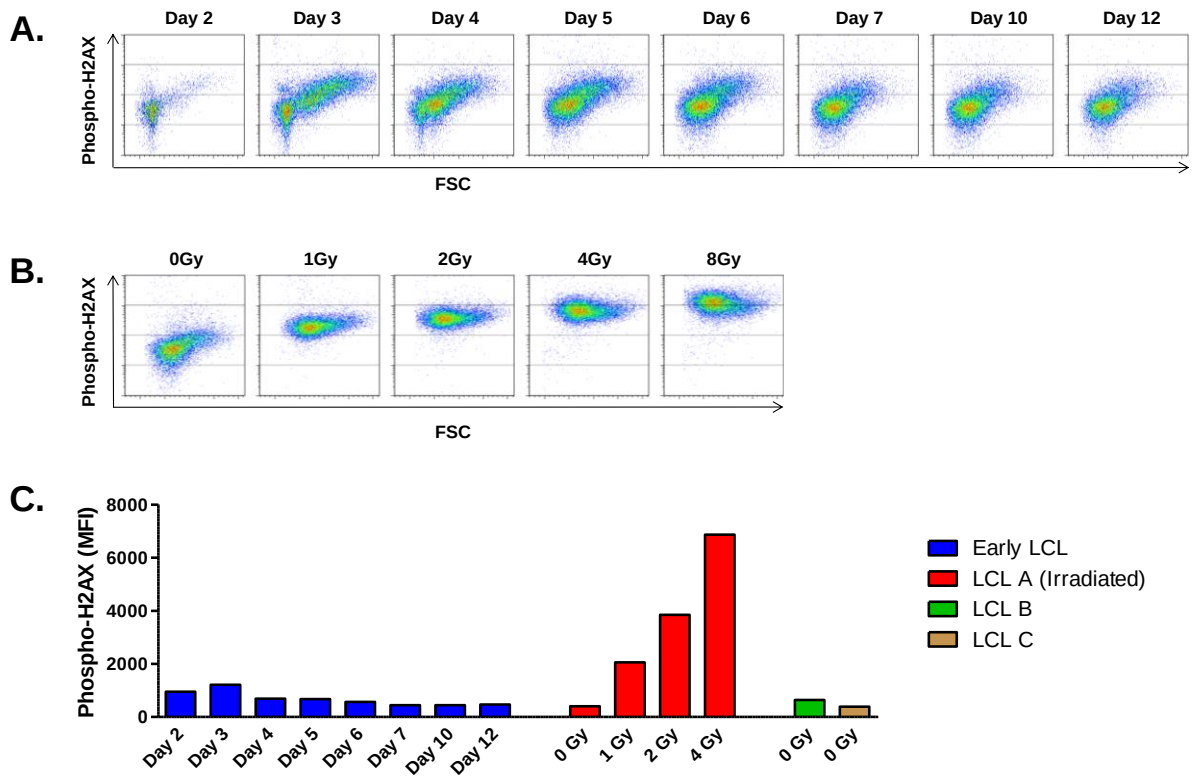

Figure 56. Analysis of Phospho-H2AX in Early EBV-Infected B-Cells

Phospho-H2AX levels were analysed in early EBV-infected B-cell cultures using intracellular flow cytometry. A. Plots showing phospho-H2AX staining versus FSC for a culture harvested on days 2 – 12. All plots display events after exclusion of dead cells and doublets. B. Plots for an established LCL irradiated with 0 – 8 Gray and harvested after 1 hour. C. Summary of phospho-H2AX MFI data for the early EBV-infected culture, the irradiated LCL and 2 other established LCLs (non-irradiated).

increase in signal for some cells around 3 - 4 days after infection, this was probably artefactual due to a co-incident increase in cell size at this time. Consequently, we found little evidence to support the occurrence of a prominent period of DNA damage response signalling after EBV infection. Thereafter, a direct comparison of phospho-H2AX staining in EBV-infected cells and mitogen-stimulated B-cell blasts was undertaken (analysing B-cells that had been pre-labelled with a proliferation marker similar to CFSE). This showed that B-cell blasts contain at least as much phospho-H2AX as EBV-infected B-cells (Figure 57 shows staining representative of at least 3 separate experiments). In light of this, we conclude that there appears to be little difference in the degree of genomic instability present in early EBV-infected and B-cells blast cultures. Consequently, this places doubt on the likelihood that early DNA damage signalling events are responsible for observed differences in clonal outgrowth.

6.4 Evaluation of AID-Associated Mutations in LCLs

We were also interested in the possibility that 'off-target' AID-induced mutations might influence the clonal outgrowth of LCLs. Notably, Epeldegui et al. have previously reported that EBV-infection leads to the accrual of AID-induced mutations in the genes BCL6 and p53[244]. However, it remains uncertain to what extent these off-target mutations are *de novo* events, or whether they represent pre-existing mutations which are selected during the course of clonal outgrowth.

To address these issues, we elected to analyse BCL6 and p53 sequences in LCLs generated from alterative cell types. Thus, LCLs were generated from $CD19^+$ B-cells isolated from a healthy adult donor (Total LCL), as well as $CD27^-IgD^+$ naive B-cells isolated from a healthy

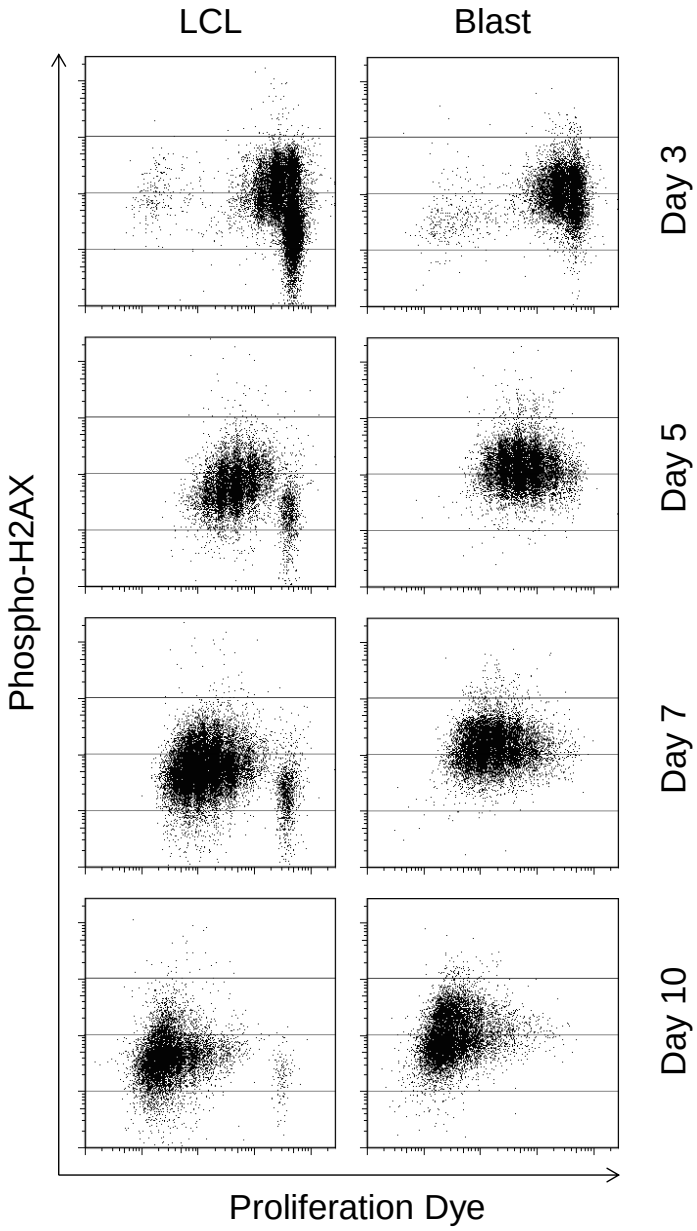

Figure 57. Comparison of Phospho-H2AX in EBV-Infected and B-Cell Blast Cultures

Phospho-H2AX levels were simultaneously analysed in EBV-infected and B-cell blast cultures harvested on days 3, 5, 7 and 10 using intracellular flow cytometry. B-cells used to generate the cultures were stained with a violet proliferation dye (similar to CFSE) and dead cells, contaminating L-cells and doublets were excluded from the displayed plots. Levels of phospho-H2AX observed in the B-cell blast were similar to, or higher than, those seen in the EBV-infected culture.

adult donor (Naive LCL) and $CD19^+$ B-cells from an umbilical cord donor (Cord LCL). The Total LCL was analysed to assess reproducibility of the observation that mutations progressively accumulate in LCLs. Meanwhile, the Naive and Cord LCLs were included as important controls; given that naive and umbilical cord blood B-cells are antigen-inexperienced cells that do not possess AID-induced mutations, we can infer that any mutations detected in these LCLs are likely to be the result of *de novo* mutation events.

All cultures were generated by infecting isolated B-cells with wild type 2089 EBV. Samples were collected at intervals following infection and DNA extracted from these was analysed by cloning and Sanger sequencing. The PCR primers used for BCL6 and p53 genes were identical to those employed by Epeldegui et al.[244] These amplified a 5' noncoding region of the BCL6 gene, and a coding region of p53. These regions had originally been selected as they have been found to be mutated in NHL[52,608]. Importantly, PCRs were performed using a high-fidelity DNA polymerase with a proofreading capability, in order to minimise the PCR error rate. For each time point, a total of 10 BCL6 and 10 p53 sequences were cloned and sequenced, and the results were analysed to determine the proportion of mutated sequences and the total number of mutations.

As summarised in Figure 58, analysis of BCL6 sequences revealed progressive accumulation of mutations in both the Total LCL and the Naive LCL, but not in the Cord LCL. At baseline, the Total LCL revealed 3 mutations (in 2 sequences), in keeping with the presence of memory B-cells carrying pre-existing BCL6 mutations in this sample. Unfortunately a baseline sample for the Naive LCL was not available but we expect this would not have exhibited any mutations. Meanwhile, no mutations were observed at baseline for the Cord LCL, as

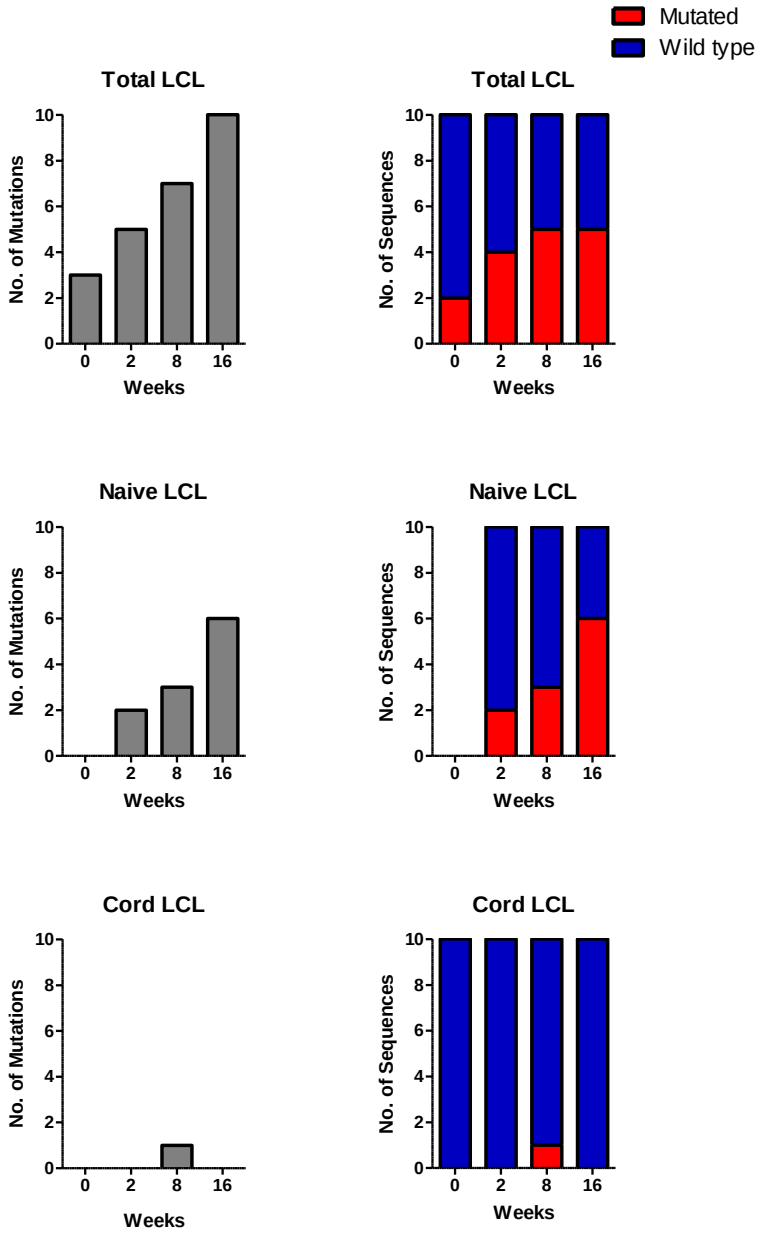

Figure 58. BCL6 Mutations in LCLs

BCL6 sequences were analysed at 0, 2, 8 and 16 week time points in LCLs generated from adult total B-cells, adult naive B-cells or umbilical cord B-cells. 10 sequences were analysed for each time point. The number of mutations (plots on the left) and the number of mutated sequences (plots on the right) at each time point are displayed. Progressive accumulation of mutations was noted in the total B-cell and naive B-cell LCLs but not the cord LCL.

expected. By 16 weeks, the Total LCL had accumulated 10 mutations (in 5 sequences). Interestingly, the Naive LCL had also accumulated 6 mutations (in 6 sequences) by this time. In contrast, the Cord LCL exhibited only 1 mutation, apparent at the 8 week time point. Subsequent inspection of the individual BCL6 mutations revealed additional information. As such, whilst most BCL6 mutations in the Total LCL were non-recurring, in the 16 week sample identical mutations were noted for 2 sequences, and these matched a third sequence from the 8 week time point (Table 23). A similar pattern was observed for the Naive LCL, in that 3 sequences contained identical mutations at the 16 week time point, with 1 matching sequence identified at 8 weeks (Table 24).

Figure 59 shows data for the corresponding p53 sequences. Notably, this revealed a markedly different pattern to that observed for the BCL6 sequences, with a lower number of mutations generally and, more importantly, no accumulation of mutations. However, single mutations were noted in the Cord LCL at 2, 8 and 16 week time points.

6.5 Discussion

Our group has previously reported that EBV-infected B-cell cultures derived from isolated $CD27^{-}IgD^{+}$ naive B-cells develop oligo- and mono-clonality within a few weeks of infection, a result not seen with naive B-cell blasts generated by CD40L/IL4 stimulation. Interestingly, the clones which dominate these naive LCL cultures are often found to carry mutated Ig sequences, indicating that EBV may induce SHM *in vitro*. While it is difficult to envisage a scenario in which a mutated Ig gene might confer a growth advantage *in vitro*, it was hypothesised that off-target effects of AID might generate a pool of precursors carrying cellular mutations from which the fittest clone would emerge. However AID activity might

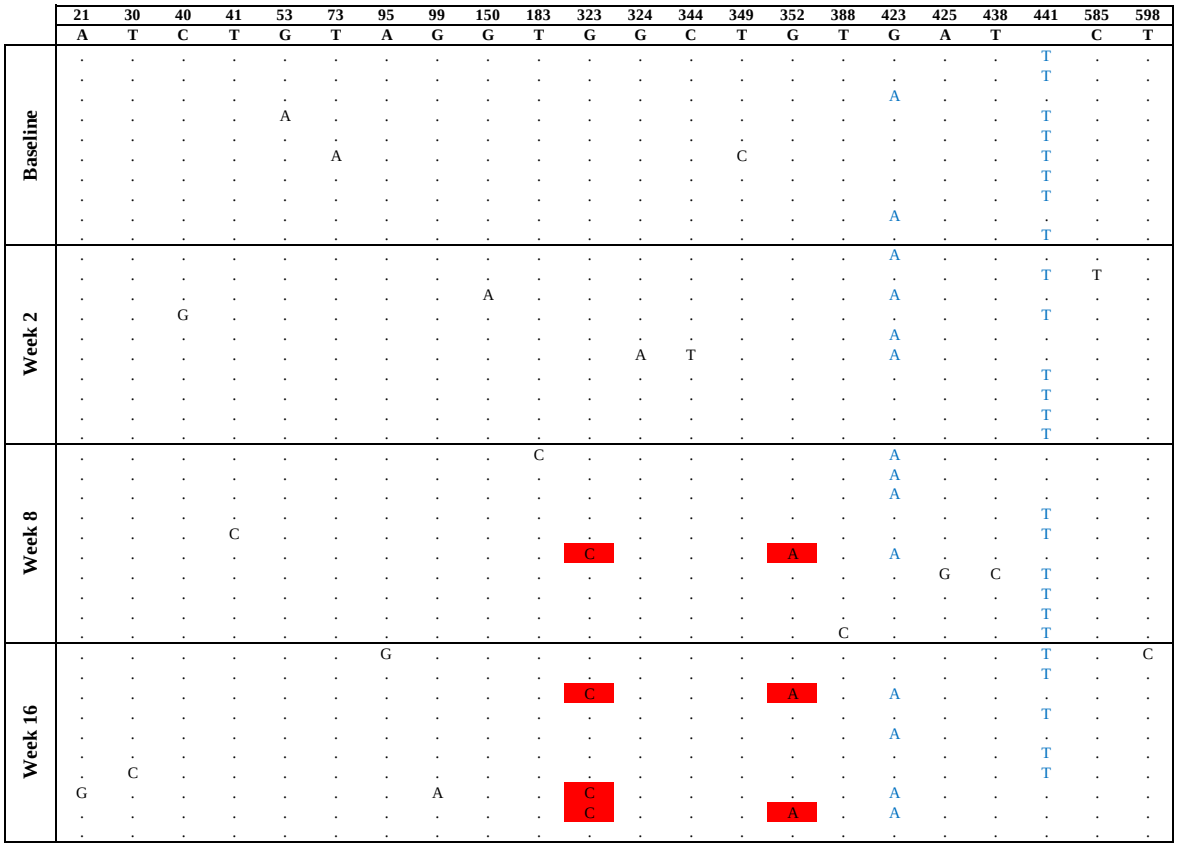

Table 23. BCL6 Mutations in the Total LCL

BCL6 sequences from an LCL generated from total adult B-cells, harvested at 0, 2, 8 and 16 week time points are aligned (10 sequences per sample). Mutations are shown in comparison to a reference BCL6 sequence. Recurring mutations are apparent at positions 323 and 352 (highlighted in red) for 8 and 16 week time points, consistent with emergence of clonality in the LCL culture. Notably, 2 mutually exclusive polymorphisms (blue colour font) previously described in dbSNP database were observed at positions 423 (G to A; rs114991887) and 441 (T insertion; rs3832246) for which this donor is heterozygous. Changes at these positions were not included in the analysis but they indicate that sequence data was successfully obtained from both alleles.

	11	29	119	224	418	441	462	482	577
	A	A	T	G	C		T	T	A
Week 2	.	.	.	.	.	T	.	.	.
	.	.	.	.	.	T	.	.	.
	.	.	.	.	.	T	.	.	G
	.	.	.	.	.	T	.	.	.
	.	.	.	.	.	T	.	.	.
	.	.	.	.	.	T	.	C	.
	.	.	.	.	.	T	.	.	.
	.	.	.	.	.	T	.	.	.
	.	.	.	.	.	T	.	.	.
	.	.	.	.	.	T	.	.	.
Week 8	.	.	.	.	.	T	.	.	.
	.	.	.	.	.	T	.	.	.
	.	.	.	.	.	T	.	.	.
	.	.	.	.	.	T	.	.	.
	.	.	.	.	.	T	.	.	.
	.	.	.	.	.	T	.	.	.
	C	.	.	.	.	T	.	.	.
	.	G	.	.	.	T	.	.	.
	.	.	.	.	.	T	C	.	.
	.	.	.	.	.	T	.	.	.
Week 16	.	.	.	.	.	T	.	.	.
	.	.	.	.	.	T	.	.	.
	.	.	.	.	T	T	.	.	.
	C	.	.	.	.	T	.	.	.
	.	.	.	.	.	T	.	.	.
	C	.	.	.	.	T	.	.	.
	.	.	.	A	.	T	.	.	.
	.	.	C	.	.	T	.	.	.
	.	.	.	.	.	T	.	.	.
	C	.	.	.	.	T	.	.	.

Table 24. BCL6 Mutations in the Naive LCL

BCL6 sequences from an LCL generated from naive adult B-cells, harvested at 2, 8 and 16 week time points are aligned (10 sequences per sample). Mutations are shown in comparison to a reference BCL6 sequence. A known polymorphism (blue font) is observed at position 441 (T insertion; rs3832246), for which this donor is homozygous; changes at this position were not included in the analysis. Recurring mutations are apparent at position 11 (highlighted in red) for 8 and 16 week time points, consistent with emergence of clonality in the LCL culture.

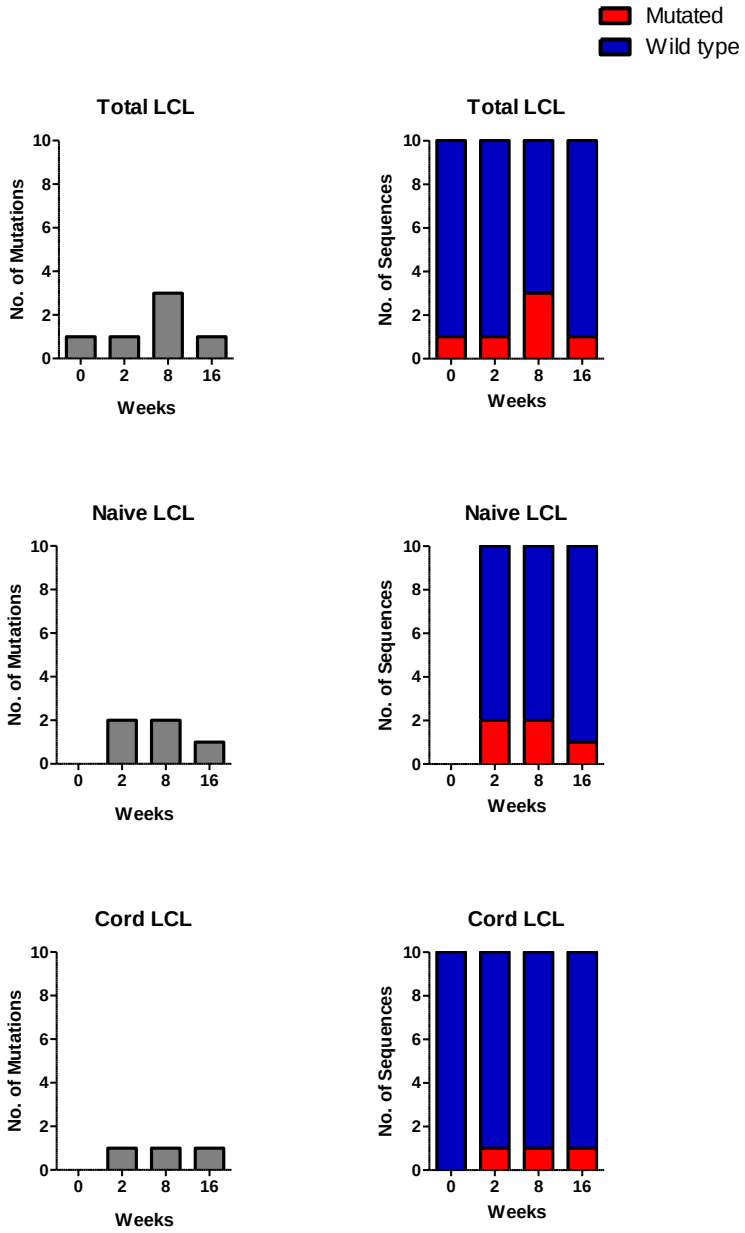

Figure 59. p53 Mutations in LCLs

p53 sequences were analysed at 0, 2, 8 and 16 week time points in LCLs generated from adult total B-cells, adult naive B-cells or umbilical cord B-cells. 10 sequences were analysed for each time point. The number of mutations (plots on the left) and the number of mutated sequences (plots on the right) at each time point are displayed. Progressive accumulation of mutations was not observed in any of the cultures.

not be sufficient for this observed clonal evolution in LCL cultures, since mitogen stimulation also induces AID expression yet does not cause Ig gene mutation or clonal outgrowth. This raises the possibility that other mechanisms might drive the emergence of clonality in LCLs but not B-cell blasts. Given this, experiments in this chapter were primarily designed to investigate differences between EBV-infected B-cells and mitogen-stimulated B-cell blasts that might determine their alternative patterns of clonal outgrowth.

Patterns of Clonal Outgrowth

We first showed that LCLs generated from total and FACS-sorted naive adult B-cells exhibit clonal outgrowth within a few weeks of infection, whereas B-cell blasts remain polyclonal. These findings confirm our group's previous data demonstrating clonal emergence in naive LCLs[236], and are consistent with earlier reports which have analysed clonality in LCLs established from total B-cells. Thus, Ryan et al. used CDR3 spectratyping to show that LCLs generated from 5 adult donors developed monoclonality by around 8 weeks [238], whereas Plagnol et al. made similar observations using X chromosome inactivation as a measure of clonality[239]. Lacoste et al. subsequently demonstrated the acquisition of clonality in LCLs using karyotyping[237].

We extended our understanding by showing that LCLs generated from umbilical cord blood B-cells also exhibit clonal outgrowth. This result is important because preliminary data had suggested that umbilical cord LCLs might remain polyclonal in culture. Given that our group has also previously shown that umbilical cord LCLs rarely acquire AID-associated Ig gene mutations, we speculated that this might be linked to the preservation of polyclonality within these cultures. Therefore, our current findings that umbilical cord LCLs *do* develop clonality,

provides evidence that clonal outgrowth is not necessarily related to the occurrence of AID-induced Ig gene mutation.

We also assessed the effect on clonal outgrowth of a BZLF1 defective strain of EBV. This was performed since EBV lytic cycle gene expression has been demonstrated as a potentially important influence in the pathogenesis of PTLD[445-448]. Thus lytic gene expression is often found within PTLD tumours, and BZLF1 KO LCLs show impaired growth when transplanted into SCID mice[445], an effect that may result, at least in part, by up-regulation of paracrine factors such as IL6 in response to IE lytic gene expression[445,446]. Lytic cycle gene expression has also been associated with increased DNA damage response signalling; it is also at least conceivable that low level lytic cycle gene expression might contribute to clonality if it were to trigger the generation of mutations in cells that subsequently revert to latent infection. However, our results for BZLF1 KO LCLs were indistinguishable from those generated using the wild type 2089 strain of EBV. This indicates that lytic cycle gene expression probably does not have a significant effect on clonal outgrowth.

It should be noted that in undertaking these studies, we employed IgH CDR3 spectratyping as the principal method to assess clonal outgrowth. This technique is advantageous compared to the previously employed ‘clone and sequence’ approach because it simultaneously samples all available IgVH loci, and it is also much less labour intensive. However, the technique also has significant limitations. Thus, it is important to acknowledge that it is a qualitative rather than quantitative measure of clonality. Indeed, several groups have attempted to derive quantitative data from spectratypes using a variety of algorithms, but Euroclonality Guidelines state these are unreliable and that the assay should be regarded more as a 'molecular morphological

assay'[602]. Therefore, the technique may be unable to detect more subtle differences in clonality. Our validation of the assay also revealed that it is possible for a single spectratype peak to contain more than 1 clone, due to clones that by chance exhibiting CDR3 amplicons of identical length. Furthermore, unlike the conventional 'clone and sequence' approach, it does not provide information on individual CDR3 sequences and thus cannot be used to detect IgVH mutations. These limitations mean that, in retrospect, IgH CDR3 spectratyping may not have been best suited to the current experiments.

Differences in Cell Proliferation and Survival

A series of investigations were also undertaken to explore how differences in proliferation and cell survival might explain the contrasting patterns of clonal outgrowth observed in LCL and B-cell blast cultures. Thus, comparison of growth rates in the first 6 weeks revealed that LCLs exhibit a relatively stable growth rate after an initial lag period. In contrast, B-cell blast cultures showed a brisk growth rate for the first 3 - 4 weeks before slowing considerably, consistent with previous studies[32]. Despite these differences in growth kinetics, estimated total cell counts showed that B-cell blasts had undergone at least as many cell divisions as the LCLs over these first weeks when clonality emerges. We therefore conclude that the alternative patterns of clonality do not simply reflect differences in the overall degree of proliferation between cultures.

Analysis of events in the first few days of culture revealed other potentially important differences between EBV-infected and B-cell blast cultures. In particular, the proportion of B-cells activated to a blastoid state was found to differ substantially between them. Thus, in B-cell blast cultures almost all cells were successfully activated to became blastoid, whereas in

EBV-infected cultures a high proportion of cells appeared to die rather than become blastoid (Figure 49). As a consequence B-cell blasts were found to be numerically superior after 10 days of culture, despite evidence of a longer delay before the first cell division provided by analysis of CFSE data (FlowJo methodology).

Interestingly, others have already observed relatively high rates of cell death following EBV-infection of B-cells[609], although this finding has not been emphasised in the literature. Why this occurs is not clear, but we speculate that some cells may apoptose because they fail to be infected, or because they are infected by a defective virus that fails to initiate transcription, or even because they do not enter cell cycle despite EBNA-LP or EBNA2 expression; however, the latter theory is contrary to evidence that successful B-cell infection almost always leads to cell cycle entry[228]. In contrast, B-cell blasts may show superior blastoid activation thanks to the CD40L expressing fibroblast layer on which they are grown, as well as the presence of soluble IL4. These factors may provide an environment that efficiently maintains cell survival and promotes activation such that almost all input B-cells become blastoid.

In light of these results we hypothesised that clonal emergence might be favoured in LCLs, either because the number of infected cells is reduced by the amount of early cell death, or because the feeder layer and/or IL4 might deliver signals throughout the life of a B-cell blast culture that ameliorate the processes that drive clonal selection in LCLs. However, when these possibilities were tested by culturing LCLs on feeder layers, with or without CD40L stimulation and supplementary IL4, they were found to exhibit clonal emergence just as normal.

Hyperproliferation and Genomic Instability

Previous studies have suggested that EBV might cause genomic instability in infected cells. Thus, Lacoste et al. showed that LCLs often display karyotypic abnormalities and increased numbers of phospho-H2AX foci compared to B-cell blasts[237]. Meanwhile work from the Masucci group has shown that the EBV latent proteins EBNA1, LMP1 and EBNA3C can also contribute to genomic instability[242,243]. Furthermore, Nikitin et al. have reported that a period of hyperproliferation-associated genomic instability follows EBV-infection of B-cells, as measured by the accumulation of phospho-H2AX foci[158]. Prompted by such work, we speculated that patterns of clonal outgrowth might be related to genomic instability and/or DNA damage signalling during the first few days in culture. Indeed, if early genomic instability results in mutations that are not repaired (EBV might even block repair pathways) then this might generate a pool of cells carrying genetic damage from which the fittest clone may emerge.

Initial work focussed on characterising proliferation rates in EBV-infected and B-cell blast cultures, in anticipation of finding a similar period of hyperproliferation in EBV cultures to that found by Nikitin et al. (who had not included B-cells blasts as a comparator). However, we were surprised to find little evidence for hyperproliferation. Thus, analysis of CFSE data, using FlowJo methodology, revealed linear outgrowth of EBV-infected B-cells (Figure 53). Importantly, although reanalysis of our CFSE data using the Hawkins et al. methodology (which had been employed by Nikitin et al.) revealed a period of apparent hyperproliferation in EBV-infected cultures, closer inspection revealed this to be artefactual. Thus, as stated by Hawkins et al., data points with a mean division number less than 1.5 should be regarded as unreliable[557]. Interestingly, it is also notable that Nikitin et al. analysed CFSE-labelled

cultures at time points as long as 13 days post-infection. Notably, CSFE data is highly unreliable at these time points and their inclusion is likely to grossly underestimate the number of cell divisions and give a false impression that cells are proliferating more slowly than previously.

Subsequent work involved the characterisation of DNA damage signalling in early cultures, which was initially attempted with Western blotting. However, it rapidly became apparent that this was inappropriate for the current application, due to the hitherto underappreciated differences in the ratio of dead cells to blastoid cells in these cultures, as well as the significant risk of contamination by irradiated fibroblast cells. Consequently, intracellular flow cytometry was developed as a method to assay phospho-H2AX. This technique proved particularly useful because it was possible to gate out non-viable cells from the analysed cultures, allowing for a fair comparison of EBV-infected and B-cell blast cultures. However, newly infected B-cells were only found to exhibit levels of phospho-H2AX similar to those found in established LCLs. Furthermore, phospho-H2AX levels were not found to be substantially different in a direct comparison of EBV-infected B-cells versus B-cells blasts.

From these data we conclude that there is insufficient evidence to suggest that levels of genomic instability in EBV-infected cultures are any greater than those found in B-cell blasts, or that this is a mechanism to explain the observed differences in clonal outgrowth found in these cultures. Additionally, our data contradict the findings of Nikitin et al., as we found little evidence for a period of hyperproliferation-induced DNA damage signalling.

Assessment of Off-Target AID Mutations in LCLs

We were also interested by the observation of Epeldegui et al. that AID-associated mutations in BCL6 and p53 genes accumulate in newly generated LCLs[244]. Given that our laboratory has previously demonstrated that dominant clonotypes in naive LCLs often exhibit AID-induce Ig mutations[236], we hypothesised that new off-target AID-induced mutations might contribute to clonal outgrowth observed in LCLs. However, given that Epeldegui et al. had generated LCLs from total adult B-cells, which contain memory B-cells with pre-existing off target AID-induced mutations , we could not be confident that these findings did not represent selection of cells carrying pre-existing mutations rather the appearance of *de novo* mutations. In support of the former possibility, several groups have reported that AID expression is up-regulated following EBV-induced growth transformation[219,227-229]. Furthermore, analysis of Ig gene sequences has indicated evidence of ongoing SHM in EBV-infected cultures[236]. On the other hand, up to 30% of GC-experienced cells are thought to carry off-target AID-induced mutations[49]. If memory B-cells carrying such mutations exhibit clonal outgrowth, either randomly or due to selective growth or survival advantage, this could also explain the apparent accumulation of mutations in LCLs. On this point, AID is also reported to only target genes that are actively transcribed, which is at odds with the observation that BCL6 is not expressed in LCLs[236,610].

Using a 'clone and sequence' approach to compare BCL6 and p53 sequences in LCLs generated from either total adult B-cells, naive adult B-cells or umbilical cord B-cells, we showed an accumulation of BCL6 mutations in the Total and Naive LCL cultures. As such, our findings are in keeping with the work of Epeldegui et al.[244] However, it is also notable that fewer mutations were noted in the Naive LCL than in the Total LCL. Also, as evidenced

by the appearance of recurrent mutations in these cultures (Tables 23 and 24), it is apparent that at least some of the progressive increase in mutations could be accounted for by the emergence of clonality. Given this, we conclude that clonal outgrowth may act to exaggerate the apparent mutation rate in LCLs.

Interestingly, whilst the BCL6 data was very similar to that of Epeldegui et al., a different pattern was observed for p53 sequences. As such, no progressive accumulation of mutations was observed in p53. It is uncertain why these results should be so different but it is notable that p53 has been shown to be an infrequent target of AID mutation[51]. Also, the p53 amplicon lies within a coding region of the gene and this is a less common target for AID, which preferentially causes mutations in 5' noncoding regions[51,52]. Furthermore, mutations affecting this coding region may have resulted in amino acid changes in the p53 protein, and these will have been subject to selection pressures in culture.

The results for the umbilical cord LCL were particularly intriguing because this showed no accumulation of mutations in either the BCL6 or p53 loci. This is remarkable in light of our previous data showing that umbilical cord LCLs exhibit clonal outgrowth, because it suggests that BCL6 mutations are unimportant as drivers of clonal selection. Furthermore, the result suggests 2 alternative interpretations as to why umbilical cord LCLs fail to develop AID-induced mutations. Thus, one possibility is that umbilical cord blood LCLs exhibit a unique property such that they are insensitive to AID-induced mutations. This may be due to differences in the chromatin configuration at the Ig locus, or other epigenetic changes, that preclude AID-induced mutation in these cells. However, an alternative explanation is that the principal mechanism by which mutations accumulate in LCLs may be by selection of pre-

existing mutations. These are absent in cord blood B-cells but may be present at low frequency in FACS-sorted naive B-cell populations as a result of contamination with memory B-cells. If this is the case then it would imply remarkably strong selection of the contaminating memory B-cells, given that FACS purity is typically >98%.

Ultimately, due to the relatively low number of sequences analysed at each time point during the course of these experiments, it is difficult to draw firm conclusions as to whether the accumulation of mutations apparent in LCLs primarily derives from the appearance of *de novo* AID-induced off-target events, or whether selection of pre-exciting mutations is the predominant mechanism. This needs to be addressed in future experiments, with analysis of larger numbers of sequences, amplified from a broader range of loci.

7. DLI Salvage Therapy for Rituximab-Refractory PTLD arising after Allo-HSCT: *In Vivo* Expansion of Functional EBV Epitope-Specific T-Cells

Rituximab has significantly improved PTLD-related mortality following allo-HSCT[521]. In particular, its use to pre-emptively treat individuals who develop high-level EBV DNAemia in the weeks following transplant, as identified by EBV qPCR monitoring, has led to a marked reduction in mortality relative to historic cohorts[498-501]. Nevertheless, a proportion of patients develop Rituximab-refractory PTLD and are consequently at high risk of mortality[520,521]. The management of such patients is often challenging. Thus, whilst cytotoxic chemotherapy such as CHOP may result in good outcomes for Rituximab-refractory PTLD in the setting of solid organ transplantation, this has not been the case after allo-HSCT, where very poor outcomes are likely to be a consequence of increased toxicity in this patient group.[520,572] However, considerably better responses have been achieved using cellular therapies. Thus, transplant donor-derived unselected donor lymphocyte infusions (DLI), which contain EBV-specific T-cells whenever the donor is EBV-seropositive, have successfully been used as salvage therapy for established PTLD, with response rates of around 70%[523-526]. Unfortunately this approach is limited by the risk of generating alloreactive T-cell responses, which may result in potentially life threatening GvHD. Alternatively, EBV CTL infusions, prepared by *in vitro* stimulation of donor or third party lymphocytes, overcome this problem. These have been used both as effective prophylaxis for PTLD and in the treatment of established disease, resulting in response rates similar to those achieved with DLI, without evidence of alloreactivity[499,527,530,531].

Despite their benefits, EBV CTLs are still not universally available, due in part to the

laborious and costly nature of their production[611]. Novel approaches including the development of protocols for rapid *ex vivo* selection of virus-specific T-cells[534,535,612], or the use of genetically engineered T-cells[613], are seeking to address this issue. Yet these are reliant on knowledge of the antigenic specificity and function of cells with greatest therapeutic potential. Whilst DLI and EBV CTLs appear efficacious for the treatment of PTLD, to date little is known about the factors which might determine response to treatment. Thus, although the expansion of adoptively transferred cells has been correlated with successful clinical outcome, additional properties such as dynamic changes in the specificity and functional characteristics of individual EBV epitope-specific T-cells remain poorly characterised. In order to address this issue, EBV-specific T-cell responses were studied in 2 patients with Rituximab-refractory PTLD who were successfully treated with DLI.

7.1 Patient Presentation and Treatment

This study used clinical data and samples collected from 2 patients who underwent treatment with DLI for Rituximab-refractory PTLD arising after allo-HSCT. Baseline and transplant characteristics for the patients are summarised in Table 25. Patient A underwent allo-HSCT for lymphocytoplasmacytic lymphoma in partial remission using fludarabine and BEAM preparative conditioning, with an HLA-matched unrelated donor with a single HLA-A antigen mismatch (HLA A26 for A32). Due to graft failure, a second transplant from the same donor was performed using fludarabine, cyclophosphamide and ATG conditioning. EBV qPCR testing of whole blood revealed low-level EBV DNAemia on day 71 (post second transplant), with a virus load of 760 copies/ml (Figure 60). Despite weaning cyclosporin, this subsequently rose to high-level EBV DNAemia (28,150 copies/ml) by day 99. The patient was therefore pre-emptively treated with Rituximab 375 mg/m^2, administered weekly to a

	Patient A	Patient B
Age at Transplant, years	51	62
Sex	Female	Female
Diagnosis	LPL	AML
First Transplant		
Donor	Unrelated	Sibling
Conditioning	Flu BEAM	Flu Mel
T Depletion	Alemtuzumab	Alemtuzumab
Second Transplant		
Donor	Unrelated	Sibling
Conditioning	Flu-Cy	FLAMSA-Bu
T Depletion	ATG	ATG
EBV Serology		
Recipient	+	+
Donor	+	+
HLA Type		
A	02, 32*	01, 24
B	44, 49	07, 14
C	05, 07	07, 08
DRB1	01, 15	07, 15
DQB1	05, 06	02, 06

Table 25. Characteristics of Patients Treated with DLI for Rituximab-Refractory PTLD
Both patients developed PTLD following a second allo-HSCT which used ATG for T-cell depletion. *Patient A had a single HLA-A antigen mismatch with their donor (A26 for A32).

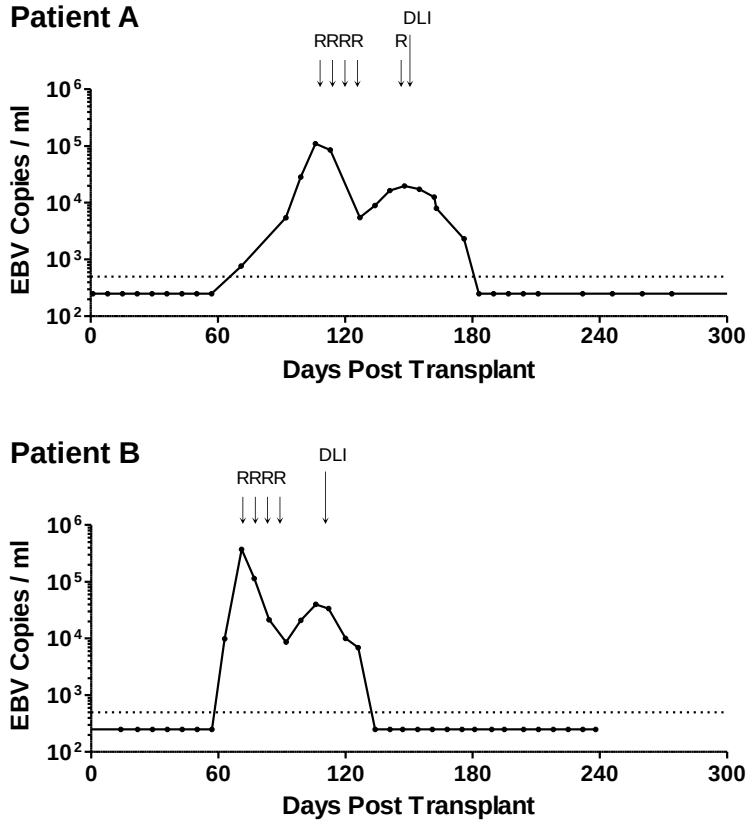

Figure 60. Use of DLI for Rescue of Rituximab-Refractory PTLD after Allo-HSCT

Serial EBV load in whole blood following allo-HSCT for patients A and B. Day 0 is the time of second transplant. The dotted line represents the 500 copies/ml threshold of sensitivity for the EBV qPCR assay. Values <500 copies/ml are arbitrarily shown as 250 copies/ml. R indicates infusion of Rituximab 375 mg/m2; DLI, donor lymphocyte infusion of 1 x106/Kg.

total of 4 infusions, resulting in a decline in EBV load to a nadir of 5470 copies/ml on day 127. However, 7 days after the fourth infusion of Rituximab there was recrudescence of EBV DNAemia which progressed on further testing. This was accompanied by severe oropharyngeal inflammation and ulceration causing absolute dysphagia and airway compromise which progressed despite empirical antimicrobial therapy and systemic steroids. Imaging including PET-CT revealed active disease principally involving Waldeyer's Ring and confluent, full-length oesophageal involvement (Figure 61A). An oropharyngeal biopsy confirmed monomorphic PTLD of DLBCL subtype, which was positive for EBV by EBER *in situ* hybridisation but negative for CD20 immunohistochemistry, consistent with prior Rituximab exposure (Figure 61B)[614].

Patient B underwent allo-HSCT for AML in first complete remission, with fludarabine, melphalan and Alemtuzumab preparative conditioning, using PBSC from a fully HLA-antigen matched sibling donor. A second allograft from the same donor was performed approximately 18 months later (day 0) following relapse of primary disease, with FLAMSA and busulphan conditioning. EBV monitoring revealed a viral load of 9810 copies/ml on day 63 (post second transplant) which progressed to 370,000 copies/ml on day 71 (Figure 60). Consequently, pre-emptive therapy with Rituximab 375 mg/m^2 was administered to a total of 4 weekly infusions. This resulted in reduction of EBV load to a nadir of 8625 copies/ml after the third infusion of Rituximab. However, 6 days following the fourth infusion there was recrudescence of EBV DNAemia with a virus load of 20,760 copies/ml which subsequently increased. This was associated with general malaise and B symptoms, and PET imaging revealed active disease involving the nasopharynx, spleen and multiple lymph nodes (Figure 61A). In the absence of an amenable biopsy site, a diagnosis of probable PTLD was made

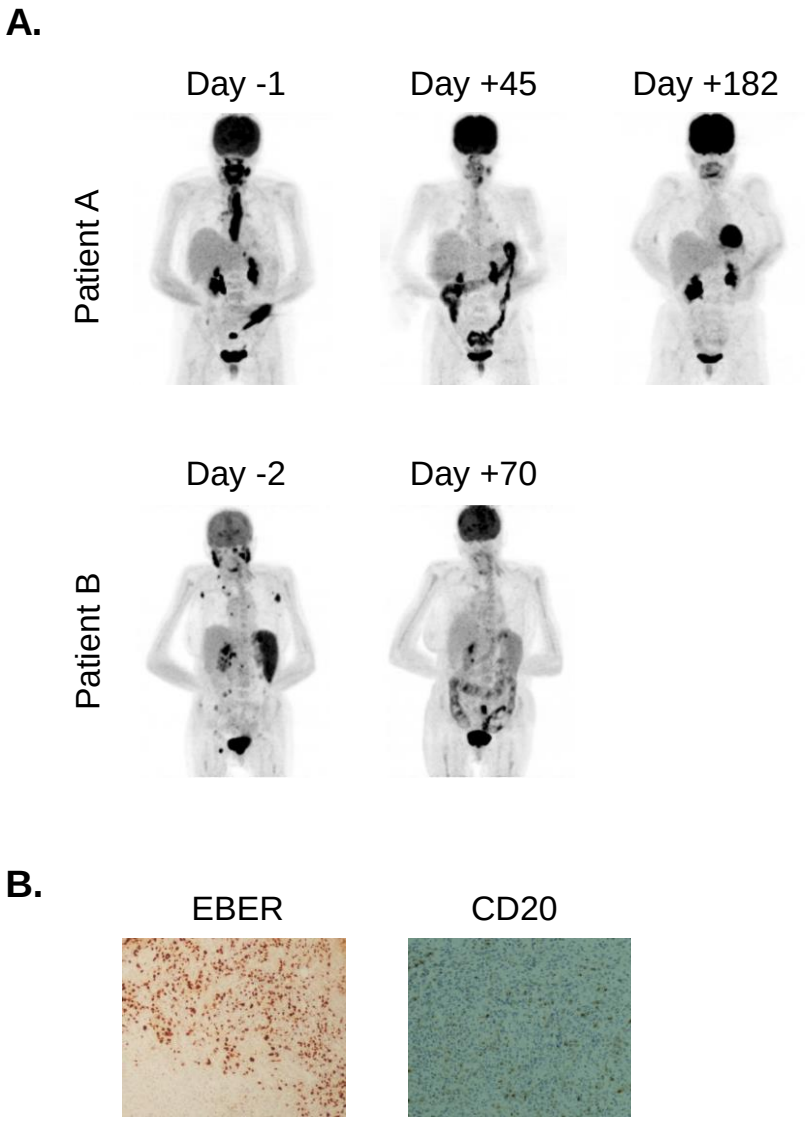

Figure 61. Investigations Pre- and Post-DLI

A. Positron emission tomography imaging taken pre- and post-DLI treatment for Patients A and B. Patient A had active disease principally located in the oropharynx and oesophagus. Patient B had active disease in the oropharynx, spleen and lymph nodes. Excellent responses were observed following DLI. Day 0 is the day of DLI treatment. B. Sections of formalin-fixed and paraffin-embedded biopsy tissue from Patient A showing widespread positivity for EBERs on in situ hybridisation but predominantly negative immunohistochemistry for CD20. Images are magnified 40x.

consistent with published diagnostic criteria[496].

The patients were subsequently treated with single infusions of 1 $x10^6$/Kg unselected donor lymphocytes derived from their EBV immune stem cell donors. In both, a rapid and sustained response to DLI was observed, comprising reduction of EBV load to undetectable levels (Figure 60), resolution of symptoms, and complete metabolic response defined by CT-PET (Figure 61A). Except for stage 1 skin GvHD in Patient A, administration of DLI was tolerated without complication. Patient A remains well after more than 2 years of follow-up. Patient B remained in remission from PTLD but died from treatment-refractory AML around 8 months following their second transplant.

7.2 Expansion of Lymphocyte Subsets Following DLI

Blood samples were collected prospectively following administration of DLI, with the aim of monitoring *in vivo* immune responses. Inspection of total lymphocyte counts revealed a similar pattern of lymphocyte expansion following DLI infusion in both patients (Figure 62). Thus, lymphopenia was noted prior to infusion, with lymphocyte counts of only 300 cells/μl in both (normal range 1000 – 4000 cells/μl). Although the counts were unchanged at 2 weeks following infusion, by 4 weeks there was a marked increase to 2500 cells/μl and 1100 cells/μl for Patients A and B respectively. Thereafter, the lymphocyte counts decreased to near baseline frequencies by 13 weeks in Patient A, and by 8 weeks in Patient B (although there was a further increase at the 10 week time point in the latter). In order to characterise lymphocyte subsets, PBMCs were analysed using a multicolour flow cytometry panel to enumerate $CD3^+$ T-cells (including $CD8^+$ and $CD4^+$ subsets), $CD56^+$ NK-cells and $CD19^+$ B-cells (Figure 62). This revealed a predominance of NK-cells, and few T-cells, in the pre-DLI

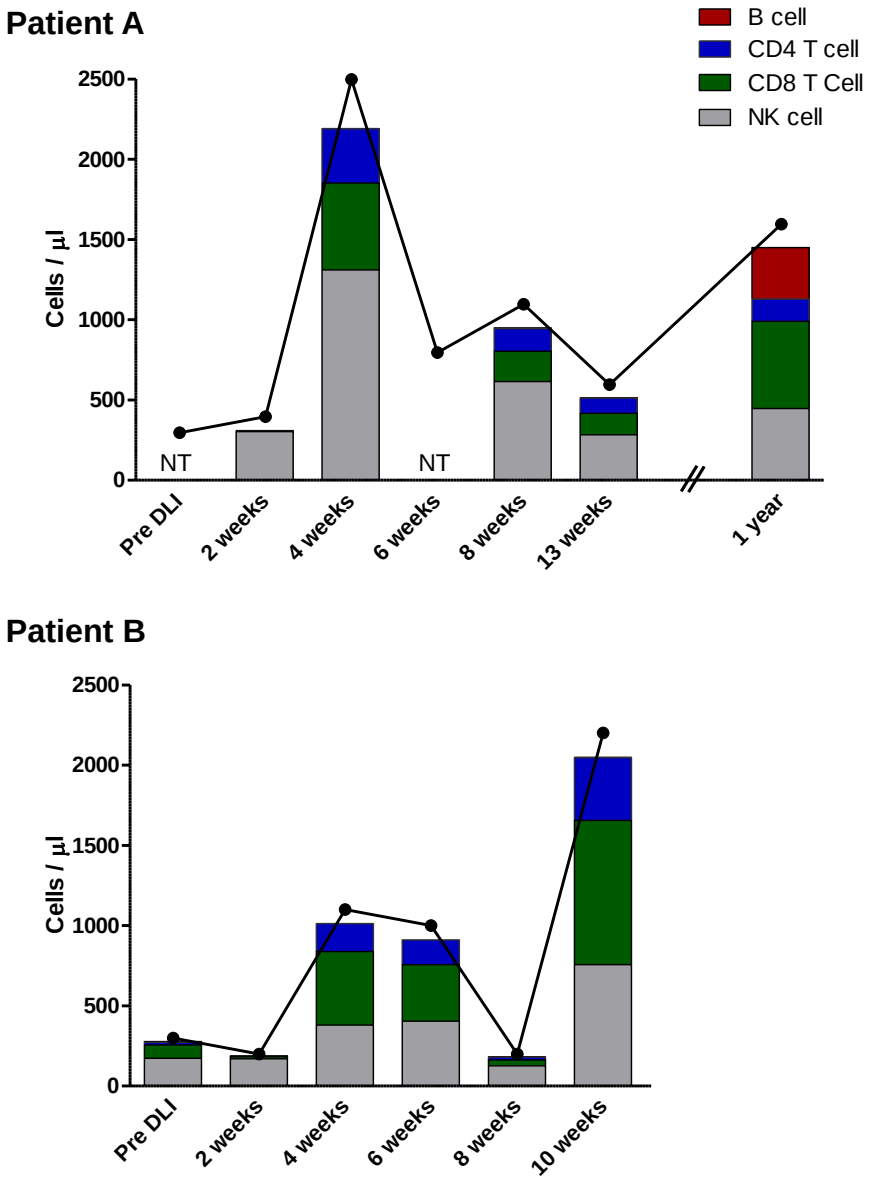

Figure 62. Lymphocyte Counts and Subsets after DLI

Total lymphocyte (joined black dots) and main lymphocyte subset counts (stacked columns) pre- and post-DLI infusion for Patients A and B. NT indicates not tested. Expansion of $CD4^+$ and $CD8^+$ T-cell and NK-cell subsets was observed at 4 weeks after DLI treatment in both patients.

and 2 week time points. However, by 4 weeks both the $CD8^+$ and $CD4^+$ T-cell subsets underwent marked expansion, accompanied by a similar increase in NK-cells. Regarding $CD19^+$ B-cells, despite prior Rituximab therapy these constituted 1.0% of lymphocytes at 2 weeks post DLI-infusion in Patient A but reduced to 0.1% by the 4 week time point, and remained at trace levels at 13 weeks (maximum 0.3%). In Patient B, B-cells made up 1.6% of lymphocytes pre-DLI, falling to 0.6% at 2 weeks post-DLI and remained at trace levels at 10 weeks (maximum 0.2%). Overall, these data suggest that DLI-derived $CD8^+$ and $CD4^+$ T-cells and NK-cells had undergone *in vivo* expansion following infusion, co-incident with elimination of residual circulating B-cells.

7.3 Characterisation of EBV Epitope-Specific T-cell Responses

Whilst previous studies have demonstrated expansion of EBV-specific T-cells following administration of DLI, the antigenic specificities of these cells have not been characterised[525,615]. To enumerate EBV epitope-specific T-cell responses for study patients, PBMCs were stimulated overnight with EBV peptides and responding $CD8^+$ and $CD4^+$ T-cells were quantified using IFN-γ release Elispot assay. Initially, aliquots of donor lymphocytes were tested, revealing EBV-specific $CD8^+$ and $CD4^+$ T-cell responses typical of healthy EBV seropositive individuals[287]. Thus, responses to a range of EBV antigens were observed, with prominent responses to immunodominant epitopes (Figure 63). Patient A exhibited strong responses to the $CD8^+$ T-cell peptides EEN (EBNA3C), KEH (EBNA3C), CLG (LMP2) and YVL (BRLF1), whilst the DLI for Patient B showed prominent responses against the $CD8^+$ T-cell peptides TYS (EBNA3B), TYG (LMP2) and RPP (EBNA3A), and the $CD4^+$ T-cell peptide PRS (EBNA2). In contrast, analysis of patient PBMCs collected prior to DLI infusion showed responses undetectable above background DMSO. Responses

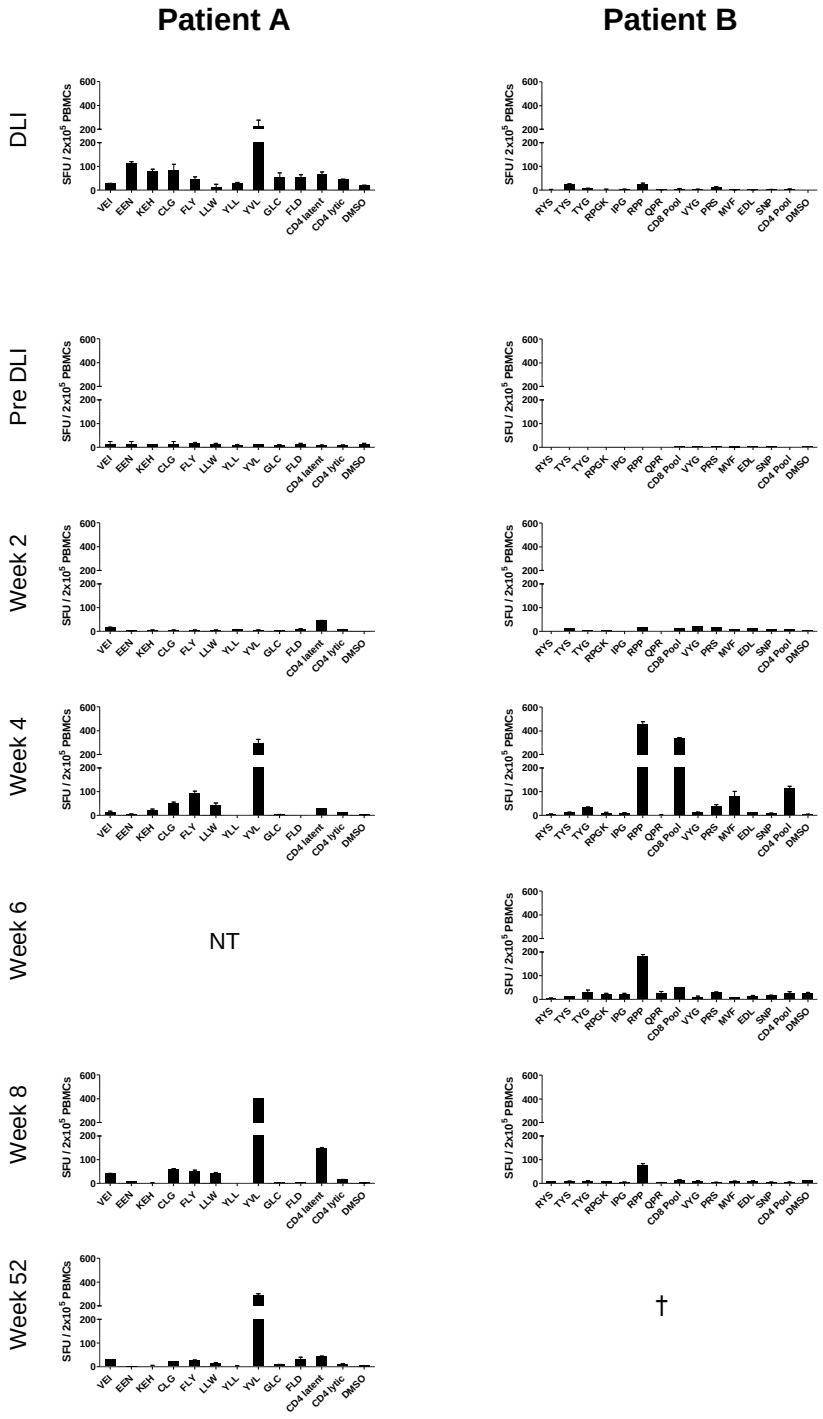

Figure 63. IFN-γ Elispot Analysis of EBV Epitope-Specific T-Cells after DLI

Aliquots of donor lymphocytes or PBMCs from patients A and B were stimulated overnight with selected panels of previously determined HLA class I and II EBV epitope-specific peptides before responding cells were enumerated using IFN-γ Elispot. Mean spot forming units (SFUs) per 2 x105 cells are displayed. NT, indicates not tested; † indicates death.

remained poor at 2 weeks after DLI. However, by 4 weeks there was a very marked increase in EBV-specific T-cell frequency. Importantly, these responses included some, but not all, of the epitope specificities identified in the corresponding DLI samples. Thus, in Patient A the $CD8^+$ response was dominated by reactivity against the $CD8^+$ YVL (BRLF1) peptide, with weaker responses to the LMP2 peptides FLY, CLG and LLW, whereas in Patient B the RPP (EBNA3A) peptide and the $CD8^+$ peptide pool (a composite of lytic antigen peptides) elicited the strongest responses. Epitope-specific $CD4^+$ T-cells were also detected in both patients, most evidently against the pool of $CD4^+$ latent epitope peptides in Patient A, and the MVF (EBNA1) peptide and $CD4^+$ peptide pool (a composite of lytic antigens plus EBNA3C peptides) in Patient B. Interestingly, $CD4^+$ T-cell responses may have preceded those of $CD8^+$ T-cells in Patient A, as responses to the $CD4^+$ latent pool were detected at 2 weeks. The responses persisted in both patients, most notably in Patient A in whom EBV-specific T-cells were detected at 2 years following DLI (data not shown).

Given that IFN-γ release may underestimate the total frequency of antigen-specific T-cells[302], we subsequently sought to quantify EBV-specific T-cells by flow cytometry, using MHC class I tetramers. Reagents were available for the HLA A*02 restricted EBV latent epitope CLG (LMP2) and the EBV lytic epitopes YVL (BRLF1) and GLC (BMLF1). These were used to analyse PBMCs from the HLA A*02-positive Patient A, to determine responding T-cells as a proportion of circulating $CD8^+$ T-cells (Figure 64). Responses to all 3 tetramers were undetectable at 2 weeks following DLI, consistent with a general absence of $CD8^+$ T-cells at this time point (as demonstrated by Figure 62). However, by 4 weeks after DLI, responses to YVL (BRLF1) and GLC (BMLF1) tetramers were markedly increased, comprising 5.7% and 1.9% of circulating $CD8^+$ T-cells respectively (Figure 64). These

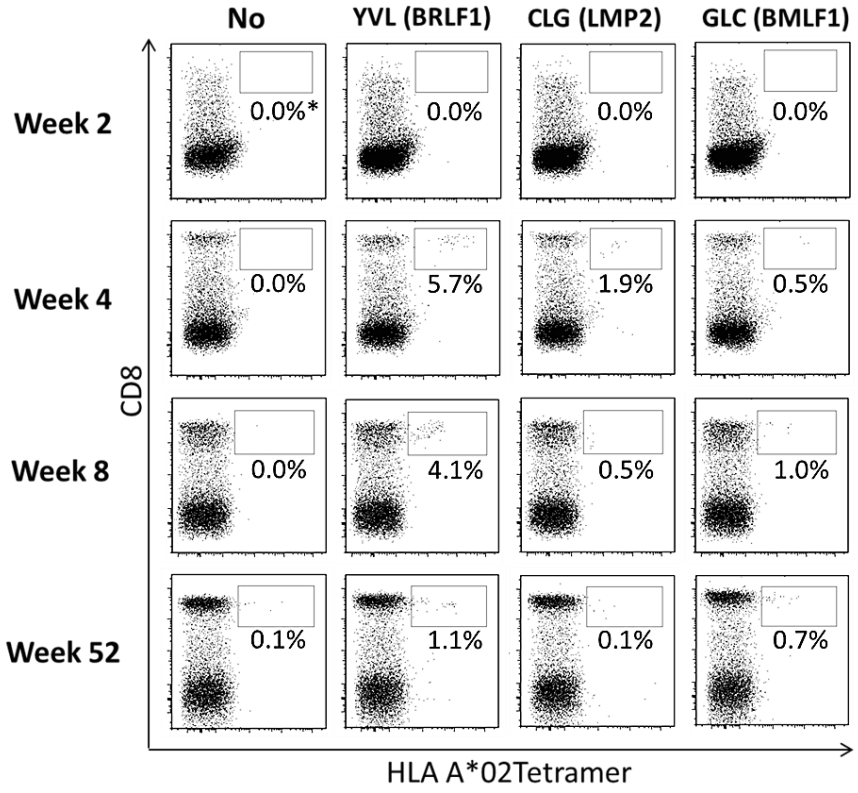

Figure 64. HLA Class I Tetramer-Specific CD8$^+$ T-Cells after DLI

PBMCs from HLA A*02-positive Patient A were stained with the HLA A*02 tetramers YVL (BRLF1), CLG (LMP2) and GLC (BMLF1). Cell populations within the boxes indicate the percentage of tetramer-positive cells within the CD8$^+$ T-cell population. A no tetramer control (left column) was also included. Tetramer staining performed by Dr H. Long, University of Birmingham.

responses were maximal at this time point and remained elevated at 8 weeks. The response to GLC (BMLF1) was less marked but also increased to a maximum of 1.0% of $CD8^+$ T-cells at 8 weeks. Notably, by 12 months after infusion of DLI, the frequencies of MHC class I tetramer-specific cells within the $CD8^+$ T-cell subset had fallen to levels typically found in healthy EBV-seropositive adults[287]. The frequency (cells/μl) of EBV tetramer-specific $CD8^+$ T-cells was subsequently calculated (Figure 65), revealing the full magnitude and kinetics of these responses. Importantly, this demonstrated a close correlation between EBV epitope-specific $CD8^+$ T-cell expansion and resolution of viral DNAemia, particularly for the immunodominant EBV lytic peptide epitope YVL (BRLF1).

7.4 Expression of EBV T-cell Target Antigens in PTLD Tissue

Having documented EBV antigen-specific $CD8^+$ and $CD4^+$ T-cell responses following DLI, we wished to confirm the presence of corresponding viral antigens within PTLD tumour tissue. As such, sections from the PTLD biopsy available from Patient A were subjected to immunohistochemistry for a selected range of EBV proteins (Figure 66). This showed expression of EBNA1, EBNA2, LMP1 and LMP2 latent proteins, consistent with a Latency III, growth-transforming, pattern of virus gene expression. Importantly, these included several proteins recognised by the T-cells that had been found to expand *in vivo* post-DLI (Figures 63 and 64). Notably, the EBV lytic cycle antigen BZLF1, expression of which is responsible for initiating the virus replication programme, was also readily detected. However, late lytic cycle gp350, which contributes to the virus envelope and is one of the final proteins to be expressed from the EBV genome, was absent.

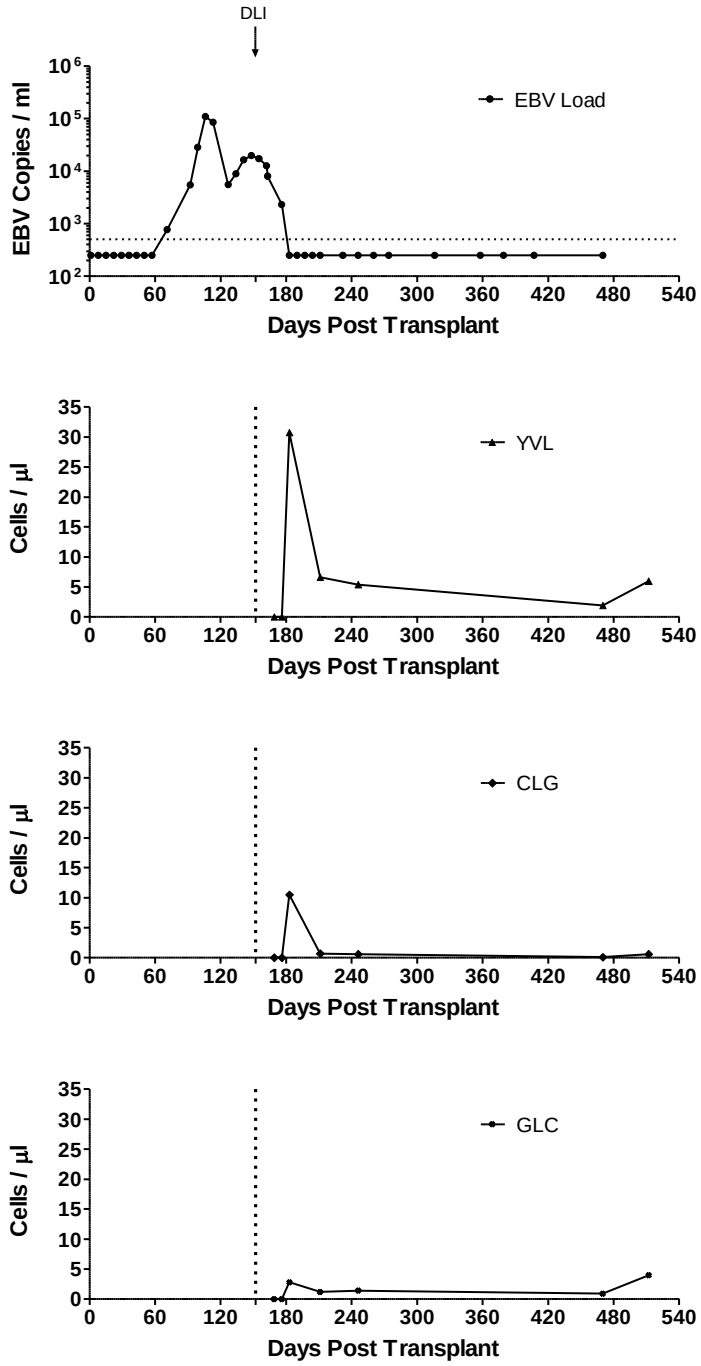

Figure 65. Frequency of HLA Class I Tetramer-Specific CD8$^+$ T-Cells after DLI

The number of CD8$^+$ T-cells specific to the HLA class I tetramers YVL (BRLF1), CLG (LMP2) and GLC (BMLF1) were determined for Patient A following DLI. Responses are plotted alongside whole blood EBV loads. The dotted lines indicate the timing of DLI treatment.

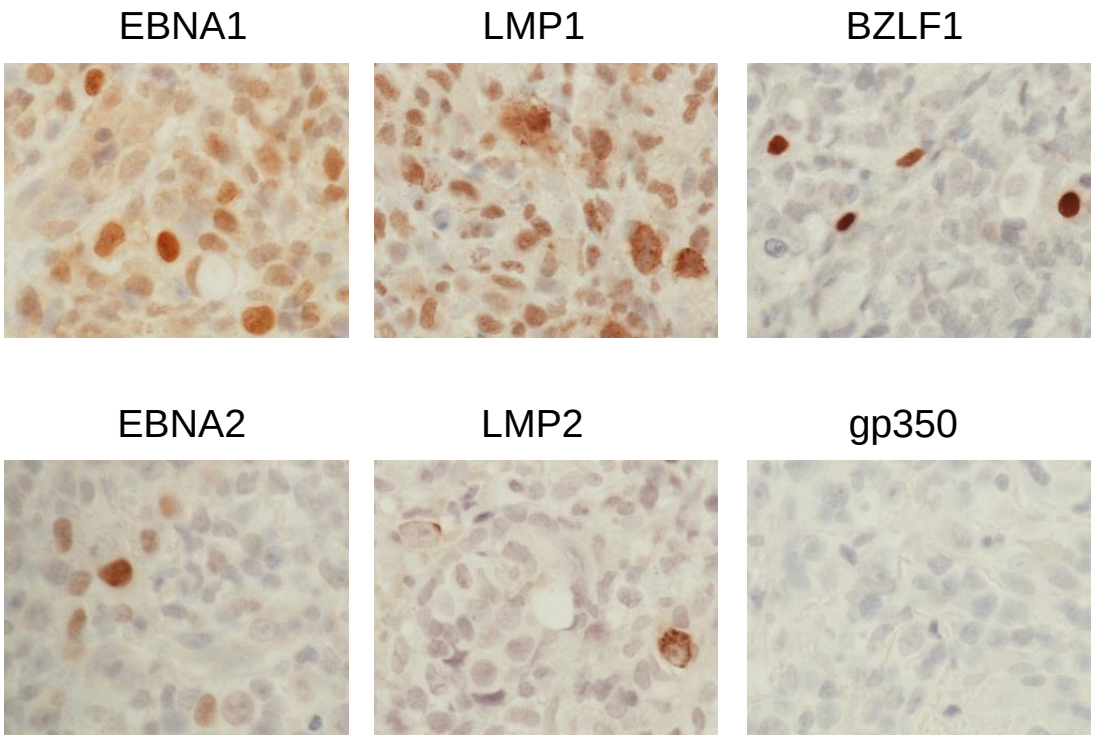

Figure 66. EBV Antigen Expression in PTLD Biopsy Tissue

Immunohistochemistry performed on sections of formalin-fixed and paraffin-embedded PTLD biopsy material from Patient A revealed strong positivity for EBV latent antigens EBNA1, EBNA2, LMP1 and LMP1, as well as the EBV lytic antigen BZLF1, but absence of late lytic antigen gp350. Images are magnified 60x. Immunohistochemistry was performed by Dr E. Nagy, Cancer Sciences, University of Birmingham.

7.5 Discussion

Whilst pre-emptive Rituximab therapy constitutes an effective strategy to reduce the incidence of PTLD-associated mortality after allo-HSCT, it nevertheless remains suboptimal. Treatment itself is not devoid of side effects[616], and a significant proportion of patients develop established, Rituximab-refractory, disease. Given the disappointing outcomes observed with cytotoxic chemotherapy, cellular therapies currently offer the best chance of rescue. However, effective responses to DLI or EBV CTLs are also not universal, and approximately 30% of patients exhibit treatment failure[525]. Retrospective analysis of the viral and immunological variables that may influence outcome is therefore likely to be crucial for the optimisation of future adoptive immunotherapeutic approaches. In this chapter the potential value of performing detailed immune characterisation following administration of cellular therapy is exemplified with 2 cases of Rituximab-refractory PTLD successfully rescued with DLI.

Both study patients received single doses of 1 $x10^6$/kg unselected transplant donor-derived lymphocytes. In each, infusion resulted in complete clinical response, comprising sustained resolution of EBV DNAemia and remission of radiological abnormalities. Notably, this was accompanied by marked expansion in circulating lymphocytes, with peak frequencies observed within 4 weeks of DLI therapy. The lymphocyte expansions contained both $CD8^+$ and $CD4^+$ T-cells, consistent with previous reports that successful treatment of established PTLD correlates with restoration of T-cell numbers[525]. Interestingly, we also observed simultaneous increases in $CD3^-CD56^+$ NK-cell numbers. Notably, *in vitro* studies have shown that this lymphocyte subset, some of which are primed for rapid IFN-γ production[617], may play a role in limiting B-cell transformation by EBV[306,307]. However, their contribution to the

clinical responses seen against established PTLD following DLI is yet to be determined.

We went on to analyse the specificity of the expanded $CD8^+$ and $CD4^+$ T-cells in PBMCs collected before and after DLI. Previous studies, undertaken in similarly treated patients, have estimated EBV-specific T-cell numbers using LCL or peptide pool stimulation followed by limiting dilution or chromium release assays[382,525], and by detecting IFN-γ production by flow cytometry[525] or Elispot[532]. Whilst these assays are good measures of total EBV-specific responses, data regarding individual epitope specificities are not captured. In the present study, we instead used panels of patient HLA-relevant EBV epitope peptides to determine the frequency of individual responses, initially by IFN-γ Elispot. This approach has previously been used to track the kinetics of infused peptide-selected T-cells of known specificity[534]. In both patients, expanded T-cells contained immunodominant responses identical to those present in the DLI prior to infusion, i.e. YVL (BRLF1) for Patient A, and RPP (EBNA3A) for Patient B, and subdominant responses to a range of other $CD8^+$ and $CD4^+$ peptides. Crucially, detection of IFN-γ release in these assays demonstrated that the expanded T-cells are able to function in response to their cognate antigen. Furthermore, we were also able to quantify absolute numbers of EBV epitope-specific $CD8^+$ T-cells for Patient A, whose HLA I type was amenable to analysis with HLA-A*02 restricted EBV peptide MHC I tetramers. Significantly, the peak frequencies of tetramer positive cells in the blood coincided with the dynamics of total lymphocyte expansion, in line with reports of clinical responses occurring concurrently with expansion of LCL-reactive cells[525,615]. At this time, greater than 8% of all circulating $CD8^+$ T-cells were specific for the 3 available MHC I tetramers. Given that the observed responses represent only 3 epitopes from the entire virus genome, restricted through a single HLA I allele, it is likely that detected responses are under-representative of all those present

and that the majority of the expanded $CD8^+$ T-cells are in fact virus-specific.

Importantly, we also observed notable differences in the repertoire of responses present in the DLI prior to infusion compared to those appearing *in vivo* after infusion. Thus, for Patient A the FLY (LMP2) peptide elicited the second largest response following infusion, whilst 2 stronger responses in the DLI, EEN (EBNA3C) and KEH (EBNA3C), were almost undetectable. Similarly, in Patient B, reactivity against the $CD8^+$ peptide pool was more prominent 4 weeks post infusion than in the DLI, whereas the TYS response of the DLI was undetectable after infusion. These differing patterns indicate non-uniform expansion of EBV epitope-specific T-cells present in the DLI following administration, and suggest that antigen encounter *in vivo* may shape the observed responses. Furthermore, they may explain why attempts to simply correlate antigen specificities present in heterogeneous therapeutic cell preparations with clinical outcome have thus far been unsuccessful[532,618].

Immunohistochemistry on biopsy material from Patient A demonstrated expression of several proteins associated with the viral latency III programme. Importantly, this included proteins that were targets of the expanded $CD8^+$ T-cell response. Additionally, we detected unequivocal expression of the IE lytic cycle protein BZLF1. This transcription factor is the key initiator of EBV lytic cycle, and drives sequential expression of over 80 viral proteins involved in virus replication[10]. However, despite widespread BZLF1 expression in the biopsy, we could not detect expression of the L structural protein gp350. Such observations accord with earlier evidence that lytic cycle does not always progress to the final stages in PTLD tumours[439,443], and that lytic cycle expression may therefore be abortive. Interestingly, it has been suggested that IE and E lytic gene expression, whether abortive or not, might enhance

PTLD tumourigenesis, possibly by stimulating the secretion of cytokines[445,448]. Notably, this pattern was reflected in the T-cell specificities expanded *in vivo*. Thus the immunodominant reactivity in the blood of Patient A following DLI was against the IE epitope YVL (BRLF1), whereas L epitope FLD (BALF4) responses were absent during the time of PTLD resolution. Together, these data indicate that tumour antigen expression can drive T-cell expansion, and suggest that T-cells active against latent and early lytic antigens may be more therapeutically important than L antigen-specific responses in the setting of PTLD. Further analysis of post-DLI expanded T-cells in a larger series of patients will help to identify key therapeutic responses required for clinical efficacy. Such knowledge will be crucial to enhance the success of novel approaches using *ex vivo* selected T-cells[534,535] or genetically engineered T-cells[613].

In summary, this work confirms that DLI can be an effective therapeutic option for Rituximab-refractory PTLD arising after allo-HSCT when EBV CTLS are not available, although the risk of alloreactivity should be borne in mind. Moreover, we have described several novel properties pertaining to the virus-specific immune response which develops *in vivo* following adoptive transfer. Thus, resolution of disease coincided with a marked increase in lymphocytes, including in particular functional EBV epitope-specific $CD8^+$ and $CD4^+$ T-cells. These exhibited reactivity against a range of latent and IE lytic antigens expressed in biopsy material. Importantly, expansion of specificities present in the DLI did not appear to be uniform, indicating that presentation of epitopes from viral antigens expressed in the tumour can drive the *in vivo* immune response. Further analyses on similarly treated patients are required to define the most clinically important epitopes against which therapy should be targeted.

8. Conclusions and Further Work

This thesis presents a series of complementary studies exploring a central theme of EBV-associated PTLD. Initially, retrospective studies undertaken in the solid allograft and allo-HSCT clinical settings are reported; focusing on outcomes, incidence and risk factors, these studies exemplify the problem posed by PTLD and provide important clinical context for subsequent data. Thereafter, emphasis shifts to exploring the pathogenesis of PTLD, with insights generated by *ex vivo* analysis of samples collected from patients undergoing allo-HSCT, and work exploring the clonal evolution of LCLs *in vitro* as a model for PTLD. Finally, consideration is given to the treatment of PTLD using DLI, with findings relevant to the future optimisation of adoptive immunotherapeutic strategies.

8.1 PTLD Arising after Solid Organ Transplant

For patients with biopsy-proven PTLD following solid organ transplant we report 74% versus 59% (P = 0.52) 2-year overall survival for those treated with first-line R-mono or R-CHOP chemotherapy respectively, noting that those selected to receive R-CHOP generally had higher risk disease. This work confirms that R-mono *can* be a successful therapy for some patients with low risk disease. More importantly, using a modified prognostic scoring system we were able to identify a subset of patients who exhibited very poor outcome, irrespective of initial therapy. Thus, patients scoring ≥2 points using the 4-point modified IPI had a 2-year overall survival of only 43%. Notably, these results represent an interim analysis, because data on at least 50 further cases of PTLD are still due to be contributed from collaborating centres. Once completed, this will be among the largest series of its kind.

Given the current paucity of data on outcomes and prognostic factors for PTLD treated in the Rituximab era, this study is of substantial value. However, more importantly, it also provides a foundation for the development of future studies. In this respect, it is hoped that the availability of a large series of clinically annotated PTLD cases, drawn from a network of collaborating centres, will facilitate future work to undertake molecular profiling of PTLD tumours, in order to identify markers of prognostic or therapeutic importance. Furthermore, in follow-up to our study, a Phase II/III randomised controlled trial is currently being developed, with Dr Sridhar Chaganti as chief investigator, to address the pressing need for novel therapeutic strategies for patients with high risk PTLD. Examining the role of upfront EBV CTLs in PTLD after solid allograft, this trial will randomise patients with high risk or R-mono refractory (EBV-associated) PTLD between R-CHOP chemotherapy or third party EBV CTLs. The latter will be sourced from a cryopreserved bank of EBV CTLs generated from third party donors by Prof Mark Vickers from the University of Aberdeen. These will be selected on the basis of partial HLA-antigen matching, an approach already used for PTLD unresponsive to other therapies with encouraging results[531]. If the EBV CTLs prove non-inferior to conventional upfront chemotherapy then this will be a landmark study in the field of adoptive immunotherapy.

8.2 EBV Reactivation and PTLD after Allo-HSCT

In what is, as far as we know, the largest study to examine incidence and risk factors for EBV reactivation and PTLD in patients undergoing Alemtuzumab-conditioned T-cell deplete allo-HSCT, we report a cumulative incidence of high-level EBV reactivation (≥ 20,000 copies/ml whole blood) of 18% by 1 year after transplant amongst a cohort of 186 adults patients, with 8 cases of PTLD and 3 PTLD-related deaths. We therefore conclude that Alemtuzumab-

conditioned allo-HSCT *does* carry a significant risk of risk of PTLD, even in the context of EBV monitoring and pre-emptive Rituximab therapy. Interestingly, viral reactivation events occurred up to, and beyond, 6 months post-transplant. This suggests that monitoring for a period of 3 months, as recommended in current guidelines from the Second European Conference on Infections in Leukemia[496], may be insufficient. Importantly, we also report the novel finding that patients with a diagnosis of NHL, most of whom received Rituximab therapy within 6 months prior to transplant, appear to exhibit a greatly reduced incidence of EBV reactivation and PTLD compared to other diagnostic groups. This is intriguing because it suggests that pre-transplant Rituximab might protect such patients from developing PTLD.

In light of the above findings, it is foreseeable that Rituximab delivered in the peri-transplant period i.e. shortly before or after transplant, might be an effective method of prophylaxis for patients undergoing allo-HSCT, perhaps where the risk of PTLD is particularly high, such as after a second transplant or when ATG has been used. Given this, further research should be performed to explore the mechanism by which pre-transplant Rituximab might confer protection. Thus, efforts should be made to confirm or refute the observation by Van Dorp et al. that pre-transplant Rituximab therapy (delivered within 6 months prior to transplant) results in delayed reconstitution of the B-cell compartment[578]. Furthermore, studies to characterise the origin of EBV strains contributing to viral reactivation and PTLD, similar to those presented in Section 5.15, should be undertaken on larger patient cohorts. If the predominant viral strain present at the time of EBV reactivation is shown to be of recipient origin, then this would support the hypothesis that Rituximab results in protection by suppressing recipient virus prior to transplant. Ultimately, a randomised controlled clinical trial will be required to determine if Rituximab can indeed provide effective prophylaxis from

PTLD. One possibility would be to randomise patients undergoing T-cell deplete allo-HSCT to receive infusions of Rituximab on transplant day -7 and day +7, or not. The primary outcome measure for such a trial should be incidence of EBV DNAemia, with secondary outcomes including incidence of PTLD and non-relapse morality.

8.3 Studies on the Persistence of EBV in Patients Undergoing Allo-HSCT

To explore the relationship between EBV persistence and immune reconstitution following allo-HSCT, blood samples collected from patients who exhibited high-level EBV reactivation were compared to those from patients who had never developed significant EBV DNA. This led to the novel finding that whereas most allo-HSCT patients exhibit a marked deficiency of $CD27^+$ memory B-cells for many months after transplant, those with high-level EBV reactivation show a highly significant increase in both the proportion and number of circulating $CD27^+$ memory B-cells. These cells were not present prior to viral reactivation, and up to around 90% were shown to carry viral genomes. Intriguingly, a high proportion of these $CD27^+$ memory B-cells also exhibited an activated phenotype, given that they expressed plasmablastic-cell surface markers, had increased cell size, and around half of the cells showed positivity for the proliferation marker Ki-67. Importantly, although analysis of EBV gene expression revealed some Latency III expression within FACS-sorted $CD27^+$ B-cells, the finding of a disproportionately low level of these transcripts suggested that a highly restricted pattern of viral gene expression is present in most EBV-infected cells. These data are important because they allow us to establish a more complete understanding of the pathophysiology of EBV reactivation after allo-HSCT. Furthermore, they show that EBV, quite remarkably, maintains selectivity for the memory B-cell compartment even in the setting of allo-HSCT where naive B-cells normally predominate. This raises important questions as

to how this selectivity is maintained.

In future work, effort should be directed at confirming our observation that a high proportion of circulating $CD27^+$ memory B-cells are indeed activated cells, many of which are proliferating. One strategy would be to perform cell cycle analysis using non-toxic DNA-specific fluorescent dyes, in combination with cell surface marker staining, in order to facilitate the FACS-sorting of $CD27^+$ memory B-cells in S or G2/M phases of the cell cycle. These cells could be subsequently analysed using EBV qPCR in order to confirm the presence of EBV within actively proliferating cells. Furthermore, FACS-sorted single cells could be analysed with emerging techniques to assay EBV gene expression within single cells, in order to further characterise patterns of EBV latent gene expression. Such aims could also be addressed at the protein level by performing immunofluorescence staining on FACS-sorted cells, assuming that the significant technical challenges associated with such an approach could be overcome. Meanwhile, other work should be undertaken to address the question as to the origin of the $CD27^+$ memory B-cells i.e. do they derive from mature B-cells transferred across with the donor stem cell graft, or do they originate from engrafted donor haematopoietic stem cells? One potential approach to this challenging problem would be to perform 'kappa-deleting recombination excision' (KREC) analysis, which provides an indication of the replication history of B-cells[619,620]. Additional insights may be obtained by examining EBV reactivation in recipients of umbilical cord stem cell grafts, given that these do not contain memory B-cells.

8.4 Modelling the Clonal Evolution of PTLD *in Vitro*

A series of investigations were also undertaken to explore the previously observed

phenomenon of clonal outgrowth in LCLs. Thus, IgH CDR3 spectratyping was used to confirm that LCLs generated from total or naive B-cells exhibit this effect, whereas B-cell blasts remain polyclonal in culture. Thereafter, novel observations were made that clonal outgrowth also occurs in LCLs generated from umbilical cord B-cells, and those established using a BZLF1 KO strain of EBV. Subsequently, differences observed in early EBV-infected and B-cell blast cultures led to the hypothesis that effects on cell survival and proliferation, possibly conferred by the mouse fibroblast layer used to generate B-cell blasts, might explain the observed patterns of clonal outgrowth. However, it was ultimately revealed that LCLs exhibit clonal outgrowth even when cultured on mouse fibroblasts, with or without CD40L/IL4 stimulation. Interestingly, little evidence was found to support the hypothesis that genomic instability or DNA damage response signalling in the first few days of culture has a significant influence on clonal outgrowth, particularly as levels of phospo-H2AX were found to be no lower in B-cell blasts that they are in LCLs. Furthermore, our data appear to contradict the results of Nikitin et al.[158] because EBV-infection of B-cells was not found to be associated with a period of hyperproliferation or DNA damage response signalling.

In light of the above findings, further studies are required to characterise potential influences on clonal outgrowth. Although no evidence was found to suggest that DNA damage response signalling, or genomic instability, in the first few days influence clonal outgrowth, further experiments are required to examine these factors, particularly at later time points. One approach may be to maintain cultures in the presence of small molecule inhibitors of the signalling proteins ATM and Chk2, to assess the effect of inhibition on outgrowth. Furthermore, cultures generated from individuals with inherited mutations of ATM or AID could be studied. Notably, to overcome difficulties with the comparison of LCL and B-cell

blast cultures, introduced by the requirement for a fibroblast feeder layer to generate the blasts, it would also be beneficial to assess clonal outgrowth in blasts generated using only soluble factors; this would allow better comparison using techniques such as Western blotting. In addition, given limitations identified with the current methods for assessing clonality, including the qualitative (as opposed to quantitative) nature of the data generated by IgH CDR3 spectratyping, and the labour intensive demands of sequencing individually cloned IgVH rearrangements, Next Generation Sequencing (NGS) technologies could be used to analyse Ig sequences. By simultaneously sequencing huge numbers of rearranged IgVH loci, NGS technologies would allow quantitative assessment of clonality in such a way that subtle differences in the clonal evolution of *in vitro* cultures (or PTLD tumours) might be studied, as well as yielding data on the evolution of specific sequences in culture.

The acquisition of off-target AID-induced mutations was also explored as a possible influence on clonal outgrowth. This revealed that BCL6 (but not p53) mutations accumulate in LCLs following infection but also that clonal outgrowth may exaggerate the apparent number of mutations found. Importantly, the finding that umbilical cord LCLs do not accumulate BCL6 mutations, yet they still exhibit clonal outgrowth, suggests that these mutations are not important drivers of clonal selection, contrary to expectation. However, the relatively small number of sequences analysed during these studies precluded definite conclusions. In follow-up to this work, mutations accumulating in LCLs and B-cell blasts generated from alternative B-cells subsets, including umbilical cord B-cells, should be characterised with NGS. This would allow mutation rates at multiple target loci to be determined from high numbers of sequence reads. It would also be interesting to perform experiments to confirm whether, and why, umbilical cord B-cells remain refractory to AID-induced mutations. Furthermore,

additional experiments are warranted to explore why LCLs apparently accumulate BCL6 mutations when they do not express BCL6, which is contradictory to the view that only transcribed genes can acquire AID-associated mutations.

8.5 DLI Therapy for Rituximab-Refractory PTLD

By studying patients treated with DLI for Rituximab-refractory PTLD arising after allo-HSCT, insights about the properties of *in vivo* EBV-specific immune responses consequent upon DLI treatment were gained. Thus, in both patients studied, $CD8^+$ and $CD4^+$ T-cells, as well as NK-cells, were shown to exhibit marked expansion around 4 weeks after DLI treatment, coincident with excellent clinical responses. Furthermore, using IFN-γ Elispot and MHC-class I tetramer staining, individual EBV epitope-specific T-cell responses were characterised, revealing evidence of *in vivo* antigen-driven T-cell expansion. Importantly, this work highlights the value of adoptive immunotherapy as effective treatment for PTLD. Furthermore, it demonstrates a potentially informative approach by which adoptive immunotherapy might be optimised in future, by facilitating the identification of EBV antigens, and specific epitopes, against which CTL preparations should be directed to achieve effective anti-tumour responses.

In follow-up to this work, we aim to undertake further studies in the near future to characterise *in vivo* immune responses in other patients with PTLD treated with adoptive immunotherapy. In particular, we are currently preparing a project proposal, with Dr Heather Long as chief investigator, to characterise EBV-specific immune responses in patients treated with EBV CTL therapy in the context of the aforementioned clinical trial for patients with PTLD arising after solid organ transplant. Thus, we aim to prospectively follow all patients

treated with cell therapy, in order to determine the kinetics, specificity and functional characteristics of EBV specific T-cell responses. Additional work will be undertaken to characterise the banked EBV CTLs used to treat patients. These findings will be correlated with clinical responses in order to identify potentially important determinants of clinical outcome.

9. References

1. Crawford DH, Rickinson AB, Johannessen I. Cancer virus: the story of Epstein-Barr virus. Oxford: Oxford University Press; 2014.
2. Epstein MA, Barr YM. Cultivation in vitro of human lymphoblasts from Burkitt's malignant lymphoma. *Lancet*. 1964;1(7327):252-253.
3. Henle G, Henle W, Diehl V. Relation of Burkitt's tumor-associated herpes-ytpe virus to infectious mononucleosis. *Proc Natl Acad Sci U S A*. 1968;59(1):94-101.
4. zur Hausen H, Schulte-Holthausen H, Klein G, et al. EBV DNA in biopsies of Burkitt tumours and anaplastic carcinomas of the nasopharynx. *Nature*. 1970;228(5276):1056-1058.
5. Weiss LM, Strickler JG, Warnke RA, Purtilo DT, Sklar J. Epstein-Barr viral DNA in tissues of Hodgkin's disease. *Am J Pathol*. 1987;129(1):86-91.
6. Jones JF, Shurin S, Abramowsky C, et al. T-cell lymphomas containing Epstein-Barr viral DNA in patients with chronic Epstein-Barr virus infections. *N Engl J Med*. 1988;318(12):733-741.
7. Kikuta H, Taguchi Y, Tomizawa K, et al. Epstein-Barr virus genome-positive T lymphocytes in a boy with chronic active EBV infection associated with Kawasaki-like disease. *Nature*. 1988;333(6172):455-457.
8. Kawa-Ha K, Ishihara S, Ninomiya T, et al. CD3-negative lymphoproliferative disease of granular lymphocytes containing Epstein-Barr viral DNA. *J Clin Invest*. 1989;84(1):51-55.
9. Crawford DH, Thomas JA, Janossy G, et al. Epstein Barr virus nuclear antigen positive lymphoma after cyclosporin A treatment in patient with renal allograft. *Lancet*. 1980;1(8182):1355-1356.
10. Rickinson AB, Kieff E. Fields Virology. Vol. 2 (ed 5). Philadelphia, PA: Lippincott Williams & Wilkins; 2007.
11. Schroeder HW, Jr., Cavacini L. Structure and function of immunoglobulins. *J Allergy Clin Immunol*. 2010;125(2 Suppl 2):S41-52.
12. Treanor B. B-cell receptor: from resting state to activate. *Immunology*. 2012;136(1):21-27.
13. Fried AJ, Bonilla FA. Pathogenesis, diagnosis, and management of primary antibody deficiencies and infections. *Clin Microbiol Rev*. 2009;22(3):396-414.
14. Schatz DG, Ji Y. Recombination centres and the orchestration of V(D)J recombination. *Nat Rev Immunol*. 2011;11(4):251-263.
15. Soulas-Sprauel P, Rivera-Munoz P, Malivert L, et al. V(D)J and immunoglobulin class switch recombinations: a paradigm to study the regulation of DNA end-joining. *Oncogene*. 2007;26(56):7780-7791.
16. von Boehmer H, Melchers F. Checkpoints in lymphocyte development and autoimmune disease. *Nat Immunol*. 2010;11(1):14-20.
17. Vettermann C, Schlissel MS. Allelic exclusion of immunoglobulin genes: models and mechanisms. *Immunol Rev*. 2010;237(1):22-42.
18. Tangye SG, Good KL. Human IgM+CD27+ B cells: memory B cells or "memory" B cells? *J Immunol*. 2007;179(1):13-19.

19. Carsetti R, Kohler G, Lamers MC. Transitional B cells are the target of negative selection in the B cell compartment. *J Exp Med*. 1995;181(6):2129-2140.
20. Sims GP, Ettinger R, Shirota Y, Yarboro CH, Illei GG, Lipsky PE. Identification and characterization of circulating human transitional B cells. *Blood*. 2005;105(11):4390-4398.
21. Cuss AK, Avery DT, Cannons JL, et al. Expansion of functionally immature transitional B cells is associated with human-immunodeficient states characterized by impaired humoral immunity. *J Immunol*. 2006;176(3):1506-1516.
22. Suryani S, Fulcher DA, Santner-Nanan B, et al. Differential expression of CD21 identifies developmentally and functionally distinct subsets of human transitional B cells. *Blood*. 2010;115(3):519-529.
23. Goodnow CC, Vinuesa CG, Randall KL, Mackay F, Brink R. Control systems and decision making for antibody production. *Nat Immunol*. 2010;11(8):681-688.
24. Harwood NE, Batista FD. Early events in B cell activation. *Annu Rev Immunol*. 2010;28:185-210.
25. Krieg AM. CpG motifs in bacterial DNA and their immune effects. *Annu Rev Immunol*. 2002;20:709-760.
26. Janeway CA, Jr., Medzhitov R. Innate immune recognition. *Annu Rev Immunol*. 2002;20:197-216.
27. Glynne R, Akkaraju S, Healy JI, Rayner J, Goodnow CC, Mack DH. How self-tolerance and the immunosuppressive drug FK506 prevent B-cell mitogenesis. *Nature*. 2000;403(6770):672-676.
28. Reif K, Ekland EH, Ohl L, et al. Balanced responsiveness to chemoattractants from adjacent zones determines B-cell position. *Nature*. 2002;416(6876):94-99.
29. Elgueta R, Benson MJ, de Vries VC, Wasiuk A, Guo Y, Noelle RJ. Molecular mechanism and function of CD40/CD40L engagement in the immune system. *Immunol Rev*. 2009;229(1):152-172.
30. Bour-Jordan H, Esensten JH, Martinez-Llordella M, Penaranda C, Stumpf M, Bluestone JA. Intrinsic and extrinsic control of peripheral T-cell tolerance by costimulatory molecules of the CD28/ B7 family. *Immunol Rev*. 2011;241(1):180-205.
31. Banchereau J, de Paoli P, Valle A, Garcia E, Rousset F. Long-term human B cell lines dependent on interleukin-4 and antibody to CD40. *Science*. 1991;251(4989):70-72.
32. O'Nions J, Allday MJ. Proliferation and differentiation in isogenic populations of peripheral B cells activated by Epstein-Barr virus or T cell-derived mitogens. *J Gen Virol*. 2004;85(Pt 4):881-895.
33. Coffey F, Alabyev B, Manser T. Initial clonal expansion of germinal center B cells takes place at the perimeter of follicles. *Immunity*. 2009;30(4):599-609.
34. Victora GD, Nussenzweig MC. Germinal centers. *Annu Rev Immunol*. 2012;30:429-457.
35. Shlomchik MJ, Weisel F. Germinal centers. *Immunol Rev*. 2012;247(1):5-10.
36. Klein U, Dalla-Favera R. Germinal centres: role in B-cell physiology and malignancy. *Nat Rev Immunol*. 2008;8(1):22-33.
37. Shaffer AL, Yu X, He Y, Boldrick J, Chan EP, Staudt LM. BCL-6 represses genes that function in lymphocyte differentiation, inflammation, and cell cycle control. *Immunity*. 2000;13(2):199-212.
38. Shaffer AL, Lin KI, Kuo TC, et al. Blimp-1 orchestrates plasma cell differentiation by extinguishing the

mature B cell gene expression program. *Immunity*. 2002;17(1):51-62.

39. Reljic R, Wagner SD, Peakman LJ, Fearon DT. Suppression of signal transducer and activator of transcription 3-dependent B lymphocyte terminal differentiation by BCL-6. *J Exp Med*. 2000;192(12):1841-1848.
40. Sciammas R, Shaffer AL, Schatz JH, Zhao H, Staudt LM, Singh H. Graded expression of interferon regulatory factor-4 coordinates isotype switching with plasma cell differentiation. *Immunity*. 2006;25(2):225-236.
41. Kuppers R. B cells under influence: transformation of B cells by Epstein-Barr virus. *Nat Rev Immunol*. 2003;3(10):801-812.
42. Muramatsu M, Kinoshita K, Fagarasan S, Yamada S, Shinkai Y, Honjo T. Class switch recombination and hypermutation require activation-induced cytidine deaminase (AID), a potential RNA editing enzyme. *Cell*. 2000;102(5):553-563.
43. Arakawa H, Hauschild J, Buerstedde JM. Requirement of the activation-induced deaminase (AID) gene for immunoglobulin gene conversion. *Science*. 2002;295(5558):1301-1306.
44. Nagaoka H, Muramatsu M, Yamamura N, Kinoshita K, Honjo T. Activation-induced deaminase (AID)-directed hypermutation in the immunoglobulin Smu region: implication of AID involvement in a common step of class switch recombination and somatic hypermutation. *J Exp Med*. 2002;195(4):529-534.
45. Muramatsu M, Sankaranand VS, Anant S, et al. Specific expression of activation-induced cytidine deaminase (AID), a novel member of the RNA-editing deaminase family in germinal center B cells. *J Biol Chem*. 1999;274(26):18470-18476.
46. Stavnezer J, Guikema JE, Schrader CE. Mechanism and regulation of class switch recombination. *Annu Rev Immunol*. 2008;26:261-292.
47. Shlomchik MJ, Weisel F. Germinal center selection and the development of memory B and plasma cells. *Immunol Rev*. 2012;247(1):52-63.
48. Avery DT, Bryant VL, Ma CS, de Waal Malefyt R, Tangye SG. IL-21-induced isotype switching to IgG and IgA by human naive B cells is differentially regulated by IL-4. *J Immunol*. 2008;181(3):1767-1779.
49. Pasqualucci L, Migliazza A, Fracchiolla N, et al. BCL-6 mutations in normal germinal center B cells: evidence of somatic hypermutation acting outside Ig loci. *Proc Natl Acad Sci U S A*. 1998;95(20):11816-11821.
50. Wang CL, Harper RA, Wabl M. Genome-wide somatic hypermutation. *Proc Natl Acad Sci U S A*. 2004;101(19):7352-7356.
51. Liu M, Duke JL, Richter DJ, et al. Two levels of protection for the B cell genome during somatic hypermutation. *Nature*. 2008;451(7180):841-845.
52. Migliazza A, Martinotti S, Chen W, et al. Frequent somatic hypermutation of the 5' noncoding region of the BCL6 gene in B-cell lymphoma. *Proc Natl Acad Sci U S A*. 1995;92(26):12520-12524.
53. Pasqualucci L, Neumeister P, Goossens T, et al. Hypermutation of multiple proto-oncogenes in B-cell diffuse large-cell lymphomas. *Nature*. 2001;412(6844):341-346.

54. Gaidano G, Pasqualucci L, Capello D, et al. Aberrant somatic hypermutation in multiple subtypes of AIDS-associated non-Hodgkin lymphoma. *Blood*. 2003;102(5):1833-1841.

55. Greeve J, Philipsen A, Krause K, et al. Expression of activation-induced cytidine deaminase in human B-cell non-Hodgkin lymphomas. *Blood*. 2003;101(9):3574-3580.

56. Smit LA, Bende RJ, Aten J, Guikema JE, Aarts WM, van Noesel CJ. Expression of activation-induced cytidine deaminase is confined to B-cell non-Hodgkin's lymphomas of germinal-center phenotype. *Cancer Res*. 2003;63(14):3894-3898.

57. Pasqualucci L, Guglielmino R, Houldsworth J, et al. Expression of the AID protein in normal and neoplastic B cells. *Blood*. 2004;104(10):3318-3325.

58. Robbiani DF, Bunting S, Feldhahn N, et al. AID produces DNA double-strand breaks in non-Ig genes and mature B cell lymphomas with reciprocal chromosome translocations. *Mol Cell*. 2009;36(4):631-641.

59. Klein IA, Resch W, Jankovic M, et al. Translocation-capture sequencing reveals the extent and nature of chromosomal rearrangements in B lymphocytes. *Cell*. 2011;147(1):95-106.

60. Chiarle R, Zhang Y, Frock RL, et al. Genome-wide translocation sequencing reveals mechanisms of chromosome breaks and rearrangements in B cells. *Cell*. 2011;147(1):107-119.

61. Maurer D, Fischer GF, Fae I, et al. IgM and IgG but not cytokine secretion is restricted to the CD27+ B lymphocyte subset. *J Immunol*. 1992;148(12):3700-3705.

62. Agematsu K, Nagumo H, Yang FC, et al. B cell subpopulations separated by CD27 and crucial collaboration of CD27+ B cells and helper T cells in immunoglobulin production. *Eur J Immunol*. 1997;27(8):2073-2079.

63. Klein U, Rajewsky K, Kuppers R. Human immunoglobulin (Ig)M+IgD+ peripheral blood B cells expressing the CD27 cell surface antigen carry somatically mutated variable region genes: CD27 as a general marker for somatically mutated (memory) B cells. *J Exp Med*. 1998;188(9):1679-1689.

64. Tangye SG, Liu YJ, Aversa G, Phillips JH, de Vries JE. Identification of functional human splenic memory B cells by expression of CD148 and CD27. *J Exp Med*. 1998;188(9):1691-1703.

65. Crotty S, Aubert RD, Glidewell J, Ahmed R. Tracking human antigen-specific memory B cells: a sensitive and generalized ELISPOT system. *J Immunol Methods*. 2004;286(1-2):111-122.

66. Tangye SG, van de Weerdt BC, Avery DT, Hodgkin PD. CD84 is up-regulated on a major population of human memory B cells and recruits the SH2 domain containing proteins SAP and EAT-2. *Eur J Immunol*. 2002;32(6):1640-1649.

67. Ehrhardt GR, Hsu JT, Gartland L, et al. Expression of the immunoregulatory molecule FcRH4 defines a distinctive tissue-based population of memory B cells. *J Exp Med*. 2005;202(6):783-791.

68. Ma CS, Pittaluga S, Avery DT, et al. Selective generation of functional somatically mutated IgM+CD27+, but not Ig isotype-switched, memory B cells in X-linked lymphoproliferative disease. *J Clin Invest*. 2006;116(2):322-333.

69. Fecteau JF, Cote G, Neron S. A new memory CD27-IgG+ B cell population in peripheral blood expressing VH genes with low frequency of somatic mutation. *J Immunol*. 2006;177(6):3728-3736.

70. Seifert M, Kuppers R. Molecular footprints of a germinal center derivation of human IgM+(IgD+)CD27+ B cells and the dynamics of memory B cell generation. *J Exp Med*. 2009;206(12):2659-2669.

71. Wu YC, Kipling D, Leong HS, Martin V, Ademokun AA, Dunn-Walters DK. High-throughput immunoglobulin repertoire analysis distinguishes between human IgM memory and switched memory B-cell populations. *Blood*. 2010;116(7):1070-1078.

72. Weller S, Faili A, Garcia C, et al. CD40-CD40L independent Ig gene hypermutation suggests a second B cell diversification pathway in humans. *Proc Natl Acad Sci U S A*. 2001;98(3):1166-1170.

73. Weller S, Braun MC, Tan BK, et al. Human blood IgM "memory" B cells are circulating splenic marginal zone B cells harboring a prediversified immunoglobulin repertoire. *Blood*. 2004;104(12):3647-3654.

74. Facchetti F, Appiani C, Salvi L, Levy J, Notarangelo LD. Immunohistologic analysis of ineffective CD40-CD40 ligand interaction in lymphoid tissues from patients with X-linked immunodeficiency with hyper-IgM. Abortive germinal center cell reaction and severe depletion of follicular dendritic cells. *J Immunol*. 1995;154(12):6624-6633.

75. Gulino AV, Notarangelo LD. Hyper IgM syndromes. *Curr Opin Rheumatol*. 2003;15(4):422-429.

76. Agematsu K, Nagumo H, Shinozaki K, et al. Absence of IgD-CD27(+) memory B cell population in X-linked hyper-IgM syndrome. *J Clin Invest*. 1998;102(4):853-860.

77. Ma CS, Hare NJ, Nichols KE, et al. Impaired humoral immunity in X-linked lymphoproliferative disease is associated with defective IL-10 production by CD4+ T cells. *J Clin Invest*. 2005;115(4):1049-1059.

78. Ma CS, Nichols KE, Tangye SG. Regulation of cellular and humoral immune responses by the SLAM and SAP families of molecules. *Annu Rev Immunol*. 2007;25:337-379.

79. Warnatz K, Bossaller L, Salzer U, et al. Human ICOS deficiency abrogates the germinal center reaction and provides a monogenic model for common variable immunodeficiency. *Blood*. 2006;107(8):3045-3052.

80. Kruetzmann S, Rosado MM, Weber H, et al. Human immunoglobulin M memory B cells controlling Streptococcus pneumoniae infections are generated in the spleen. *J Exp Med*. 2003;197(7):939-945.

81. Weller S, Mamani-Matsuda M, Picard C, et al. Somatic diversification in the absence of antigen-driven responses is the hallmark of the IgM+ IgD+ CD27+ B cell repertoire in infants. *J Exp Med*. 2008;205(6):1331-1342.

82. Willenbrock K, Jungnickel B, Hansmann ML, Kuppers R. Human splenic marginal zone B cells lack expression of activation-induced cytidine deaminase. *Eur J Immunol*. 2005;35(10):3002-3007.

83. Wang F. Nonhuman primate models for Epstein-Barr virus infection. *Curr Opin Virol*. 2013;3(3):233-237.

84. Moghaddam A, Rosenzweig M, Lee-Parritz D, Annis B, Johnson RP, Wang F. An animal model for acute and persistent Epstein-Barr virus infection. *Science*. 1997;276(5321):2030-2033.

85. Cho Y, Ramer J, Rivailler P, et al. An Epstein-Barr-related herpesvirus from marmoset lymphomas.

Proc Natl Acad Sci U S A. 2001;98(3):1224-1229.

86. Rivailler P, Cho YG, Wang F. Complete genomic sequence of an Epstein-Barr virus-related herpesvirus naturally infecting a new world primate: a defining point in the evolution of oncogenic lymphocryptoviruses. *J Virol*. 2002;76(23):12055-12068.
87. Kieff E, Rickinson AB. Fields Virology. Vol. 2 (ed 5). Philadelphia, PA: Lippincott Williams & Wilkins; 2007.
88. Baer R, Bankier AT, Biggin MD, et al. DNA sequence and expression of the B95-8 Epstein-Barr virus genome. *Nature*. 1984;310(5974):207-211.
89. Parker BD, Bankier A, Satchwell S, Barrell B, Farrell PJ. Sequence and transcription of Raji Epstein-Barr virus DNA spanning the B95-8 deletion region. *Virology*. 1990;179(1):339-346.
90. Zeng MS, Li DJ, Liu QL, et al. Genomic sequence analysis of Epstein-Barr virus strain GD1 from a nasopharyngeal carcinoma patient. *J Virol*. 2005;79(24):15323-15330.
91. Dolan A, Addison C, Gatherer D, Davison AJ, McGeoch DJ. The genome of Epstein-Barr virus type 2 strain AG876. *Virology*. 2006;350(1):164-170.
92. Liu P, Fang X, Feng Z, et al. Direct sequencing and characterization of a clinical isolate of Epstein-Barr virus from nasopharyngeal carcinoma tissue by using next-generation sequencing technology. *J Virol*. 2011;85(21):11291-11299.
93. Kwok H, Tong AH, Lin CH, et al. Genomic sequencing and comparative analysis of Epstein-Barr virus genome isolated from primary nasopharyngeal carcinoma biopsy. *PLoS One*. 2012;7(5):e36939.
94. Lin Z, Wang X, Strong MJ, et al. Whole-genome sequencing of the Akata and Mutu Epstein-Barr virus strains. *J Virol*. 2013;87(2):1172-1182.
95. Tso KK, Yip KY, Mak CK, et al. Complete genomic sequence of Epstein-Barr virus in nasopharyngeal carcinoma cell line C666-1. *Infect Agent Cancer*. 2013;8(1):29.
96. Tsai MH, Raykova A, Klinke O, et al. Spontaneous lytic replication and epitheliotropism define an Epstein-Barr virus strain found in carcinomas. *Cell Rep*. 2013;5(2):458-470.
97. Sample J, Young L, Martin B, Chatman T, Kieff E, Rickinson A. Epstein-Barr virus types 1 and 2 differ in their EBNA-3A, EBNA-3B, and EBNA-3C genes. *J Virol*. 1990;64(9):4084-4092.
98. Rickinson AB, Young LS, Rowe M. Influence of the Epstein-Barr virus nuclear antigen EBNA 2 on the growth phenotype of virus-transformed B cells. *J Virol*. 1987;61(5):1310-1317.
99. Cohen JI, Wang F, Mannick J, Kieff E. Epstein-Barr virus nuclear protein 2 is a key determinant of lymphocyte transformation. *Proc Natl Acad Sci U S A*. 1989;86(23):9558-9562.
100. Habeshaw G, Yao QY, Bell AI, Morton D, Rickinson AB. Epstein-barr virus nuclear antigen 1 sequences in endemic and sporadic Burkitt's lymphoma reflect virus strains prevalent in different geographic areas. *J Virol*. 1999;73(2):965-975.
101. Mainou BA, Raab-Traub N. LMP1 strain variants: biological and molecular properties. *J Virol*. 2006;80(13):6458-6468.
102. Khanim F, Yao QY, Niedobitek G, Sihota S, Rickinson AB, Young LS. Analysis of Epstein-Barr virus gene polymorphisms in normal donors and in virus-associated tumors from different geographic

locations. *Blood*. 1996;88(9):3491-3501.

103. Khanim F, Dawson C, Meseda CA, Dawson J, Mackett M, Young LS. BHRF1, a viral homologue of the Bcl-2 oncogene, is conserved at both the sequence and functional level in different Epstein-Barr virus isolates. *J Gen Virol*. 1997;78 (Pt 11):2987-2999.
104. Yao QY, Tierney RJ, Croom-Carter D, et al. Frequency of multiple Epstein-Barr virus infections in T-cell-immunocompromised individuals. *J Virol*. 1996;70(8):4884-4894.
105. Sitki-Green D, Covington M, Raab-Traub N. Compartmentalization and transmission of multiple epstein-barr virus strains in asymptomatic carriers. *J Virol*. 2003;77(3):1840-1847.
106. Rowe M, Lear AL, Croom-Carter D, Davies AH, Rickinson AB. Three pathways of Epstein-Barr virus gene activation from EBNA1-positive latency in B lymphocytes. *J Virol*. 1992;66(1):122-131.
107. Sample J, Hummel M, Braun D, Birkenbach M, Kieff E. Nucleotide sequences of mRNAs encoding Epstein-Barr virus nuclear proteins: a probable transcriptional initiation site. *Proc Natl Acad Sci U S A*. 1986;83(14):5096-5100.
108. Speck SH, Pfitzner A, Strominger JL. An Epstein-Barr virus transcript from a latently infected, growth-transformed B-cell line encodes a highly repetitive polypeptide. *Proc Natl Acad Sci U S A*. 1986;83(24):9298-9302.
109. Bodescot M, Perricaudet M. Epstein-Barr virus mRNAs produced by alternative splicing. *Nucleic Acids Res*. 1986;14(17):7103-7114.
110. Woisetschlaeger M, Yandava CN, Furmanski LA, Strominger JL, Speck SH. Promoter switching in Epstein-Barr virus during the initial stages of infection of B lymphocytes. *Proc Natl Acad Sci U S A*. 1990;87(5):1725-1729.
111. Tierney R, Nagra J, Hutchings I, et al. Epstein-Barr virus exploits BSAP/Pax5 to achieve the B-cell specificity of its growth-transforming program. *J Virol*. 2007;81(18):10092-10100.
112. Tierney RJ, Nagra JK, Rowe M, Bell A, Rickinson A. The Epstein-Barr virus BamHI C promoter is not essential for B cell immortalisation but greatly enances B cell growth transformation. *J Virol*. 2014;Submitted.
113. Johannsen E, Koh E, Mosialos G, Tong X, Kieff E, Grossman SR. Epstein-Barr virus nuclear protein 2 transactivation of the latent membrane protein 1 promoter is mediated by J kappa and PU.1. *J Virol*. 1995;69(1):253-262.
114. Wang F, Tsang SF, Kurilla MG, Cohen JI, Kieff E. Epstein-Barr virus nuclear antigen 2 transactivates latent membrane protein LMP1. *J Virol*. 1990;64(7):3407-3416.
115. Zimber-Strobl U, Suentzenich KO, Laux G, et al. Epstein-Barr virus nuclear antigen 2 activates transcription of the terminal protein gene. *J Virol*. 1991;65(1):415-423.
116. Schaefer BC, Strominger JL, Speck SH. Redefining the Epstein-Barr virus-encoded nuclear antigen EBNA-1 gene promoter and transcription initiation site in group I Burkitt lymphoma cell lines. *Proc Natl Acad Sci U S A*. 1995;92(23):10565-10569.
117. Nonkwelo C, Skinner J, Bell A, Rickinson A, Sample J. Transcription start sites downstream of the Epstein-Barr virus (EBV) Fp promoter in early-passage Burkitt lymphoma cells define a fourth

promoter for expression of the EBV EBNA-1 protein. *J Virol*. 1996;70(1):623-627.

118. Kelly G, Bell A, Rickinson A. Epstein-Barr virus-associated Burkitt lymphomagenesis selects for downregulation of the nuclear antigen EBNA2. *Nat Med*. 2002;8(10):1098-1104.
119. Kelly GL, Milner AE, Tierney RJ, et al. Epstein-Barr virus nuclear antigen 2 (EBNA2) gene deletion is consistently linked with EBNA3A, -3B, and -3C expression in Burkitt's lymphoma cells and with increased resistance to apoptosis. *J Virol*. 2005;79(16):10709-10717.
120. Kelly GL, Milner AE, Baldwin GS, Bell AI, Rickinson AB. Three restricted forms of Epstein-Barr virus latency counteracting apoptosis in c-myc-expressing Burkitt lymphoma cells. *Proc Natl Acad Sci U S A*. 2006;103(40):14935-14940.
121. Kelly GL, Long HM, Stylianou J, et al. An Epstein-Barr virus anti-apoptotic protein constitutively expressed in transformed cells and implicated in burkitt lymphomagenesis: the Wp/BHRF1 link. *PLoS Pathog*. 2009;5(3):e1000341.
122. Rowe M, Kelly GL, Bell AI, Rickinson AB. Burkitt's lymphoma: the Rosetta Stone deciphering Epstein-Barr virus biology. *Semin Cancer Biol*. 2009;19(6):377-388.
123. Rowe M, Rowe DT, Gregory CD, et al. Differences in B cell growth phenotype reflect novel patterns of Epstein-Barr virus latent gene expression in Burkitt's lymphoma cells. *EMBO J*. 1987;6(9):2743-2751.
124. Gregory CD, Rowe M, Rickinson AB. Different Epstein-Barr virus-B cell interactions in phenotypically distinct clones of a Burkitt's lymphoma cell line. *J Gen Virol*. 1990;71 (Pt 7):1481-1495.
125. Fahraeus R, Fu HL, Ernberg I, et al. Expression of Epstein-Barr virus-encoded proteins in nasopharyngeal carcinoma. *Int J Cancer*. 1988;42(3):329-338.
126. Young LS, Dawson CW, Clark D, et al. Epstein-Barr virus gene expression in nasopharyngeal carcinoma. *J Gen Virol*. 1988;69 (Pt 5):1051-1065.
127. Gilligan K, Sato H, Rajadurai P, et al. Novel transcription from the Epstein-Barr virus terminal EcoRI fragment, DIJhet, in a nasopharyngeal carcinoma. *J Virol*. 1990;64(10):4948-4956.
128. Imai S, Koizumi S, Sugiura M, et al. Gastric carcinoma: monoclonal epithelial malignant cells expressing Epstein-Barr virus latent infection protein. *Proc Natl Acad Sci U S A*. 1994;91(19):9131-9135.
129. Sugiura M, Imai S, Tokunaga M, et al. Transcriptional analysis of Epstein-Barr virus gene expression in EBV-positive gastric carcinoma: unique viral latency in the tumour cells. *Br J Cancer*. 1996;74(4):625-631.
130. Niedobitek G, Deacon EM, Young LS, Herbst H, Hamilton-Dutoit SJ, Pallesen G. Epstein-Barr virus gene expression in Hodgkin's disease. *Blood*. 1991;78(6):1628-1630.
131. Pallesen G, Sandvej K, Hamilton-Dutoit SJ, Rowe M, Young LS. Activation of Epstein-Barr virus replication in Hodgkin and Reed-Sternberg cells. *Blood*. 1991;78(5):1162-1165.
132. Chiang AK, Tao Q, Srivastava G, Ho FC. Nasal NK- and T-cell lymphomas share the same type of Epstein-Barr virus latency as nasopharyngeal carcinoma and Hodgkin's disease. *Int J Cancer*. 1996;68(3):285-290.
133. Yates J, Warren N, Reisman D, Sugden B. A cis-acting element from the Epstein-Barr viral genome

that permits stable replication of recombinant plasmids in latently infected cells. *Proc Natl Acad Sci U S A*. 1984;81(12):3806-3810.

134. Reisman D, Sugden B. trans activation of an Epstein-Barr viral transcriptional enhancer by the Epstein-Barr viral nuclear antigen 1. *Mol Cell Biol*. 1986;6(11):3838-3846.
135. Sugden B, Warren N. A promoter of Epstein-Barr virus that can function during latent infection can be transactivated by EBNA-1, a viral protein required for viral DNA replication during latent infection. *J Virol*. 1989;63(6):2644-2649.
136. Altmann M, Pich D, Ruiss R, Wang J, Sugden B, Hammerschmidt W. Transcriptional activation by EBV nuclear antigen 1 is essential for the expression of EBV's transforming genes. *Proc Natl Acad Sci U S A*. 2006;103(38):14188-14193.
137. Gahn TA, Sugden B. An EBNA-1-dependent enhancer acts from a distance of 10 kilobase pairs to increase expression of the Epstein-Barr virus LMP gene. *J Virol*. 1995;69(4):2633-2636.
138. Sample J, Henson EB, Sample C. The Epstein-Barr virus nuclear protein 1 promoter active in type I latency is autoregulated. *J Virol*. 1992;66(8):4654-4661.
139. Sung NS, Wilson J, Davenport M, Sista ND, Pagano JS. Reciprocal regulation of the Epstein-Barr virus BamHI-F promoter by EBNA-1 and an E2F transcription factor. *Mol Cell Biol*. 1994;14(11):7144-7152.
140. Yin Y, Manoury B, Fahraeus R. Self-inhibition of synthesis and antigen presentation by Epstein-Barr virus-encoded EBNA1. *Science*. 2003;301(5638):1371-1374.
141. Tellam J, Smith C, Rist M, et al. Regulation of protein translation through mRNA structure influences MHC class I loading and T cell recognition. *Proc Natl Acad Sci U S A*. 2008;105(27):9319-9324.
142. Hammerschmidt W, Sugden B. Genetic analysis of immortalizing functions of Epstein-Barr virus in human B lymphocytes. *Nature*. 1989;340(6232):393-397.
143. Zimber-Strobl U, Kremmer E, Grasser F, Marschall G, Laux G, Bornkamm GW. The Epstein-Barr virus nuclear antigen 2 interacts with an EBNA2 responsive cis-element of the terminal protein 1 gene promoter. *EMBO J*. 1993;12(1):167-175.
144. Grossman SR, Johannsen E, Tong X, Yalamanchili R, Kieff E. The Epstein-Barr virus nuclear antigen 2 transactivator is directed to response elements by the J kappa recombination signal binding protein. *Proc Natl Acad Sci U S A*. 1994;91(16):7568-7572.
145. Hsieh JJ, Hayward SD. Masking of the CBF1/RBPJ kappa transcriptional repression domain by Epstein-Barr virus EBNA2. *Science*. 1995;268(5210):560-563.
146. Kaiser C, Laux G, Eick D, Jochner N, Bornkamm GW, Kempkes B. The proto-oncogene c-myc is a direct target gene of Epstein-Barr virus nuclear antigen 2. *J Virol*. 1999;73(5):4481-4484.
147. Finke J, Rowe M, Kallin B, et al. Monoclonal and polyclonal antibodies against Epstein-Barr virus nuclear antigen 5 (EBNA-5) detect multiple protein species in Burkitt's lymphoma and lymphoblastoid cell lines. *J Virol*. 1987;61(12):3870-3878.
148. Allan GJ, Rowe DT. Size and stability of the Epstein-Barr virus major internal repeat (IR-1) in Burkitt's lymphoma and lymphoblastoid cell lines. *Virology*. 1989;173(2):489-498.
149. Tierney RJ, Kao KY, Nagra JK, Rickinson AB. Epstein-Barr virus BamHI W repeat number limits

EBNA2/EBNA-LP coexpression in newly infected B cells and the efficiency of B-cell transformation: a rationale for the multiple W repeats in wild-type virus strains. *J Virol*. 2011;85(23):12362-12375.

150. Mannick JB, Cohen JI, Birkenbach M, Marchini A, Kieff E. The Epstein-Barr virus nuclear protein encoded by the leader of the EBNA RNAs is important in B-lymphocyte transformation. *J Virol*. 1991;65(12):6826-6837.
151. Sinclair AJ, Palmero I, Peters G, Farrell PJ. EBNA-2 and EBNA-LP cooperate to cause G0 to G1 transition during immortalization of resting human B lymphocytes by Epstein-Barr virus. *EMBO J*. 1994;13(14):3321-3328.
152. Nitsche F, Bell A, Rickinson A. Epstein-Barr virus leader protein enhances EBNA-2-mediated transactivation of latent membrane protein 1 expression: a role for the W1W2 repeat domain. *J Virol*. 1997;71(9):6619-6628.
153. Peng R, Tan J, Ling PD. Conserved regions in the Epstein-Barr virus leader protein define distinct domains required for nuclear localization and transcriptional cooperation with EBNA2. *J Virol*. 2000;74(21):9953-9963.
154. Anderton E, Yee J, Smith P, Crook T, White RE, Allday MJ. Two Epstein-Barr virus (EBV) oncoproteins cooperate to repress expression of the proapoptotic tumour-suppressor Bim: clues to the pathogenesis of Burkitt's lymphoma. *Oncogene*. 2008;27(4):421-433.
155. Skalska L, White RE, Franz M, Ruhmann M, Allday MJ. Epigenetic repression of p16(INK4A) by latent Epstein-Barr virus requires the interaction of EBNA3A and EBNA3C with CtBP. *PLoS Pathog*. 2010;6(6):e1000951.
156. Maruo S, Zhao B, Johannsen E, Kieff E, Zou J, Takada K. Epstein-Barr virus nuclear antigens 3C and 3A maintain lymphoblastoid cell growth by repressing p16INK4A and p14ARF expression. *Proc Natl Acad Sci U S A*. 2011;108(5):1919-1924.
157. Krauer KG, Burgess A, Buck M, Flanagan J, Sculley TB, Gabrielli B. The EBNA-3 gene family proteins disrupt the G2/M checkpoint. *Oncogene*. 2004;23(7):1342-1353.
158. Nikitin PA, Yan CM, Forte E, et al. An ATM/Chk2-mediated DNA damage-responsive signaling pathway suppresses Epstein-Barr virus transformation of primary human B cells. *Cell Host Microbe*. 2010;8(6):510-522.
159. Jiang H, Cho YG, Wang F. Structural, functional, and genetic comparisons of Epstein-Barr virus nuclear antigen 3A, 3B, and 3C homologues encoded by the rhesus lymphocryptovirus. *J Virol*. 2000;74(13):5921-5932.
160. White RE, Ramer PC, Naresh KN, et al. EBNA3B-deficient EBV promotes B cell lymphomagenesis in humanized mice and is found in human tumors. *J Clin Invest*. 2012;122(4):1487-1502.
161. Graham JP, Arcipowski KM, Bishop GA. Differential B-lymphocyte regulation by CD40 and its viral mimic, latent membrane protein 1. *Immunol Rev*. 2010;237(1):226-248.
162. Kaye KM, Izumi KM, Kieff E. Epstein-Barr virus latent membrane protein 1 is essential for B-lymphocyte growth transformation. *Proc Natl Acad Sci U S A*. 1993;90(19):9150-9154.
163. Kilger E, Kieser A, Baumann M, Hammerschmidt W. Epstein-Barr virus-mediated B-cell proliferation

is dependent upon latent membrane protein 1, which simulates an activated CD40 receptor. *EMBO J*. 1998;17(6):1700-1709.

164. Dirmeier U, Neuhierl B, Kilger E, Reisbach G, Sandberg ML, Hammerschmidt W. Latent membrane protein 1 is critical for efficient growth transformation of human B cells by epstein-barr virus. *Cancer Res*. 2003;63(11):2982-2989.
165. Wang D, Liebowitz D, Kieff E. An EBV membrane protein expressed in immortalized lymphocytes transforms established rodent cells. *Cell*. 1985;43(3 Pt 2):831-840.
166. Baichwal VR, Sugden B. Transformation of Balb 3T3 cells by the BNLF-1 gene of Epstein-Barr virus. *Oncogene*. 1988;2(5):461-467.
167. Moorthy RK, Thorley-Lawson DA. All three domains of the Epstein-Barr virus-encoded latent membrane protein LMP-1 are required for transformation of rat-1 fibroblasts. *J Virol*. 1993;67(3):1638-1646.
168. Devergne O, Hatzivassiliou E, Izumi KM, et al. Association of TRAF1, TRAF2, and TRAF3 with an Epstein-Barr virus LMP1 domain important for B-lymphocyte transformation: role in NF-kappaB activation. *Mol Cell Biol*. 1996;16(12):7098-7108.
169. Devergne O, Cahir McFarland ED, Mosialos G, Izumi KM, Ware CF, Kieff E. Role of the TRAF binding site and NF-kappaB activation in Epstein-Barr virus latent membrane protein 1-induced cell gene expression. *J Virol*. 1998;72(10):7900-7908.
170. Izumi KM, Kieff ED. The Epstein-Barr virus oncogene product latent membrane protein 1 engages the tumor necrosis factor receptor-associated death domain protein to mediate B lymphocyte growth transformation and activate NF-kappaB. *Proc Natl Acad Sci U S A*. 1997;94(23):12592-12597.
171. Floettmann JE, Rowe M. Epstein-Barr virus latent membrane protein-1 (LMP1) C-terminus activation region 2 (CTAR2) maps to the far C-terminus and requires oligomerisation for NF-kappaB activation. *Oncogene*. 1997;15(15):1851-1858.
172. Huen DS, Henderson SA, Croom-Carter D, Rowe M. The Epstein-Barr virus latent membrane protein-1 (LMP1) mediates activation of NF-kappa B and cell surface phenotype via two effector regions in its carboxy-terminal cytoplasmic domain. *Oncogene*. 1995;10(3):549-560.
173. Mitchell T, Sugden B. Stimulation of NF-kappa B-mediated transcription by mutant derivatives of the latent membrane protein of Epstein-Barr virus. *J Virol*. 1995;69(5):2968-2976.
174. Brodeur SR, Cheng G, Baltimore D, Thorley-Lawson DA. Localization of the major NF-kappaB-activating site and the sole TRAF3 binding site of LMP-1 defines two distinct signaling motifs. *J Biol Chem*. 1997;272(32):19777-19784.
175. Kieser A, Kilger E, Gires O, Ueffing M, Kolch W, Hammerschmidt W. Epstein-Barr virus latent membrane protein-1 triggers AP-1 activity via the c-Jun N-terminal kinase cascade. *EMBO J*. 1997;16(21):6478-6485.
176. Eliopoulos AG, Young LS. Activation of the cJun N-terminal kinase (JNK) pathway by the Epstein-Barr virus-encoded latent membrane protein 1 (LMP1). *Oncogene*. 1998;16(13):1731-1742.
177. Gires O, Kohlhuber F, Kilger E, et al. Latent membrane protein 1 of Epstein-Barr virus interacts with

JAK3 and activates STAT proteins. *EMBO J*. 1999;18(11):3064-3073.

178. Dawson CW, Tramountanis G, Eliopoulos AG, Young LS. Epstein-Barr virus latent membrane protein 1 (LMP1) activates the phosphatidylinositol 3-kinase/Akt pathway to promote cell survival and induce actin filament remodeling. *J Biol Chem*. 2003;278(6):3694-3704.
179. Mosialos G, Birkenbach M, Yalamanchili R, VanArsdale T, Ware C, Kieff E. The Epstein-Barr virus transforming protein LMP1 engages signaling proteins for the tumor necrosis factor receptor family. *Cell*. 1995;80(3):389-399.
180. Gires O, Zimber-Strobl U, Gonnella R, et al. Latent membrane protein 1 of Epstein-Barr virus mimics a constitutively active receptor molecule. *EMBO J*. 1997;16(20):6131-6140.
181. Zimber-Strobl U, Kempkes B, Marschall G, et al. Epstein-Barr virus latent membrane protein (LMP1) is not sufficient to maintain proliferation of B cells but both it and activated CD40 can prolong their survival. *EMBO J*. 1996;15(24):7070-7078.
182. Uchida J, Yasui T, Takaoka-Shichijo Y, et al. Mimicry of CD40 signals by Epstein-Barr virus LMP1 in B lymphocyte responses. *Science*. 1999;286(5438):300-303.
183. Henderson S, Rowe M, Gregory C, et al. Induction of bcl-2 expression by Epstein-Barr virus latent membrane protein 1 protects infected B cells from programmed cell death. *Cell*. 1991;65(7):1107-1115.
184. Finke J, Fritzen R, Ternes P, et al. Expression of bcl-2 in Burkitt's lymphoma cell lines: induction by latent Epstein-Barr virus genes. *Blood*. 1992;80(2):459-469.
185. Eliopoulos AG, Gallagher NJ, Blake SM, Dawson CW, Young LS. Activation of the p38 mitogen-activated protein kinase pathway by Epstein-Barr virus-encoded latent membrane protein 1 coregulates interleukin-6 and interleukin-8 production. *J Biol Chem*. 1999;274(23):16085-16096.
186. Vockerodt M, Haier B, Buttgereit P, Tesch H, Kube D. The Epstein-Barr virus latent membrane protein 1 induces interleukin-10 in Burkitt's lymphoma cells but not in Hodgkin's cells involving the p38/SAPK2 pathway. *Virology*. 2001;280(2):183-198.
187. Longnecker R. Epstein-Barr virus latency: LMP2, a regulator or means for Epstein-Barr virus persistence? *Adv Cancer Res*. 2000;79:175-200.
188. Bieging KT, Swanson-Mungerson M, Amick AC, Longnecker R. Epstein-Barr virus in Burkitt's lymphoma: a role for latent membrane protein 2A. *Cell Cycle*. 2010;9(5):901-908.
189. Fruehling S, Longnecker R. The immunoreceptor tyrosine-based activation motif of Epstein-Barr virus LMP2A is essential for blocking BCR-mediated signal transduction. *Virology*. 1997;235(2):241-251.
190. Miller CL, Longnecker R, Kieff E. Epstein-Barr virus latent membrane protein 2A blocks calcium mobilization in B lymphocytes. *J Virol*. 1993;67(6):3087-3094.
191. Miller CL, Lee JH, Kieff E, Longnecker R. An integral membrane protein (LMP2) blocks reactivation of Epstein-Barr virus from latency following surface immunoglobulin crosslinking. *Proc Natl Acad Sci U S A*. 1994;91(2):772-776.
192. Caldwell RG, Wilson JB, Anderson SJ, Longnecker R. Epstein-Barr virus LMP2A drives B cell development and survival in the absence of normal B cell receptor signals. *Immunity*. 1998;9(3):405-411.

193. Portis T, Longnecker R. Epstein-Barr virus (EBV) LMP2A mediates B-lymphocyte survival through constitutive activation of the Ras/PI3K/Akt pathway. *Oncogene*. 2004;23(53):8619-8628.

194. Mancao C, Hammerschmidt W. Epstein-Barr virus latent membrane protein 2A is a B-cell receptor mimic and essential for B-cell survival. *Blood*. 2007;110(10):3715-3721.

195. Rovedo M, Longnecker R. Epstein-barr virus latent membrane protein 2B (LMP2B) modulates LMP2A activity. *J Virol*. 2007;81(1):84-94.

196. Rechsteiner MP, Berger C, Zauner L, et al. Latent membrane protein 2B regulates susceptibility to induction of lytic Epstein-Barr virus infection. *J Virol*. 2008;82(4):1739-1747.

197. Marchini A, Tomkinson B, Cohen JI, Kieff E. BHRF1, the Epstein-Barr virus gene with homology to Bc12, is dispensable for B-lymphocyte transformation and virus replication. *J Virol*. 1991;65(11):5991-6000.

198. Arrand JR, Rymo L. Characterization of the major Epstein-Barr virus-specific RNA in Burkitt lymphoma-derived cells. *J Virol*. 1982;41(2):376-389.

199. Lerner MR, Andrews NC, Miller G, Steitz JA. Two small RNAs encoded by Epstein-Barr virus and complexed with protein are precipitated by antibodies from patients with systemic lupus erythematosus. *Proc Natl Acad Sci U S A*. 1981;78(2):805-809.

200. Wu TC, Mann RB, Charache P, et al. Detection of EBV gene expression in Reed-Sternberg cells of Hodgkin's disease. *Int J Cancer*. 1990;46(5):801-804.

201. Swaminathan S, Tomkinson B, Kieff E. Recombinant Epstein-Barr virus with small RNA (EBER) genes deleted transforms lymphocytes and replicates in vitro. *Proc Natl Acad Sci U S A*. 1991;88(4):1546-1550.

202. Iwakiri D, Takada K. Role of EBERs in the pathogenesis of EBV infection. *Adv Cancer Res*. 2010;107:119-136.

203. Nanbo A, Inoue K, Adachi-Takasawa K, Takada K. Epstein-Barr virus RNA confers resistance to interferon-alpha-induced apoptosis in Burkitt's lymphoma. *EMBO J*. 2002;21(5):954-965.

204. Ruf IK, Lackey KA, Warudkar S, Sample JT. Protection from interferon-induced apoptosis by Epstein-Barr virus small RNAs is not mediated by inhibition of PKR. *J Virol*. 2005;79(23):14562-14569.

205. Wong HL, Wang X, Chang RC, et al. Stable expression of EBERs in immortalized nasopharyngeal epithelial cells confers resistance to apoptotic stress. *Mol Carcinog*. 2005;44(2):92-101.

206. Iwakiri D, Eizuru Y, Tokunaga M, Takada K. Autocrine growth of Epstein-Barr virus-positive gastric carcinoma cells mediated by an Epstein-Barr virus-encoded small RNA. *Cancer Res*. 2003;63(21):7062-7067.

207. Yang L, Aozasa K, Oshimi K, Takada K. Epstein-Barr virus (EBV)-encoded RNA promotes growth of EBV-infected T cells through interleukin-9 induction. *Cancer Res*. 2004;64(15):5332-5337.

208. Laing KG, Elia A, Jeffrey I, et al. In vivo effects of the Epstein-Barr virus small RNA EBER-1 on protein synthesis and cell growth regulation. *Virology*. 2002;297(2):253-269.

209. Yamamoto N, Takizawa T, Iwanaga Y, Shimizu N. Malignant transformation of B lymphoma cell line BJAB by Epstein-Barr virus-encoded small RNAs. *FEBS Lett*. 2000;484(2):153-158.

210. Repellin CE, Tsimbouri PM, Philbey AW, Wilson JB. Lymphoid hyperplasia and lymphoma in transgenic mice expressing the small non-coding RNA, EBER1 of Epstein-Barr virus. *PLoS One*. 2010;5(2):e9092.

211. Sadler RH, Raab-Traub N. Structural analyses of the Epstein-Barr virus BamHI A transcripts. *J Virol*. 1995;69(2):1132-1141.

212. Fabian MR, Sonenberg N, Filipowicz W. Regulation of mRNA translation and stability by microRNAs. *Annu Rev Biochem*. 2010;79:351-379.

213. Klinke O, Feederle R, Delecluse HJ. Genetics of Epstein-Barr virus microRNAs. *Semin Cancer Biol*. 2014;26:52-59.

214. Countryman J, Miller G. Activation of expression of latent Epstein-Barr herpesvirus after gene transfer with a small cloned subfragment of heterogeneous viral DNA. *Proc Natl Acad Sci U S A*. 1985;82(12):4085-4089.

215. Chevallier-Greco A, Manet E, Chavrier P, Mosnier C, Daillie J, Sergeant A. Both Epstein-Barr virus (EBV)-encoded trans-acting factors, EB1 and EB2, are required to activate transcription from an EBV early promoter. *EMBO J*. 1986;5(12):3243-3249.

216. Biggin M, Bodescot M, Perricaudet M, Farrell P. Epstein-Barr virus gene expression in P3HR1-superinfected Raji cells. *J Virol*. 1987;61(10):3120-3132.

217. Countryman J, Jenson H, Seibl R, Wolf H, Miller G. Polymorphic proteins encoded within BZLF1 of defective and standard Epstein-Barr viruses disrupt latency. *J Virol*. 1987;61(12):3672-3679.

218. Rooney CM, Rowe DT, Ragot T, Farrell PJ. The spliced BZLF1 gene of Epstein-Barr virus (EBV) transactivates an early EBV promoter and induces the virus productive cycle. *J Virol*. 1989;63(7):3109-3116.

219. Lieberman PM, Hardwick JM, Sample J, Hayward GS, Hayward SD. The zta transactivator involved in induction of lytic cycle gene expression in Epstein-Barr virus-infected lymphocytes binds to both AP-1 and ZRE sites in target promoter and enhancer regions. *J Virol*. 1990;64(3):1143-1155.

220. Hardwick JM, Lieberman PM, Hayward SD. A new Epstein-Barr virus transactivator, R, induces expression of a cytoplasmic early antigen. *J Virol*. 1988;62(7):2274-2284.

221. Hammerschmidt W, Sugden B. Identification and characterization of oriLyt, a lytic origin of DNA replication of Epstein-Barr virus. *Cell*. 1988;55(3):427-433.

222. Edson CM, Thorley-Lawson DA. Epstein-Barr virus membrane antigens: characterization, distribution, and strain differences. *J Virol*. 1981;39(1):172-184.

223. Biggin M, Farrell PJ, Barrell BG. Transcription and DNA sequence of the BamHI L fragment of B95-8 Epstein-Barr virus. *EMBO J*. 1984;3(5):1083-1090.

224. Gong M, Ooka T, Matsuo T, Kieff E. Epstein-Barr virus glycoprotein homologous to herpes simplex virus gB. *J Virol*. 1987;61(2):499-508.

225. Fingeroth JD, Weis JJ, Tedder TF, Strominger JL, Biro PA, Fearon DT. Epstein-Barr virus receptor of human B lymphocytes is the C3d receptor CR2. *Proc Natl Acad Sci U S A*. 1984;81(14):4510-4514.

226. Li Q, Spriggs MK, Kovats S, et al. Epstein-Barr virus uses HLA class II as a cofactor for infection of B

lymphocytes. *J Virol*. 1997;71(6):4657-4662.

227. Wang X, Hutt-Fletcher LM. Epstein-Barr virus lacking glycoprotein gp42 can bind to B cells but is not able to infect. *J Virol*. 1998;72(1):158-163.
228. Shannon-Lowe C, Baldwin G, Feederle R, Bell A, Rickinson A, Delecluse HJ. Epstein-Barr virus-induced B-cell transformation: quantitating events from virus binding to cell outgrowth. *J Gen Virol*. 2005;86(Pt 11):3009-3019.
229. Siemer D, Kurth J, Lang S, Lehnerdt G, Stanelle J, Kuppers R. EBV transformation overrides gene expression patterns of B cell differentiation stages. *Mol Immunol*. 2008;45(11):3133-3141.
230. Calender A, Billaud M, Aubry JP, Banchereau J, Vuillaume M, Lenoir GM. Epstein-Barr virus (EBV) induces expression of B-cell activation markers on in vitro infection of EBV-negative B-lymphoma cells. *Proc Natl Acad Sci U S A*. 1987;84(22):8060-8064.
231. Wang F, Gregory CD, Rowe M, et al. Epstein-Barr virus nuclear antigen 2 specifically induces expression of the B-cell activation antigen CD23. *Proc Natl Acad Sci U S A*. 1987;84(10):3452-3456.
232. Cordier M, Calender A, Billaud M, et al. Stable transfection of Epstein-Barr virus (EBV) nuclear antigen 2 in lymphoma cells containing the EBV P3HR1 genome induces expression of B-cell activation molecules CD21 and CD23. *J Virol*. 1990;64(3):1002-1013.
233. Alfieri C, Birkenbach M, Kieff E. Early events in Epstein-Barr virus infection of human B lymphocytes. *Virology*. 1991;181(2):595-608.
234. Sugden B, Mark W. Clonal transformation of adult human leukocytes by Epstein-Barr virus. *J Virol*. 1977;23(3):503-508.
235. Henderson E, Miller G, Robinson J, Heston L. Efficiency of transformation of lymphocytes by Epstein-Barr virus. *Virology*. 1977;76(1):152-163.
236. Heath E, Begue-Pastor N, Chaganti S, et al. Epstein-Barr virus infection of naive B cells in vitro frequently selects clones with mutated immunoglobulin genotypes: implications for virus biology. *PLoS Pathog*. 2012;8(5):e1002697.
237. Lacoste S, Wiechec E, Dos Santos Silva AG, et al. Chromosomal rearrangements after ex vivo Epstein-Barr virus (EBV) infection of human B cells. *Oncogene*. 2010;29(4):503-515.
238. Ryan JL, Kaufmann WK, Raab-Traub N, Oglesbee SE, Carey LA, Gulley ML. Clonal evolution of lymphoblastoid cell lines. *Lab Invest*. 2006;86(11):1193-1200.
239. Plagnol V, Uz E, Wallace C, et al. Extreme clonality in lymphoblastoid cell lines with implications for allele specific expression analyses. *PLoS One*. 2008;3(8):e2966.
240. Derheimer FA, Kastan MB. Multiple roles of ATM in monitoring and maintaining DNA integrity. *FEBS Lett*. 2010;584(17):3675-3681.
241. Cimprich KA, Cortez D. ATR: an essential regulator of genome integrity. *Nat Rev Mol Cell Biol*. 2008;9(8):616-627.
242. Halazonetis TD, Gorgoulis VG, Bartek J. An oncogene-induced DNA damage model for cancer development. *Science*. 2008;319(5868):1352-1355.
243. Vafa O, Wade M, Kern S, et al. c-Myc can induce DNA damage, increase reactive oxygen species, and

mitigate p53 function: a mechanism for oncogene-induced genetic instability. *Mol Cell*. 2002;9(5):1031-1044.

244. Epeldegui M, Hung YP, McQuay A, Ambinder RF, Martinez-Maza O. Infection of human B cells with Epstein-Barr virus results in the expression of somatic hypermutation-inducing molecules and in the accrual of oncogene mutations. *Mol Immunol*. 2007;44(5):934-942.
245. He B, Raab-Traub N, Casali P, Cerutti A. EBV-encoded latent membrane protein 1 cooperates with BAFF/BLyS and APRIL to induce T cell-independent Ig heavy chain class switching. *J Immunol*. 2003;171(10):5215-5224.
246. Gil Y, Levy-Nabot S, Steinitz M, Laskov R. Somatic mutations and activation-induced cytidine deaminase (AID) expression in established rheumatoid factor-producing lymphoblastoid cell line. *Mol Immunol*. 2007;44(4):494-505.
247. Turnell AS, Grand RJ. DNA viruses and the cellular DNA-damage response. *J Gen Virol*. 2012;93(Pt 10):2076-2097.
248. Chaurushiya MS, Weitzman MD. Viral manipulation of DNA repair and cell cycle checkpoints. *DNA Repair (Amst)*. 2009;8(9):1166-1176.
249. Mietz JA, Unger T, Huibregtse JM, Howley PM. The transcriptional transactivation function of wild-type p53 is inhibited by SV40 large T-antigen and by HPV-16 E6 oncoprotein. *EMBO J*. 1992;11(13):5013-5020.
250. McCarthy SA, Symonds HS, Van Dyke T. Regulation of apoptosis in transgenic mice by simian virus 40 T antigen-mediated inactivation of p53. *Proc Natl Acad Sci U S A*. 1994;91(9):3979-3983.
251. Debbas M, White E. Wild-type p53 mediates apoptosis by E1A, which is inhibited by E1B. *Genes Dev*. 1993;7(4):546-554.
252. Scheffner M, Werness BA, Huibregtse JM, Levine AJ, Howley PM. The E6 oncoprotein encoded by human papillomavirus types 16 and 18 promotes the degradation of p53. *Cell*. 1990;63(6):1129-1136.
253. Kudoh A, Fujita M, Zhang L, et al. Epstein-Barr virus lytic replication elicits ATM checkpoint signal transduction while providing an S-phase-like cellular environment. *J Biol Chem*. 2005;280(9):8156-8163.
254. Sato Y, Shirata N, Kudoh A, et al. Expression of Epstein-Barr virus BZLF1 immediate-early protein induces p53 degradation independent of MDM2, leading to repression of p53-mediated transcription. *Virology*. 2009;388(1):204-211.
255. Wu CC, Liu MT, Chang YT, et al. Epstein-Barr virus DNase (BGLF5) induces genomic instability in human epithelial cells. *Nucleic Acids Res*. 2010;38(6):1932-1949.
256. Allday MJ, Inman GJ, Crawford DH, Farrell PJ. DNA damage in human B cells can induce apoptosis, proceeding from G1/S when p53 is transactivation competent and G2/M when it is transactivation defective. *EMBO J*. 1995;14(20):4994-5005.
257. Allday MJ, Sinclair A, Parker G, Crawford DH, Farrell PJ. Epstein-Barr virus efficiently immortalizes human B cells without neutralizing the function of p53. *EMBO J*. 1995;14(7):1382-1391.
258. Kamranvar SA, Gruhne B, Szeles A, Masucci MG. Epstein-Barr virus promotes genomic instability in

Burkitt's lymphoma. *Oncogene*. 2007;26(35):5115-5123.

259. Gruhne B, Sompallae R, Masucci MG. Three Epstein-Barr virus latency proteins independently promote genomic instability by inducing DNA damage, inhibiting DNA repair and inactivating cell cycle checkpoints. *Oncogene*. 2009;28(45):3997-4008.
260. Gruhne B, Sompallae R, Marescotti D, Kamranvar SA, Gastaldello S, Masucci MG. The Epstein-Barr virus nuclear antigen-1 promotes genomic instability via induction of reactive oxygen species. *Proc Natl Acad Sci U S A*. 2009;106(7):2313-2318.
261. Kamranvar SA, Masucci MG. The Epstein-Barr virus nuclear antigen-1 promotes telomere dysfunction via induction of oxidative stress. *Leukemia*. 2011;25(6):1017-1025.
262. Kamranvar SA, Chen X, Masucci MG. Telomere dysfunction and activation of alternative lengthening of telomeres in B-lymphocytes infected by Epstein-Barr virus. *Oncogene*. 2013;32(49):5522-5530.
263. Henle G, Henle W, Clifford P, et al. Antibodies to Epstein-Barr virus in Burkitt's lymphoma and control groups. *J Natl Cancer Inst*. 1969;43(5):1147-1157.
264. Niederman JC, Evans AS, Subrahmanyan L, McCollum RW. Prevalence, incidence and persistence of EB virus antibody in young adults. *N Engl J Med*. 1970;282(7):361-365.
265. Henle G, Henle W. Observations on Childhood Infections with the Epstein-Barr Virus. *Journal of Infectious Diseases*. 1970;121(3):303-310.
266. Young LS, Rickinson AB. Epstein-Barr virus: 40 years on. *Nat Rev Cancer*. 2004;4(10):757-768.
267. Crawford DH, Macsween KF, Higgins CD, et al. A cohort study among university students: identification of risk factors for Epstein-Barr virus seroconversion and infectious mononucleosis. *Clin Infect Dis*. 2006;43(3):276-282.
268. Balfour HH, Jr., Odumade OA, Schmeling DO, et al. Behavioral, virologic, and immunologic factors associated with acquisition and severity of primary Epstein-Barr virus infection in university students. *J Infect Dis*. 2013;207(1):80-88.
269. Hoagland J. The transmission of infectious mononucleosis. *Am J Med Sci*. 1955;229(3):262-272.
270. Gerber P, Lucas S, Nonoyama M, Perlin E, Goldstein LI. Oral excretion of Epstein-Barr virus by healthy subjects and patients with infectious mononucleosis. *Lancet*. 1972;2(7785):988-989.
271. Anagnostopoulos I, Hummel M, Kreschel C, Stein H. Morphology, immunophenotype, and distribution of latently and/or productively Epstein-Barr virus-infected cells in acute infectious mononucleosis: implications for the interindividual infection route of Epstein-Barr virus. *Blood*. 1995;85(3):744-750.
272. Kurth J, Spieker T, Wustrow J, et al. EBV-infected B cells in infectious mononucleosis: viral strategies for spreading in the B cell compartment and establishing latency. *Immunity*. 2000;13(4):485-495.
273. Niedobitek G, Agathanggelou A, Herbst H, Whitehead L, Wright DH, Young LS. Epstein-Barr virus (EBV) infection in infectious mononucleosis: virus latency, replication and phenotype of EBV-infected cells. *J Pathol*. 1997;182(2):151-159.
274. Tomkinson BE, Wagner DK, Nelson DL, Sullivan JL. Activated lymphocytes during acute Epstein-Barr virus infection. *J Immunol*. 1987;139(11):3802-3807.
275. Silins SL, Cross SM, Elliott SL, et al. Development of Epstein-Barr virus-specific memory T cell

receptor clonotypes in acute infectious mononucleosis. *J Exp Med*. 1996;184(5):1815-1824.

276. Silins SL, Sherritt MA, Silleri JM, et al. Asymptomatic primary Epstein-Barr virus infection occurs in the absence of blood T-cell repertoire perturbations despite high levels of systemic viral load. *Blood*. 2001;98(13):3739-3744.
277. Balfour HH, Jr., Holman CJ, Hokanson KM, et al. A prospective clinical study of Epstein-Barr virus and host interactions during acute infectious mononucleosis. *J Infect Dis*. 2005;192(9):1505-1512.
278. Sixbey JW, Nedrud JG, Raab-Traub N, Hanes RA, Pagano JS. Epstein-Barr virus replication in oropharyngeal epithelial cells. *N Engl J Med*. 1984;310(19):1225-1230.
279. Conley ME, Rohrer J, Minegishi Y. X-linked agammaglobulinemia. *Clin Rev Allergy Immunol*. 2000;19(2):183-204.
280. Faulkner GC, Burrows SR, Khanna R, Moss DJ, Bird AG, Crawford DH. X-Linked agammaglobulinemia patients are not infected with Epstein-Barr virus: implications for the biology of the virus. *J Virol*. 1999;73(2):1555-1564.
281. Turk SM, Jiang R, Chesnokova LS, Hutt-Fletcher LM. Antibodies to gp350/220 enhance the ability of Epstein-Barr virus to infect epithelial cells. *J Virol*. 2006;80(19):9628-9633.
282. Shannon-Lowe CD, Neuhierl B, Baldwin G, Rickinson AB, Delecluse HJ. Resting B cells as a transfer vehicle for Epstein-Barr virus infection of epithelial cells. *Proc Natl Acad Sci U S A*. 2006;103(18):7065-7070.
283. Imai S, Nishikawa J, Takada K. Cell-to-cell contact as an efficient mode of Epstein-Barr virus infection of diverse human epithelial cells. *J Virol*. 1998;72(5):4371-4378.
284. Haque T, Johannessen I, Dombagoda D, et al. A mouse monoclonal antibody against Epstein-Barr virus envelope glycoprotein 350 prevents infection both in vitro and in vivo. *J Infect Dis*. 2006;194(5):584-587.
285. Paul JR, Bunnell WW. The presence of heterophile antibodies in infectious mononucleosis. *The American Journal of the Medical Sciences*. 1932;183(1):90-103.
286. Davidsohn I. Serologic diagnosis of infectious mononucleosis. *JAMA*. 1937;108(4):289-295.
287. Hislop AD, Taylor GS, Sauce D, Rickinson AB. Cellular responses to viral infection in humans: lessons from Epstein-Barr virus. *Annu Rev Immunol*. 2007;25:587-617.
288. McNally JM, Welsh RM. Bystander T cell activation and attrition. *Curr Top Microbiol Immunol*. 2002;263:29-41.
289. Sutkowski N, Conrad B, Thorley-Lawson DA, Huber BT. Epstein-Barr virus transactivates the human endogenous retrovirus HERV-K18 that encodes a superantigen. *Immunity*. 2001;15(4):579-589.
290. Callan MF, Steven N, Krausa P, et al. Large clonal expansions of CD8+ T cells in acute infectious mononucleosis. *Nat Med*. 1996;2(8):906-911.
291. Steven NM, Leese AM, Annels NE, Lee SP, Rickinson AB. Epitope focusing in the primary cytotoxic T cell response to Epstein-Barr virus and its relationship to T cell memory. *J Exp Med*. 1996;184(5):1801-1813.
292. Steven NM, Annels NE, Kumar A, Leese AM, Kurilla MG, Rickinson AB. Immediate early and early

lytic cycle proteins are frequent targets of the Epstein-Barr virus-induced cytotoxic T cell response. *J Exp Med*. 1997;185(9):1605-1617.

293. Callan MF, Tan L, Annels N, et al. Direct visualization of antigen-specific CD8+ T cells during the primary immune response to Epstein-Barr virus In vivo. *J Exp Med*. 1998;187(9):1395-1402.
294. Hoshino Y, Morishima T, Kimura H, Nishikawa K, Tsurumi T, Kuzushima K. Antigen-driven expansion and contraction of CD8+-activated T cells in primary EBV infection. *J Immunol*. 1999;163(10):5735-5740.
295. Catalina MD, Sullivan JL, Bak KR, Luzuriaga K. Differential evolution and stability of epitope-specific CD8(+) T cell responses in EBV infection. *J Immunol*. 2001;167(8):4450-4457.
296. Hislop AD, Annels NE, Gudgeon NH, Leese AM, Rickinson AB. Epitope-specific evolution of human CD8(+) T cell responses from primary to persistent phases of Epstein-Barr virus infection. *J Exp Med*. 2002;195(7):893-905.
297. Pudney VA, Leese AM, Rickinson AB, Hislop AD. CD8+ immunodominance among Epstein-Barr virus lytic cycle antigens directly reflects the efficiency of antigen presentation in lytically infected cells. *J Exp Med*. 2005;201(3):349-360.
298. Woodberry T, Suscovich TJ, Henry LM, et al. Differential targeting and shifts in the immunodominance of Epstein-Barr virus--specific CD8 and CD4 T cell responses during acute and persistent infection. *J Infect Dis*. 2005;192(9):1513-1524.
299. Hislop AD, Kuo M, Drake-Lee AB, et al. Tonsillar homing of Epstein-Barr virus-specific CD8+ T cells and the virus-host balance. *J Clin Invest*. 2005;115(9):2546-2555.
300. Callan MF, Fazou C, Yang H, et al. CD8(+) T-cell selection, function, and death in the primary immune response in vivo. *J Clin Invest*. 2000;106(10):1251-1261.
301. Tamaru Y, Miyawaki T, Iwai K, et al. Absence of bcl-2 expression by activated CD45RO+ T lymphocytes in acute infectious mononucleosis supporting their susceptibility to programmed cell death. *Blood*. 1993;82(2):521-527.
302. Long HM, Chagoury OL, Leese AM, et al. MHC II tetramers visualize human CD4+ T cell responses to Epstein-Barr virus infection and demonstrate atypical kinetics of the nuclear antigen EBNA1 response. *J Exp Med*. 2013;210(5):933-949.
303. Williams H, McAulay K, Macsween KF, et al. The immune response to primary EBV infection: a role for natural killer cells. *Br J Haematol*. 2005;129(2):266-274.
304. Lotz M, Tsoukas CD, Fong S, Carson DA, Vaughan JH. Regulation of Epstein-Barr virus infection by recombinant interferons. Selected sensitivity to interferon-gamma. *Eur J Immunol*. 1985;15(5):520-525.
305. Chijioke O, Muller A, Feederle R, et al. Human natural killer cells prevent infectious mononucleosis features by targeting lytic Epstein-Barr virus infection. *Cell Rep*. 2013;5(6):1489-1498.
306. Strowig T, Brilot F, Arrey F, et al. Tonsilar NK cells restrict B cell transformation by the Epstein-Barr virus via IFN-gamma. *PLoS Pathog*. 2008;4(2):e27.
307. Lunemann A, Vanoaica LD, Azzi T, Nadal D, Munz C. A distinct subpopulation of human NK cells restricts B cell transformation by EBV. *J Immunol*. 2013;191(10):4989-4995.

308. Yao QY, Rickinson AB, Epstein MA. A re-examination of the Epstein-Barr virus carrier state in healthy seropositive individuals. *Int J Cancer*. 1985;35(1):35-42.

309. Niedobitek G, Young LS, Lau R, et al. Epstein-Barr virus infection in oral hairy leukoplakia: virus replication in the absence of a detectable latent phase. *J Gen Virol*. 1991;72 (Pt 12):3035-3046.

310. Young LS, Lau R, Rowe M, et al. Differentiation-associated expression of the Epstein-Barr virus BZLF1 transactivator protein in oral hairy leukoplakia. *J Virol*. 1991;65(6):2868-2874.

311. Niedobitek G, Herbst H, Young LS, et al. Patterns of Epstein-Barr virus infection in non-neoplastic lymphoid tissue. *Blood*. 1992;79(10):2520-2526.

312. Tao Q, Srivastava G, Chan AC, Chung LP, Loke SL, Ho FC. Evidence for lytic infection by Epstein-Barr virus in mucosal lymphocytes instead of nasopharyngeal epithelial cells in normal individuals. *J Med Virol*. 1995;45(1):71-77.

313. Khan G, Miyashita EM, Yang B, Babcock GJ, Thorley-Lawson DA. Is EBV persistence in vivo a model for B cell homeostasis? *Immunity*. 1996;5(2):173-179.

314. Miyashita EM, Yang B, Lam KM, Crawford DH, Thorley-Lawson DA. A novel form of Epstein-Barr virus latency in normal B cells in vivo. *Cell*. 1995;80(4):593-601.

315. Miyashita EM, Yang B, Babcock GJ, Thorley-Lawson DA. Identification of the site of Epstein-Barr virus persistence in vivo as a resting B cell. *J Virol*. 1997;71(7):4882-4891.

316. Babcock GJ, Decker LL, Volk M, Thorley-Lawson DA. EBV persistence in memory B cells in vivo. *Immunity*. 1998;9(3):395-404.

317. Laichalk LL, Hochberg D, Babcock GJ, Freeman RB, Thorley-Lawson DA. The dispersal of mucosal memory B cells: evidence from persistent EBV infection. *Immunity*. 2002;16(5):745-754.

318. Souza TA, Stollar BD, Sullivan JL, Luzuriaga K, Thorley-Lawson DA. Peripheral B cells latently infected with Epstein-Barr virus display molecular hallmarks of classical antigen-selected memory B cells. *Proc Natl Acad Sci U S A*. 2005;102(50):18093-18098.

319. Qu L, Rowe DT. Epstein-Barr virus latent gene expression in uncultured peripheral blood lymphocytes. *J Virol*. 1992;66(6):3715-3724.

320. Tierney RJ, Steven N, Young LS, Rickinson AB. Epstein-Barr virus latency in blood mononuclear cells: analysis of viral gene transcription during primary infection and in the carrier state. *J Virol*. 1994;68(11):7374-7385.

321. Babcock GJ, Hochberg D, Thorley-Lawson AD. The expression pattern of Epstein-Barr virus latent genes in vivo is dependent upon the differentiation stage of the infected B cell. *Immunity*. 2000;13(4):497-506.

322. Benninger-Doring G, Pepperl S, Deml L, Modrow S, Wolf H, Jilg W. Frequency of CD8(+) T lymphocytes specific for lytic and latent antigens of Epstein-Barr virus in healthy virus carriers. *Virology*. 1999;264(2):289-297.

323. Saulquin X, Ibisch C, Peyrat MA, et al. A global appraisal of immunodominant CD8 T cell responses to Epstein-Barr virus and cytomegalovirus by bulk screening. *Eur J Immunol*. 2000;30(9):2531-2539.

324. Bihl F, Frahm N, Di Giammarino L, et al. Impact of HLA-B alleles, epitope binding affinity, functional

avidity, and viral coinfection on the immunodominance of virus-specific CTL responses. *J Immunol*. 2006;176(7):4094-4101.

325. Leen A, Meij P, Redchenko I, et al. Differential immunogenicity of Epstein-Barr virus latent-cycle proteins for human CD4(+) T-helper 1 responses. *J Virol*. 2001;75(18):8649-8659.
326. Long HM, Haigh TA, Gudgeon NH, et al. CD4+ T-cell responses to Epstein-Barr virus (EBV) latent-cycle antigens and the recognition of EBV-transformed lymphoblastoid cell lines. *J Virol*. 2005;79(8):4896-4907.
327. Long HM, Leese AM, Chagoury OL, et al. Cytotoxic CD4+ T cell responses to EBV contrast with CD8 responses in breadth of lytic cycle antigen choice and in lytic cycle recognition. *J Immunol*. 2011;187(1):92-101.
328. Merlo A, Turrini R, Bobisse S, et al. Virus-Specific Cytotoxic CD4+ T Cells for the Treatment of EBV-Related Tumors. *The Journal of Immunology*. 2010;184(10):5895-5902.
329. Thorley-Lawson DA. Epstein-Barr virus: exploiting the immune system. *Nat Rev Immunol*. 2001;1(1):75-82.
330. Joseph AM, Babcock GJ, Thorley-Lawson DA. Cells expressing the Epstein-Barr virus growth program are present in and restricted to the naive B-cell subset of healthy tonsils. *J Virol*. 2000;74(21):9964-9971.
331. Chaganti S, Heath EM, Bergler W, et al. Epstein-Barr virus colonization of tonsillar and peripheral blood B-cell subsets in primary infection and persistence. *Blood*. 2009;113(25):6372-6381.
332. Thorley-Lawson DA, Gross A. Persistence of the Epstein-Barr virus and the origins of associated lymphomas. *N Engl J Med*. 2004;350(13):1328-1337.
333. Crawford DH, Ando I. EB virus induction is associated with B-cell maturation. *Immunology*. 1986;59(3):405-409.
334. Niedobitek G, Agathanggelou A, Steven N, Young LS. Epstein-Barr virus (EBV) in infectious mononucleosis: detection of the virus in tonsillar B lymphocytes but not in desquamated oropharyngeal epithelial cells. *Mol Pathol*. 2000;53(1):37-42.
335. Laichalk LL, Thorley-Lawson DA. Terminal differentiation into plasma cells initiates the replicative cycle of Epstein-Barr virus in vivo. *J Virol*. 2005;79(2):1296-1307.
336. Ehlin-Henriksson B, Gordon J, Klein G. B-lymphocyte subpopulations are equally susceptible to Epstein-Barr virus infection, irrespective of immunoglobulin isotype expression. *Immunology*. 2003;108(4):427-430.
337. Roughan JE, Torgbor C, Thorley-Lawson DA. Germinal center B cells latently infected with Epstein-Barr virus proliferate extensively but do not increase in number. *J Virol*. 2010;84(2):1158-1168.
338. Chaganti S, Ma CS, Bell AI, et al. Epstein-Barr virus persistence in the absence of conventional memory B cells: IgM+IgD+CD27+ B cells harbor the virus in X-linked lymphoproliferative disease patients. *Blood*. 2008;112(3):672-679.
339. Taylor AL, Watson CJ, Bradley JA. Immunosuppressive agents in solid organ transplantation: Mechanisms of action and therapeutic efficacy. *Crit Rev Oncol Hematol*. 2005;56(1):23-46.

340. Fishman JA. Infection in solid-organ transplant recipients. *N Engl J Med*. 2007;357(25):2601-2614.

341. Chapman JR, Webster AC, Wong G. Cancer in the transplant recipient. *Cold Spring Harb Perspect Med*. 2013;3(7).

342. Mackall C, Fry T, Gress R, Peggs K, Storek J, Toubert A. Background to hematopoietic cell transplantation, including post transplant immune recovery. *Bone Marrow Transplant*. 2009;44(8):457-462.

343. Powles R, Mehta J, Kulkarni S, et al. Allogeneic blood and bone-marrow stem-cell transplantation in haematological malignant diseases: a randomised trial. *Lancet*. 2000;355(9211):1231-1237.

344. Storek J, Dawson MA, Storer B, et al. Immune reconstitution after allogeneic marrow transplantation compared with blood stem cell transplantation. *Blood*. 2001;97(11):3380-3389.

345. Kolb HJ. Graft-versus-leukemia effects of transplantation and donor lymphocytes. *Blood*. 2008;112(12):4371-4383.

346. Ruggeri L, Mancusi A, Burchielli E, et al. NK cell alloreactivity and allogeneic hematopoietic stem cell transplantation. *Blood Cells Mol Dis*. 2008;40(1):84-90.

347. Chang YJ, Huang XJ. Donor lymphocyte infusions for relapse after allogeneic transplantation: when, if and for whom? *Blood Rev*. 2013;27(1):55-62.

348. Markey KA, MacDonald KP, Hill GR. The biology of graft-versus-host disease: experimental systems instructing clinical practice. *Blood*. 2014;124(3):354-362.

349. Bacigalupo A. Antilymphocyte/thymocyte globulin for graft versus host disease prophylaxis: efficacy and side effects. *Bone Marrow Transplant*. 2005;35(3):225-231.

350. Finke J, Bethge WA, Schmoor C, et al. Standard graft-versus-host disease prophylaxis with or without anti-T-cell globulin in haematopoietic cell transplantation from matched unrelated donors: a randomised, open-label, multicentre phase 3 trial. *Lancet Oncol*. 2009;10(9):855-864.

351. Waldmann H, Polliak A, Hale G, et al. Elimination of graft-versus-host disease by in-vitro depletion of alloreactive lymphocytes with a monoclonal rat anti-human lymphocyte antibody (CAMPATH-1). *Lancet*. 1984;2(8401):483-486.

352. Kanda J, Lopez RD, Rizzieri DA. Alemtuzumab for the prevention and treatment of graft-versus-host disease. *Int J Hematol*. 2011;93(5):586-593.

353. Tomblyn M, Chiller T, Einsele H, et al. Guidelines for preventing infectious complications among hematopoietic cell transplantation recipients: a global perspective. *Biol Blood Marrow Transplant*. 2009;15(10):1143-1238.

354. Storek J, Geddes M, Khan F, et al. Reconstitution of the immune system after hematopoietic stem cell transplantation in humans. *Semin Immunopathol*. 2008;30(4):425-437.

355. Lewin SR, Heller G, Zhang L, et al. Direct evidence for new T-cell generation by patients after either T-cell-depleted or unmodified allogeneic hematopoietic stem cell transplantations. *Blood*. 2002;100(6):2235-2242.

356. Mackall CL, Granger L, Sheard MA, Cepeda R, Gress RE. T-cell regeneration after bone marrow transplantation: differential CD45 isoform expression on thymic-derived versus thymic-independent

progeny. *Blood*. 1993;82(8):2585-2594.

357. Jameson SC. Maintaining the norm: T-cell homeostasis. *Nat Rev Immunol*. 2002;2(8):547-556.

358. Mackall CL, Bare CV, Granger LA, Sharrow SO, Titus JA, Gress RE. Thymic-independent T cell regeneration occurs via antigen-driven expansion of peripheral T cells resulting in a repertoire that is limited in diversity and prone to skewing. *J Immunol*. 1996;156(12):4609-4616.

359. Weinberg K, Annett G, Kashyap A, Lenarsky C, Forman SJ, Parkman R. The effect of thymic function on immunocompetence following bone marrow transplantation. *Biol Blood Marrow Transplant*. 1995;1(1):18-23.

360. Dumont-Girard F, Roux E, van Lier RA, et al. Reconstitution of the T-cell compartment after bone marrow transplantation: restoration of the repertoire by thymic emigrants. *Blood*. 1998;92(11):4464-4471.

361. Mackall CL, Fleisher TA, Brown MR, et al. Distinctions between CD8+ and CD4+ T-cell regenerative pathways result in prolonged T-cell subset imbalance after intensive chemotherapy. *Blood*. 1997;89(10):3700-3707.

362. Bemark M, Holmqvist J, Abrahamsson J, Mellgren K. Translational Mini-Review Series on B cell subsets in disease. Reconstitution after haematopoietic stem cell transplantation - revelation of B cell developmental pathways and lineage phenotypes. *Clin Exp Immunol*. 2012;167(1):15-25.

363. Storek J, Witherspoon RP, Storb R. Reconstitution of membrane IgD- (mIgD-) B cells after marrow transplantation lags behind the reconstitution of mIgD+ B cells. *Blood*. 1997;89(1):350-351.

364. Avanzini MA, Locatelli F, Dos Santos C, et al. B lymphocyte reconstitution after hematopoietic stem cell transplantation: functional immaturity and slow recovery of memory CD27+ B cells. *Exp Hematol*. 2005;33(4):480-486.

365. Suzuki I, Milner EC, Glas AM, et al. Immunoglobulin heavy chain variable region gene usage in bone marrow transplant recipients: lack of somatic mutation indicates a maturational arrest. *Blood*. 1996;87(5):1873-1880.

366. Sarantopoulos S, Stevenson KE, Kim HT, et al. Altered B-cell homeostasis and excess BAFF in human chronic graft-versus-host disease. *Blood*. 2009;113(16):3865-3874.

367. Marie-Cardine A, Divay F, Dutot I, et al. Transitional B cells in humans: characterization and insight from B lymphocyte reconstitution after hematopoietic stem cell transplantation. *Clin Immunol*. 2008;127(1):14-25.

368. Auffermann-Gretzinger S, Lossos IS, Vayntrub TA, et al. Rapid establishment of dendritic cell chimerism in allogeneic hematopoietic cell transplant recipients. *Blood*. 2002;99(4):1442-1448.

369. van Tol MJ, Gerritsen EJ, de Lange GG, et al. The origin of IgG production and homogeneous IgG components after allogeneic bone marrow transplantation. *Blood*. 1996;87(2):818-826.

370. Wahren B, Gahrton G, Linde A, et al. Transfer and persistence of viral antibody-producing cells in bone marrow transplantation. *J Infect Dis*. 1984;150(3):358-365.

371. Ljungman P, Wiklund-Hammarsten M, Duraj V, et al. Response to tetanus toxoid immunization after allogeneic bone marrow transplantation. *J Infect Dis*. 1990;162(2):496-500.

372. Atkinson K, Storb R, Prentice RL, et al. Analysis of late infections in 89 long-term survivors of bone marrow transplantation. *Blood*. 1979;53(4):720-731.

373. Engelhard D, Cordonnier C, Shaw PJ, et al. Early and late invasive pneumococcal infection following stem cell transplantation: a European Bone Marrow Transplantation survey. *Br J Haematol*. 2002;117(2):444-450.

374. Winston DJ, Schiffman G, Wang DC, et al. Pneumococcal infections after human bone-marrow transplantation. *Ann Intern Med*. 1979;91(6):835-841.

375. Ljungman P, Engelhard D, de la Camara R, et al. Vaccination of stem cell transplant recipients: recommendations of the Infectious Diseases Working Party of the EBMT. *Bone Marrow Transplant*. 2005;35(8):737-746.

376. Dilly SA, Sloane JP. Cellular composition of the spleen after human allogeneic bone marrow transplantation. *J Pathol*. 1988;155(2):151-160.

377. Sale GE, Alavaikko M, Schaefers KM, Mahan CT. Abnormal CD4:CD8 ratios and delayed germinal center reconstitution in lymph nodes of human graft recipients with graft-versus-host disease (GVHD): an immunohistological study. *Exp Hematol*. 1992;20(8):1017-1021.

378. Storek J, Witherspoon RP, Webb D, Storb R. Lack of B cells precursors in marrow transplant recipients with chronic graft-versus-host disease. *Am J Hematol*. 1996;52(2):82-89.

379. Storek J, Wells D, Dawson MA, Storer B, Maloney DG. Factors influencing B lymphopoiesis after allogeneic hematopoietic cell transplantation. *Blood*. 2001;98(2):489-491.

380. Crawford DH, Edwards JM, Sweny P, Hoffbrand AV, Janossy G. Studies on long-term T-cell-mediated immunity to Epstein-Barr virus in immunosuppressed renal allograft recipients. *Int J Cancer*. 1981;28(6):705-709.

381. Yao QY, Rickinson AB, Gaston JS, Epstein MA. In vitro analysis of the Epstein-Barr virus: host balance in long-term renal allograft recipients. *Int J Cancer*. 1985;35(1):43-49.

382. Lucas KG, Small TN, Heller G, Dupont B, O'Reilly RJ. The development of cellular immunity to Epstein-Barr virus after allogeneic bone marrow transplantation. *Blood*. 1996;87(6):2594-2603.

383. Chakrabarti S, Milligan DW, Pillay D, et al. Reconstitution of the Epstein-Barr virus-specific cytotoxic T-lymphocyte response following T-cell-depleted myeloablative and nonmyeloablative allogeneic stem cell transplantation. *Blood*. 2003;102(3):839-842.

384. Gulley ML, Tang W. Using Epstein-Barr viral load assays to diagnose, monitor, and prevent posttransplant lymphoproliferative disorder. *Clin Microbiol Rev*. 2010;23(2):350-366.

385. Chan KC, Zhang J, Chan AT, et al. Molecular characterization of circulating EBV DNA in the plasma of nasopharyngeal carcinoma and lymphoma patients. *Cancer Res*. 2003;63(9):2028-2032.

386. Babcock GJ, Decker LL, Freeman RB, Thorley-Lawson DA. Epstein-barr virus-infected resting memory B cells, not proliferating lymphoblasts, accumulate in the peripheral blood of immunosuppressed patients. *J Exp Med*. 1999;190(4):567-576.

387. Rose C, Green M, Webber S, Ellis D, Reyes J, Rowe D. Pediatric solid-organ transplant recipients carry chronic loads of Epstein-Barr virus exclusively in the immunoglobulin D-negative B-cell compartment.

J Clin Microbiol. 2001;39(4):1407-1415.

388. Parker A, Bowles K, Bradley JA, et al. Diagnosis of post-transplant lymphoproliferative disorder in solid organ transplant recipients - BCSH and BTS Guidelines. *Br J Haematol*. 2010;149(5):675-692.
389. Opelz G, Dohler B. Lymphomas after solid organ transplantation: a collaborative transplant study report. *Am J Transplant*. 2004;4(2):222-230.
390. Leblond V, Davi F, Charlotte F, et al. Posttransplant lymphoproliferative disorders not associated with Epstein-Barr virus: a distinct entity? *J Clin Oncol*. 1998;16(6):2052-2059.
391. Dotti G, Fiocchi R, Motta T, et al. Epstein-Barr virus-negative lymphoproliferate disorders in long-term survivors after heart, kidney, and liver transplant. *Transplantation*. 2000;69(5):827-833.
392. Landgren O, Gilbert ES, Rizzo JD, et al. Risk factors for lymphoproliferative disorders after allogeneic hematopoietic cell transplantation. *Blood*. 2009;113(20):4992-5001.
393. Birkeland SA, Hamilton-Dutoit S. Is posttransplant lymphoproliferative disorder (PTLD) caused by any specific immunosuppressive drug or by the transplantation per se? *Transplantation*. 2003;76(6):984-988.
394. Swinnen LJ, Costanzo-Nordin MR, Fisher SG, et al. Increased incidence of lymphoproliferative disorder after immunosuppression with the monoclonal antibody OKT3 in cardiac-transplant recipients. *N Engl J Med*. 1990;323(25):1723-1728.
395. Caillard S, Lamy FX, Quelen C, et al. Epidemiology of posttransplant lymphoproliferative disorders in adult kidney and kidney pancreas recipients: report of the French registry and analysis of subgroups of lymphomas. *Am J Transplant*. 2012;12(3):682-693.
396. Fernberg P, Edgren G, Adami J, et al. Time trends in risk and risk determinants of non-Hodgkin lymphoma in solid organ transplant recipients. *Am J Transplant*. 2011;11(11):2472-2482.
397. Duvoux C, Pageaux GP, Vanlemmens C, et al. Risk factors for lymphoproliferative disorders after liver transplantation in adults: an analysis of 480 patients. *Transplantation*. 2002;74(8):1103-1109.
398. Bakker NA, van Imhoff GW, Verschuuren EA, et al. HLA antigens and post renal transplant lymphoproliferative disease: HLA-B matching is critical. *Transplantation*. 2005;80(5):595-599.
399. Dharnidharka VR, Tejani AH, Ho PL, Harmon WE. Post-transplant lymphoproliferative disorder in the United States: young Caucasian males are at highest risk. *Am J Transplant*. 2002;2(10):993-998.
400. Opelz G, Henderson R. Incidence of non-Hodgkin lymphoma in kidney and heart transplant recipients. *Lancet*. 1993;342(8886-8887):1514-1516.
401. Sampaio MS, Cho YW, Qazi Y, Bunnapradist S, Hutchinson IV, Shah T. Posttransplant malignancies in solid organ adult recipients: an analysis of the U.S. National Transplant Database. *Transplantation*. 2012;94(10):990-998.
402. van Leeuwen MT, Grulich AE, Webster AC, et al. Immunosuppression and other risk factors for early and late non-Hodgkin lymphoma after kidney transplantation. *Blood*. 2009;114(3):630-637.
403. Sampaio MS, Cho YW, Shah T, Bunnapradist S, Hutchinson IV. Impact of Epstein-Barr virus donor and recipient serostatus on the incidence of post-transplant lymphoproliferative disorder in kidney transplant recipients. *Nephrol Dial Transplant*. 2012;27(7):2971-2979.

404. Quinlan SC, Pfeiffer RM, Morton LM, Engels EA. Risk factors for early-onset and late-onset post-transplant lymphoproliferative disorder in kidney recipients in the United States. *Am J Hematol*. 2011;86(2):206-209.

405. Ho M, Miller G, Atchison RW, et al. Epstein-Barr virus infections and DNA hybridization studies in posttransplantation lymphoma and lymphoproliferative lesions: the role of primary infection. *J Infect Dis*. 1985;152(5):876-886.

406. Dharnidharka VR, Sullivan EK, Stablein DM, Tejani AH, Harmon WE. Risk factors for posttransplant lymphoproliferative disorder (PTLD) in pediatric kidney transplantation: a report of the North American Pediatric Renal Transplant Cooperative Study (NAPRTCS). *Transplantation*. 2001;71(8):1065-1068.

407. Hale G, Waldmann H. Risks of developing Epstein-Barr virus-related lymphoproliferative disorders after T-cell-depleted marrow transplants. CAMPATH Users. *Blood*. 1998;91(8):3079-3083.

408. Sundin M, Le Blanc K, Ringden O, et al. The role of HLA mismatch, splenectomy and recipient Epstein-Barr virus seronegativity as risk factors in post-transplant lymphoproliferative disorder following allogeneic hematopoietic stem cell transplantation. *Haematologica*. 2006;91(8):1059-1067.

409. Carpenter B, Dimopoulou M, Manji N, et al. T Cell Depletion with Alemtuzumab Is Associated with a High Incidence of EBV Viraemia but Low Risk of PTLD Following Allogeneic Stem Cell Transplantation. *ASH Annual Meeting Abstracts*. 2008;112(11):1177-.

410. Peric Z, Cahu X, Chevallier P, et al. Features of EBV reactivation after reduced intensity conditioning unrelated umbilical cord blood transplantation. *Bone Marrow Transplant*. 2012;47(2):251-257.

411. Dumas PY, Ruggeri A, Robin M, et al. Incidence and risk factors of EBV reactivation after unrelated cord blood transplantation: a Eurocord and Societe Francaise de Greffe de Moelle-Therapie Cellulaire collaborative study. *Bone Marrow Transplant*. 2013;48(2):253-256.

412. Ho AY, Adams S, Shaikh H, Pagliuca A, Devereux S, Mufti GJ. Fatal donor-derived Epstein-Barr virus-associated post-transplant lymphoproliferative disorder following reduced intensity volunteer-unrelated bone marrow transplant for myelodysplastic syndrome. *Bone Marrow Transplant*. 2002;29(10):867-869.

413. Bordon V, Padalko E, Benoit Y, Dhooge C, Laureys G. Incidence, kinetics, and risk factors of Epstein-Barr virus viremia in pediatric patients after allogeneic stem cell transplantation. *Pediatr Transplant*. 2012;16(2):144-150.

414. Peggs KS, Banerjee L, Thomson K, Mackinnon S. Post transplant lymphoproliferative disorders following reduced intensity conditioning with in vivo T cell depletion. *Bone Marrow Transplant*. 2003;31(8):725-726; author reply 727.

415. Cohen J, Gandhi M, Naik P, et al. Increased incidence of EBV-related disease following paediatric stem cell transplantation with reduced-intensity conditioning. *Br J Haematol*. 2005;129(2):229-239.

416. van der Velden WJ, Mori T, Stevens WB, et al. Reduced PTLD-related mortality in patients experiencing EBV infection following allo-SCT after the introduction of a protocol incorporating pre-emptive rituximab. *Bone Marrow Transplant*. 2013;48(11):1465-1471.

417. Liu Q, Xuan L, Liu H, et al. Molecular monitoring and stepwise preemptive therapy for Epstein-Barr virus viremia after allogeneic stem cell transplantation. *Am J Hematol*. 2013;88(7):550-555.

418. Zallio F, Primon V, Tamiazzo S, et al. Epstein-Barr virus reactivation in allogeneic stem cell transplantation is highly related to cytomegalovirus reactivation. *Clin Transplant*. 2013;27(4):E491-497.

419. Auger S, Orsini M, Ceballos P, et al. Controlled Epstein-Barr virus reactivation after allogeneic transplantation is associated with improved survival. *Eur J Haematol*. 2014;92(5):421-428.

420. Hoegh-Petersen M, Goodyear D, Geddes MN, et al. High incidence of post transplant lymphoproliferative disorder after antithymocyte globulin-based conditioning and ineffective prediction by day 28 EBV-specific T lymphocyte counts. *Bone Marrow Transplant*. 2011;46(8):1104-1112.

421. Swerdlow SH, Campo E, Harris NL. WHO Classification of Tumours of Haematopoietic and Lymphoid Tissues. Lyon, France: IARC Press; 2008.

422. Wu TT, Swerdlow SH, Locker J, et al. Recurrent Epstein-Barr virus-associated lesions in organ transplant recipients. *Hum Pathol*. 1996;27(2):157-164.

423. Chadburn A, Chen JM, Hsu DT, et al. The morphologic and molecular genetic categories of posttransplantation lymphoproliferative disorders are clinically relevant. *Cancer*. 1998;82(10):1978-1987.

424. Lones MA, Mishalani S, Shintaku IP, Weiss LM, Nichols WS, Said JW. Changes in tonsils and adenoids in children with posttransplant lymphoproliferative disorder: report of three cases with early involvement of Waldeyer's ring. *Hum Pathol*. 1995;26(5):525-530.

425. Knowles DM, Cesarman E, Chadburn A, et al. Correlative morphologic and molecular genetic analysis demonstrates three distinct categories of posttransplantation lymphoproliferative disorders. *Blood*. 1995;85(2):552-565.

426. Frizzera G, Hanto DW, Gajl-Peczalska KJ, et al. Polymorphic diffuse B-cell hyperplasias and lymphomas in renal transplant recipients. *Cancer Res*. 1981;41(11 Pt 1):4262-4279.

427. Hanto DW, Gajl-Peczalska KJ, Frizzera G, et al. Epstein-Barr virus (EBV) induced polyclonal and monoclonal B-cell lymphoproliferative diseases occurring after renal transplantation. Clinical, pathologic, and virologic findings and implications for therapy. *Ann Surg*. 1983;198(3):356-369.

428. Harris NL, Ferry JA, Swerdlow SH. Posttransplant lymphoproliferative disorders: summary of Society for Hematopathology Workshop. *Semin Diagn Pathol*. 1997;14(1):8-14.

429. Sun X, Peterson LC, Gong Y, Traynor AE, Nelson BP. Post-transplant plasma cell myeloma and polymorphic lymphoproliferative disorder with monoclonal serum protein occurring in solid organ transplant recipients. *Mod Pathol*. 2004;17(4):389-394.

430. Caillard S, Agodoa LY, Bohen EM, Abbott KC. Myeloma, Hodgkin disease, and lymphoid leukemia after renal transplantation: characteristics, risk factors and prognosis. *Transplantation*. 2006;81(6):888-895.

431. Dockrell DH, Strickler JG, Paya CV. Epstein-Barr virus-induced T cell lymphoma in solid organ transplant recipients. *Clin Infect Dis*. 1998;26(1):180-182.

432. Tsao L, Draoua HY, Mansukhani M, Bhagat G, Alobeid B. EBV-associated, extranodal NK-cell lymphoma, nasal type of the breast, after heart transplantation. *Mod Pathol*. 2004;17(1):125-130.

433. Nalesnik MA, Randhawa P, Demetris AJ, Casavilla A, Fung JJ, Locker J. Lymphoma resembling Hodgkin disease after posttransplant lymphoproliferative disorder in a liver transplant recipient. *Cancer*. 1993;72(9):2568-2573.

434. Rowlings PA, Curtis RE, Passweg JR, et al. Increased incidence of Hodgkin's disease after allogeneic bone marrow transplantation. *J Clin Oncol*. 1999;17(10):3122-3127.

435. Rowe M, Niedobitek G, Young LS. Epstein-Barr virus gene expression in post-transplant lymphoproliferative disorders. *Springer Semin Immunopathol*. 1998;20(3-4):389-403.

436. Young LS, Finerty S, Brooks L, Scullion F, Rickinson AB, Morgan AJ. Epstein-Barr virus gene expression in malignant lymphomas induced by experimental virus infection of cottontop tamarins. *J Virol*. 1989;63(5):1967-1974.

437. Rowe M, Young LS, Crocker J, Stokes H, Henderson S, Rickinson AB. Epstein-Barr virus (EBV)-associated lymphoproliferative disease in the SCID mouse model: implications for the pathogenesis of EBV-positive lymphomas in man. *J Exp Med*. 1991;173(1):147-158.

438. Brink AA, Dukers DF, van den Brule AJ, et al. Presence of Epstein-Barr virus latency type III at the single cell level in post-transplantation lymphoproliferative disorders and AIDS related lymphomas. *J Clin Pathol*. 1997;50(11):911-918.

439. Oudejans JJ, Jiwa M, van den Brule AJ, et al. Detection of heterogeneous Epstein-Barr virus gene expression patterns within individual post-transplantation lymphoproliferative disorders. *Am J Pathol*. 1995;147(4):923-933.

440. Shaknovich R, Basso K, Bhagat G, et al. Identification of rare Epstein-Barr virus infected memory B cells and plasma cells in non-monomorphic post-transplant lymphoproliferative disorders and the signature of viral signaling. *Haematologica*. 2006;91(10):1313-1320.

441. Delecluse HJ, Kremmer E, Rouault JP, Cour C, Bornkamm G, Berger F. The expression of Epstein-Barr virus latent proteins is related to the pathological features of post-transplant lymphoproliferative disorders. *Am J Pathol*. 1995;146(5):1113-1120.

442. Niedobitek G, Mutimer DJ, Williams A, et al. Epstein-Barr virus infection and malignant lymphomas in liver transplant recipients. *Int J Cancer*. 1997;73(4):514-520.

443. Rea D, Fourcade C, Leblond V, et al. Patterns of Epstein-Barr virus latent and replicative gene expression in Epstein-Barr virus B cell lymphoproliferative disorders after organ transplantation. *Transplantation*. 1994;58(3):317-324.

444. Montone KT, Hodinka RL, Salhany KE, Lavi E, Rostami A, Tomaszewski JE. Identification of Epstein-Barr virus lytic activity in post-transplantation lymphoproliferative disease. *Mod Pathol*. 1996;9(6):621-630.

445. Hong GK, Gulley ML, Feng WH, Delecluse HJ, Holley-Guthrie E, Kenney SC. Epstein-Barr virus lytic infection contributes to lymphoproliferative disease in a SCID mouse model. *J Virol*. 2005;79(22):13993-14003.

446. Jones RJ, Seaman WT, Feng WH, et al. Roles of lytic viral infection and IL-6 in early versus late passage lymphoblastoid cell lines and EBV-associated lymphoproliferative disease. *Int J Cancer*. 2007;121(6):1274-1281.

447. Ma SD, Hegde S, Young KH, et al. A new model of Epstein-Barr virus infection reveals an important role for early lytic viral protein expression in the development of lymphomas. *J Virol*. 2011;85(1):165-177.

448. Ma SD, Yu X, Mertz JE, et al. An Epstein-Barr Virus (EBV) mutant with enhanced BZLF1 expression causes lymphomas with abortive lytic EBV infection in a humanized mouse model. *J Virol*. 2012;86(15):7976-7987.

449. Ghobrial IM, Habermann TM, Macon WR, et al. Differences between early and late posttransplant lymphoproliferative disorders in solid organ transplant patients: are they two different diseases? *Transplantation*. 2005;79(2):244-247.

450. Nelson BP, Nalesnik MA, Bahler DW, Locker J, Fung JJ, Swerdlow SH. Epstein-Barr virus-negative post-transplant lymphoproliferative disorders: a distinct entity? *Am J Surg Pathol*. 2000;24(3):375-385.

451. Shimizu N, Tanabe-Tochikura A, Kuroiwa Y, Takada K. Isolation of Epstein-Barr virus (EBV)-negative cell clones from the EBV-positive Burkitt's lymphoma (BL) line Akata: malignant phenotypes of BL cells are dependent on EBV. *J Virol*. 1994;68(9):6069-6073.

452. Srinivas SK, Sample JT, Sixbey JW. Spontaneous loss of viral episomes accompanying Epstein-Barr virus reactivation in a Burkitt's lymphoma cell line. *J Infect Dis*. 1998;177(6):1705-1709.

453. Matsushima AY, Strauchen JA, Lee G, et al. Posttransplantation plasmacytic proliferations related to Kaposi's sarcoma-associated herpesvirus. *Am J Surg Pathol*. 1999;23(11):1393-1400.

454. Kapelushnik J, Ariad S, Benharroch D, et al. Post renal transplantation human herpesvirus 8-associated lymphoproliferative disorder and Kaposi's sarcoma. *Br J Haematol*. 2001;113(2):425-428.

455. Dotti G, Fiocchi R, Motta T, et al. Primary effusion lymphoma after heart transplantation: a new entity associated with human herpesvirus-8. *Leukemia*. 1999;13(5):664-670.

456. Chen W, Huang Q, Zuppan CW, et al. Complete absence of KSHV/HHV-8 in posttransplant lymphoproliferative disorders: an immunohistochemical and molecular study of 52 cases. *Am J Clin Pathol*. 2009;131(5):632-639.

457. Paessler M, Kossev P, Tsai D, et al. Expression of SHP-1 phosphatase indicates post-germinal center cell derivation of B-cell posttransplant lymphoproliferative disorders. *Lab Invest*. 2002;82(11):1599-1606.

458. Brauninger A, Spieker T, Mottok A, Baur AS, Kuppers R, Hansmann ML. Epstein-Barr virus (EBV)-positive lymphoproliferations in post-transplant patients show immunoglobulin V gene mutation patterns suggesting interference of EBV with normal B cell differentiation processes. *Eur J Immunol*. 2003;33(6):1593-1602.

459. Capello D, Cerri M, Muti G, et al. Molecular histogenesis of posttransplantation lymphoproliferative disorders. *Blood*. 2003;102(10):3775-3785.

460. Timms JM, Bell A, Flavell JR, et al. Target cells of Epstein-Barr-virus (EBV)-positive post-transplant

lymphoproliferative disease: similarities to EBV-positive Hodgkin's lymphoma. *Lancet*. 2003;361(9353):217-223.

461. Capello D, Rossi D, Gaidano G. Post-transplant lymphoproliferative disorders: molecular basis of disease histogenesis and pathogenesis. *Hematol Oncol*. 2005;23(2):61-67.
462. Kuppers R. Mechanisms of B-cell lymphoma pathogenesis. *Nat Rev Cancer*. 2005;5(4):251-262.
463. Johnson LR, Nalesnik MA, Swerdlow SH. Impact of Epstein-Barr virus in monomorphic B-cell posttransplant lymphoproliferative disorders: a histogenetic study. *Am J Surg Pathol*. 2006;30(12):1604-1612.
464. Alizadeh AA, Eisen MB, Davis RE, et al. Distinct types of diffuse large B-cell lymphoma identified by gene expression profiling. *Nature*. 2000;403(6769):503-511.
465. Lenz G, Wright G, Dave SS, et al. Stromal gene signatures in large-B-cell lymphomas. *N Engl J Med*. 2008;359(22):2313-2323.
466. Kanzler H, Kuppers R, Hansmann ML, Rajewsky K. Hodgkin and Reed-Sternberg cells in Hodgkin's disease represent the outgrowth of a dominant tumor clone derived from (crippled) germinal center B cells. *J Exp Med*. 1996;184(4):1495-1505.
467. Kuppers R, Rajewsky K, Zhao M, et al. Hodgkin disease: Hodgkin and Reed-Sternberg cells picked from histological sections show clonal immunoglobulin gene rearrangements and appear to be derived from B cells at various stages of development. *Proc Natl Acad Sci U S A*. 1994;91(23):10962-10966.
468. Chadburn A, Suciu-Foca N, Cesarman E, Reed E, Michler RE, Knowles DM. Post-transplantation lymphoproliferative disorders arising in solid organ transplant recipients are usually of recipient origin. *Am J Pathol*. 1995;147(6):1862-1870.
469. Larson RS, Scott MA, McCurley TL, Vnencak-Jones CL. Microsatellite analysis of posttransplant lymphoproliferative disorders: determination of donor/recipient origin and identification of putative lymphomagenic mechanism. *Cancer Res*. 1996;56(19):4378-4381.
470. Weissmann DJ, Ferry JA, Harris NL, Louis DN, Delmonico F, Spiro I. Posttransplantation lymphoproliferative disorders in solid organ recipients are predominantly aggressive tumors of host origin. *Am J Clin Pathol*. 1995;103(6):748-755.
471. Capello D, Rasi S, Oreste P, et al. Molecular characterization of post-transplant lymphoproliferative disorders of donor origin occurring in liver transplant recipients. *J Pathol*. 2009;218(4):478-486.
472. Gong JZ, Bayerl MG, Sandhaus LM, et al. Posttransplant lymphoproliferative disorder after umbilical cord blood transplantation in children. *Am J Surg Pathol*. 2006;30(3):328-336.
473. Zutter MM, Martin PJ, Sale GE, et al. Epstein-Barr virus lymphoproliferation after bone marrow transplantation. *Blood*. 1988;72(2):520-529.
474. Vakiani E, Nandula SV, Subramaniyam S, et al. Cytogenetic analysis of B-cell posttransplant lymphoproliferations validates the World Health Organization classification and suggests inclusion of florid follicular hyperplasia as a precursor lesion. *Hum Pathol*. 2007;38(2):315-325.
475. Djokic M, Le Beau MM, Swinnen LJ, et al. Post-transplant lymphoproliferative disorder subtypes correlate with different recurring chromosomal abnormalities. *Genes Chromosomes Cancer*.

2006;45(3):313-318.

476. Poirel HA, Bernheim A, Schneider A, et al. Characteristic pattern of chromosomal imbalances in posttransplantation lymphoproliferative disorders: correlation with histopathological subcategories and EBV status. *Transplantation*. 2005;80(2):176-184.

477. Locker J, Nalesnik M. Molecular genetic analysis of lymphoid tumors arising after organ transplantation. *Am J Pathol*. 1989;135(6):977-987.

478. Craig FE, Gulley ML, Banks PM. Posttransplantation lymphoproliferative disorders. *Am J Clin Pathol*. 1993;99(3):265-276.

479. Cesarman E, Chadburn A, Liu YF, Migliazza A, Dalla-Favera R, Knowles DM. BCL-6 gene mutations in posttransplantation lymphoproliferative disorders predict response to therapy and clinical outcome. *Blood*. 1998;92(7):2294-2302.

480. Rinaldi A, Capello D, Scandurra M, et al. Single nucleotide polymorphism-arrays provide new insights in the pathogenesis of post-transplant diffuse large B-cell lymphoma. *Br J Haematol*. 2010;149(4):569-577.

481. Kwee I, Capello D, Rinaldi A, et al. Genomic aberrations affecting the outcome of immunodeficiency-related diffuse large B-cell lymphoma. *Leuk Lymphoma*. 2012;53(1):71-76.

482. Craig FE, Johnson LR, Harvey SA, et al. Gene expression profiling of Epstein-Barr virus-positive and -negative monomorphic B-cell posttransplant lymphoproliferative disorders. *Diagn Mol Pathol*. 2007;16(3):158-168.

483. Vakiani E, Basso K, Klein U, et al. Genetic and phenotypic analysis of B-cell post-transplant lymphoproliferative disorders provides insights into disease biology. *Hematol Oncol*. 2008;26(4):199-211.

484. Morscio J, Dierickx D, Tousseyn T. Molecular pathogenesis of B-cell posttransplant lymphoproliferative disorder: what do we know so far? *Clin Dev Immunol*. 2013;2013:150835.

485. VanBuskirk AM, Malik V, Xia D, Pelletier RP. A gene polymorphism associated with posttransplant lymphoproliferative disorder. *Transplant Proc*. 2001;33(1-2):1834.

486. Bogunia-Kubik K, Mlynarczewska A, Jaskula E, Lange A. The presence of IFNG 3/3 genotype in the recipient associates with increased risk for Epstein-Barr virus reactivation after allogeneic haematopoietic stem cell transplantation. *Br J Haematol*. 2006;132(3):326-332.

487. Lee TC, Savoldo B, Barshes NR, et al. Use of cytokine polymorphisms and Epstein-Barr virus viral load to predict development of post-transplant lymphoproliferative disorder in paediatric liver transplant recipients. *Clin Transplant*. 2006;20(3):389-393.

488. Thomas RV, McAulay K, Higgins C, Wilkie G, Crawford DH. Interferon gamma (IFN-gamma) polymorphism in posttransplantation lymphoproliferative disease. *Blood*. 2005;106(4):1502-1503; author reply 1503.

489. Babel N, Vergopoulos A, Trappe RU, et al. Evidence for genetic susceptibility towards development of posttransplant lymphoproliferative disorder in solid organ recipients. *Transplantation*. 2007;84(3):387-391.

490. McAulay KA, Haque T, Crawford DH. Tumour necrosis factor gene polymorphism: a predictive factor for the development of post-transplant lymphoproliferative disease. *Br J Cancer*. 2009;101(6):1019-1027.

491. Kasztelewicz B, Jankowska I, Pawlowska J, Teisseyre J, Dzierzanowska-Fangrat K. The impact of cytokine gene polymorphisms on Epstein-Barr virus infection outcome in pediatric liver transplant recipients. *J Clin Virol*. 2012;55(3):226-232.

492. Pourfarziani V, Einollahi B, Taheri S, Nemati E, Nafar M, Kalantar E. Associations of Human Leukocyte Antigen (HLA) haplotypes with risk of developing lymphoproliferative disorders after renal transplantation. *Ann Transplant*. 2007;12(4):16-22.

493. Subklewe M, Marquis R, Choquet S, et al. Association of human leukocyte antigen haplotypes with posttransplant lymphoproliferative disease after solid organ transplantation. *Transplantation*. 2006;82(8):1093-1100.

494. Reshef R, Luskin MR, Kamoun M, et al. Association of HLA polymorphisms with post-transplant lymphoproliferative disorder in solid-organ transplant recipients. *Am J Transplant*. 2011;11(4):817-825.

495. San-Juan R, Comoli P, Caillard S, Moulin B, Hirsch HH, Meylan P. Epstein-Barr virus-related post-transplant lymphoproliferative disorder in solid organ transplant recipients. *Clin Microbiol Infect*. 2014;20 Suppl 7:109-118.

496. Styczynski J, Reusser P, Einsele H, et al. Management of HSV, VZV and EBV infections in patients with hematological malignancies and after SCT: guidelines from the Second European Conference on Infections in Leukemia. *Bone Marrow Transplant*. 2009;43(10):757-770.

497. Pescovitz MD. Rituximab, an anti-cd20 monoclonal antibody: history and mechanism of action. *Am J Transplant*. 2006;6(5 Pt 1):859-866.

498. van Esser JW, Niesters HG, van der Holt B, et al. Prevention of Epstein-Barr virus-lymphoproliferative disease by molecular monitoring and preemptive rituximab in high-risk patients after allogeneic stem cell transplantation. *Blood*. 2002;99(12):4364-4369.

499. Comoli P, Basso S, Zecca M, et al. Preemptive therapy of EBV-related lymphoproliferative disease after pediatric haploidentical stem cell transplantation. *Am J Transplant*. 2007;7(6):1648-1655.

500. Wagner HJ, Cheng YC, Huls MH, et al. Prompt versus preemptive intervention for EBV lymphoproliferative disease. *Blood*. 2004;103(10):3979-3981.

501. Carpenter B, Haque T, Dimopoulou M, et al. Incidence and dynamics of Epstein-Barr virus reactivation after alemtuzumab-based conditioning for allogeneic hematopoietic stem-cell transplantation. *Transplantation*. 2010;90(5):564-570.

502. Preiksaitis JK, Pang XL, Fox JD, Fenton JM, Caliendo AM, Miller GG. Interlaboratory comparison of epstein-barr virus viral load assays. *Am J Transplant*. 2009;9(2):269-279.

503. Gil L, Styczynski J, Komarnicki M. Strategy of pre-emptive management of Epstein-Barr virus post-transplant lymphoproliferative disorder after stem cell transplantation: results of European transplant centers survey. *Contemp Oncol (Pozn)*. 2012;16(4):338-340.

504. Fryer JF, Heath AB, Wilkinson DE, Minor PD. Collaborative study to evaluate the proposed 1st WHO

International Standard for Epstein-Barr virus (EBV) for nucleic acid amplification (NAT)-based assays. *WHO ECBS Report*. 2011;WHO/BS/11.2172.

505. Clave E, Agbalika F, Bajzik V, et al. Epstein-Barr virus (EBV) reactivation in allogeneic stem-cell transplantation: relationship between viral load, EBV-specific T-cell reconstitution and rituximab therapy. *Transplantation*. 2004;77(1):76-84.
506. Annels NE, Kalpoe JS, Bredius RG, et al. Management of Epstein-Barr virus (EBV) reactivation after allogeneic stem cell transplantation by simultaneous analysis of EBV DNA load and EBV-specific T cell reconstitution. *Clin Infect Dis*. 2006;42(12):1743-1748.
507. Worth A, Conyers R, Cohen J, et al. Pre-emptive rituximab based on viraemia and T cell reconstitution: a highly effective strategy for the prevention of Epstein-Barr virus-associated lymphoproliferative disease following stem cell transplantation. *Br J Haematol*. 2011;155(3):377-385.
508. Parker A, Bowles K, Bradley JA, et al. Management of post-transplant lymphoproliferative disorder in adult solid organ transplant recipients - BCSH and BTS Guidelines. *Br J Haematol*. 2010;149(5):693-705.
509. Tsai DE, Hardy CL, Tomaszewski JE, et al. Reduction in immunosuppression as initial therapy for posttransplant lymphoproliferative disorder: analysis of prognostic variables and long-term follow-up of 42 adult patients. *Transplantation*. 2001;71(8):1076-1088.
510. Reshef R, Vardhanabhuti S, Luskin MR, et al. Reduction of immunosuppression as initial therapy for posttransplantation lymphoproliferative disorder. *Am J Transplant*. 2011;11(2):336-347.
511. Swinnen LJ, LeBlanc M, Grogan TM, et al. Prospective study of sequential reduction in immunosuppression, interferon alpha-2B, and chemotherapy for posttransplantation lymphoproliferative disorder. *Transplantation*. 2008;86(2):215-222.
512. Oertel SH, Verschuuren E, Reinke P, et al. Effect of anti-CD 20 antibody rituximab in patients with post-transplant lymphoproliferative disorder (PTLD). *Am J Transplant*. 2005;5(12):2901-2906.
513. Choquet S, Leblond V, Herbrecht R, et al. Efficacy and safety of rituximab in B-cell post-transplantation lymphoproliferative disorders: results of a prospective multicenter phase 2 study. *Blood*. 2006;107(8):3053-3057.
514. Gonzalez-Barca E, Domingo-Domenech E, Capote FJ, et al. Prospective phase II trial of extended treatment with rituximab in patients with B-cell post-transplant lymphoproliferative disease. *Haematologica*. 2007;92(11):1489-1494.
515. Jain AB, Marcos A, Pokharna R, et al. Rituximab (chimeric anti-CD20 antibody) for posttransplant lymphoproliferative disorder after solid organ transplantation in adults: long-term experience from a single center. *Transplantation*. 2005;80(12):1692-1698.
516. Elstrom RL, Andreadis C, Aqui NA, et al. Treatment of PTLD with rituximab or chemotherapy. *Am J Transplant*. 2006;6(3):569-576.
517. Taylor AL, Bowles KM, Callaghan CJ, et al. Anthracycline-based chemotherapy as first-line treatment in adults with malignant posttransplant lymphoproliferative disorder after solid organ transplantation. *Transplantation*. 2006;82(3):375-381.

518. Buadi FK, Heyman MR, Gocke CD, et al. Treatment and outcomes of post-transplant lymphoproliferative disease: a single institution study. *Am J Hematol*. 2007;82(3):208-214.

519. Trappe R, Oertel S, Leblond V, et al. Sequential treatment with rituximab followed by CHOP chemotherapy in adult B-cell post-transplant lymphoproliferative disorder (PTLD): the prospective international multicentre phase 2 PTLD-1 trial. *Lancet Oncol*. 2012;13(2):196-206.

520. Fox CP, Burns D, Parker AN, et al. EBV-associated post-transplant lymphoproliferative disorder following in vivo T-cell-depleted allogeneic transplantation: clinical features, viral load correlates and prognostic factors in the rituximab era. *Bone Marrow Transplant*. 2014;49(2):280-286.

521. Styczynski J, Gil L, Tridello G, et al. Response to rituximab-based therapy and risk factor analysis in Epstein Barr Virus-related lymphoproliferative disorder after hematopoietic stem cell transplant in children and adults: a study from the Infectious Diseases Working Party of the European Group for Blood and Marrow Transplantation. *Clin Infect Dis*. 2013;57(6):794-802.

522. Burns DM, Crawford DH. Epstein-Barr virus-specific cytotoxic T-lymphocytes for adoptive immunotherapy of post-transplant lymphoproliferative disease. *Blood Rev*. 2004;18(3):193-209.

523. Papadopoulos EB, Ladanyi M, Emanuel D, et al. Infusions of donor leukocytes to treat Epstein-Barr virus-associated lymphoproliferative disorders after allogeneic bone marrow transplantation. *N Engl J Med*. 1994;330(17):1185-1191.

524. O'Reilly RJ, Lacerda JF, Lucas KG, Rosenfield NS, Small TN, Papadopoulos EB. Adoptive cell therapy with donor lymphocytes for EBV-associated lymphomas developing after allogeneic marrow transplants. *Important Adv Oncol*. 1996:149-166.

525. Doubrovina E, Oflaz-Sozmen B, Prockop SE, et al. Adoptive immunotherapy with unselected or EBV-specific T cells for biopsy-proven EBV+ lymphomas after allogeneic hematopoietic cell transplantation. *Blood*. 2012;119(11):2644-2656.

526. Heslop HE, Brenner MK, Rooney CM. Donor T cells to treat EBV-associated lymphoma. *N Engl J Med*. 1994;331(10):679-680.

527. Rooney CM, Smith CA, Ng CY, et al. Infusion of cytotoxic T cells for the prevention and treatment of Epstein-Barr virus-induced lymphoma in allogeneic transplant recipients. *Blood*. 1998;92(5):1549-1555.

528. Heslop HE, Slobod KS, Pule MA, et al. Long-term outcome of EBV-specific T-cell infusions to prevent or treat EBV-related lymphoproliferative disease in transplant recipients. *Blood*. 2010;115(5):925-935.

529. Comoli P, Maccario R, Locatelli F, et al. Treatment of EBV-related post-renal transplant lymphoproliferative disease with a tailored regimen including EBV-specific T cells. *Am J Transplant*. 2005;5(6):1415-1422.

530. Gustafsson A, Levitsky V, Zou JZ, et al. Epstein-Barr virus (EBV) load in bone marrow transplant recipients at risk to develop posttransplant lymphoproliferative disease: prophylactic infusion of EBV-specific cytotoxic T cells. *Blood*. 2000;95(3):807-814.

531. Haque T, Wilkie GM, Jones MM, et al. Allogeneic cytotoxic T-cell therapy for EBV-positive posttransplantation lymphoproliferative disease: results of a phase 2 multicenter clinical trial. *Blood*. 2007;110(4):1123-1131.

532. Leen AM, Bollard CM, Mendizabal AM, et al. Multicenter study of banked third-party virus-specific T cells to treat severe viral infections after hematopoietic stem cell transplantation. *Blood*. 2013;121(26):5113-5123.

533. Haque T, McAulay KA, Kelly D, Crawford DH. Allogeneic T-cell therapy for Epstein-Barr virus-positive posttransplant lymphoproliferative disease: long-term follow-up. *Transplantation*. 2010;90(1):93-94.

534. Moosmann A, Bigalke I, Tischer J, et al. Effective and long-term control of EBV PTLD after transfer of peptide-selected T cells. *Blood*. 2010;115(14):2960-2970.

535. Icheva V, Kayser S, Wolff D, et al. Adoptive transfer of epstein-barr virus (EBV) nuclear antigen 1-specific t cells as treatment for EBV reactivation and lymphoproliferative disorders after allogeneic stem-cell transplantation. *J Clin Oncol*. 2013;31(1):39-48.

536. Gerdemann U, Vera JF, Rooney CM, Leen AM. Generation of multivirus-specific T cells to prevent/treat viral infections after allogeneic hematopoietic stem cell transplant. *J Vis Exp*. 2011(51).

537. Gerdemann U, Katari UL, Papadopoulou A, et al. Safety and clinical efficacy of rapidly-generated trivirus-directed T cells as treatment for adenovirus, EBV, and CMV infections after allogeneic hematopoietic stem cell transplant. *Mol Ther*. 2013;21(11):2113-2121.

538. Carbone PP, Kaplan HS, Musshoff K, Smithers DW, Tubiana M. Report of the Committee on Hodgkin's Disease Staging Classification. *Cancer Res*. 1971;31(11):1860-1861.

539. Lister TA, Crowther D, Sutcliffe SB, et al. Report of a committee convened to discuss the evaluation and staging of patients with Hodgkin's disease: Cotswolds meeting. *J Clin Oncol*. 1989;7(11):1630-1636.

540. Rohatiner A, d'Amore F, Coiffier B, et al. Report on a workshop convened to discuss the pathological and staging classifications of gastrointestinal tract lymphoma. *Ann Oncol*. 1994;5(5):397-400.

541. Cheson BD, Pfistner B, Juweid ME, et al. Revised response criteria for malignant lymphoma. *J Clin Oncol*. 2007;25(5):579-586.

542. Gallagher A, Armstrong AA, MacKenzie J, et al. Detection of Epstein-Barr virus (EBV) genomes in the serum of patients with EBV-associated Hodgkin's disease. *Int J Cancer*. 1999;84(4):442-448.

543. Klein G, Dombos L, Gothoskar B. Sensitivity of Epstein-Barr virus (EBV) producer and non-producer human lymphoblastoid cell lines to superinfection with EB-virus. *Int J Cancer*. 1972;10(1):44-57.

544. Ressing ME, Keating SE, van Leeuwen D, et al. Impaired transporter associated with antigen processing-dependent peptide transport during productive EBV infection. *J Immunol*. 2005;174(11):6829-6838.

545. Rooney CM, Gregory CD, Rowe M, et al. Endemic Burkitt's lymphoma: phenotypic analysis of tumor biopsy cells and of derived tumor cell lines. *J Natl Cancer Inst*. 1986;77(3):681-687.

546. Graham FL, Smiley J, Russell WC, Nairn R. Characteristics of a human cell line transformed by DNA from human adenovirus type 5. *J Gen Virol*. 1977;36(1):59-74.

547. Delecluse HJ, Hilsendegen T, Pich D, Zeidler R, Hammerschmidt W. Propagation and recovery of intact, infectious Epstein-Barr virus from prokaryotic to human cells. *Proc Natl Acad Sci U S A*.

1998;95(14):8245-8250.

548. Feederle R, Kost M, Baumann M, et al. The Epstein-Barr virus lytic program is controlled by the co-operative functions of two transactivators. *EMBO J*. 2000;19(12):3080-3089.

549. Garrone P, Neidhardt EM, Garcia E, Galibert L, van Kooten C, Banchereau J. Fas ligation induces apoptosis of CD40-activated human B lymphocytes. *J Exp Med*. 1995;182(5):1265-1273.

550. Bell AI, Groves K, Kelly GL, et al. Analysis of Epstein-Barr virus latent gene expression in endemic Burkitt's lymphoma and nasopharyngeal carcinoma tumour cells by using quantitative real-time PCR assays. *J Gen Virol*. 2006;87(Pt 10):2885-2890.

551. Tierney RJ, Shannon-Lowe CD, Fitzsimmons L, Bell AI, Rowe M. Unexpected patterns of Epstein–Barr virus transcription revealed by a High throughput PCR array for absolute quantification of viral mRNA. *Virology*. 2015;474(0):117-130.

552. Midgley RS, Bell AI, McGeoch DJ, Rickinson AB. Latent gene sequencing reveals familial relationships among Chinese Epstein-Barr virus strains and evidence for positive selection of A11 epitope changes. *J Virol*. 2003;77(21):11517-11530.

553. Frey B, Suppmann B. Demonstration of the Expand^{TM} PCR system's greater fidelity and higher yields with a lacI-based PCR fidelity assay. *Biochemica (Roche)*. 1995;2:8-9.

554. Fecteau JF, Neron S. CD40 stimulation of human peripheral B lymphocytes: distinct response from naive and memory cells. *J Immunol*. 2003;171(9):4621-4629.

555. FlowJo version 7.6.5 Manual: Tree Star Inc.

556. Roederer M. Interpretation of cellular proliferation data: avoid the panglossian. *Cytometry A*. 2011;79(2):95-101.

557. Hawkins ED, Hommel M, Turner ML, Battye FL, Markham JF, Hodgkin PD. Measuring lymphocyte proliferation, survival and differentiation using CFSE time-series data. *Nat Protoc*. 2007;2(9):2057-2067.

558. Aubin J, Davi F, Nguyen-Salomon F, et al. Description of a novel FR1 IgH PCR strategy and its comparison with three other strategies for the detection of clonality in B cell malignancies. *Leukemia*. 1995;9(3):471-479.

559. Inoue H, Nojima H, Okayama H. High efficiency transformation of Escherichia coli with plasmids. *Gene*. 1990;96(1):23-28.

560. Brochet X, Lefranc MP, Giudicelli V. IMGT/V-QUEST: the highly customized and integrated system for IG and TR standardized V-J and V-D-J sequence analysis. *Nucleic Acids Res*. 2008;36(Web Server issue):W503-508.

561. Zimmermann H, Trappe RU. EBV and posttransplantation lymphoproliferative disease: what to do? *Hematology Am Soc Hematol Educ Program*. 2013;2013:95-102.

562. Choquet S, Trappe R, Leblond V, Jager U, Davi F, Oertel S. CHOP-21 for the treatment of post-transplant lymphoproliferative disorders (PTLD) following solid organ transplantation. *Haematologica*. 2007;92(2):273-274.

563. Leblond V, Dhedin N, Mamzer Bruneel MF, et al. Identification of prognostic factors in 61 patients

with posttransplantation lymphoproliferative disorders. *J Clin Oncol*. 2001;19(3):772-778.

564. Ghobrial IM, Habermann TM, Maurer MJ, et al. Prognostic analysis for survival in adult solid organ transplant recipients with post-transplantation lymphoproliferative disorders. *J Clin Oncol*. 2005;23(30):7574-7582.
565. Knight JS, Tsodikov A, Cibrik DM, Ross CW, Kaminski MS, Blayney DW. Lymphoma after solid organ transplantation: risk, response to therapy, and survival at a transplantation center. *J Clin Oncol*. 2009;27(20):3354-3362.
566. Evens AM, David KA, Helenowski I, et al. Multicenter analysis of 80 solid organ transplantation recipients with post-transplantation lymphoproliferative disease: outcomes and prognostic factors in the modern era. *J Clin Oncol*. 2010;28(6):1038-1046.
567. Cang S, Mukhi N, Wang K, Liu D. Novel CD20 monoclonal antibodies for lymphoma therapy. *J Hematol Oncol*. 2012;5:64.
568. Younes A, Gopal AK, Smith SE, et al. Results of a pivotal phase II study of brentuximab vedotin for patients with relapsed or refractory Hodgkin's lymphoma. *J Clin Oncol*. 2012;30(18):2183-2189.
569. Petrich A. Brentuximab Vedotin + Rituximab as Frontline Therapy for Pts w/ CD30+ and/or EBV+ Lymphomas; 2014.
570. Akinleye A, Chen Y, Mukhi N, Song Y, Liu D. Ibrutinib and novel BTK inhibitors in clinical development. *J Hematol Oncol*. 2013;6:59.
571. Heslop HE. How I treat EBV lymphoproliferation. *Blood*. 2009;114(19):4002-4008.
572. Styczynski J, Einsele H, Gil L, Ljungman P. Outcome of treatment of Epstein-Barr virus-related post-transplant lymphoproliferative disorder in hematopoietic stem cell recipients: a comprehensive review of reported cases. *Transpl Infect Dis*. 2009;11(5):383-392.
573. Kottaridis PD, Milligan DW, Chopra R, et al. In vivo CAMPATH-1H prevents graft-versus-host disease following nonmyeloablative stem cell transplantation. *Blood*. 2000;96(7):2419-2425.
574. Savani BN, Pohlmann PR, Jagasia M, et al. Does peritransplantation use of rituximab reduce the risk of EBV reactivation and PTLPD? *Blood*. 2009;113(24):6263-6264.
575. Petropoulou AD, Porcher R, Peffault de Latour R, et al. Increased infection rate after preemptive rituximab treatment for Epstein-Barr virus reactivation after allogeneic hematopoietic stem-cell transplantation. *Transplantation*. 2012;94(8):879-883.
576. McIver Z, Stephens N, Grim A, Barrett AJ. Rituximab administration within 6 months of T cell-depleted allogeneic SCT is associated with prolonged life-threatening cytopenias. *Biol Blood Marrow Transplant*. 2010;16(11):1549-1556.
577. Morris EC, Rebello P, Thomson KJ, et al. Pharmacokinetics of alemtuzumab used for in vivo and in vitro T-cell depletion in allogeneic transplantations: relevance for early adoptive immunotherapy and infectious complications. *Blood*. 2003;102(1):404-406.
578. van Dorp S, Pietersma F, Wolfl M, et al. Rituximab treatment before reduced-intensity conditioning transplantation associates with a decreased incidence of extensive chronic GVHD. *Biol Blood Marrow Transplant*. 2009;15(6):671-678.

579. Gratama JW, Oosterveer MA, Zwaan FE, Lepoutre J, Klein G, Ernberg I. Eradication of Epstein-Barr virus by allogeneic bone marrow transplantation: implications for sites of viral latency. *Proc Natl Acad Sci U S A*. 1988;85(22):8693-8696.

580. Gratama JW, Oosterveer MA, Lepoutre JM, et al. Serological and molecular studies of Epstein-Barr virus infection in allogeneic marrow graft recipients. *Transplantation*. 1990;49(4):725-730.

581. van Kooij B, Thijsen SF, Meijer E, et al. Sequence analysis of EBV DNA isolated from mouth washings and PBMCs of healthy individuals and blood of EBV-LPD patients. *J Clin Virol*. 2003;28(1):85-92.

582. Meijer E, Spijkers S, Moschatsis S, et al. Active Epstein-Barr virus infection after allogeneic stem cell transplantation: re-infection or reactivation? *Transpl Infect Dis*. 2005;7(1):4-10.

583. Hopwood PA, Brooks L, Parratt R, et al. Persistent Epstein-Barr virus infection: unrestricted latent and lytic viral gene expression in healthy immunosuppressed transplant recipients. *Transplantation*. 2002;74(2):194-202.

584. Qu L, Green M, Webber S, Reyes J, Ellis D, Rowe D. Epstein-Barr virus gene expression in the peripheral blood of transplant recipients with persistent circulating virus loads. *J Infect Dis*. 2000;182(4):1013-1021.

585. Scholzen T, Gerdes J. The Ki-67 protein: from the known and the unknown. *J Cell Physiol*. 2000;182(3):311-322.

586. Holmes MV, Caplin B, Atkinson C, et al. Prospective monitoring of Epstein-Barr virus DNA in adult renal transplant recipients during the early posttransplant period: role of mycophenolate mofetil. *Transplantation*. 2009;87(6):852-856.

587. Bamoulid J, Courivaud C, Coaquette A, et al. Subclinical Epstein-Barr virus viremia among adult renal transplant recipients: incidence and consequences. *Am J Transplant*. 2013;13(3):656-662.

588. Bakker NA, Verschuuren EA, Erasmus ME, et al. Epstein-Barr virus-DNA load monitoring late after lung transplantation: a surrogate marker of the degree of immunosuppression and a safe guide to reduce immunosuppression. *Transplantation*. 2007;83(4):433-438.

589. Meij P, van Esser JW, Niesters HG, et al. Impaired recovery of Epstein-Barr virus (EBV)--specific CD8+ T lymphocytes after partially T-depleted allogeneic stem cell transplantation may identify patients at very high risk for progressive EBV reactivation and lymphoproliferative disease. *Blood*. 2003;101(11):4290-4297.

590. Rose C, Green M, Webber S, et al. Detection of Epstein-Barr virus genomes in peripheral blood B cells from solid-organ transplant recipients by fluorescence in situ hybridization. *J Clin Microbiol*. 2002;40(7):2533-2544.

591. Calattini S, Sereti I, Scheinberg P, Kimura H, Childs RW, Cohen JI. Detection of EBV genomes in plasmablasts/plasma cells and non-B cells in the blood of most patients with EBV lymphoproliferative disorders using Immuno-FISH. *Blood*. 2010.

592. Decker LL, Klaman LD, Thorley-Lawson DA. Detection of the latent form of Epstein-Barr virus DNA in the peripheral blood of healthy individuals. *J Virol*. 1996;70(5):3286-3289.

593. Wagner HJ, Bein G, Bitsch A, Kirchner H. Detection and quantification of latently infected B lymphocytes in Epstein-Barr virus-seropositive, healthy individuals by polymerase chain reaction. *J Clin Microbiol*. 1992;30(11):2826-2829.

594. Sugden B, Phelps M, Domoradzki J. Epstein-Barr virus DNA is amplified in transformed lymphocytes. *J Virol*. 1979;31(3):590-595.

595. Shannon-Lowe C, Adland E, Bell AI, Delecluse HJ, Rickinson AB, Rowe M. Features distinguishing Epstein-Barr virus infections of epithelial cells and B cells: viral genome expression, genome maintenance, and genome amplification. *J Virol*. 2009;83(15):7749-7760.

596. Wimperis JZ, Gottlieb D, Duncombe AS, Heslop HE, Prentice HG, Brenner MK. Requirements for the adoptive transfer of antibody responses to a priming antigen in man. *J Immunol*. 1990;144(2):541-547.

597. Lausen BF, Hougs L, Schejbel L, Heilmann C, Barington T. Human memory B cells transferred by allogenic bone marrow transplantation contribute significantly to the antibody repertoire of the recipient. *J Immunol*. 2004;172(5):3305-3318.

598. Yao QY, Czarnecka H, Rickinson AB. Spontaneous outgrowth of Epstein-Barr virus-positive B-cell lines from circulating human B cells of different buoyant densities. *Int J Cancer*. 1991;48(2):253-257.

599. Weller S, Reynaud CA, Weill JC. Splenic marginal zone B cells in humans: where do they mutate their Ig receptor? *Eur J Immunol*. 2005;35(10):2789-2792.

600. Agematsu K, Futatani T, Hokibara S, et al. Absence of memory B cells in patients with common variable immunodeficiency. *Clin Immunol*. 2002;103(1):34-42.

601. Dharnidharka VR, Douglas-Nikitin V. Hodgkin's-like PTLD versus true Hodgkin's disease. *Pediatr Transplant*. 2004;8(6):581-582.

602. Langerak AW, Groenen PJ, Bruggemann M, et al. EuroClonality/BIOMED-2 guidelines for interpretation and reporting of Ig/TCR clonality testing in suspected lymphoproliferations. *Leukemia*. 2012;26(10):2159-2171.

603. Kataoka Y, Bindokas VP, Duggan RC, Murley JS, Grdina DJ. Flow cytometric analysis of phosphorylated histone H2AX following exposure to ionizing radiation in human microvascular endothelial cells. *J Radiat Res*. 2006;47(3-4):245-257.

604. Huang X, Darzynkiewicz Z. Cytometric assessment of histone H2AX phosphorylation: a reporter of DNA damage. *Methods Mol Biol*. 2006;314:73-80.

605. Ismail IH, Wadhra TI, Hammarsten O. An optimized method for detecting gamma-H2AX in blood cells reveals a significant interindividual variation in the gamma-H2AX response among humans. *Nucleic Acids Res*. 2007;35(5):e36.

606. Kuo LJ, Yang LX. Gamma-H2AX - a novel biomarker for DNA double-strand breaks. *In Vivo*. 2008;22(3):305-309.

607. Tanaka T, Huang X, Halicka HD, et al. Cytometry of ATM activation and histone H2AX phosphorylation to estimate extent of DNA damage induced by exogenous agents. *Cytometry A*. 2007;71(9):648-661.

608. Chen Y, Xiang Z, Li H, Yang N, Zhang H. P53 gene mutations in non-Hodgkin's lymphoma. *J Tongji*

Med Univ. 1999;19(1):27-30.

609. Iskra S, Kalla M, Delecluse HJ, Hammerschmidt W, Moosmann A. Toll-like receptor agonists synergistically increase proliferation and activation of B cells by epstein-barr virus. *J Virol*. 2010;84(7):3612-3623.
610. Carbone A, Gaidano G, Gloghini A, et al. BCL-6 protein expression in AIDS-related non-Hodgkin's lymphomas: inverse relationship with Epstein-Barr virus-encoded latent membrane protein-1 expression. *Am J Pathol*. 1997;150(1):155-165.
611. Bollard CM, Rooney CM, Heslop HE. T-cell therapy in the treatment of post-transplant lymphoproliferative disease. *Nat Rev Clin Oncol*. 2012;9(9):510-519.
612. Uhlin M, Okas M, Gertow J, Uzunel M, Brismar TB, Mattsson J. A novel haplo-identical adoptive CTL therapy as a treatment for EBV-associated lymphoma after stem cell transplantation. *Cancer Immunol Immunother*. 2010;59(3):473-477.
613. Cieri N, Mastaglio S, Oliveira G, Casucci M, Bondanza A, Bonini C. Adoptive immunotherapy with genetically modified lymphocytes in allogeneic stem cell transplantation. *Immunol Rev*. 2014;257(1):165-180.
614. Teng YK, Ioan-Facsinay A, van Laar JM. CD20 epitope masking by rituximab: comment on the article by Gunnarsson et al. *Arthritis Rheum*. 2008;58(2):634; author reply 634.
615. De Pasquale MD, Mastronuzzi A, De Vito R, et al. Unmanipulated donor lymphocytes for EBV-related PTLD after T-cell depleted HLA-haploidentical transplantation. *Pediatrics*. 2012;129(1):e189-194.
616. Petropoulou AD, Porcher R, de Latour RP, et al. Increased Infection Rate After Preemptive Rituximab Treatment for Epstein-Barr Virus Reactivation After Allogeneic Hematopoietic Stem-Cell Transplantation. *Transplantation*. 2012.
617. Ferlazzo G, Pack M, Thomas D, et al. Distinct roles of IL-12 and IL-15 in human natural killer cell activation by dendritic cells from secondary lymphoid organs. *Proc Natl Acad Sci U S A*. 2004;101(47):16606-16611.
618. McAulay KA, Haque T, Urquhart G, Bellamy C, Guiretti D, Crawford DH. Epitope specificity and clonality of EBV-specific CTLs used to treat posttransplant lymphoproliferative disease. *J Immunol*. 2009;182(6):3892-3901.
619. van Zelm MC, Szczepanski T, van der Burg M, van Dongen JJ. Replication history of B lymphocytes reveals homeostatic proliferation and extensive antigen-induced B cell expansion. *J Exp Med*. 2007;204(3):645-655.
620. Mensen A, Ochs C, Stroux A, et al. Utilization of TREC and KREC quantification for the monitoring of early T- and B-cell neogenesis in adult patients after allogeneic hematopoietic stem cell transplantation. *J Transl Med*. 2013;11:188.

10. Appendix

Assay	Primer/Probe	Genome Co-ordinates*	Sequence	20x conc.
Wp	W0	14391–14410	CGCCAGGAGTCCACACAAAT	2µM
	W1W2	14709–14701/ 14619–14612	GAGGGGACCCTCTGGCC	2µM
Cp	C1C2	11467–11479/ 11626–11639	AATCATCTAAACCGACTGAAGAAACAG	20µM
	W1W2	14709–14701/ 14619–14612	GAGGGGACCCTCTGGCC	20µM
Wp/Cp	W probe	14564–14588	ACCGAAGTGAAGGCCCTGGACCAAC	10µM
EBNA1	Q	62440–62456	GTGCGCTACCGGATGGC	20µM
	Y3	48422–48440	TGCCTGAACCTGTGGTTGG	20µM
	F primer	50099-50115	GGGTGAGGCCACGCTTT	20µM
	U	55247-55269	CTGCAGCCCAGAGAGTAGTCTCA	20µM
	U1	55326-55304	CAGGTCTACTGGCGGTCTATGAT	
	K	107952–107941/ 67649–67636	CATGATTCACACTTAAAGGAGACGG	20µM
	U probe	67563–67587	TCCTCTGGAGCCTGACCTGTGATCG	10µM
EBNA2	EBNA2 Type1 F	35702-35711 36098-36109/	GCTTAGCCAGTAACCCAGCACT	6 µM
	EBNA2 Type2 F		GCTTAGCCAGTAACTCAGCGCT	6 µM
	EBNA2 R	36181-36160	TGCTTAGAAGGTTGTTGGCATG	6 µM
	EBNA2 probe	36127-36153	CCCAACCACAGGTTCAGGCAAAACTTT	10µM
EBNA3A	EBNA3A F	81944-81929	CCCCTTAACTCAACCCATTAACC	6 µM
	EBNA3A R	82313-82335	CGGCCCCTCCATTGGT	6 µM
	EBNA3A probe	82343-82363	ACCCGCAGCCCATTTCCTCCA	10µM
EBNA3B	EBNA3B F	83265-83281	TGCCGCTGCAAGAGAGG	20µM
	EBNA3B R	83510-83500/ 83421-83413	AGGTCCGATTGCAACATGGA	20µM
	EBNA3B probe	83347-83374	CCTAGATTTGTGGATGTGAACCCAACGC	10µM
EBNA3C	EBNA3C F	88813-88831	TACGCCCCATTCCAACAAG	6 µM
	EBNA3C R	88876-88858	CCCACGGCCATGCTATCTT	6 µM
	EBNA3C probe	88835-88856	CCCCCCTCCCCCTATGCCGTTA	10µM
BHRF1	W2	14810-14830	TGGTAAGCGGTTCACCTTCAG	6µM
	Y2	35706-35680	GAGGATGAAGACTAAGTCACAGGCTTA	6µM
	H2	41596-41607/ 42047-42055	GGCTTACCTCGGTTCCCTCTT	6µM
	HF	42134-42111	TCCCGTATACACAGGGCTAACAGT	6µM
	Probe	42067-42097	TGCCAGATCTTGTAGAGCAAGATGGCCTATT	10µM
LMP1	LMP1 F	168644-168625	AATTTGCACGGACAGGCATT	6 µM
	LMP1R	168435-168454	AAGGCCAAAAGCTGCCAGAT	6 µM
	LMP 1 probe (B95)	168951-168965/ 169042-169060	TCCAGATACCTAAGACAAGTAAGCACCCGAAGAT	10µM
	LMP1 probe (Cao)		TCCAGAGACCTAAGACAAGTAAGCAGCCAAAGAT	10µM
LMP1-TR	LMP1-TR F (B95)	169013-168994	CCCCTCTCAAGGTCGTGTTC	6 µM

	LMP1-TR F (Cao)		GCGTCTCAAGGTCGCGTTC	6 µM
	LMP1-TR R (B95)	169099-169080	CGTAGCCGCCCTACATAAGC	6 µM
	LMP1-TR R (Cao)		TCGTAGGCGGCCTACATAACC	6 µM
	LMP1-TR probe (B95)	169017-169040	CCTCAGGGCAGTGTGTCAGGAGCA	10µM
	LMP1-TR probe (Cao)		TGCTCCTGCCACACTACCCTGACCA	10µM
LMP2 (total)	LMP2exon6 F	1027-1049	GGTTCTCCTGATTTGCTCTTCGT	6 µM
	LMP2exon6 R	1129-1113	CGCGGAGGCTAGCAACA	6 µM
	LMP2exon6 probe	1074-1103	TCCTTCTGGCACGACTGTTCCTATATGCTC	10µM
LMP2A	LMP2A exon1 F	166109-166129	TCCCTAGAAATGGTGCCAATG	6 µM
	LMP2A exon1 R	166215-166195	GAAGAGCCAGAAGCAGATGGA	6 µM
	LMP2A probe	166142-166160	CCTAGCCCCGGCGGGGATC	10µM
LMP2B	LMP2B exon1F	169365-169385	GTAATCTGCACAAAGAGGCGC	6 µM
	LMP2B exon1R	169436-169421	AAAGCACGGCCTCCCG	6 µM
	LMP2B probe	169399-169418	TGCCGCCAACGACCTCCCAA	10µM
LMP2-TR	LMP2-TR F	28-50	ACTTTTCTTCTTGCCCGTTCTCT	6 µM
	LMP2-TR R	114-133	GAAACACGAGGCGGCAATAG	6 µM
	LMP2-TR probe	66-92	CAGTATGCCTGCCTGTAATTGTTGCGC	10µM
BZLF1	BZLF1 F	90859-90835	CCCAAACTCGACTTCTGAAGATGTA	20x
	BZLF1 R	90767-90791	TGATAGACTCTGGTAGCTTGGTCAA	custom
	BZLF1probe	90803-90820	CCCATACCAGGTGCCTTT	assay
BRLF1	BRLF1 F	92662-92644	TTGGGCCATTCTCCGAAAC	6 µM
	BRLF1 R	92581-92590	TATAGGGCACGCGATGGAA	6 µM
	BRLF1probe	92611-92631	AGACGGGCTGAGAATGCCGGC	10µM
BMLF1	BMLF1 F	71978-71958	CCCGAACTAGCAGCATTTCCT	6 µM
	BMLF1 R	71805-71824	GACCGCTTCGAGTTCCAGAA	6 µM
	BMLF1 probe	71941-71955	AACGAGGATCCCGCAGAGAGCCA	10µM
BALF1	BALF1 F	164694-169676	GGGCAAAGACACGCACGTA	6 µM
	BALF1 R	164615-164633	GCCGCGACCAGTAGTCGTA	6 µM
	BALF1 probe	164650-164670	CATCATCAGCGTCCTGCGCGC	10µM
BALF2	BALF2F	164131-164113	CGGGCTTCAGCATCAATGT	6 µM
	BALF2R	164053-164074	TGATAGGAGGTAGCGCGTAGGA	6 µM
	BALF2 probe	164080-164101	ACAGGAGGCCCGACCCCAACTG	10µM
BARF1	BARF1 F	165586-165606	GGGAGCCTCTCTGTTGCTGTT	6 µM
	BARF1 R	165658-165639	TTTTCCCAACGCAGGTCACT	6 µM
	BARF1 probe	165608-165631	ACCTGTCACTTCCCAAGCCCTGGC	10µM
BGLF5	BGLF5F	108930-108913	GCAAGCCCGGGAGAGACT	6 µM
	BGFL5R	108862-108879	GAGGCGACCGTTTTCGAA	6 µM
	BGLF5 probe	108881-108904	CGGGTGAACATTGTGACGGCCTTC	10µM

Table 26. Primers and Probes for Fluidigm RT-PCR

* Coordinates taken from accession number NC007605 (Human Herpesvirus 4 type 1, complete genome)

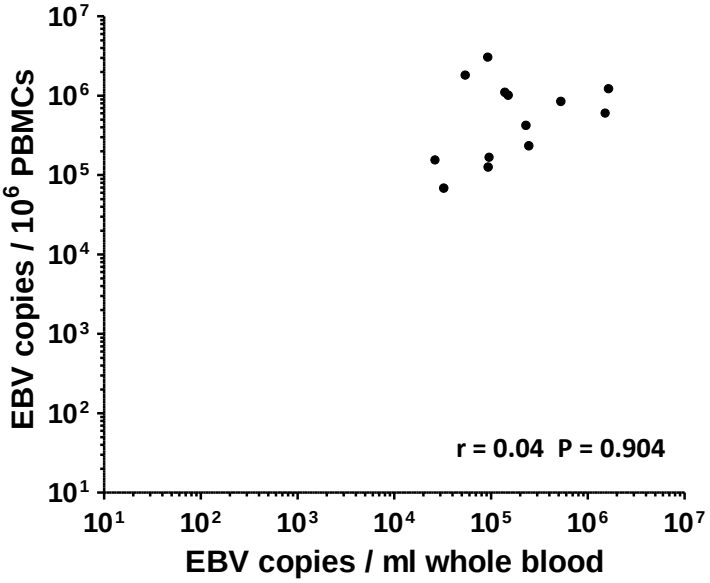

Figure 67. Whole Blood versus PBMC EBV Loads for High EBV Allo-HSCT Patients

EBV loads determined by the clinical whole blood EBV qPCR assay (EBV copies / ml of whole blood) are plotted against corresponding virus loads determined within isolated PBMCs (EBV copies / 10^6 PBMCs) for allo-HSCT patients with high-level EBV reactivation. Pearson correlation was non-significant within the group.